AUTONOMIC AND PHARMACOLOGIC MODULATION OF THE FREQUENCY-DEPENDENT PROPERTIES OF THE ATRIOVENTRICULAR NODE

by

Mohsen Nayebpour, Pharm.D

Department of Pharmacology and Therapeutics

A thesis submitted to the Faculty of Graduate Studies and Research,

McGill University, Montreal

December, 1990 in partial fulfillment of the requirements

for the degree of Doctor of Philosophy

This thesis is dedicated to

my wife, Azita, whose support and encouragement were fundamental during the course of my graduate studies were it not from her patience, understanding and motivation during all these years, this thesis may have never been completed.

to my sons: Mohammad Amin and Mohammad Mehdi

Thanks for your patience.

ABSTRACT

The responses of the atrioventricular node (AVN) to changes in activation rate is complex. A variety of approaches have been used to explain the different responds of AVN, but none has been able to describe fully nodal behavior. Three rate-dependent nodal properties referred to as recovery, facilitation, and fatigue contribute to rate-induced changes in nodal conduction time. We developed a model incorporating a quantitative description of these properties that was able to accurately predict AV node conduction during steady state atrial pacing. This model provides a mathematical framework through which interventions such as changes in the autonomic tone may affect AV nodal conduction. This was evaluated by studying effects of vagal stimulation (VS), isoproterenol (IP), and beta blockade (BB) on AVN conduction. Experimental results and mathematical modelling revealed that these interventions alter the ways in which the AVN responds to changes in activation rate. These changes result in enhanced rate-dependent AVN conduction slowing with VS and BB, and reduced rate-dependent slowing with IP.

The potential implications of the rate-dependent properties of the AVN were studied by evaluating whether the depressant effects of diltiazem (D) on the AVN are enhanced during arrhythmias which increase AVN activation rate. The relative magnitude of D's effects on the AVN during tachycardia (atrial fibrillation, and circus movement tachycardia) were significantly magnified compared to the effects at races comparable to sinus rhythm in man. Rate-dependent calcium channel-blocking properties of D were an intrinsic property, though their intensity was modulated by autonomic tone. This thesis provides a link between basic theories of rate dependent properties and physiologic and pharmacologic implications.

RESUME

La réponse du noeud auriculo-ventriculaire lors de changements de fréquence d'activation est complexe. Une variété d'approches ont été utilisées pour expliquer les différentes réponses du noeud AV, mais aucune a été capable de décrire complètement le comportement nodal. Trois propriétés, dépendantes en fréquence, du noeud AV telles que récupération, facilitation et fatigue contribuent aux changements dans le temps de conduction du noeud. Nous avons développé un modèle, incorporant une description quantitative de ces propriétés, étant capable de prédire précisément la conduction du noeud AV durant la stimulation auriculaire pendant l'état constant. Ce modèle nous donne une structure mathématique incluant les interventions pouvant affecter la conduction du noeud AV comme les changements au niveau du tonus autonomique. Ceci a été évalué en étudiant les effets de la stimulation vagale (SV), isoprotérénol (IP) et bloqueur beta (BB) sur la conduction du noeud AV. Les résultats expérimentaux et ceux provenant du modèle mathématique ont révélés que ces interventions altèrent les façons à laquelle le noeud AV répond lors de changements de la fréquence d'activation. Ces changements résultent en une intensification du ralentissement de la conduction dépendante en fréquence avec SV et BB et réduit ce ralentissement de la conduction dépendante en fréquence avec IP.

Les implications potentielles des propriétés dépendantes en fréquence du noeud AV, ont été étudiées, en évaluant si les effets dépressants de diltiazem (D) sur le noeud AV sont intensifiés durant les arythmies, celles-ci augmentant la fréquence d'activation. L'amplitude relative des effets de diltiazem sur le noeud AV durant une tachycardie (fibrillation auriculaire et tachycardie de réentrée) était amplifée significativement en comparaison à celle obtenue durant des fréquences comparables au rythme sinusal chez l'homme. Les propriétés dépendantes en fréquence des bloqueurs des canaux calciques par diltiazem étaient des propriétés intrinsèques bien que leur intensité était modulé par le tonus autonomique. Cette thèse fournit un lien entre les théories fondamentales des propriétés dépendantes en fréquence et les implications physiologiques et pharmacologiques.

ACKNOWLEDGMENTS

Doctor Stanley Nattel, my supervisor, for his guidance, suggestions, inspiration, and for providing an excellent learning environment Were it not from his constant availability, and his constructive criticism and careful proof-reading of the thesis, this thesis may have never been completed.

Doctor A.C. Cuello, Chairman of the Department of Pharmacology for giving me the opportunity to pursue my graduate studies

Doctor M. Quik, my advisor, thanks for the helpful discussions and advice through the years.

Doctor Mario Talajic, my friend, thanks for the helpful discussions and advice through the years.

I also wish to express my attachment to the students with whom I went through these learning years including Rafael Cabeza, Zigua Wang, Suzan Ranger, Susan Bayly, Wuhua Jing, Lorella Gorafalo, Nicole Laudignon, Howard Mount, Jean. C. Martel, R. Mosqueda, William Potvin, Michael Poulter, Ligia Stern, William Toy, Steve Fergusson, Suzan Geertsen, Anurag Tandon, Ronith Afar, Katia Betito.

Special thanks to Carol Mathews, Christine Villemaire, Nancy Turmel for their friendship and for invaluable assistance in different aspects of my work.

PREFACE

Note on the Format of this Thesis

In accordance with the Faculty of Graduate Studies and Research the candidate has the option of including as part of his thesis the text of original papers already published by learned journals, and original papers submitted or suitable for submission to learned journals. The exact wording relating to this option is as follows.

> The Candidate has the option, subject to the approval of the Department, of including as part of the thesis the text of an original paper, or papers, suitable for submission to learned journals for publication. In this case the thesis must still conform to all requirements explained in this document, and additional material (e.g. experimental data, details of equipment and experimental design) may need to be provided. In any case, abstract, full introduction and conclusion must be included, and where more than one manuscript appears, connecting texts and common abstract, introduction and conclusion are required. A mere collection of manuscripts is not acceptable, nor can reprints of published paper be accepted. While the inclusion of manuscripts co-authored by the Candidate and others is not prohibited for a test period, the Candidate is warned to make an explicit statement on who contributed to such work and to what extent. Copyright clearance from the co-author or co-authors must be included when the thesis is submitted. Supervisors and others will have to bear witness to the accuracy of such claims before the Oral Committee. It should be noted that the task of the External Examiner is much more difficult in such cases.

Chapter 2:

Mohsen Navebpour, Mario Talajic, Stanley Nattel. Quantification of Dynamic AV Nodal Properties and Application to Predict Rate-Dependent AV Conduction. Accepted for publication in Am. J. of Physiology, November, 1990.

Chapter 3:

Mohsen Nayebpour, Mario Talajic, Christine Villemaire, Stanley Nattel. Vagal Modulation of the Rate-Dependent Properties of the Atroventricular Node. Circ. Res. 1990;67.1152-1160.

Chapter 4:

Mohsen Nayebpour, Mario Talajic, Stanley Nattel. The Effects of Beta-Adrenergic Stimulation and Blockade on Rate-Dependent AV Node Properties. Submitted to Circ. Res. November, 1990.

Chapter 5:

Mario Talajic, Mohsen Nayebpour, Wuhua Jing, Stanley Nattel. Frequency-Dependent Effects of Diltiazem on the Atrioventricular Node During Experimental Atrial Fibrillation. Circulation 1989, 80: 380-389

Chapter 6:

Talajic Mario, Papadatos D, Villemaire C, Nayebpour M, Nattel S. Antiarrhythmic Actions of Diltiazem During Experimental Atrioventricular Reentrant Tachycardias- Importance of Use-Dependent Calcium Channel-Blocking Properties. Circulation 1990,81:334-342

Chapter 7:

Mohsen Nayebpour, Mario Talajic, Wuhua Jing and Stanley Nattel. Autonomic Modulation of the Frequency-Dependent Actions of Diltiazem on the Atrioventricular Node in Anesthetized Dogs. The J of Pharmacol. and Exper. Ther; 235: 353-361,1990.

TABLE OF CONTENTS

INDEX OF FIGURES

CHAPTER 1

CHAPTER 2

CHAPTER 5

CHAPTER 6

LIST OF TABLES

CHAPTER 2

CHAPTER 3

CHAPTER 4

CHAPTER 5

CHAPTER 6

CHAPTER 7

Statement of Authorship

This thesis is comprised of six papers co-authored by myself and others. The following is a statement regarding the contributions of myself and others to this work.

The papers entitled "Quantification of dynamic AV nodal properties and application to predict rate-dependent AV conduction" (Nayebpour et al, 1990),"Vagal modulation of the rate-dependent properties of the AV node" (Nayebpour et al, 1990), and "The effects of beta adrenergic receptor stimulation and blockade on rate-dependent AV node properties." (Nayebpour et al, 1990) describe research in which the initial ideas and hypotheses, design of studies, and analysis of data were almost exclusively my own. For these studies, Dr Nattel served in an supervisory capacity, helping me clarify ideas, analysing the data, and improve the writing. Mathematical quantification of "Facilitation" was suggested by Dr. Nattel. Dr. Talajic participated in discussing the data, giving suggestions, and reading the manuscripts. Christine Villemaire assisted me in analysing some of the data presented in the second paper

The papers entitled "Frequency-dependent effects of diltiazem on the atrioventricular node during experimental atrial fibrillation" (Talajic et al, 1989), and "The antiarrhythmic actions of diltiazem during AV reentrant tachycardias-Relationship to use-dependent calcium channel blocking properties" (Talajic et al, 1990) were more of a collaborative effort It was Dr. Talajic's idea to test the frequency-dependent effects of diltiazem on the AV node during experimental tachycardias. In the first study I was responsible for performing the experiments, and analysing the data. Some of the experiments were conducted by Dr Ting

Dr. Nattel served as supervisor. In the second study I participated in performing some of the experiments While not exclusively my own work, these two papers are included in the body of the thesis because of its place in the sequence of research I am presenting. Their inclusion will show the relationship between the frequency-dependent properties of the AV node and drug efficacy in the treatment of tachycardias involving the AV node

The paper entitled "Autonomic modulation of the frequency-dependent actions of diltiazem on the atrioventricular node in anesthetized dogs" (Nayebpour et al, 1990) describes research in which the initial ideas, design of studies, and analyses of data were almost all my own. For this study, Dr. Nattel served in an supervisory capacity, and improved the writing Although, it was Dr. Talajic's initial idea to test the frequency-dependent effects of diltiazem during atrial fibrillation (see manuscript discussed above), the importance of autonomic tone in modulating the frequency-dependent drug effect was not tested He participated in discussing the data and helping in analysing some of the data Dr. Jing participated in performing some of the experiments.

Chapter 1

INTRODUCTION

1. ATRIOVENTRICULAR NODE

1.1- Functional significance

Although the AV (atrioventricular) bundle was first described in 1893 by Wilhelm His, Jr., a much more comprehensive report was given by Sunao Tawara in 1906 (Tawara, 1906; cited in Meijler and Janse, 1988). The name *node* was given to the initial portion of the AV conducting system because of the peculiar network-like arrangement of the muscular fibers and not because of the macroscopic appearance of a node-like swelling or thickening. The AV node, with its junctional fibers, links the atria to the ventricles. The strategic position of the AV node makes this structure an important part of the specialized conduction system An important function of the AV conduction system is the transmission of impulses from the atria to the ventricles. In addition, the cardiac impulse is delayed in the central portion of the AV node This allows sufficient time for atrial contraction to contribute to the filling of the ventricles. One of the important functions of the AV node is to protect the ventricles from excessively rapid rhythms In addition the AV node may act as a pacemaker for the ventricles when the sinus node pacemaker fails

1.2- Location and organization

The AV node is situated in the lower posterior portion of the atrial septum on the right side near the AV border. In the adult human it measures 5 to 7 mm in length and 2 to 5 mm in width (James, 1961). The AV node is positioned in a triangle bounded by the orifice of the coro-

nary sinus, the orifice of the superior vena cava, the coronary sinus, the orifice of the inferior vena cava and the small septal cusp of the tricuspid valve (Roberts, 1959). This triangle, originally described by Koch (Koch, 1909), is named the triangle of Koch It is close to the coronary sinus, its upper border being just beneath and a few millimeters to the right of this vein. The lower border of the AV node lies on the right side of the root of the aorta and above the septum membranaceum, and is situated between the limbus of the fossa ovalis and the tricuspid valve.

1.3- Distribution of cell types within the AV node

Most of our knowledge about the electrophysiology, innervation, histology, and ultrastructure of conduction tissue has been obtained from studies on animal species, particularly the rabbit. There are very few studies of AV node histology in human hearts. Most studies of human AV node have been performed either in tissues obtained at post mortem examination or in hearts obtained from recipients of cardiac transplants. James and Sherf (1968) were able to identify four different cell types in the human AV node on the basis of light microscopic examinations. The first cell type at the atrionodal margin resembles ordinary working myocardium. These cells are linked via intercalated disks to the other cell types within the AV node, but never with cells located centrally in the node These cells contain more myofibrils than those located centrally and their sarcoplasmic reticulum is fully developed This type of cells has not been reported in the rabbit AV node

The second cell type which is by far the most common in the human AV node is called the transitional cell type. These cells are slender and elongated, and resemble working myocardial cells except that their internal organization is somewhat simpler (James and Sherf, 1968). These cells provide a network which contacts all four cell types. The junctions between these cells and either working or Purkinje cells are provided by intercalated discs. These intercalated discs have a simple structure compared to those of working myocardium. In these cells the myofibrils are located in a parallel fashion along the long axis of the cells, and as the number of myofibrils increases, so does the number of mitochondria. These cells resemble transitional cells described in the rabbit heart (Anderson et al, 1974). However, in the rabbit these cells are subdivided into three distinct groups the posterior, midnodal, and anterior group of transitional cells.

The third cell type is that of "P" cells. They are rounded or ovoid in shape, have a poorly developed sarcoplasmic reticulum, and are located centrally in the AV node. One of the most striking differences between midnodal cells and those of the working myocardium or transitional cells is the lack of fully developed intercalated discs, either among these cells or between them and neighboring cells (James and Sherf, 1968) This lack of intercalated disks may contribute to the slow conduction which occurs in this region of the AV node. These cells contain relatively few myofibrils and sarcomeres, and have little sarcoplasmic reticulum. They correspond midnodal or "N" cells in the rabbit heart (Anderson et al, 1974), which are small and not separated by much connective tissue (Anderson et al, 1974).

The fourth cell type in the human AV node occupies the distal portion of the node and resembles Purkinje cells. In these cells the myofibrils are fewer in number than in working myocardium, but they are sarcosome-rich like the transitional cells. This may explain the pacemaker activity observed in this region. These cells correspond to cells in the distal portion of the rabbit AV node, called lower nodal cells or "NH" cells (Anderson et al, 1974) In the rabbit AV node the lower nodal cells are separated by connective tissue and it is easy to distinguish these cells from His bundle cells.

1.4- Structural-Electrophysiological correlation

In 1960 Paes de Carvalho and de Almeida divided the AV nodal area into three zones based on electrophysiological properties. Subsequently, other authors confirmed the existence of these zones in the AV node (Strackee et al, 1971; Anderson et al, 1974, Billette et al, 1976) These different zones are usually designated AN (atrionodal), N (nodal), and NH (nodal-His) AN cells have action potential configurations which gradually change from a typical atrial action potential (rapid upstroke, constant level of membrane potential during phase 4, rapid repolarization) toward a more typical nodal action potential (less negative resting potential, slow diastolic depolarization, and slow upstroke) (Hoffman and Cranefield, 1960, Mendez and Moe, 1966, Billette, 1987) "N" cells are located more centrally and have typical nodal action potentials as described above The NH zone is distal to the "N" zone and is a transitional region between the "N" zone and the His bundle. Therefore, their action potential configurations gradually/

change from a typical "N" cell action potential to a typical action potential from the His bundle (more negative membrane potential, long action potential duration, phase 2 and 3 of action potential clearly differentiated) (Hoffman and Cranefield, 1960).

Since the identification of these zones, several attempts have been made to correlate these electrophysiologically distinct zones with morphological characteristics (Anderson et al, 1974, Billette et al, 1976, Sherf, et al 1985) Anderson et al (1974) identified these zones on the basis of action potential differences and then injected cobalt chloride through the microelectrodes from which action potentials had been recorded Subsequent histological identification of cobalt staining showed a close correlation between different electrophysiological zones and morphologically distinct cells (Figure 1.1). In this study AN potentials were recorded from transitional cells and NH potentials from lower nodal cells in the distal AV node.

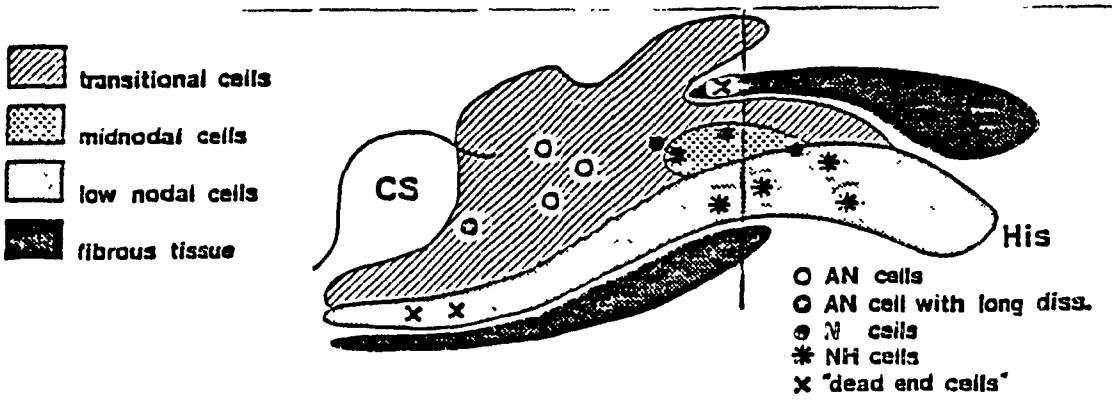

Figure 1.1. Diagram showing distribution of morphologically different cell types in AV node.The positions of the 15 verified cobalt spots are superimposed on this map. Each of the symbols represents 1 cobalt spot NH cells are confined to the anterior lower nodal cells The N cells are adjacent to the midnodal cells, and all AN cells are in transitional cells This Figure is taken from a paper by Anderson et al, Circ Res, Vol 35, 1974.

Typical nodal potentials (N potentials) were recorded from the central portion of the AV node. Billette et al (1986) studied cycle length-dependent properties of AV nodal activation and related them to subsequent morphological analysis, confirming the above results. However, Billette's results showed that the proximal portion of the AV node, known as the AN zone, appeared to occupy a larger area in the atrial portion of the AV node, and another type of AN cells (so called "double-component AN cells") was identified between AN cells and N cells. Subsequently, Billette (1987) subdivided the proximal portion of the AV node into AN cells, ANCO cells, and ANL cells based on electrophysiological properties.

Based on these studies it can be concluded that the architecture of the AV node is designed to subserve its specialized function. The distribution of morphologically distinct cells from the proximal to the distal portion of the node determines the conduction of atrial impulses through the AV node. In the following section the significance of these different zones in determining AV nodal conduction delay will be discussed.

2 ELECTROPHYSIOLOGY OF THE AV NODE

2.1- Cellular electrophysiology

2.1.1- Action Potential Characteristics

The action potential characteristics of cells in the AV node are different from those of cells elsewhere in the specialized conduction system (Hoffman and Cranefield 1960). In cells of the specialized conduction system the resting membrane potential (RMP) ranges from

aproximately -65 mV in the AV node to approximately -95 mV in the Purkinje system (Hoffman and Cranefield, 1960). Action potentials recorded from typical nodal cells (N cells) have low amplitude and either a small overshoot or no overshoot at all (Hoffman and Cranefield, 1960; Mendez and Moe, 1966). The maximum rate of rise of membrane potential during phase 0 (V_{max}) is slow (Hoffman and Cranefield, 1960, Paes de Carvalho and Almeida, 1960; Mendez and Moe 1966) Phase 1 repolarization is not clearly demarcated, and the duration of the action potential is somewhat longer than that of atrial cells but shorter than for Purkinje cells (Billette, 1987) AV nodal cells nearer the His bundle have a more negative resting membrane potential, and their action potential durations are longer with greater V_{max} and amplitude (Hoffman et al 1959, Mendez and Moe 1966; Billette, 1987) Along with the geometry and architecture of the AV node, these action potential characteristics are critical in determining conduction through the AV node

2.1.2- Membrane Currents in AV nodal cells

Although the voltage clamp technique has been available since 1952, there are few studies using this technique to analyze the membrane current systems in the AV node. Some indirect information on ionic currents of the AV node has been obtained by analyzing action potential characteristics and their response to pharmacologic agents (Zipes and Mendez 1973; Wit and Cranefield 1974). These studies suggest that the slow inward current (I_{si}) is responsible for phase zero of the AV nodal action potential Zipes and Mendez (1973) showed that 2 mM $MnCl_2$

supresses activity in nodal cells without altering activity in the atrium or His bundle. On the other hand, tetrodotoxin eliminates activity in the His bundle and atrium without importantly altering the function of AV nodal cells These observations suggested the concept that calcium entry through so-called "slow channels" is responsible for the activation of AV nodal tissue.

The major limitation to studying ionic currents in the AV node in the a multicellular preparation is the heterogeneity of the AV node As discussed earlier, the AV node consists of different cell types with different electrical properties. The short space constant in the AV node (Noma et al, 1980) adds another restriction, by limiting the size of preparations in which voltage control is possible The introduction of the patch clamp technique allows for the study of ionic currents at the level of a single cell or single channel (Hamill et al, 1981) A few laboratories have been successful in using whole cell voltage clamp with a patch electrode to study the membrane currents in the AV node (Kokubun et al, 1982 and 1985, Nakayama et al, 1984, Nakayama and Irisawa, 1985)

2 1.2 1- Transient Inward Calcium Current, I_{si}

Noma et al (1980a) and later Kokubun et al (1982) characterized ionic currents in the AV node using small specimens of the rabbit AV node They found that the upstroke of the action potential in the AV node is dependent on the calcium slow inward current sensitive to D 600 and insensitive to tetrodotoxin (TTX) Taniguchi et al (1981) and Nakayama et al (1984) characterized the ionic current in the AV node

using single pace-making cells from the AV node of rabbit hearts. The slow inward current in single cells was comparable to that obtained in small AV nodal specimens. The slow inward current can be recorded in both sodium-free and calcium-free Tyrode solutions, and in both cases the current is sensitive to D-600 and insensitive to TTX (Kokubun et al, 1982). This implies that the slow inward current in AV nodal cells can be carried by calcium or sodium ions through the slow inward current channels, although in the physiological situations Ca^{++} is the main charge carrier. There has been dispute as to whether the fast sodium inward current (I_{Na}) can also contribute to phase zero of action potentials in the AV node. Membrane hyperpolarization either in multicellular preparations (Van Capelle and Janse, 1976; Kokubun et al, 1982) or in single cells isolated from the AV node (Nakayama et al, 1984) can allow sodium inward current sensitive to tetrodotoxin (TTX) to be elicited. Kokubun et al (1982) showed that the upstroke of the action potential elicited from a hyperpolarizing prepulse to -83 mV is biphasic, and that the fast initial phase is sensitive to TTX. These findings are comparable with other observations (Ruiz-Ceretti, 1976; Kokubun et al, 1985) suggesting a potential contribution of the fast sodium inward current in the AV node.

2.1.2.2- Potassium outward currents

2.1.2.2.1- Delayed rectifier (I_K)

It is known that the termination of the action potential in Purkinje fibers is in part due to activation of a delayed rectifier potassium current (Nobel and Tsien, 1969). For many years, the characterization of I_K was complicated by the potential for potassium fluctuations in the

extracellular space of multicellular preparations. The introduction of single cell and single channel recording has diminished these problems. I_K activates slowly upon depolarization and decays gradually after repolarization to the holding potential, and has been identified in the AV node (Noma et al, 1980a; Kokubun et al, 1982, Taniguchi et al, 1981). Kokubun et al (1982) found that the time course of the outward current tail was biexponential, like the outward tail current in the SA node (DiFrancesco et al, 1979; Irisawa, 1978 and Brown, 1982) It has been suggested that the fast component plays an important role in the repolarization of the AV node (Kokubun et al, 1982)

2.1 2 2.2-Transient outward current I_{to}

Another potential voltage gated potassium channel in the AV node is the transient outward current (I_{to}) which is also called the early outward current. This current was demonstrated in the sheep Purkinje fiber as early as 1964 (Deck and Trautwein, 1964), and has been extensively studied in various cardiac cells (Fozzard and Hiraoka, 1973 Powell and Gibbons, 1979; Coraboeuf and Carmeliet, 1982, Josephson et al, 1984 Tseng and Hoffman , 1989) Recently Nakayama and Irisawa (1985) have characterized I_{to} in quiescent cells of the AV node of the rabbit They found that this outward current can be activated upon depolarization from hyperpolarized potentials, and then quickly decays Although I_{to} is carried mainly by potassium ions, the channel may also be permeable to sodium (Nakayama and Irisawa, 1985). However, Kokubun et al (1982) did not record I_{to} in multicellular specimens at physiologic potentials

Therefore the exact contribution of this current to AV nodal physiology is not known.

2.1.2.3-The hyperpolarization activated current (I_f)

Hyperpolarization of the SA node induces a gradually increasing inward current. This current has been referred to as hyperpolarization activated current or I_f (Brown et al, 1979; Noma et al, 1980b, Yanagihara and Irisawa, 1980) Kokubun et al (1982) found I_f in small specimens of the AV node, and later Nakayama et al (1984) demonstrated its presence in cells isolated from the rabbit AV node. The properties of the current were similar to those of I_f in the SA node Since I_f is inactivated at the normal resting potential of the AV node, the exact contribution of this current in the AV nodal physiology is not known

2.1.3-Passive electrical properties of the AV node

In order to understand passive properties it is useful to think of the cardiac membrane as an electrical analogue containing resistors and capacitors (Arnsdorf, 1984) (Figure 1.2A) The resistance of the cardiac membrane to the flow of ions and charged species is provided by its finite structure (the thin lipid bilayer). This structure is able to store charges of opposite sign on its two sides (capacitor) The internal resistance of the cardiac fiber per unit length is r_i, and r_m is the membrane resistance over the same length, while the capacity of the fiber per unit length is c_m. These electrical constants can be measured by the analyzing the changes in membrane potential produced by a square

wave pulses of current. The decrement of the injected current that occurs along the length of an cardiac fiber depends upon the values of r_m and r_i, and the ratio between these factors determines the longitudinal spread of current. The steady-state voltage falls exponentially with distance from the point of current injection (Figure 1.2B), and can be expressed mathematically as: $V_x = V_0 e^{-x/lambda}$ in which lambda is the space constant.

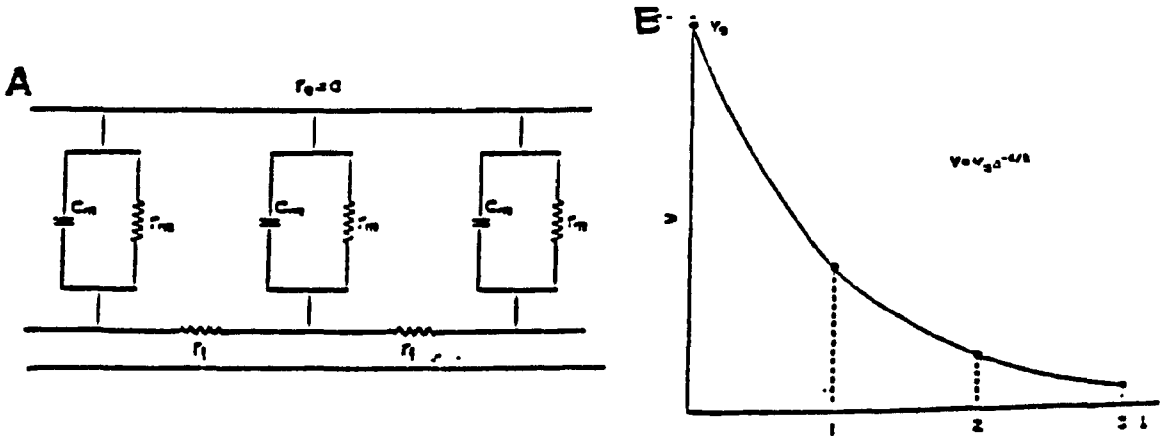

Figure 1.2A: Equivalent electrical circuit for the passive properties of a cardiac fiber. C_m: Capacity of fiber per unit length; r_m: Membrane resistance; r_i: The internal resistance; r_o: external resistance.

Figure 1.2B: Electrotonic decay with distance in an infinitely long cable-like fiber. Ordinate: transmembrane potential; Abscissa. distance in terms of the space constant.

In the AV node r_i is much larger than in Purkinje fibers and ventricular muscle, and r_m is smaller (De Mello, 1977; Nishimura et al, 1988). Consequently, the space constant in the AV node is shorter than in Purkinje fibers and ventricular muscle, tending to cause slow conduction. De Mello (1977) calculated the space constant of the AV node fiber to be about 0.43 mm and Kokubun et al (1982) reported a value of 0 69 mm (1/3-1/2 that of other myocardial fibers).

3- MACROSCOPIC AV NODE ELECTROPHYSIOLOGY

3 1-The P-R interval

The P-R interval on the surface electrocardiogram (ECG) represent the time taken for the impulse to pass from the atria to ventricles. This interval represents the time required for the propagation of the impulse through the atria, AV node, AV bundle, and bundle branches (Figure 1.3A).

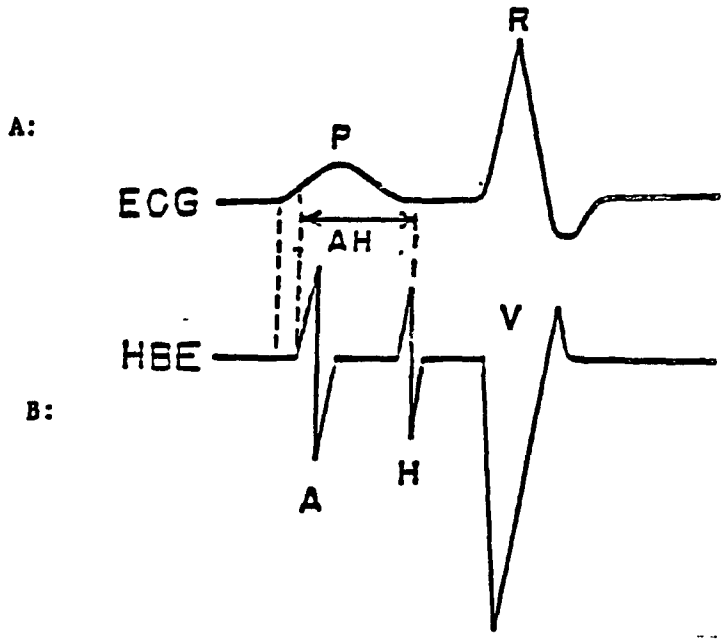

Figure 1.3· An example of a simultaneous ECG and His bundle electrogram (HBE) showing P-R and A-H intervals.

Only a fraction of the normal P-R interval represents the passage of excitation through the AV node. The AV node conduction time can be more closely estimated using an intracardiac electrogram (Scherlag et al, 1969). A bipolar catheter electrode is introduced into the right atrium and positioned across the tricuspid valve. The resulting electrogram includes a sharp deflection (H, Figure 1 3B) that represents His bundle activation The time taken from atrial depolarization (A) to the

His electrogram (H) (refered as the AH interval) represents AV conduction time.

Although the AH interval is the best available measurement of the AV node conduction time, the P-R interval still is a clinically useful index of AV conduction time. The intra-atrial conduction time (P A interval), and infranodal conduction time (H-V interval) are normally 20 to 50 and 35 to 55 msec in the adult human heart respectively (Ross and Mandel, 1987) These intervals are not significantly affected by the autonomic nervous system or by other physiological interventions. The P-R interval in the normal adult human heart is 120 to 200 msec, and the A-H interval is 50 to 120 msec (Ross and Mandel, 1987) The A H interval is highly dependent on heart rate and on the state of the autonomic nervous system.

3 2-The site of conduction delay

There is some disagreement regarding the contribution of different zones of the AV node in determining the AV nodal conduction delay. Hoffman et al (1968) showed that premature AV nodal stimulation causes a delay in the proximal AV node Billette et al (1976) found that a delay in conduction through AN cells accounts for a large fraction of the total nodal delay during pacing at a slow rate In another study James (1976) perfused ethylenediaminetetraacetic acid (EDTA) into the AV node artery of the dog to map the site of delay. He concluded that the cells at the junction of the AV node and His bundle are the site of delay in AV conduction. The most complete study of the contribution of different zones to AV nodal conduction delay was performed recently by Billette

(1987). He showed that 25% of the conduction delay upon premature stimulation takes place in proximal cells of the node (AN, ANCO, ANL, and N cells), and the majority of the AV nodal delay takes place between the N and NH zones.

3.3- The cause of AV nodal conduction delay

Hoffman et al (1959) estimated the speed of conduction in the AV node to be 0.05-0.02 m/sec, much less than in the ventricles (0.4 m/sec), atria (0.8-1 m/sec), and Purkinje fibers (4 m/sec). Lewis and Master (1925) proposed that the slow conduction in the AV node is due to a longer refractory period of the node compared to that of atrial or Purkinje fibers. Krayer et al (1951) proposed a synaptic type of transmission to explain AV nodal delay. Later Hoffman et al (1958), and Hoffman and Cranefield (1959, 1960) performed studies on rabbit and dog hearts and concluded that the AV delay is due to slow conduction rather than to refractoriness of nodal tissue or to delay due to chemical transmission.

In addition to slow conduction (uniform propagation at a low velocity) as a basic mechanism for the conduction delay in the AV node, Hoffman also proposed that conduction is decremental (Hoffman et al,1959, Hoffman and Cranefield,1960; Hoffman et al, 1958). Decremental conduction occurs when a normal action potential enters a region of the myocardium in which changes in the properties of the fiber ahead of the action potential diminish the efficiency of the action potential as a stimulus. Changes in fiber diameter, threshold potential, and cable properties can result in decremental conduction. Another mechanism for

AV node conduction delay could involve the electrotonic spread of an impulse across an inexcitable gap (Mendez and Moe, 1966, Billette et al, 1976). Hoffman et al (1959) considered this possibility, but judged it to be unlikely. The mapping studies done by Billette et al (1976) and Billette (1987) provided evidence that an inexcitable gap is located between N cells and NH cells. With increasing premature stimulation, action potentials in the N zone dissociate progressively into two components, that are synchronous with action potentials recorded proximal and distal to the N zone respectively (Billette et al, 1976 Billette 1987). The fact that no action potentials could be recorded during the interval between these two components suggests that the proximal impulse is unable to cross this area, but electrotonic current spread brings distal excitable cells to threshold. The longer the duration of the stagnation the longer the delay, until block occurs (Billette 1987)

3.4- Refractory period of the AV node

The inability of a tissue to be re-excited immediately after an action potential is called refractoriness, and the period during which excitability is reduced is called the refractory period As it shown in Figure 1 4, the effective refractory period (ERP), during which stimuli of any strength are unable to initiate a propagated action potential, is followed by the relative refractory period (RRP), during which only stimuli greater than those which normally reach threshold can cause a propagated action potential. Refractory periods of the AV conduction system can be determined by the atrial extrastimulus technique (Ur et al, 1970, Denes et al, 1974) With this technique, an atrial extra

stimulus (A_2) is applied at decreasing coupling intervals after a series of sinus or atrial driven beats (A_1) (Figure 1.5A). In a plot of A_2-H_2 (conduction time of premature beat) vs A_1-A_2 (coupling interval) (Figure 1.5B), AV nodal RRP is the longest A_1-A_2 producing prolongation of A_2-H_2 relative to A_1-H_1, and AVERP is the longest A_1-A_2 where A_2 is not followed by an H_2. In a plot of H_1-H_2 (output interval) vs A_1-A_2 (input interval) (Figure 1.5C), AV nodal FRP is the shortest attainable H_1-H_2 interval

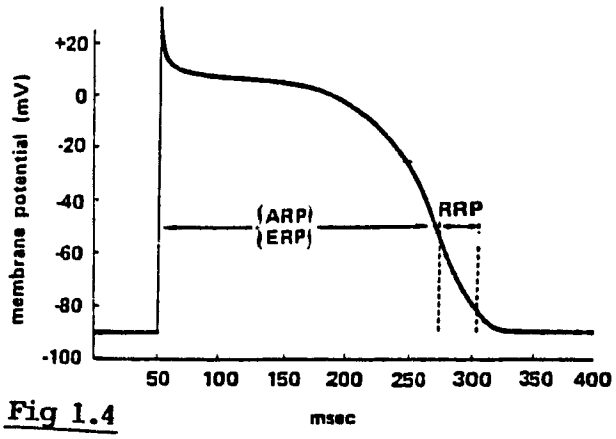

Fig 1.4

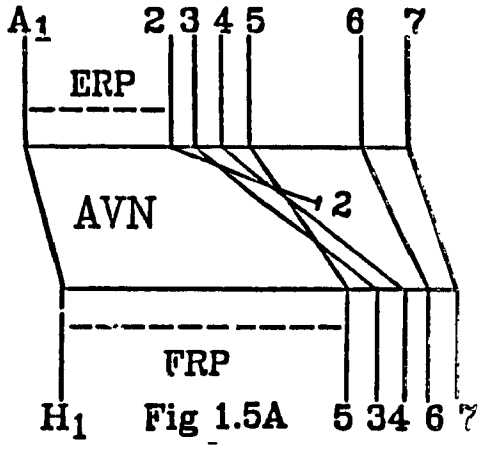

Fig 1.5A

Figure 1.4: Schematic drawing of the relationship between transmembrane potential from a single cardiac fiber and excitability of that fiber to stimulation (modified from Hoffman and Cranefield, 1960)

Figure 1.5A. A diagram of the extrastimulus technique shows the last of a series of 20 basic (A_1) and one premature beat at different coupling intervals (2-7)

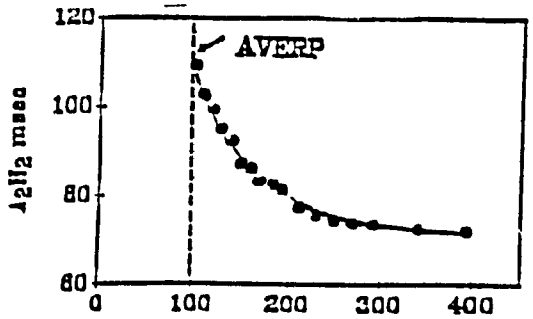

Fig 1.5B A_1A_2 (msec)

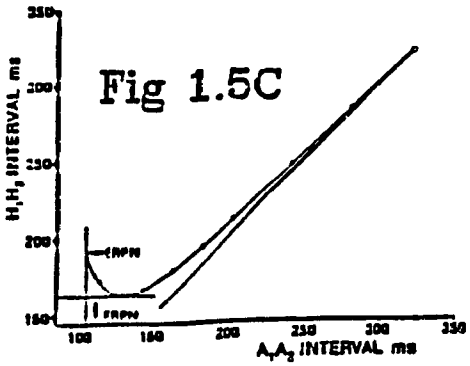

Figure 1.5B: Diagrammatic representation of A_1A_2-A_2H_2 curve showing effective refractory period of the AV node.

Figure 1.5C: Diagrammatic representation of A_1A_2-H_1H_2 curve showing functional refractory period of the AV node

Billette (1987) used simultaneous intracellular recording of different zones in the AV node to demonstrate that the ERP and FRP were related to the minimum intervals between successive upstrokes at the node entrance (AN and ANCO cells) and outlet (NH cells) respectively.

The validity of the AVFRP as an index of AV nodal refractoriness has been debated. Ferrier and Dresel (1974), and Simson et al (1979) showed that the AVFRP and AVERP are inversely related, and suggested that AVERP is an indicator of nodal conduction. Recently Billette and Metayer (1989), by studing the rate-induced changes of AVFRP and taking into consideration the effects of facilitation and fatigue on AVERP, suggested that AVFRP is related to nodal refractoriness. AVFRP is also a useful measure of the maximum ventricular rate that can occur during rapid atrial rhythms such as atrial fibrillation (Magalev et al, 1987, Billette et al, 1974; Billette et al, 1975). The effective refractory period on the other hand is a useful measurement to evaluate the effects of antiarrhythmic drugs on the AV node. Most antiarrhythmic drugs suppress various supraventricular tachyarrhythmias by prolongation of AVERP (eg. calcium channel blockers, and beta blockers).

3.5- Concealed conduction

Lewis and Master (1925) first noted that the AV nodal conduction time of propagated impulses during 2:1 response (two atrial and one ventricular response) is longer than during 1:1 conduction with the same RR interval. Incomplete penetration of an atrial impulse into the AV node may block or delay the passage of a subsequent atrial impulse. This phenomenon was later termed "concealed conduction" by Langendorf

(1948) and defined as the effect of blocked impulses on the formation and conduction of subsequent impulses. Hoffman et al (1961) showed that concealed conduction can take place in any part of the conduction system. Later, Moe et al (1964) characterized this phenomenon and showed that concealment is regularly demonstrable after thoracic sympathectomy and during vagal stimulation. Concealed conduction is determined by a "zone of concealment" (Moe et al, 1964) during which an impulse can excite the atrium and penetrate into the AV node, but blocks somewhere within the node because of AV node refractoriness.

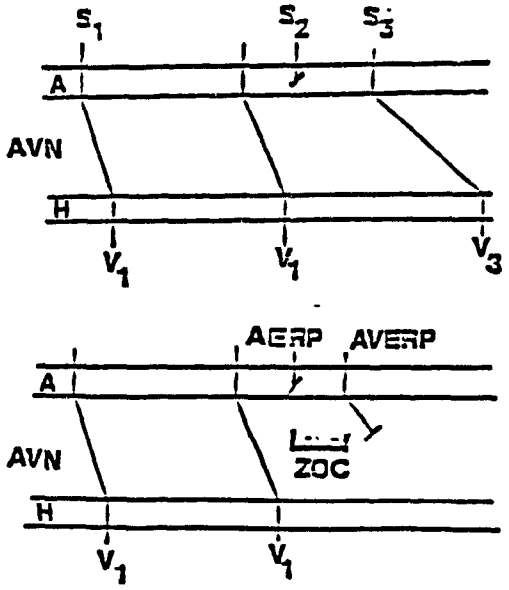

Top: A, AVN, H, and V, respectively, represent atrium, AV node, His bundle, and ventricle V_1, V_3 are ventricular responses to the driving stimuli of S_1, and S_3 respectively. S_2 is the blocked premature stimulus.

Bottom: S_3 is blocked within the AV node. Shaded area represents the zone of concealment "ZOC" which is the interval between AVERP and AERP

Figure 1.6

Since penetration into the AV node has occurred, the concealed impulse leaves the node partially refractory despite not having propagated to the ventricles. The duration of the zone of concealment (ZOC) is determined by the difference between atrial effective refractory period (AERP) and AV node effective refractory period (AVERP) (Figure 1.6). The ZOC can be increased by interventions that increase AV node refractoriness, such as vagal stimulation (Moe et al, 1964) and calcium

channel blockers (Talajic et al, 1989) The timing of the blocked atrial beat in the ZOC determines the conduction of a subsequent conducted beat (Moe et al, 1964). Concealed conduction within the AV node is one of the major determinants of the ventricular response during atrial fibrillation (Langendorf, 1948; Langendorf et al, 1965, Moore, 196)

4 FREQUENCY-DEPENDENT PROPERTIES OF AV NODE

Changes in driving rate have no significant effect on conduction in the atrium, Purkinje fibers, and ventricular muscle until phase 3 block occurs (Hoffman and Cranefield, 1960; Merideth et al, 1968, Talajic and Nattel, 1986). In fact, Ferrier and Dreifus (1973) demonstrated a period of supernormal conductivity in both the interatrial septum and the ventricles prior to conduction block In the AV node, however, as the rate increases, the conduction time increases until AV block occurs (Mobitz, 1924; Lewis and Master, 1925) As long as the interval between two consecutive atrial impulses is longer than the time required for full recovery of AV nodal excitability there are no major changes in AV conduction time As the rate increases, impulses enter the AV node at relatively earlier points in the refractory period, thereby increasing the AV conduction time Denes et al (1974) reported a statistically significant correlation between AV conduction time (AH interval) and AV node effective refractory period (AVERP) in man. They found that as the AVERP got longer as a result of increases in rate, the AV conduction time lengthened Rate dependent increases in AV conduction time and refractoriness constitute one of the important properties of the AV node in protecting the ventricles from

rapid rhythms such as atrial fibrillation. Rate-dependent conduction properties of the AV node determine the occurrence and/or manifestations of supraventricular arrhythmias.

4.1-Patterns of response of the AV node to rate change

4.1.1- Response of AV node conduction time to single premature atrial stimuli

Mobitz (1924) and shortly thereafter Lewis and Master (1925) reported that conduction time of single atrial extrastimuli was inversely and nonlinearly related to the elapsed time from the preceding ventricular activation. They found that P-R interval increases with increasing prematurity of the propagated atrial impulse. They related this phenomenon to the phase of nodal recovery in which atrial impulses penetrate the node. The curve relating the conduction time of the premature impulse (measured as P2R2, A2V2, or A2H2) to the coupling test interval (R1P2, V1A2, H1A2, or A1A2) is called the AV node recovery curve or refractory curve (Figure 1.7).

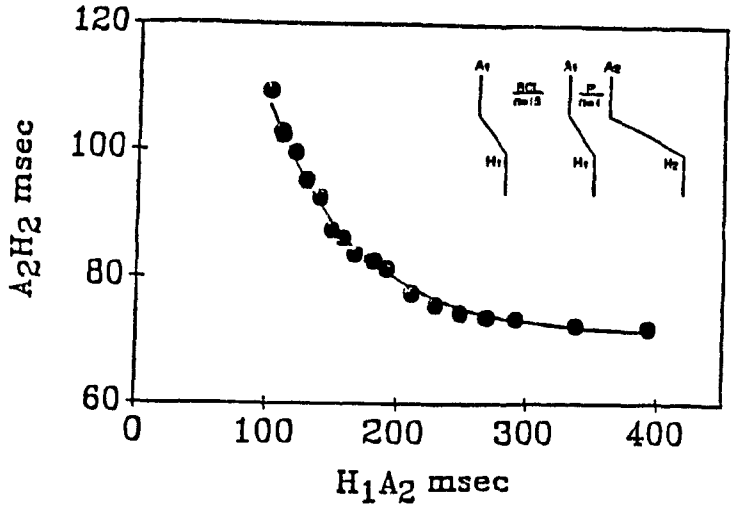

Figure 1.7: Diagrammatic representation of A_2H_2, H_1A_2 curve.

Wit et al (1970) and Damato et al (1969) studied the same relationship in man and found that the response of the AV node to single premature atrial impulses was similar to the one described for animals. The response of AV conduction time to single premature atrial impulses is frequently used in clinical electrophysiology to study nodal refractoriness

4.1.2-Response of AV conduction time to increased rate

4.1.2.1- Incremental pacing (ramp changes in heart rate)

Loeb et al (1985) studied the beat-to-beat changes of AV conduction during ramp changes in heart rate in autonomically decentralized dogs. They found that linearly increased heart rate resulted in an increase in AV conduction time which was parallel to the rising phase of heart rate. The response of AV conduction time to linearly decreased heart rate was not symmetric, showing a hysteresis phenomenon (Figure 1.8). Moreover, they found that as the rate of change of heart rate increased the loop of 1:1 conduction happened at a higher level of heart rate (Figure 1.9). They concluded that changes in AV conduction are dependent not only on the number of atrial impulses per unit time but also on the rate of change of atrial impulses per unit time

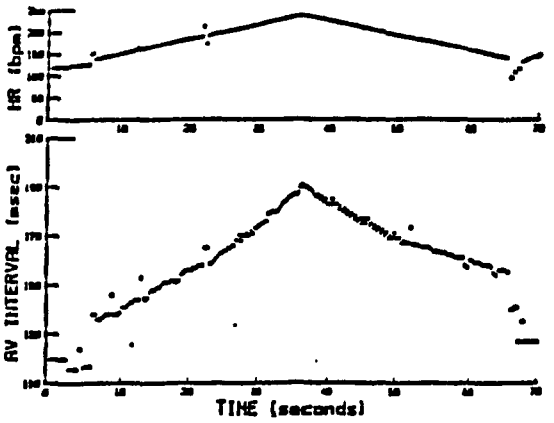

Figure 1.8. Effect of linear heart rate increment and linear heart rate decrement on AV interval. Upper curve reflects heart rate plotted vs. time and lower curve represents AV interval plotted vs time (taken from Loeb et al, 1985)

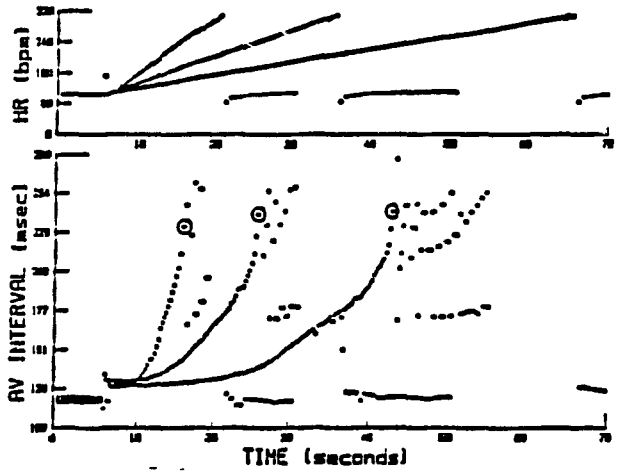

Figure 1.9 Relationship between the rate of changes of heart rate and the loss of 1:1 conduction. Upper graph shows linear heart rate ramps of 200 beats/min above control rate. Lower graph shows associated AV intervals (taken from Loeb et al, 1985)

4 1 2 2-Response to single-step and multiple step increments in heart rate

AV nodal response to a sudden or multiple step increases in heart rate is generally characterized by progressive prolongation of AV node conduction time for a variable number of beats until a new steady state value is achieved. This phenomenon has been called AV accommodation (Loeb et al, 1987) Lewis and Master (1925) and Meredith et al (1968)

examined the response of AV conduction time to multiple-step increments in heart rate and found that as the rate increased the AV conduction time increased in a cumulative manner. The same kind of nodal response was shown by Loeb et al (1987), and Billette et al (1986), they found that the intrinsic response of the AV node to heart rates changes was not only dependent on the absolute level of heart rate, but also on the potential cumulative effects of earlier heart rate Figure 1 10 shows an example of this kind of nodal response.

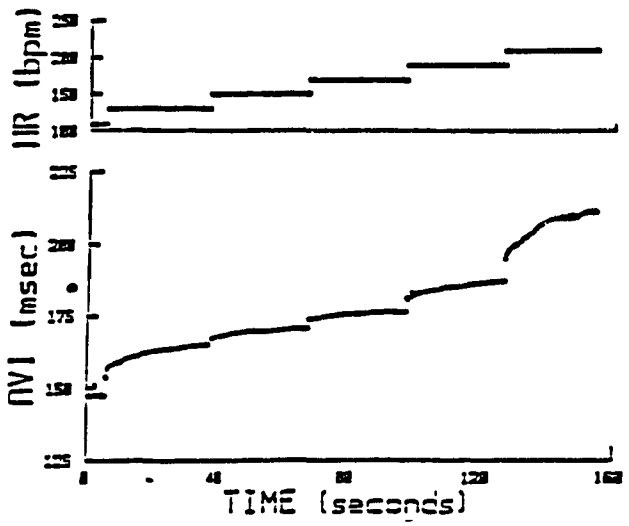

Figure 1.10: An example of multiple-step increments in heart rate Top panel, heart rate (beat/min); bottom panel, AV interval vs time (taken from loeb et al, 1987)

These data indicate that stepwise increments in heart rate of identical magnitude are associated with different degrees of AV prolongation This cumulative effect is more pronounced at a higher heart rate The response of AV conduction time to the single step change in heart rate is different from the one which resulted from multi-step or stepwise changes in heart rate in terms of the time course of the changes in AV conduction time. The response of AV node conduction to sudden changes (single step) in heart rate commonly happens at the onset of

supraventricular tachycardia when the heart rate abruptly changes from the sinus rhythm to a very fast heart rate.

Two kinds of approaches have been used to study the response of the AV node to a sudden change in heart rate. In the first approach, the heart rate is changed from a slow heart rate to a fast rate with a constant interstimulus interval. Loeb et al (1987) used this approach and found that there was a time dependent prolongation in the AV conduction time until a new steady state was achieved. A very fast heart rate resulted in a gradual conduction slowing followed by the loss of 1 1 conduction. Lehmann et al (1984) studied the patterns of the human AV nodal response to a sudden increase in atrial rate Depending on the interval between the last beat (S1) at the slow rate (S1S1) and the first beat (S2) of the fast rate (S2S2), S1S2, three potential patterns of nodal response were observed. These consisted of "crescendo" accommodation, which was characterized by a gradual increase in AV conduction time until steady state was achieved, an "instantaneous pattern", in which AV conduction time reached its steady state within one beat, and "decrescendo" accommodation, in which the response of the AV node was characterized by a sudden initial increase in AV conduction time which was longer than the eventual steady state, andthen progressively decreased to attain the steady state value.

The second approach involves the response of AV conduction time to sudden changes in rate with a constant VA or HA interval Clinically this kind of sudden change in heart rate occurs during reentrant tachycardias associated with the Wolff-Parkinson-White syndrome (Durrer et al, 1970, Gallagher et al, 1975). During such tachycardias the bypass pathway (VA) interval has little variation in conduction time (Gallagher

et al, 1975, Narula, 1972), whereas the AV interval initially increases to a maximum value and then oscillates over several beats until it reaches a new steady state.

4.1 3-Patterns of AV block

In addition to the different patterns of nodal response to the rate changes described above, the response of the AV node to a very fast heart rate may be manifested as different degrees of AV block.

First-degree AV block is manifested electrocardiographically as a prolongation of the P-R interval. The P-R interval consists of three components: PA, intra-atrial conduction time, AH interval, the AV nodal conduction time, and the HV interval, conduction time through the His-Purkinje system. Although first-degree AV block can be due to slowing anywhere in the conducting system (Narula et al, 1971), it has been shown that it tends to be due to slowing in the AV node (Narula, 1979).

Second-degree AV block is characterized by the failure of one but not all, atrial impulses to traverse the AV node. Therefore, the ratio between atrial impulses and ventricular responses is greater than one. If every other atrial impulse is blocked, the resulting abnormality is called 2:1 AV block (Katz and Pick, 1956). In 4 3 AV block every fourth P wave is not followed by a QRS complex. A feature of some cases of second-degree AV block is the Wenckebach Phenomenon, which normally occurs during a fast atrial rate. The electrocardiographic manifestation of this phenomenon is a progressive prolongation of the P-P interval (AV conduction time) leading ultimately to a dropped beat (Wenckebach, 1899).

4 2-What are the properties of the AV node determining rate- induced changes in AV nodal conduction?

In the previous section different patterns of AVCT to different stimulation protocols was described. Three factors have been identified which contribute to rate-induced changes in AVCT AV nodal recovery, fatigue, and facilitation

4 2 1-AV nodal recovery

The major determinant of the nodal respons to alterations in input rate comes from the slow recovery of AV node conduction after activation, and is most simply demonstrated in the conduction of a single premature beat (section 4 1.1, and Figure 1.7 in this section) Two kinds of approaches have been used to construct AV recovery curves Lewis and Master (1925), Levy et al (1974), and Billette (1976) analyzed AV node recovery plotting conduction time of the test impulse (PR or AV or AH) versus corresponding ventriculo-atrial (RP or VA) or His atrial (HA) intervals On the other hand, Meredith et al (1967), Simon et al (1978), and Ferrier and Dresel (1974) used preceding atrial (A_1A_2) intervals as an index of recovery time. There are data to support either approach Both approaches suggest that as the heart rate increases the atrial impulse progressively encounters the steep portion of the AV recovery curve and as a result AV conduction increases until AV refractoriness is encountered

4.2.2-Fatigue

The cumulative effects of rapid AV nodal stimulation result in progressive lengthening of AV conduction time to a new steady state, a process called fatigue by Lewis and Master (1925), Levy and Lester (1925), Meredith et al (1968), and Ferrier and Moe et al (1973) demonstrated this phenomenon by showing that the AV conduction time of beats elicited after a pause increased as the basic cycle length of stimulation decreased, implying that this effect could be dissociated from incomplete recovery. Fatigue results in an upward shift of the AV recovery curve constructed at the fast heart rate compared to the one at the slow heart rate (Billette et al, 1988). Narula and Bungo et al and Lehmann et al (1984) found that in response to sudden and sustained increases in atrial rate there is a progressive lengthening of AV conduction time to a new steady state. Jenkins and Belardinelli et al (1988) showed in isolated guinea pig hearts that during sustained fast atrial pacing, after an initial prolongation in AV conduction time that occurs with the first beat at the new rate, there is a time dependent phase of AV prolongation which takes 20-30 second to reach a new steady state. The functional characteristics of rate-induced fatigue have been recently studied by Billette et al (1988) in the isolated rabbit AV node. They found that the onset and dissipation of the fatigue follow a monoexponential time course.

4.2.3-Facilitation

Lewis and Master (1925) first noted that the second beat of a fast train of stimulation, despite having the same RP interval, had a faster conduction than the first beat. This property, termed facilitation, has been studied in detail by Billette (1981) and Billette et al (1986, 1988, 1989). This property describes the facilitatory effect of closely coupled atrial impulses on the conduction of a subsequent impulse, and reaches its maximum value after one beat of the fast rate. In vitro data (Billette, 1987) shows that premature AV nodal action potentials can have a decreased duration, possibly providing a cellular basis for facilitation.

4.3-Underlying cellular mechanisms of the rate-dependent properties of the AV node

Microelectrode studies in isolated cardiac tissues have demonstrated that the action potential durations and refractory periods of atrial muscle, ventricular muscle, and His-Purkinje cells shorten as the cycle length decreases (Hoffman and Cranefield, 1960). In the AV node, since the recovery of excitability exceeds beyond full repolarization, the duration of the AV node action potential is not the most important determinant of the refractory period. Therefore, as rate increases the AVERP fails to shorten (Denes et al, 1974; Gagin et al, 1973). In cardiac muscle cells and His-Purkinje fibers, electrical excitability is completely restored when repolarization is completed (Hoffman and Cranefield, 1960). In contrast, in the AV node excitability lags beyond

full repolarization and the tissue can remain relatively refractory for a significant period after the termination of the action potential (Merideth et al, 1968). This contributes importantly by the frequency dependence of AV conduction velocity and refractoriness. Since excitability is one of the determinants of conduction velocity (Cranefield, 1977), changes in excitability would have a profound effect on the conduction velocity. Merideth et al (1968) found that at higher driving rates, the gap between complete repolarization and recovery of excitability increases further. This has a profound effect on AV conduction time and refractoriness.

As explained in section (3.3) the aditional conduction delay during premature AV nodal stimulation may be due to electrotonic propagation in the N-NH region. The source current in the N region is the slow calcium inward current, and the recovery of this current is one of the determinants of the delay (Billette et al 1976, and 1987). Slow inward current I_{si} activates upon depolarization and then inactivates during the action potential. Therefore, time is required after each action potential for the recovery of calcium inward current from inactivation. If an atrial impulse arrives in the AV node at a time when the calcium inward current (I_{sj}) has not fully recovered from inactivation there is less inward current available, and as a result the conduction is slowed. The time constant of the AV nodal recovery curve (60-80 msec) (Talajic and Nattel, 1986) is in the same range as the time constant of recovery of L-type calcium currents in isolated canine cardiac Purkinje cells (Hirano et al, 1989) and for slow inward current in multicellular preparations (McDonald, 1982). It is quite likely that the time dependent recovery of AV nodal conduction is related to the recovery of

L-type calcium channels from their inactivation during the preceding action potential. It has been shown that the recovery of calcium current can be further delayed by calcium channel blockers (Uehara and Hume, 1985). In vivo studies have also shown that these drugs slow AV node recovery by adding a component related to recovery of drug-associated channels (Talajic and Nattel, 1986).

5-INNERVATION OF THE AV NODE

The atrioventricular nodal region is richly innervated by both sympathetic and parasympathetic systems (Randall and Armour, 1977) While sympathetic discharges tend to accelerate AV nodal conduction, parasympathetic discharges impede AV conduction (Hamlin and Smith, 1968, Randall and Armour, 1977; Levy, 1971). In the physiologic situation the interaction of these two effects is not algebraically additive (Levy, 1971). While changes in autonomic tone directly alter AV nodal conduction, alteration in sinus rate induced by changes in autonomic tone also affect nodal conduction. Thus, changes in AV nodal conduction can result from either direct effects or altered sinus rate This is discussed in more detail in section 6.2.4.

5.1- Parasympathetic control of the AV node.

5.1.1-Vagal innervation of the AV node.

Efferent vagal activity in the intact animal can occur as discrete bursts in the cardiac cycle (Jewett, 1964) It has been shown that continuous supramaximal trains of left vagus stimulation prolong AV conduction time after a latency of less than one second, while right

vagus stimulation has relatively lesser effects (Cohen, 1912, Cohen and Lewis, 1913, Irisawa et al, 1971; Hageman et al,1975) However, Hamlin and Smith (1968) and Spear and Moore (1973) stimulated both right and left vagi with submaximal stimulation and found no difference in AV conduction slowing. In these studies constant stimulation parameters were not used, and the influences of the changes in heart rate evoked by vagal stimulation were not taken into account In a more carefully controlled anatomical and functional study by Ardell and Randall (1986) it was shown that in spite of anatomically distinct vagal pathways for control of SA node and AV node, supramaximal stimulation of left and right vagi had parallel negative dromotropic effects on AV node

5.1.2- Phase-dependent effects of vagal stimulation.

Spontaneous efferent vagal activity to the heart is manifested by brief bursts of impulses that are synchronized with each cardiac cycle (Jewett, 1964, Katona et al, 1970, Kunze, 1972) This means that the timing of a single vagal stimulus (Brown and Eccles, 1934) or brief bursts of impulses (Levy et al, 1969) relative to the phase of the cardiac cycle is an important determinant of the response This phenomenon generally is refered to as "phasic effects of vagal discharge" The phasic effects of vagal nerve stimulation on the SA node and heart rate have been extensively studied by numerous investigators (Katona et al 1969, Dong and Reiyz, 1970, Levy et al, 1972, Spear and Moore, 1973, Levy et al, 1978; Jalife and Moe, 1979, Spear et al 1979, Sasyniuk et al, 1984). A common finding in these studies is the effect of the time the vagal stimulus was delivered at progressively [illegible]

cardiac cycle, the sinus cycle length (P-P interval) continued to increase until a maximum prolongation of the P-P interval was obtained when the vagal stimulation was placed near the end of the sinus cycle

In contrast, the situation in the AV node is more complex than the SA node because of the concomitant effects of vagal stimulation on sinus cycle length, which decreases the input rate to the AV node and tends to improve conduction (Levy et al 1970, Spear and Moore, 1973, Martin, 1977a, Martin, 1977b), and the direct depressant effect of vagal stimulation on the AV node. The detailed investigations of Mazgalev et al (1986a and 1986b) overcome the difficulties posed by these interactions, and they showed that a brief postganglionic burst of stimuli causes a transient membrane hyperpolarization lasting about 300 msec Therefore the membrane voltage level at the time of arrival of the atrial beat in the central portion of the AV node may vary depending on the time of the vagal discharges which has significant effects on the conduction of the atrial impulse

5.1 3-Cellular effects of cholinergic stimulation on the AV node

Cranefield et al (1959) found that the application of ACh slowed depolarization, decreased action potential amplitude, and caused notching in the upstroke of the action potential at the atrial margin of the AV node They did not record simultaneously from different zones of the AV node, and thought that the effects of ACh were limited to cells in the atrial margin of the node. Vincenzi and West (1963) and West and Foda (1967) used field stimulation to show that the release of ACh from nerve endings abolished action potentials from the N region AN action potentials showed a decrease in duration, amplitude and hyper-

polarization, but they were not abolished Using similar techniques, Mazgalev et al (1986a, 1986b) found that postganglionic vagal stimulation hyperpolarized cells located in the N zone A. a result, atrial activation results in either no action potential in the N one or an action potential with a slower rate of rise, smaller amplitude and duration, and depressed conduction (Mazgalev et al 1986a) On the other hand, changes in the AN, and NH regions of the node were negligible

5 1 4-Rate-dependent effects of vagal nerve stimulation on the AV node

Wallick et al (1982) noted significant interaction between cardiac frequency and vagal effects on the AV conduction time This implies that the intrinsic rate-dependent properties of the AV node can be influenced by vagal stimulation

5 1 5- Cellular mechanisms underlying ACh-induced conduction slowing in the AV node

Since the phase zero of the action potential in the AV node is dependent on the Ca^{++} inward current (Zipes and Mendez, 1973 Nomura et al 1980a), inhibition of Ca^{++} influx would be expected to slow conduction Nishimura et al (1988) found that ACh only slightly reduced I_{Ca} On the other hand, they found that ACh strongly increased the outward current, thus decreasing the net phase zero inward current and slowing AV nodal conduction. Therefore, the effects of ACh on AV node conduction could be considered in terms of ACh effects on both K^+ and Ca^{++} currents

5.1.5.1-Effects of ACh on potassium current

Burgen and Terroux (1953) found that ACh increased gK^+. Shortly thereafter this was confirmed in a radiotracer study in which the rate of atrial uptake of $^{42}K^+$ was found to be increased by ACh (Rayner and Weatherall, 1959). Noma and Trautwein (1978) showed that the reversal potential of the ACh-activated outward current in the rabbit SA node was dependent on extracellular potassium. Since the current-voltage relation of ACh-increased gK^+ was similar to the one described for the I_{K1} (inward rectifier), it was suggested that ACh increases gK^+ through existing inwardly rectifying potassium channels (Garnier et al, 1978). However, the validity of this suggestion was questioned by Noma and Trautwein (1978), who found that ACh-activated current exhibits time dependence, in contrast to I_{K1}, which depens only on voltage at physiologic potentials. Subsequent voltage clamp studies showed that ACh increased gK^+ (Shibata and Giles, 1984; Nishimura et al, 1988) in preparations where no I_{K1} could be found. The Ach-sensitive outward K^+ current has been named I_{ACh}.

5.1.5.2-Effects of ACh on passive electrical properties of AV node.

Although ACh-induced AV nodal conduction slowing appears to be due predominately to effects of ACh on gK, the passive electrical properties of the AV node should be taken into account to understand the mechanisms responsible for the effects of ACh on AV node conduction. Nishimura et al (1988) found that the passive electrical properties of AV node tissue were changed as a result of the ACh activated $I_{K.ACh}$ current. By

increasing the resting membrane conductance, ACh reduced the membrane resistance As a result of decreases in the membrane resistance ACh shortened the space constant. The longitudinal resistance in the AV node is higher than in other cardiac tissue, implying that fewer gap junctions are present in the AV node (Defelice and Challice, 1969, Weidmann, 1952). This contributes to the slow conduction through the AV node, which can be further slowed by ACh-increased longitudinal resistance and -decreased space constant These effects, along with the effects of ACh on membrane currents, may explain the negative dromotropic actions of ACh on the AV node.

5 1.5 3-Effects of ACh on calcium current

Another mechanism by which ACh depresses AV node conduction is by depressing slow inward current I_{si} In 1973 Prolope al et al suggested that ACh has the same effects on the action potential as those of manganese (a Ca^{++} channel blocker) This suggestion has been confirmed by voltage clamp experiments in which ACh depressed I_{si} in bullfrog atrial strips (Giles and Noble, 1976) and mammalian atrial trabeculae (Hartfield et al, 1976) However, this effect of ACh varies greatly as a function of species, cardiac cell type, and concentration of ACh Hartfield et al (1976) demonstrated that ACh reduced twitch tension by 30% The concluded that the negative inotropic effect of ACh was completely due to shortening of action potential duration, and consequent reduction in calcium entry during the plateau However, at higher concentrations of ACh (which reduced the twitch tension by 70-90% slow inward current was significantly reduced and even completely abolished [illegible]

1976). In a detailed study on the effects of ACh in the rabbit AV node by Nishimura et al (1988) it was shown that ACh at low concentrations reduced I_{si} by only 11%. From these results it can be concluded that low concentrations of ACh slow conduction in the AV node by increasing outward current and thereby reducing the net inward current. At higher concentrations of ACh, an additional direct effect to inhibit the slow inward current occurs.

5.1.6-Intracellular mechanisms underlying the effects of ACh on the membrane currents of the AV node.

Although the time course of ACh-activated K^+ channels suggest a multi-step process with intrinsic delays of 30-100 ms (Hill-Smith and Purves, 1978, Osterrieder et al, 1981), no second messenger system has been found to link muscarinic ACh receptor activation to the channel. Changes in cyclic nucleotide levels (cAMP and cGMP) neither mimic the effects of ACh on $^{42}K^+$ efflux (Nawrath, 1977, and Fleming et al 1981) nor modify the hyperpolarization of AV node cells by ACh (Trautwein et al, 1987). Pfaffinger et al (1985) found that intracellular guanosine 5'-triphosphate (GTP) was required for muscarinic stimulation of ACh induced $I_{K\ Ach}$. Furthermore, they showed that the inactivation of G protein by pertussis toxin (IAP) eliminated the ACh-induced $I_{K\ Ach}$. Logothetis et al (1987) showed that the beta and gamma subunits of G-proteins are involved in the ACh-induced-$I_{K\ Ach}$. These data suggest that muscarinic regulation of cardiac K^+ channels requires at least three components, the muscarinic ACh receptors, pertussis toxin-sensitive G proteins, and specific inward-rectifying K^+ channels.

(Soejima and Noma, 1984, Pfaffinger et al, 1985; Breitwieser and Sabo, 1985; Kurachi et al, 1986; Kurachi et al, 1986, , Logothetis et al, 1987). In contrast to the effects of ACh on potassium currents, cyclic AMP is involved in the regulation of I_{si} by ACh (Mirro et al 1980; Reuter, 1983). Biegon et al (1980) found that ACh decreased the formation of cAMP via an inhibitory G proteins G_i or N_i. Whether this is a result of an increase in c.GMP is doubtful. Recently it has been proposed that the muscarinic receptor-activated alpha subunit of G proteins might interact with other membrane enzymes or proteins to antagonize the activation of adenylate cyclase by beta adrenergic receptors, decreasing net calcium current (Breitwieser and Sabo, 1985).

5.2-Sympathetic control of the AV node

5.2.1-Effects of sympathetic stimulation and catecholamines

In contrast to the negative dromotropic effect of vagal nerve stimulation on the AV node, stimulation of the cardiac sympathetic nerves accelerates AV node conduction. In the pl[illegible] both heart rate and AV node conduction are modulated by [illegible] parasympathetic tone on a beat-to-beat basis (Warner et al 1986a, Warner et al, 1986b). Although in resting conscious dog[illegible] conduction is predominately modulated by changes in parasympathetic activity associated with the respiratory cycle (Warner et al 1986a), changes in arterial blood pressure result in sympathetically mediated alteration in AV node conduction (Warner and Loeb, 1986). [illegible] conducted in both man (Lister et al, 1967) and dog[illegible] (1987) have shown that although sympathetic stimulation [illegible]

rate, it decreases AV nodal conduction time. This shows that the direct effects of adrenergic stimulation on AV node conduction predominant over the effect of changes in heart rate. While the AH interval is significantly shortened by sympathetic stimulation, the HV interval is not altered (Priola, 1975; Spear and Moore, 1973).

Irisawa et al (1971) and Spear and Moore (1973) showed that in anesthetized dogs right stellate ganglion stimulation importantly shortens the R-R interval and slightly shortens the AV interval. In contrast, left stellate ganglion stimulation caused no obvious changes in the R-R interval, whereas it significantly reduced AV interval.

One of the most striking differences between the effects of vagal nerve stimulation and sympathetic stimulation on the AV node is the time course of these effects. Spear and Moore (1973) found that that the latency for the response to vagal stimulation was 0.165-0.230 second, whereas for stellate stimulation, the latency for acceleration of conduction was 1-1.5 minutes.

5.2 2-Electrophysiologic actions of beta-adrenergic stimulation on AV nodal cellular electrophysiology.

The positive dromotropic effect of either norepinephrine released from cardiac sympathetic nerves or of exogenously administered catecholamines is due to the interaction of these agents with postjunctional beta-adrenoreceptors. The most significant effect of catecholamines is to increase the rate of rise of phase zero depolarization and the action potential overshoot of AN and N cells without affecting resting membrane potential. This results in an acceleration in

conduction through the AV node (Hoffman and Singer, 196) The amplitude and rate of rise of the action potential of distal (NH) cell are not affected by catecholamines, but their diastolic phase (phase 4) accelerates which implies that pacemaker current responsible for phase depolarization is increased (TSE and Davis, 197)

The recovery of AV nodal cell excitability has not been studied in the presence of catecholamines, but in chicken ventricle the recovery of calcium-dependent action potentials from inactivation is accelerated by isoproterenol (Tsuji et al, 1985) The effects of slow channel blocker such as verapamil, which prolong the effective refractory period of AV nodal cells, can be reversed by catecholamines (Zipes and Fischer, 1974)

5.2.3-Cellular mechanisms underlying the effects of adrenergic stimulation on the AV node

5.2.3.1-Adrenergic receptors in the AV node

The effects of catecholamines are mediated by membrane bound adrenoreceptors There are two main types of adrenoreceptor alpha and beta, which have different pharmacological properties (Ahlquist 1967) These receptors have been further subdivided into $alpha_1$, $alpha_2$, $beta_1$ and $beta_2$ (Lands et al, 1967). The heart appears to contain predominantly $beta_1$ receptors (Manalan et al, 1981, Stiles et al 1983) whereas vasculature contains predominantly $beta_2$ receptors (Barnard et al, 1982) $Beta_1$ receptors mediate the positive inotropic and dromotropic effects of catecholamines on the heart, whereas $beta_2$ receptors mediate smooth-muscle relaxation However, in recent years it

become clear that $beta_2$ receptors functionally contribute to cardiac inotropic and chronotropic effects of catecholamines (Brown et al, 1986; Arnold et al, 1985; Strauss et al, 1986; Levine and Leenen, 1989).

Pharmacologic evidence suggests the presence of beta-adrenoceptors in the AV node Sympathetic effects on conduction can be blocked by beta-adrenoceptor blockers (Levy and Martin, 1979, Giudicelli and Lhoste, 1982) In a recent study Saito et al (1988) characterized beta-adrenoceptor subtypes in the AV node of the rat heart by quantitative autoradiography and estimated that the proportion of $beta_1$- and $beta_2$-adrenoceptors in the AV node were about 56% and 44% respectively However it is not known whether both subtypes of the beta-adrenoceptor mediate the dromotropic effects of catecholamines in the AV node

$Alpha_1$-receptors can increase the force of contraction of the myocardium (Watanabe et al, 1982, Homey and Graham, 1985) $alpha_2$-receptors are located on the presynaptic nerve terminal membrane and inhibit the release of norepinephrine from the terminal by a negative feedback mechanism (Watanabe et al, 1982, Homey and Graham, 1985) The existence of alpha- adrenoreceptors in the AV node has not yet been shown In a recent study Talajic et al (1990) showed that in anesthetized dogs phenylephrine, an $alpha_1$-adrenergic agonist had no effect on AV conduction time

c) 3.)-Modulation of calcium channels by catecholamines

Beta-adrenergic stimulation of the heart increases the slow inward current (I_{si}) This increase in I_{si} results in an elevation of the plateau of the action potential as well as a positive inotropic effect

(Reuter, 1983). Experiments conducted at the level of single cardiac cells using unitary channel recording suggest that the increase in amplitude of I_{si} by catecholamines occurs without any changes in the kinetics (steady state activation or inactivation) (Hess et al, 1986) Since the membrane resting potential in the AV node is more positive than in the Purkinje cells and ventricular myocytes, it is likely that the positive dromotropic effects of adrenergic neurotransmitters on the AV node are mediated through L-type calcium channels, rather than T-type channels which inactivate at more negative potentials (Hess et al, 1986). In fact, Tytgat et al (1988), and Hagiwara et al (1988) have shown that the T-type calcium channel is insensitive to isoproterenol Unitary channel recording has shown that beta-adrenergic stimulation increases the probability of the L-channel open state, and a dramatic decrease in the number of nulls (no detectable channel openings) in the recorded sweeps (Hess et al, 1986). As a result of these changes the amplitude of the whole cell calcium current will increase.

These effects are mediated by intracellular mediators such as cAMP, and can be abolished following patch excision in which both receptor and effector will be separated from intracellular mediators (Hess et al, 1986). Biochemical studies have demonstrated that activation of beta-adrenergic receptors stimulates the membrane-bound enzyme adenylate cyclase, an effect which is mediated by a stimulatory (G_s) guanine nucleotide-binding regulatory protein (Rodbell, 1980). Increases in adenylate cyclase activity catalyze the formation of cAMP from ATP cAMP then binds to the regulatory subunit of protein kinase. The released catalytic subunit of the enzyme (Cohen, 1982) then phosphorylates the calcium channel. This may result in an increse in the probabi-

lity that channels will be in the open state, or an increase in the number of calcium channels, either of which would increase calcium conductance (Reuter and Scholz, 1977).

6. ROLE OF THE AV NODE IN CARDIAC ARRHYTHMIAS.

6.1-Role of AV node in atrial fibrillation and flutter.

Very rapid activation of the atria occurs in two kinds of atrial arrhythmias: atrial fibrillation, in which the atria are activated irregularly at a very rapid rate (400-600 impulses/min), and atrial flutter, in which the atrial rate is in the range of 300/min and the rhythm is regular. In both cases the ventricular response to the atrial rhythm is not 1:1. Instead, 2:1 AV conduction is commonly seen in untreated atrial flutter, and the ventricular rhythm in atrial fibrillation is usually grossly irregular. The failure of the AV node to conduct all of the atrial impulses to the ventricles demonstrates the protective role of the AV node. Two important properties of the AV node determine the ventricular response to atrial impulses during atrial fibrillation, the AV node functional refractory period (AVFRP) and concealed AV nodal conduction resulting from intranodal impulse block (Langendorf et al, 1966, Moore, 1967, Mazgalev et al, 1982; Billette et al, 1974, Billette et al 1975)

6.2-Atrioventricular bypass tract (Wolff-Parkinson-White syndrome))

Preexcitation is defined as the activation of the ventricles by a supraventricular impulse earlier than would occur over the normal AV

conduction pathway (Gallagher et al, 1982). The most common type of preexcitation is the Wolf-Parkinson-White (WPW) syndrome, in which an accessory pathway (called a Kent bundle) connects the atrium and the ventricle. Therefore, an atrial impulse can activate the ventricles either via the AV node or via the accessory pathway. Patients with WPW are susceptible to several types of arrhythmias. One of these arrhythmias, called atrio-ventricular reentrant tachycardia or orthodromic circus movement tachycardia (CMT), is due to a macro-reentrant circuit involving the normal AV node, His bundle, bundle branches, ventricular muscle, the accessory pathway, and atria. During orthodromic CMT anterograde conduction occurs over the normal AV conduction system to the ventricle, and the impulse then passes retrograde over the Kent bundle to the atria and back through the normal AV conduction system to complete the circuit. Depending on the refractory period of the AV node or Kent bundle, an atrial impulse can either use the AV node or Kent bundle. Therefore, in this type of SVT the AV node can be used in anterograde or retrograde pathway and changes in the AV node refractory period and conduction play an important role in induction or termination of this type of tachycardia.

6.3-Paroxysmal supraventricular tachycardia (AV node reentry)

Paroxysmal supraventricular tachycardias (SVTs) are characterized by an atrial rate of 150 to 250 beats/min. The most common form of these tachycardias is AV nodal reentry (Akhtar, 1982). It has been postulated that in some individuals the AV node may be functionally or anatomically divided into two distinct pathways. The beta- or fast pathway has a

tion but a relatively long refractory period The alpha- or slow pathway has slow conduction but a short refractory period Normally, anterograde conduction occurs through the fast beta pathway and the impulse reaches the His bundle Conduction through the slow alpha-pathway arrives at the His bundle when the tissue is refractory because of prior activation from the faster beta-pathway However, if an atrial premature depolarization (APD) enters the AV node when the fast pathway is refractory,the impulse will block in the fast pathway and anterogradly conducts through the slow pathway (alpha) to the His bundle and ventricles. If the conduction over the alpha-pathway is sufficiently slow, the initially blocked beta-pathway will have time to recover As a result, the impulse can retrogradly enter the fast pathway. This can cause a circuit in the AV node and a sustained paroxysmal SVT can be established if the reentrant impulse continues to find recovered tissue ahead Therefore, in this type of tachycardia the existence of the two functionally different pathways and slow conduction in the AV node provide the substrates for the tachycardia Since this kind of arrhythmia occurs in the AV node, pharmacological agents which can depress conduction through the AV node are expected to be effective in the treatment of the arrhythmia These include agents such as propranolol (beta-blocker), digoxin, and verapamil (calcium blocker) On the other hand, agents such as isoproterenol or atropine, which enhance AV node conduction, facilitate the induction and persistence of the tachycardia

7.EFFECTS OF ANTIARRHYTHMIC AGENTS ON AV NODAL FUNCTION

7.1-Frequency-dependent effects of calcium channel blockers

Antiarrhythmic drugs have been shown to have important frequency-dependent properties. This phenomenon was initially described in 1957 by Johnson and Mckinnon who demonstrated that quinidine's depressant effects on the V_{max} of ventricular fibers in vitro were greater as the driving rate increased. Heistracher (1971) confirmed the above study and showed that there was a time-dependent decrease in V_{max} in quinidine-treated fibers. These observations along with other in vitro studies describing the frequency-dependent effects of antiarrythmic drugs (mainly sodium channel blockers) have led to the development of different models describing the mechanisms of actions of antiarrhythmic drugs on phase zero inward currents (Hondeghem and Katzung, 1977, Grant et al, 1984; Hondeghem and Katzung, 1984; Starmer and Grants, 1985; Starmer et al, 1984).

Most of the clinically used calcium channel blockers decrease the maximum rate of depolarization of the AV nodal action potential (V_{max}), and slow the conduction of the impulse through the AV node These effects are known to be due to an interaction of these agents with the slow calcium channels and inhibition of calcium inward current Frequency-dependent block has also been demonstrated for calcium channel blockers. Verapamil was initially found to produce a greater increase in rabbit atrioventricular nodal conduction time at faster atrial pacing than at slower rates (Wit and Cranefield, 1974) Subsequently, it was observed that verapamil and its methoxy derivative, D600, had a more

depressant effect on contractility as driving rate was increased (Bayer et al, 1975). Later, Ehara and Kaufmann (1978), and McDonald et al (1980) directly demonstrated frequency-dependent block of the calcium current with verapamil and D600. Kanaya and Katzung (1984), Tung and Horad (1983), Lee and Tsien (1983), and Uehara and Hume (1985) demonstrated the same phenomenon for diltiazem

/ 2-Clinical implications of frequency-dependent drug effect

According to the modulated receptor hypothesis of Hondeghem and Katzung (1977, and 1984) antiarrhythmic drugs preferentialy bind to their receptors when the channels are in the ativated or inactivated state, and dissociate during diastole. Each antiarrhythmic drug has a characteristic association and dissociation rate constant for each of the three channel states As a result of the selective affinity of drugs for activated or inactivated states, the more frequently the channels are used the more block accumulates. Consequently, the amount of block developed per activation and the rate of recovery from block during diastole determines the net block. Based on this concept, Hondeghem and Katzung (1984) proposed that antiarrhythmic drugs would have more profound effects during tachycardia and early extrasystoles, and less effect or no effect at all during sinus rhythm. Thus, a drug with a longer recovery time has more depressant effects during tachycardia than a drug with shorter recovery time This could provide a basis for selecting the appropriate drug and dose which has little effects at normal heart rate and maximum effect during tachycardia

Considering the implications of the frequency-dependent drug effects Talajic and Nattel (1986), and Ellenbogen et al (1985) evaluated the rate-dependent effects of calcium channel blockers on AV nodal conduction and refractorines in dog and man, respectively. Ellenbogen et al (1985) found that verapamil prolonged AV conduction time as the rate increased. Though they did not evaluate this effect during arrhythmias, they suggested that frequency-dependent drug effect may determine drug efficacy in the termination of paroxysmal supraventricular tachycardia. Talajic and Nattel (1986) found that the kinetics of action of calcium channel blockers in their in vivo animal model parallelled their kinetic effects in vitro (Uehara and Hume, 1985). However, the direct clinical implications of this frequency-dependence, and its importance in the treatment of arrhythmias has not been tested in either spontaneous or experimentally induced arrhythmias.

STATEMENT OF PROBLEM

The introduction presented here suggests that the rate-dependent properties of the AV node can produce complex sequences of beat-to-beat changes in conduction time and refractoriness. Although three important factors (recovery time, fatigue, facilitation) have been recognized to explain the rate-dependent functions of the AV node (Lewis and Master, 1925, Merideth et al, 1968, Billette, 1981), their specific involvement in different responses have been difficult to establish. Recent observations in in vitro rabbit AV node (Billette et al, 1987, 1988, and 1989) suggest that the different nodal responses can largely be explained in terms of interactions between the three main properties.

An important step to further this understanding would be the development of a model incorporating quantitative indices of AV node recovery, fatigue, and facilitation. A first test of this model would be its ability to predict changes in AV nodal conduction time during atrial pacing. I have developed such a model, which is presented in chapter II. The assumptions of the model are: 1) AV conduction time (AH interval) is an exponential function of the previous recovery interval (HA interval). 2) Facilitatory effects of closely coupled atrial impulses result in leftward shift of the AV recovery curve. 3) The cumulative effects of prolonged AV nodal stimulation (Fatigue) can be quantified by an exponential function. 4) An equation incorporating the quantitative indices of AV recovery, facilitation, and fatigue can accurately predict the changes in AV conduction time as a result of increases in atrial rate.

Autonomic tone has an important modulating influence on AV nodal conduction. However, prior studies have only evaluated steady-state ef-

fects without consideration of possible changes in the intrinsic frequency-dependent properties of AV nodal function. Chapters III, and IV describe experiments in which the model developed in chapter II is used to evaluate the effects of vagal stimulation, sympathetic stimulation, and beta-blockade on each of the three rate-dependent properties of the AV node. Our specific goals in these two studies are 1) to determine the interactions between the heart rate and autonomic tone on the AV node and 2) to determine the extent to which the effects of autonomic tone on AV nodal conduction are due to changes in individual functional properties at any given heart rate.

The frequency-dependent properties of the AV node play an important role in protecting the ventricle during atrial fibrillation and flutter and determine the induction and termination of reentrant supraventricular arrhythmias. Calcium channel blocking drugs are frequently used to treat these arrhythmias, with their efficacy related to their ability to block calcium channels responsible for impulse propagation in the AV node. Molecular models of antiarrhythmic drug actions assume that the maximal depression of slow inward current occurs at faster driving frequencies (Hondeghem and Katzung, 1984; Grant et al, 1984) These models suggest that calcium antagonists could selectively depress AV conduction during supraventricular tachycardias, with much less depression during sinus rhythm. Chapter V and VI describe experiments in which the potential implications of the rate dependent properties of calcium channel blockers are directly tested during two experimental models of supraventricular arrhythmias: 1) Atrial fibrillation, 2) Orthodromic circus movement tachycardia.

Sympathetic and parasympathetic influences have opposite and additive effects on AV node conduction. This might modulate the frequency-dependent effects of diltiazem on the AV node described in chapters V and VI. Chapter VII describes experiments which evaluate the frequency-dependent effects of diltiazem during atrial fibrillation in the presence of different states of autonomic tone.

Ahlquist RP (1948): A study of the adrenotropic receptors. Am J Physiol 153:586-600.

Akhtar M (1982): Supraventricular Tachycardias. In Tachycardias: Mechanism, Diagnosis, Treatment. Edited by Josephson ME, and Wellens HJJ. p.137-169.

Anderson RH, Janse MJ, Van Capelle FJL, Billette J, Becker AE, and Durrer D (1974): A combined morphological and electrophysiological study of the atrioventricular node of the rabbit heart. Circ Res. 35.909-922.

Ardell JL, and Randall WC (1986) Selective vagal innervation of sinoatrial and atrioventricular node in canine heart. Am J Physiol 251(Heart Circ Physiol 20) H764-H773

Arnold JMO, O'Conner PC, Riddell JG, Harron DWG, Shanks RG, McDevitt DG (1985) Effects of the beta$_2$-adrenoceptor antagonist ICI 118,551 on exercise tachycardia and isoprenaline-induced beta adrenoceptor responses in man. Br J Clin Pharmacol 19 619-630

Arnsdorf MF (1984): Cable properties and conduction of the action potential. In: Physiology and Pathophysiology of the Heart, edited by N. Sperelakis. Martinus Nijhoff Publishing, p 109-140

Bayer R, Henneker R, Kaufmann R, Mannhold R (1975): Inotropic and electrophysiological actions of verapamil and D600 in mammalian myocardium. I Pattern of inotropic effects of the racemic compounds Naunyn-Schmeidebergs Arch Pharmacol 290 49

Biegon RL, Epstein PM, and Pappano AJ (1980). Muscarinic antagonism of the effects of phosphodiesterase inhibitor (methylisobutylxanthine) in embryonic chick ventricle. J Pharmac. exp. Ther. 215,348-356.

Billette J, Nadeau RA, Roberge F (1974): Relation between the atrionodal H-H interval during atrial fibrillation and the functional refractory period of the AV junction. Cardiovasc Res,8 347-351

Billette J, Roberge FA, Nadeau RA (1975) Role of the atrioventricular junction in determining the ventricular response to atrial fibrillation. Can J Physiol Pharmacol,53.575-585

Billette J (1976): Preceding-His- Atrial interval as a determinant of atrioventricular nodal conduction time in the human and rabbit heart. Am J Cardiol 38: 889-896

Billette J, Janse M, Van Capeller FJL, Anderson RH, Touboul P, and Durrer D (1976): Cycle -length-dependent properties of AV nodal activation in rabbit hearts. Am J Physiol 231:1129-1139

Billette J (1981). Short time constant for rate-dependent changes of atrioventricular conduction in dogs. Am J Physiol 241 H26 H32

Billette J, Gossard JP, Lepanto L, Cartier R (1986). Common functional origin for simple and copmlex responses of atrioventricular node in dogs. Am J Physiol 251:H920-H925

Billette J (1987) Atrioventricular nodal activation during periodic premature stimulation of the atrium Am. J Physiol 252(Heart Circ, Physiol. 21):H163-H177

Billette J, Metayer R, and St-Vincent Marie (1988) Selective functional characteristics of rate-induce fatigue in rabbit atrioventricular node Circ Res; 62 /90-/99

Billette J, and Metayer R (1989). Origin, domain, and dynamics of rate induced variations of functional refractory period in rabbit atrioventricular node Circ Res, 6) 164-17)

Brettschesi GL, Szabo G (1985) Uncoupling of muscarinic and beat-adrenergic receptors from ion channels by a guanine nucleotide analogue Nature 1985, 317:536-540

Brown GL, and Eccles JC (1934) The action of a single vagal volley on the rhythm of the heart beat J Physiol. Lonnd. 82.211-241

Brown HF, DiFrancesco D, Nobel SJ (1979) How does adrenalin accelerate the heart? Nature 280.235-236.

Brown HF (1982) Electrophysiology of the sinoatrial node, Physiol Rev 62 505-530

Brown H, McLeod AA, Shand DG (1986) In support of cardiac chronotropic beta$_2$ adrenoceptors. Am J Cardiol 57 11F-16F

Burgen ASV, Terroux KG (1953). On the negative inotrophic effect in the cat's auricle J Physiol (London) 120.449-464.

Cagin NA, Kunstadt D, Wolfish P, Levitt B (1973) The influence of heart rate on the refractory period of the atrium and A-V conduction system American Heart Journal 85 (3) 358-366

Cohn AE (1912) On the differences in the effects of stimulation of the two vagus nerves on rate and conduction of the dog's heart. J Exp Med. 16.732-757.

Cohn AE, and Lewis T (1913). The predominant influence of the left vagus nerve upon conduction between the auricles and ventricles in the dogs J Exp. Med. 18:739-747.

Cohen P (1982): The role of protein phosphorylation in neural and hormonal control of cellular activity Nature 296, 613-620

Coraboeuf E, Carmeliet E (1982): Existence of two transient outward currents in sheep cardiac Purkinje fibers Pflugers Arch 392 352-359

Cranefield PF, Hoffman BF, and Paes de Carvalho A (1959). Effects of acetylcholine on single fibers of the atrioventricular node Circ Res 19-23

Damato AN, Lau SH, Patton RD, Steiner C, and Berkowit WD (1969). A study of atrioventricular conduction in man using premature atrial stimulation and His bundle recordings. Circulation 40 of 69

Deck KA, Trautwein W (1964). Ionic currents in cardiac excitation. Pflugers Arch 280: 63-80

DeFelice LJ, and Challice CE (1969) Anatomical and ultrastructural study of the electrophysiological atrioventricular node of the rabbit. Circ. Res 24:457-474

De Mello (1977): Passive electrical properties of the AV node. Pflugers Arch 371:135-139

Denes P, Wu D, Dhingra R, Pietras RJ, and Rosen KM (1973) The effect of cycle length on cardiac refractory periods in man. Circulation 49 32-41

DiFrancesco D, Noma A, Trautwein W (1979) Kinetics and magnitude of the time-dependent potassium current in the rabbit sinoatrial node: Effect of external potassium. Pflugers Arch 371 139-139

Dong E, and Reitz BA (1970) Effect of timing of vagal stimulation on heart rate in the dog. Circ Res 27.635-646

Durrer D, Schuilenburg RM, and Wellens HJJ (1970) Pre-excitation revisited. Cardiol. 25:690-697

Ehara T, Kaufmann R (1978): The voltage- and time dependent effects of (-)-verapamil on the slow inward current in isolated calf ventricular myocardium. J Pharmacol Exp Ther 207 49

Ellenbogen KA, German LD, O'Callaghan WG, Colamita PG, Kirchhoff AC, Gilbert MR, Strauss HC (1985) Frequency-dependent effects of verapamil on atrioventricular nodal conduction in man. Circulation 72 344-352.

Ferrier GR, and Dresel PE (1973): Role of the atrium in determining the functional and effective refractory period and the conduction time of the atrioventricular transmission system. Circ Res 33 [illegible]

Ferrier GR, Dresel PE (1974): Relationship of the functional refractory period to conduction in the atrioventricular node. Circ Res 34 204-214

Fleming BP, Giles W, and Lederer J (1981) Are acetylcholine-induced increases in ^{42}K efflux mediated by intracellular cyclic GMP in turtle cardiac pace-maker tissue. J Physiol (Lond.) 314 47-64

Fozzard HA, Hiraoka M (1973): The positive dynamic current and its activation properties in cardiac Purkinje fibers. J Physiol (Lond) 234 569-586

Fozzard HA (1977). Cardiac muscle: Excitability and passive electrical properties. Progress in Cardiovascular Dis. [illegible]

Gallagher JJ, Sealy WC, Cox SJ, German LD, Kasell JH, Bardy GH, Packer DL. (1982) In Tachycardias: Mechanism, Diagnosis, Treatment ed by Josephson ME and Wellens HJJ pp 260

Gallagher JJ, Svenson RH, Sealy WC, and Wallace AG (1976) The Wolff-Parkonson-White syndrome and the pre-excitation dysrhythmias. Med. Clin. North Am. 60 101-123

Gallagher JJ, Gilbert M, Svenson RH, Miller HC, Sealy WC, Kasell J, and Wallace AG (1975). Wolff-Parkinson-White syndrome the problem, evaluation and surgical correction. Circulation 51 767-785

Garnier D, Nargeot J, Ojeda C, and Rougier O (1978) The action of acetylcholine on background conductance in frog atrial trabeculate J Physiol (Lond.) 274 381-396

Giles WR, and Noble SJ (1976) Changes in membrane currents in bullfrog atrium produced by acetylcholine J Physiol (Lond.) 261.103-123

Giudicelli JF, Lhoste F (1982). Beta-adrenoceptor blockade and atrioventricular conduction in dogs Role of intrinsic sympathomimetic activity Br J Clin Pharmacol 13 167S-171S

Grant AO, Starmer CF, Strauss HC (1984): Antiarrhythmic drug action-blockade of the inward sodium current Circ Res 55 427

Hageman GR, Randall WC, and Armour JA (1975) Direct and reflex cardiac bradydysrhythmias from small vagal nerve stimulations Am Heart J. 89.338-348.

Hamill OP, Marty A, Neher E, Sakmann B, and Sigworth FJ (1981) Improved patch-clamp techniques for high-resolution current recording from cells and cell-free membrane patches Pflugers Arch 391 85-100

Hamlin RL, and Smith CR (1968): Effects of vagal stimulation on S-A and A-V nodes. Am. J Physiol 251 560-568

Herstracher P (1971): Mechanism of action of antifibrillatory drugs Naunyn-Schiedebergs Arch Pharmacol 269.199-212

Hess P, Lansman JB, Nilius B, and Tsien RW (1986). Calcium channel types in cardiac myocytes Modulation by dihydropyridines and beta-adrenergic stimulation J of Cardiovasc Pharmacol, 8(suppl 9) S11-S21.

Hill-Smith I, and Purves RD (1978): Synaptic delay in the heart An ionophoretic study J. Physiol (Lond.) 279, 31-54

Hirano Y, Fozzard HA, January CT (1989): Characteristics of L- and T-type Ca^{2+} currents in canine cardiac Purkinje cells. Am J Physiol;256:H1478-H1492.

Hoffman BF, Paes de Carvalho A, and Mello WC de (1958) Trans membrane potentials of single fibers of the atrio-ventricular node Nature, 181 66

Hoffman BF, Paes de Carvalho A, Carlos Mello W, and Cranefield PF (1959): Electrical Activity of Single Fibers of the Atrioventricular Node. Circ. Res. 7, 11-18.

Hoffman BF, and Cranefield PF (1960) Electrophysiology of the Heart McGraw-Hill, N Y

Hoffman BF, Cranefield PF, and Stuckey JH (1961) Concealed conduction Circ Res 9:194-203

Hoffman BF, Singer DH (1967): Appraisal of the effects of catecholamines on cardiac electrical activity Ann N Y Acad Sci 139 914-939

Homey CJ, and Graham RM (1985) Molecular characterization of adrenergic receptors Circ Res 56 632-650

Hondeghem LM, Katzung BG (1977) Time- and voltage dependent interactions of antiarrhythmic drugs with cardiac sodium channels Biochim Biophys Acta 472:373.

Hondeghem LM, Katzung BG (1984) Antiarrhythmic agents the modulated receptor mechanism of action of sodium and calcium channel blocking drugs. Annu Rev Pharmacol Toxicol 24 387-423

Irisawa H, Caldwell WM, and Wilson MF (1971) Neural regulation of atrioventricular conduction Jap J Physiol 21 [illegible]

Irisawa H (1978): Comparative physiology of the cardiac pacemaker mechanism Physiol Rev 58 461-498

Jalife J, and Moe GK (1979): Phasic effects of vagal stimulation on pacemaker activity of the isolated sinus node of the young cat Circ Rec 45:595-607

James TN (1961) Morphology of the human atrioventricular node with remarks pertinent to its electrophysiology Am Heart J 62 756-771

James TN, Sherf L (1968) Ultrastructure of the human atrioventricular node Circulation 37 1049-1070

James TN (1976) Selective experimental chelation of calcium in the A-V node and His bundle J Mol Cell Cardiol 8 361-374

Jenkins J, Belardinelli L (1988). atrioventricular nodal accommodation in isolated guinea pig hearts: Physiological significance and role of adenosine. Circ Res 63:97-116

Jewett DL (1964): Activity of single efferent fibers in the cervical vagus nerve of the dog, with special reference to possible cardio-inhibitory fibers J Physiol London 172 321-337

Johnson EA, McKinnon MG (1957) The differential effect of quinidine and pyrilamine on the myocardial action potential of the [illegible] stimulation J Pharmacol Exp Ther 120 460

Josephson RR, Sanchez Chapula J, Brown AM (1984): Early outward current in rat single ventricular cells Circ Res 54:157-162.

Kanaya S, Katzung BG (1984): Effects of diltiazem on transmembrane potential and current of right ventricular papillary muscle of ferrets J Pharmacol Exp Ther 228:245.

Katona PG, Poitras JW, Barnett GO, and Terry BS (1970). Cardiac vagal efferent activity and heart period in the carotid sinus reflex. Am J Physiol. 218 1030-1037

Katz LN, and Pick A (1956) Clinical Electrophysiology Part I, The Arrhythmias Lea & Febiger, Philadelphia.

Kenyon JL, Gibbons WR (1979). Influence of chloride, potassium and tetraethylammonium on the early outward current of sheep cardiac Purkinje fibers. J Gen Physiol 73. 117-138

Krayer O, Mandoki JJ, and Mendez C (1951) Studies on veratrum alkaloids XVI The action of epinephrine and veratrine on the functional refractory period of the auriculo-ventricular transmission in the heart-lung preparation of the dog , J Pharm and exper Ther , 103:412-419.

Kokubun S, Nishimura M, Noma A, and Irisawa H (1982) Membrane currents in the rabbit atrioventricural node cell. Pflugers Arch. 393 15-22

Kokubun S, Nishimura M, Noma A, Irisawa H (1985). The spontaneous action potential of the rabbit atrioventricular node cells Jpn J Physiol 30 529-540.

Kumada DL (1972). Reflex discharge patterns of cardiac vagal efferent fibers J Physiol London 222:1-15

Kurachi Y, Nakajima T, Sugimoto T (1986a) Acetylcholine activation of K^+ channels in cell-free membrane of atrial cells Am J Physiol 1986, 251:H681-H684

Kurachi Y, Nakajima T, Sugimoto T (1986b) On the mechanisms of activation of muscarinic K^+ channels by adenosine in isolated atrial cells: Involvement of GTP-binding proteins. Pfluger Arch 407 264-274.

Lands AM, Arnold A, McAuliff JP, Lunduana FP, Brown RC (1967) Differentiation of receptor systems activated by sympathomimetic amines. Nature 214:597-598.

Langendorf R (1948): Concealed A-V conduction: The effect of blocked impulses on the formation and conduction of subsequent impulses Am Heart J,52:766-778.

Langendorf R, Pick A, Katz LN (1965): Ventricular response in atrial fibrillation. Role of concealed conduction in the AV junction. Circulation 31 69-75

Lee KS, Tsien RW (1983) Mechanism of calcium channel blockade by verapamil, D600, diltiazem and nitrendipine in single dialyzed heart cells. Nature 302:790

Lehmann MH, Denker S, Mahmud R, Akhtar M (1984) Pattern of human atrioventricular nodal accommodation to a sudden acceleration of atrial rate. Am J Cardiol 53:71

Levine MAH, and Leene FHH (1989): Role of beta$_1$-receptors and vagal tone in cardiac inotropic and chronotropic responses to a beta$_1$ agonist in humans Circ. Res 79:107-115

Levy MN, Martin PJ, Iano T, and Zieske H (1969) Paradoxical effect of vagus nerve stimulation on heart rate in dogs Circ Res 25:303-314

Levy MN, Martin PJ, Iano T, and Zieske H (1970) Effects of single vagal stimuli on heart rate and atrioventricular conduction Am J Physiol. 218(5).1276-1262

Levy MN (1971). Sympathetic-Parasympathetic interactions in the heart Circ Res 29.437-445

Levy MN, Iano T and Zieske H (1972) Effects of repetitive bursts of vagal activity on heart rate Circ. Res 30.186-195

Levy MN, Martin PJ, Zieske H, Adler D (1974) Role of positive feedback in the atrioventricular nodal Wenckebach phenomenon Circ res 34:697-710

Levy MN, Wexberg S, Eckel C, and Zieske H (1978) The effect of changing interpulse intervals on the negative chronotropic response to repetitive bursts of vagal stimuli in the dog Circ Res 43:570-576

Levy MN, and Martin PJ (1979): Neural control of the heart In Handbook of Physiology, the cardiovascular system the heart Bethesda American Physiological Society, Sect 2 Vol I, chap 16, pp 581-620

Lewis T (1914): The effect of vagal stimulation upon atrioventricular rhythm Heart, 5:247-279.

Lewis T, Master AM (1925): Observations upon conduction in the mammalian heart. A-V conduction, Heart, 12:209-264

Lister JW, Stein E, Kosowsky BD, Lau SH, and Damato AN (1967): Atrioventricular conduction in man Effects of rate, exercise, isoproterenol and atropine on P-R interval Am J Cardiol 16:516-523.

Loeb JM, deTarnowsky JM, Warner MR, Whitson CC (1985): Dynamic interactions between heart rate and atrioventricular conduction Am J Physiol 249:H505-H511.

Loeb JM, deTarnowsky JM, Whitson CC, Warner MR (1987) Atrioventricular nodal accommodation.rate- and time-dependent effects. Am J Physiol 252 H578-H584

Logothetis DE, Kurach Y, Galper J, Neer EJ, and Clapham DE (1987): The beta gamma subunits of GTP-binding proteins activate the muscarinic K^+ channel in heart. Nature (Lond) 325:321-325.

Manalan AS, Besch HR, and Watanabe AM (1981). Characterization of [^{3}H](-)carazolol bindind to beta-adrenergic receptors, application to study of beta-adrenergic receptor subtypes in canine ventricular myocardium and lung. Circ Res . 49 326-336

Martin P (1977a). Paradoxical dynamic interaction of heart period and vagal activity on atrioventricular conduction in the dog. Circ Res 40 81-89.

Martin P (1977b) The influence of the parasympathetic nervous system on atrioventricular conduction. Circ. Res. 41 593-599

Mazgalev T, Dreifus LS, Bianchi J, Michelson EL (1982): Atrioventricular nodal conduction during atrial fibrillation in rabbit heart Am J Physiol.243:H754-H760

Mazgalev T, Dreifus LS, Michelson EL, Pelleg A, Pric R (1986a) Phasic effects of postganglionic vagal stimulation on atrioventricular nodal conduction Am J physiol 251.H619-H630.

Mazgalev T, Dreifus LS, Michelson EL, and Pelleg A (1986b) Vagally induced hyperpolarization in atrioventricular node. Am J Physiol 251.H631-H643.

McDonald TF, pelzer D, Trautwein W (1980)· On the mechanism of slow calcium channel block in heart. Pfluegers Arch 385.175

McDonald TF (1982)· The slow inward current in the heart Annu Rev Physiol.44 425-434.

Meijler FL, Kroneman J, Vander Tweel I, Herbschleb JN, Hecthaar RM, and C Borst (1984): Nonrandom ventricular rhythm in horses with atrial fibrillation and its significance for patients J. Am. Coll. Cardiol. 4:316-323.

Meijler F, and Janse MJ, (1988): Morphology and Electrophysiology of the Mammalian Atrioventricular Node. Physiological Reviews. 68,No 2, 608-647.

Mendez C, and Moe GK (1966): Some characteristics of transmembrane potentials of AV nodal cells during propagation of premature beats Circ. Res.19·993-1010.

Merideth J, Mendez C, Mueller WJ, and Moe GK (1968): Electrical excitability of atrioventricular nodal cells Circ Res 23:69-85

Mirro MJ, Bailey JC, and Watanabe AM (1980) The role of cyclic AMP in regulation of the slow inward current In The Slow Inward Current

and Cardiac Arrhythmias, ed. by D. P. Zipes, J. C. Bailey, and V Elharrar, pp. 111-126, Martinus Nijhoff, Boston.

Mobitz W (1924): Uber die unvollstandige Storung der Erregungs-uberleitung zwischen Vorhof und Kammer des menschlichen Herzens Zeit Gesamte Exp Med 41:180-237.

Moe GK, Abildskov JA, and Mendez C (1964): An experimental study of concealed conduction. Am. Heart J. 67:338-356.

Moe GK, Childers RW, Merideth J (1968): An appraisal of "supernormal" A-V conduction. Circulation 38:5-28.

Moore EN (1967): Observations on concealed conduction in atrial fibrillation. Circ. Res; 21:201-208.

Nakayama T, Kurachi Y, Noma A, and Irisawa H (1984): action potential and membrane currents of single pacemaker cells of the rabbit heart. Pfluegers Arch. 402:248-257.

Nakayama T, and Irisawa H (1985): Transient outward current carried by potassium and sodium in quiescent atrioventricular node cells of rabbits. Circ Res 57:65-73.

Narula OS, Scherlag BJ, Samet P, and Javier RP (1971): Atrioventricular block: Localization and classification by His bundle recording Am. J. Med., 50:146-165.

Narula OS (1972): Wolff-Parkinson-White syndrome- Circulation 47·872-887.

Narula OS, Runge M (1976): Sccommodation of A-V nodal conduction and fatigue phenomenon in the His-Purkinje system, in Wellens HJJ, Lie KI, Janse MJ (eds): The conduction system of the heart, Leiden, The Netherlands, Stenfert Kroese, pp529-544.

Narula OS (1979): In Narula OS (ed): Cardiac arrhythmias: Electrophysiology, Diagnoses and Management. Baltimore, Williams & Wilkins.

Nawrath H (1977): Does cyclic GMP mediate the negative inotropic effect of acetylcholine in the heart? Nature (Lond.) 267:72-74.

Nishimura M, Habuchi Y, Hiromasa S, and Watanabe Y (1988): Ionic basis of depressed automaticity and conduction by acetylcholine in rabbit AV node. Am. J. Physiol. 255(Heart Circ. Phsiol. 24): H7-H14

Noble D, Tsien RW (1969): Outward membrane currents activated in the plateau range of potential in cardiac Purkinje fibers. J Physiol. 200:205-231

Noma A, and Trautwein W (1978): Relaxation of the Ach-induced potassium current in the rabbit sinoatrial node cell. Pflugers Arch. 377, 193-200.

Noma A, Irisawa H, Kokubun S, Kotake H, Nishimura H, Watanabe Y (1980a) Slow current systems in the A-V node of the rabbit heart. Nature 285:228-229

Noma A, Kotake H, Irisawa H (1980b): Slow inward current and its role mediating the chronotropic effect of epinephrine in the rabbit sinoarterial node Pflugers Arch 388:1-9.

Osterrieder W, Tang QF, and Trautwein W (1981) The time course of the muscarinic response to ionophoretic acetylcholine application to the S-A node of the rabbit heart. Pflugers Arch. 389,283-291.

Pace de Carvalho A, and de Almedia DF (1960) Spread of activity through the atrioventricular node Circ Res 8 801-809

Pfaffinger PJ, Martin JM, Hunter DD, Nathanson NM, Hille B (1985) GTP-binding proteins couple cardiac muscarinic receptors to a K channel Nature 317,538-540

Priola DV (1973) Effects of beta receptor stimulation and blockade on AV nodal and bundle branch conduction in the canine heart Am J Cardiol 31:35-40

Prokopczuk A, Lewartowski B, and Czarnecka M (1973): On the cellular mechanism of the inotropic action of acetylcholine on isolated rabbit and dog atria Pflugers Arch Gen. Physiol 399, 305-316

Randall WC, and Armour JA (1977). Gross and microscopic anatomy of the cardiac innervation In: Neural regulation of the heart edited by Randall WC. New York: Oxford Univ Press, p.15-41.

Rayner B, and Weatherall N (1959). Acetylcholine and potassium movements in rabbit auricles J. Physiol. (Lond) 146,399-409

Reuter H, and Schools H (1977) The regulation of the calcium conductance of cardiac muscle by adrenalin J Physiol 264 49-62

Reuter H (1983) Calcium channel modulation by neurotransmitters, enzymes and drugs. Nature (Lond) 301 569-574

Roberts JT, (1959): Histology of the heart. The conduction system, in cardiology, an encyclopedia of cardiovascular system, ed. Luisada, A A., New York, Toronto. London, McGraw-Hill Book Company, Inc , vol.1,p.1-71.

Rodbell M (1980): The rol of hormone receptors and GTP-regulatory proteins in membrane transduction. Nature.284,17-22.

Ross TF, and Mandel WJ (1987): Invasive Cardiac Electrophysiologic Testing In: Cardiac arrhythmias Their mechanism, Diagnosis, and Management, edited by Mandel WJ Second edition p 101-142

Ruiz-Ceretti E, Ponce Zumino A (1976): Action potential changes under varied $[Na]_o$ and $[Ca]_o$ indicating the existence of two currents in cells of the rabbit atrioventricular node Circ Res 39 326-336

Saito K, Kurihara M, Cruciani R, Potter WZ, and Saavedra JM (1988) Characterization of $beta_1$- and $beta_2$- adrenoceptor subtypes in the rat atrioventricular node by quantitative autoradiography. Circ Res 62.173-177

Scherlag BJ, Lau SH, Helfant RH, Berkowitz WD, Stein E, and Damato AN (1969). Catheter technique for recording His bundle activity in man. Circulation 39:13-18

Sherf LT, James TN, and Woods WT (1983) Function of the atrioventricular node considered on the basis of observed histology and fine structure J Am Coll Cardiol 1 70-80

Shibata EF, and Giles W (1984). Cardiac pacemaker cells from bullfrog sinus venous lack an inwardly rectifying background I^+ current. Biophys J 45 136a

Shrier A, Dubarsky H, Rosengarten M, Guevara MR, Nattel S, and Glass L (1987) Prediction of complex atrioventricular conduction rhythm in humans with use of the atrioventricular nodal recovery curve. Circulation 76, 6.1196-1205

Simson MB, Spear JF, Moore EN (1978) Electrophysiologic studies on atrioventricular nodal Wenckebach cycles. Am J Cardiol 41 241-253

Simson MB, Spear J, and Moore EN (1979) The relationship between atrioventricular nodal refractoriness and the functional refractory period in the dog. Circ Res 44 121-126

Slenter VAJ, Salata JJ, and Jalife J (1984) Vagal control of pacemaker periodicity and intranodal conduction in the rabbit sinoatrial node Circ. Res 54 436-446.

Soejima M, and Noma A (1984). Mode of regulation of the ACh-sensitive K-channel by the muscarinic receptor in rabbit atrial cell Pflugers Arch gen Physiol 400 424-431

Spear JF, and Moore EN (1973) Influence of brief vagal and cardiac nerve stimulation on pacemaker activity and conduction within the atrioventricular conduction system of the dog. Circ Res 32 747-61

Spear JF, Kronhaus KD, Moore NE, and Kline R (1979) The effect of brief vagal stimulation on the isolated rabbit sinus node Circ Res. 44:75-88.

Starmer CF, Grant AO, Strauss HC (1984). Mechanism of use-dependent block of sodium channels in excitable membrane by local anesthetics. Biophys J 46.15.

Starmer CF, Grant AO (1985): Phasic ion channel blockade a kinetic model and parameter estimation procedure Mol Pharmacol 28 348

Stiles GL, Taylor S, and Lefkowitz RJ (1983) Human cardiac beta-adrenergic receptors Subtype heterogeneity delineated by direct radioligand binding Life Sci 33 467-473

Strackee J, Hoelen AJ, Zimmerman ANE, and Meijler FL (1971): Artificial atrial fibrillation in the dog. An artifact? Circ. Res 28 441-445

Strauss MH, Reeves, Smith RA, Leenen DL, (1986) The role of cardiac $beta_1$ receptors in the hemodynamic response to a $beta_2$- agonist. Clin Pharmacol Therap 40:108-115

Talajic M, and Nattel S (1986) Frequency-dependent effects of calcium antagonists on atrioventricular conduction and refractoriness: Demonstration and characterization in anesthetized dogs Circulation 74 1156-1167

Talajic M, Nayebpour M, Jing W, Nattel S (1989). Frequency-dependent effects of diltiazem on the atrioventricular node during experimental atrial fibrillation Circulation 80 380-389

Talajic M, Villemaire C, Papadatos D, Lemery R, Roy D, Nattel S (1990) Cycle length alternation during supraventricular tachycardia Occurrence and mechanism in a canine model of AV reentrant tachycardia. PACE 13.314-325.

Talajic M, Villemaire C, Nattel S (1990): Electrophysiological effects of alpha-adrenergic stimulation. PACE 13:578-582.

Taniguchi J, Kokubun S, Noma A, and Irisawa H (1981): Spontaneously active cells isolated from the sino-atrial and atrio-ventricular nodes of the rabbit heart. Jpn J Physiol 31 547-558.

Tawara S (1906) Das Reizleitungssystem des saugetierherzens. Fischer, Jena

Ten Eick R, Nawrath H, McDonald TF, and Trautwein W (1976) On the mechanism of the negative inotropic effect of acetylcholine Pflugers Arch. 316,207-213

Toshio Nakamama, and Hiroshi Irisawa (1985) Transient outward current carried by potassium and sodium in quiescent atrioventricular node cells of rabbits Circ Res 57:65-73.

Trautwein W, Taniguchi J, and Noma A (1982) The effect of intracellular cyclic nucleotides and calcium on the action potential and acetylcholine response of isolated cardiac cells Pflugers Arch 392 307-314.

TSE WW, and Davis LD (1972). Effects of epinephrine on the diastolic depolarization of the canine AV node (abstr.) Federation Proc 31: 314

Tseng GN, and Hoffman BF (1989): Two components of transient outward current in canine ventricular myocytes Circ Res 64 633-647

Tsuji Y, Inoue D, and Pappano AJ (1985) Beat-adrenoceptor agonist accelerates recovery from inactivation of calcium-dependent action potential J Mol Cell Cardiol 1 [illegible]

Tung L, Morad M (1983): Voltage- and frequency-dependent block of dil tiazem on the slow inward current and generation of tension in frog ventricular muscle. Pfluegers Arch 398.189

Tytgat J. Nilius B, Vereeck J, and Carmeliet E (1988) The T type ca channel in guinea-pig ventricular myocytes is insensitive to isoproterenol. Pflugers Arch 411 704-706

Uehara A, Hume JR (1985): Interactions of organic calcium antagonists with calcium channels in single frog atrial cells J Gen Physiol 85:621-647.

Van Capelle FJ, and Janse MJ (1976) Influences of geometry on the shape of the propagated action potential In The Conduction System of the Heart, edited by H J J Wellens, K L Lie, and M J. Janse Leiden, The Netherland· Stenfert Kroese, p 216 225

Vincenzi FF, and West TC (1963)· Release of autonomic mediators in cardiac tissue by direct subthreshold electrical stimulation J Pharmacol Exp. Ther. 141. 185-194

Wallick DW, Martin PJ, Masuda Y, Levy MN (1980) Effects of autonomic activity and changes in heart rate on atrioventricular conduction Am J Physiol 243.H523-H527.

Warner MR, DeTarnowsky JM, Whitson CC and Loeb JH (1986a) Beat by beat modulation of AV conduction II Autonomic neural mechanisms. Am. J Physiol. 251 (Heart Circ physiol 20) H1134 H1142

Warner MR, and Loeb JM (1986b). Beat-by-beat modulation of AV conduction I Heart rate and respiratory influences Am J Physiol 251(Heart Cir Physiol 20) H1126-H1133

Warner MR, and Loeb JM (1987) Reflex regulation of atrioventricular conduction. Am J Physiol 252 (Heart Cir Physiol 21) H1080 H1085

Watanabe AM, Jones LR, Manalan AS, and Besch HR (1978) Cardiac autonomic receptors. Recent concepts from radiolabeled ligand binding studies Circ Res 50.161-174

Weidmann S (1952): The electrical constants of Purkinje fibers J Physiol Lond 118 348-360

Wenckebach KF (1899)· Zur analyse des unregelmassigen pulses Z Klin Med 37 475-488.

West TC, Toda N (1967) Response of the AV node of the rabbit to stimulation of intracardiac cholinergic nerves Circ Res

Wit AL, Weiss MB, Berkowitz WD, Rosen PJ, Sherlag BJ, and Hoffman BF (1970) Patterns of atrioventricular conduction in the mammalian heart Circ Res 27 353

Wit AL, Cranefield PF (1974): Effect of verapamil on the sinoarterial and atrioventricular nodes of the rabbit and the mechanism by which it arrests reentrant atrioventricular nodal tachycardia Circ Res 35:413-425

Yamagishi S (1966): Effect of tetrodotoxin on the pacemaker action potential of the sinus node Proc Jap Acad 42: 1194

Yanagihara K, Irisawa H (1980): Inward current activated during hyperpolarization in the rabbit sinoarterial node cell Pflügers Arch 385:11-19.

Zipes DP, Mendez C (1973): Action of manganese ions and tetrodotoxin on atrioventricular nodal transmembrane potentials in isolated rabbit hearts. Circ Res 32.447-454.

Zipes DP, and Fischer JC (1974): Effects of agents which inhibit the slow channel on sinus node automaticity and atrioventricular conduction in the dog. Circulation Res 34:184-192.

CHAPTER 2

Quantification of Dynamic AV Nodal Properties and Application to Predict Rate-Dependent AV Conduction

Quantification of dynamic AV nodal properties and application to predict rate-dependent AV conduction

MOHSEN NAYEBPOUR, MARIO TALAJIC and STANLEY NATTEL

Department of Medicine, Montreal Heart Institute, Departments of Pharmacology and Therapeutics and Medicine, McGill University, and Department of Medicine, University of Montreal.

Running head title: Quantification of AV nodal properties

Submitted to the American Journal of Physiology, August, 1990.

Supported by grants from the Medical Research Council of Canada, the Quebec Heart Foundation, the Fonds de la Recherche en Santé du Québec, and the Fonds de Recherche de l'Institut de Cardiologie de Montréal.

Dr. Talajic is a Canadian Heart Foundation scholar.

Dr. Nattel is a research scholar of the Fonds de la Recherche en Santé du Québec.

Address for correspondence: Stanley Nattel, M.D., Montreal Heart Institute, 5000 Belanger Street East, Montreal, Quebec, Canada H1T 1C8
Telephone: (514) 376-3330. FAX: (514) 376-1355.

ABSTRACT

A number of functional properties of the AV node have been described in response to changes in input rate. Recent work has suggested that three of these properties, referred to as recovery, facilitation, and fatigue, operate independently and can be isolated by selective pacing protocols. The purpose of this study was to develop quantitative descriptors of these properties, and to determine whether the conduction changes predicted to occur from the combination of these properties can account for rate-dependent changes in AV nodal conduction time. Selective pacing protocols were used in autonomically-blocked, anesthetized open chest dogs. The delay in AV nodal conduction of single premature beats (recovery) was found to be an exponential function of coupling interval with a time constant of 66±2 (M±SE) msec. A single abbreviated (facilitation) cycle shifted the AV recovery curve to shorter coupling intervals, and successive cycles at the same rate caused no further shift. Facilitation did not alter the time constant of recovery or basal conduction, but shifted the recovery curve to a degree that was exponentially related to the facilitation cycle length. The induction of a tachycardia with HA interval fixed so as to control the recovery and facilitation variables resulted in a first-order onset of AV conduction slowing (fatigue). The fatigue process had a time constant (in the range of 70 beats) that was independent of tachycardia rate, and had a magnitude that was a decaying exponential function of HA interval. An equation incorporating quantitative descriptors of recovery, facilitation, and fatigue accurately predicted rate-dependent changes in AH interval. We conclude (1) that the AV nodal properties of recovery, facilitation, and fatigue are amenable to

quantitative characterization, and (2) that rate-dependent changes in AV nodal conduction time can be well described in terms of these underlying properties.

Index Terms: Cardiac conduction - electrocardiogram - cardiac arrhythmias.

CONDUCTION THROUGH THE ATRIOVENTRICULAR node responds in a complex fashion to changes in activation rate. Abrupt increases in atrial rate result in an increase in AV node conduction time, with at least two kinetically-distinguishable components (18). One component of AV nodal adaptation has a rapid time course, and is clearly demonstrable in the conduction of a single premature beat (2,3,10,17,18,20,21,23,24,31,38,). This rapid process has been attributed to incomplete AV node recovery, and has been characterized mathematically by either an exponential (9-11,30,33,37,) or hyperbolic function (9,32). The time constant of this process, in the range of 50-100 msec (30,33,37), is similar to the time constant for recovery of calcium channels from inactivation in vitro (12,19). It is presumed to result from the incomplete recovery of calcium channels responsible for conduction through critical portions of this tissue. A second component of AV nodal conduction slowing in response to abrupt rate increase develops much more slowly. This process was first noted by Lewis and Master, who coined the term "fatigue" to describe it (18).

There has been dispute as to whether the recovery interval for AV nodal activation is best represented by the time from the preceding atrial activation, or A-A interval (10,31,32), or by the period from the preceding ventricular (VA or PR) or His bundle (HA) interval (2,5,17,18,23). If an index related to activation of the distal AV node (such as the VA or HA time) is used, the second beat of a rapid train with a constant HA interval conducts more rapidly than the first. This property, first identified by Lewis and Master in 1925 (18), has been called "facilitation".

The recovery process has been defined quantitatively in many studies, as discussed above. Billette and co-workers have shown that the processes of facilitation and fatigue can be dissociated from recovery and characterized independently using selective stimulation protocols (2,7,8). However, the time dependence of fatigue and facilitation, and the determinants of their magnitude, have not been quantified. Furthermore, while changes in AV node conduction resulting from specific pacing protocols have been attributed to recovery, facilitation and fatigue, it has not been demonstrated that the changes in AV nodal conduction due to alterations in activation rate can be quantitatively explained by these properties.

This study was designed to develop quantitative descriptors of the changes in AV nodal conduction due to incomplete recovery, facilitation, and fatigue; and then to determine whether the resulting mathematical description of AV nodal conduction can account for the alterations in conduction resulting from sustained increases in activation rate. A preliminary communication of these results has appeared in abstract form (25).

METHODS

General Methods

Mongrel dogs of either sex were anesthetized with morphine (2 mg/kg) and alpha-chloralose (100 mg/kg i.v.). Catheters were inserted into both femoral veins and arteries and were kept patent with heparinized saline solution (0.9%). Dogs were ventilated *via* an endotracheal tube using a Harvard animal respirator. Tidal volume and respiratory rate were adjusted after measurement of arterial blood gases to ensure adequate oxygenation (SaO_2 >90%) and physiologic pH (7.35 to 7.45). A thoracotomy was performed through the fourth

right intercostal space and the heart was suspended in a pericardial cradle. Body temperature was monitored continuously using a thermistor within the chest cavity and was maintained at 37-38°C by a homeothermic heating blanket.

Bipolar Teflon-coated stainless steel electrodes were inserted into the lateral right atrium and high lateral right ventricle on either side of the atrioventricular ring, and into the right atrial appendage. A bipolar plunge electrode was inserted to record the His bundle electrogram (15). Atrial and ventricular electrograms were recorded with the electrodes located in the atrial appendage and lateral right ventricle. Square-wave pulses at twice late diastolic threshold (4 msec duration) were applied via the lateral right atrial electrode, with stimulus timing controlled by a programmable stimulator (Digital Cardiovascular Instruments Inc., Berkeley, CA). Electrograms were filtered at 30-500 Hz (Bloom Instruments Ltd., Flying Hills, PA), with the amplified output led into a paper recorder and/or a sensing circuit of the stimulator. A Statham P23 ID transducer (Statham Medical Instruments, Los Angeles, CA), electrophysiologic amplifiers and a Mingograf T-16 paper recorder (Siemens-Elema Ltd., Toronto, Ont.) were used to record blood pressure, electrocardiographic leads II and aVR, atrial, His bundle and ventricular electrograms, and stimulus artifacts. Recordings were obtained at a paper speed of 200 mm/sec, with a measurement accuracy of ±2.5 msec.

The sinus node was crushed (33) to allow for a wide range of pacing rates. Nadolol was used to produce beta blockade, with 0.5 mg/kg i.v. as an initial loading dose, followed by 0.25 mg/kg every two hours. This technique has been shown to produce continuous and stable blockade of cardiac beta adrenergic receptors (34). Vagal input was eliminated by ligating and cutting the cervical vagal nerves.

Experimental Protocols

Measurement of electrophysiologic variables. Wenckebach cycle length (WBCL) was measured by decreasing atrial cycle length by 10 msec every 10 beats until second degree AV block occurred. The measurement of WBCL was repeated before and after each experimental protocol to ensure stability of AV nodal function during electrophysiologic study. The effective refractory periods of the AV node (AVERP) and atrium (AERP) were measured with the extrastimulus technique. The AVERP was defined as the longest atrial (A_1A_2) interval failing to result in a propagated His bundle response. The AERP was defined as the longest interstimulus (S_1S_2) interval failing to result in a propagated atrial response.

Atrioventricular conduction was assessed from the His bundle electrogram, with the AH interval defined as the time from the first rapid deflection of the atrial electrogram (in the His signal) to the first rapid deflection of the His spike. The HV interval was defined as the time from bundle of His depolarization to the onset of earliest ventricular activation in the His signal or surface ECG leads. The HA interval was defined as the time from the His spike to atrial activity in the His electrogram.

Quantitative assessment of functional rate-dependent properties of the AV node. Stimulation protocols and analysis methods were developed to quantify AV nodal functional properties. The three properties of AV nodal recovery, facilitation, and fatigue were characterized as follows:

1. Recovery component. A constant basic (S_1S_1) cycle length was used, and the effect of changes in recovery interval on AV nodal conduction was determined. A premature or delayed stimulus (S_2) was introduced after every 15 basic stimuli, and a curve relating A_2H_2 (conduction time of the test

impulse) to H_1A_2 (recovery time) was established (Fig. 1 protocol A). The H_1A_2-A_2H_2 relationship was determined at two basic cycle lengths (one cycle length was 50 msec above the WBCL, and the second was a standard cycle length of 600 msec). Monoexponential curve-fitting techniques were used (see below) to characterize AV node recovery.

2. Facilitation component. Premature atrial activation (A_2) results in a leftward shift of the AV node recovery curve (as defined above) for a subsequent A_3 impulse (2,18). This process has been termed "facilitation" and reaches steady state after one cycle at a new rate (4). To study this process, we paced the atrium at an S_1S_1 cycle length of 1000 msec for at least 5 minutes. A premature atrial impulse (S_2) was then introduced to produce a "facilitation cycle" (S_1S_2) after every 15 basic stimuli. A test impulse (S_3) was then applied after each S_2, and the AV node response to S_3 was monitored to generate an H_2A_3-A_3H_3 recovery curve. The latter curve was studied over a wide range of (A_1A_2) facilitation cycle lengths, with A_1A_2 varied from 800 msec to 20 msec greater than refractory period of the AV conduction system (Fig. 1 protocol B). Each H_2A_3-A_3H_3 recovery curve was fitted by a monoexponential model. As facilitation cycle length (FCL) was shortened, the recovery curve of A_3 shifted to the left.

3. Fatigue component. A slow process of AV conduction slowing, independent of AV nodal recovery and facilitation, can be demonstrated after abrupt increases in atrial rate (7,10,18). We used a sensing and pacing circuit to sense each ventricular activation and pace the lateral right atrium with a selected VA interval. Prior to the onset of tachycardia, the atrium was paced at a rate of 1 Hz to produce a stable baseline. Since the HV

interval was measured and was not affected by atrial stimulation patterns, this allowed us to initiate tachycardias with a constant HA interval, thereby maintaining a constant recovery time during tachycardia (Fig. 1 protocol C) Since facilitation reaches steady state within one cycle (4), the gradual development of AH prolongation during such a tachycardia is due to neither change in recovery nor facilitation, and results solely from the process termed "fatigue".

The onset of fatigue was studied over a wide range of HA intervals. An average of 12 HA irtervals were studied in each experiment. After tachycardia was initiated at any HA interval, it was maintained for at least 5 minutes to ensure that steady state conditions had been achieved. A recovery period of at least 5 minutes was allowed for dissipation of fatigue prior to the next test run. After the onset of tachycardia, the AH interval increased as a first-order function of beat number. The time constant and magnitude of fatigue at any HA interval were determined by exponential curve fitting.

The magnitude of fatigue was assessed independently in a different way. The AV recovery curve was first determined as described above at a slow rate. We then increased the rate, and when steady state conditions were achieved, introduced after every 15 beats a delayed stimulus (S_2) with a preceding H_1A_2 interval equal to the HA interval at the slow rate. This is sufficient to completely dissipate the facilitation resulting from rapid pacing, without altering the degree of fatigue (7). We then determined the recovery curve of a beat resulting from an S_3 following each S_2, measuring the A_3H_3 interval as a function of the preceding H_2A_3 interval. This recovery curve should reflect the effects of fatigue alone. These measurements were made using the same HA values for the slow, intermediate, and fast rate in each experiment (Fig. 1 protocol D).

Data analysis. Results are reported as the mean ± SE. Multiple comparisons were made by two-way analysis of variance with Scheffé contrasts (29). Comparisons between two groups of experimental data only were made with Student's t-test. Two-tailed tests were used for all statistical comparisons and a probability of 5% or less was taken to indicate statistical significance. Exponential curve fitting was performed using Marquardt's technique on an IBM AT compatible computer (Statistical Graphics, Rockville, Md.). Twenty dogs were studied in all: recovery curves (protocol A, Figure 1) were analyzed in all dogs; facilitation (Protocol B) was characterized in 9 dogs; fatigue was studied using protocol C in 9 dogs and protocol D in 5 dogs; and the steady state relationship between atrial rate and cycle length was assessed in 9 dogs. Several dogs were studied using more than one protocol. All animal care techniques followed the recommendations of the Canadian Council on Animal Care, and research protocols were approved by the animal care committee of the Montreal Heart Institute.

RESULTS

Stability of AV nodal function during electrophysiologic study. There were no time-dependent changes in AV nodal function as indicated by Wenckebach cycle length (WBCL) over the period of each experiment. WBCL was measured approximately every 20 min, and did not change over time (Fig. 2).

Characterization of AV nodal functional properties

1. Recovery component. An example of one experiment relating A_2H_2 to H_1A_2 interval at two basic cycle lengths is shown in Fig. 3. At a fast rate, premature beats introduced late in the recovery cycle were conducted more slowly for identical H_1A_2 intervals. This appeared as an upward

shift of the curves at intermediate and long H_1A_2 intervals. However, premature beats introduced progressively earlier (shorter H_1A_2 intervals) had faster conduction (shorter A_2H_2 intervals) than at the slower rate This appeared as a leftward, and downward shift of the curves at short H_1A_2 intervals. This pattern demonstrates the combined effects of facilitation and fatigue on the AV node recovery curve at rapid rates. Each AV recovery curve was fitted by nonlinear curve-fitting techniques to an equation of the form:

$$AH = AH_\infty + A \cdot \exp(-HA/\tau_{rec}) \qquad \text{(Eq. 1)}$$

Where AH = the AH interval at any given HA interval, AH_∞ = AH interval after an infinitely long recovery time, A is the difference between the AH interval for HA = 0 and AH_∞, and τ_{rec} = the recovery time constant The mean correlation coefficient for the fits were 0.993 with a standard deviation of 0.005. The average time constant was 66±2 msec and was independent of basic cycle length.

2. Facilitation component. Single atrial premature beats (A_2) shifted the recovery curve in response to a subsequent A_3 complex to the left, in a fashion that depended on the A_1A_2 interval (FCL). Fig. 4 (top) shows raw data from a series of recovery curves obtained with varying facilitation (A_1A_2) cycle lengths. The best-fit exponential curves to the same data are also shown. Facilitation cycles shift the recovery curve of a subsequent beat to the left, and the degree of shift can be quantified by determining the HA interval for any given AH interval. We determined the HA interval corresponding to an AH value of 125 msec for the recovery curve at each FCL. This was designated the "HA_{125}", and is indicated by the intersection between the horizontal dashed line and the recovery curve at each FCL in Fig. 4.

Fig. 5 shows an analysis of the effect of FCL on AH_∞, τ_{rec}, and HA_{125}. Decreases in FCL resulted in progressive reductions in HA_{125}, but AH_∞ and τ_{rec} were not significantly changed. The effect of a facilitation cycle can therefore be viewed as a parallel leftward shift in the recovery curve. We therefore averaged the values of AH_∞ and τ_{rec} for the recovery curves associated with each of the 10 FCL studied in each experiment, and took the mean value as representative of the overall AH_∞ and τ_{rec}. The data for each recovery curve was then refitted by equation 1 keeping AH_∞ and τ_{rec} fixed at the overall mean values for that experiment. Fig. 4 (bottom) shows a series of exponential curves fitted to the raw data shown at the top of the figure according to this method. The equations characterizing each of these curves were used to solve precisely for the HA_{125} value for each set of data, using the following rearrangement of eq. 1 for an AH interval of 125 msec:

$$HA_{125} = -\tau_{rec} \ln \frac{(125-AH_\infty)}{A} \qquad \text{(Eq. 2)}$$

As shown in Figure 6, decreases in HA_{125} resulting from facilitation were well-fitted by the relationship

$$\Delta HA_{fac} = C \cdot \exp(-HA/\tau_{fac}) \qquad \text{(Eq. 3)}$$

Where ΔHA_{fac} = magnitude of facilitation-induced shift in the recovery curve as indicated by changes in HA_{125}; C = a constant reflecting the maximum magnitude of leftward shift; HA is the HA interval from the His potential of the last basic complex to the atrial activation of the facilitating impulse; and τ_{fac} = a time constant. The correlation coefficents for the nonlinear regressions to eq. 3 averaged 0.98±0.01, with a mean τ_{fac} of 148±18 msec. Repeated facilitation cycles did not result in a further shift of the recovery curve - the degree of left shift reached steady state within one cycle (Fig. 7).

Facilitation acts to attenuate the effects of recovery by shifting the recovery curve to shorter HA values as shown in Figure 4. The combined effects of recovery and facilitation at any steady state HA interval can therefore be expressed by combining equations (1) and (3) to give:

$$AH = AH_{\infty} + A \cdot \exp[-(HA + \Delta HA_{fac})/\tau_{rec}] \qquad \text{(Eq. 1a)}$$

3. Fatigue component. When the atrial rate is increased while maintaining a constant HA interval, the AH interval gradually increases to reach a steady state over several minutes, as shown in Fig. 8. Changes in AH interval from the second beat to steady state of a tachycardia with a given HA time was well-fitted (mean r=0.93±.01) by the relationship

$$\Delta AH_n = \Delta AH_{ss} [1 - \exp(-n/\tau_{fat})] \qquad \text{(Eq. 4)}$$

Where ΔAH_n = increase in AH interval for the n^{th} beat of tachycardia; ΔAH_{ss} = change in AH interval from baseline at steady state of the tachycardia; τ_{fat} = a time constant characterizing the onset of fatigue.

Mean values of ΔAH_{ss} and τ_{fat} are shown as a function of the HA interval during tachycardia in Fig. 9. While τ_{fat} was not significantly altered over the entire range of HA intervals, the magnitude of fatigue (ΔAH_{ss}) increased as HA interval decreased (i.e. tachycardia rate increased). The relationship between ΔAH_{ss} and HA interval was well-approximated by a function of the form:

$$\Delta AH_{HA} = \Delta AH_{max} \exp(-k.HA) + b \qquad \text{(Eq. 5)}$$

Where $\Delta AH_{HA} = \Delta AH_{ss}$ at any HA interval; ΔAH_{max} is a constant (equivalent to predicted ΔAH_{ss} for a tachycardia with HA = 0); and k and b are constants. The values of ΔAH_{max}, k, and b were obtained by nonlinear least-squares regression. The curve fitted to the mean data from all experiments according to eq. 5 is shown in Fig. 9 (top).

The magnitude of fatigue was also studied using the protocol illustrated at the bottom of Fig. 1. Recovery curves were obtained at three rates of stimulation, arbitrarily termed "fast", "slow", and "intermediate". Figure 9 shows a recovery curve obtained at a slow rate (with a steady state HA of 740 msec), as well as the corresponding curve at a rapid rate (HA = 200 msec). Solid lines show the best-fit curves to eq. 1 for each set of points.

The curve at the rapid rate is shifted upwards by about 12 msec. To determine whether the change in the recovery curve at a rapid rate is due solely to a tonic increase in AH_∞ in equation 1, (i.e. a parallel upward shift), a constant value equal to the shift in AH_∞ was subtracted from each point on the fast rate recovery curve. The resulting curve, shown by the dashed line, lies close to the points on the slow rate recovery curve, consistent with a parallel shift. Table 1 shows the results of nonlinear curve-fitting of the recovery curves at each rate. Rapid rates increased the AH_∞ and tended to increase the HA_{125}, while the recovery time constant was unaltered. When the change in AH_∞ at faster rates was accounted for (as shown in Fig. 9), HA_{125} values decreased into the same range as values at the slow rate.

Combined effects of recovery, facilitation, and fatigue on the AH interval at different rates. Since the response of the AV node to changes in heart rate is dependent on the three properties explained above, one can incorporate quantitative indices of recovery, facilitation, and fatigue into a mathematical model to predict AV nodal conduction as a function of HA interval. The AV conduction time at each steady state rate represents the sum of the contributions of basal conduction time, AV recovery, fatigue, and

facilitation. These can be stated mathematically at any HA interval as follows:

$$AH_{ss} = AH_{\circ} + A \cdot \exp[-(HA + \Delta HA_{fac})/\tau_{rec}] + \Delta AH_{max} \cdot \exp(-k \cdot HA) + b \quad \text{(Eq. 6)}$$

Where $AH_{\circ} = AH_{\infty}$ (from eq. 1) at a cycle length of 1000 msec, A and τ_{rec} are defined by (recovery) equation 1, ΔHA_{fac} is determined by equation 3, and ΔAH_{max}, k and b are defined by equation 5. In order to estimate the contribution of these processes to the rate-dependent changes in AV conduction time, we used mean values obtained from the results of all experiments studying each process to get overall estimates of $AH_{\circ}$, A, τ_{rec}, ΔHA_{max}, τ_{fac}, ΔAH_{max}, k and b. The predicted changes in AH interval resulting from heart-rate dependent changes in recovery, facilitation, and fatigue are shown as a function of steady state HA interval in Figure 11. At long HA intervals, the AH interval is only determined by basal conduction time ($AH_{\circ}$). The contribution of the three rate sensitive properties (recovery, facilitation, and fatigue) is almost negligible. As the HA interval is decreased further, each of the rate-sensitive nodal properties become progressively more important in determining AV conduction time (AH interval). Application of the recovery equation (1) alone would grossly overestimate the changes in AH interval as steady state HA is reduced. However, because facilitation appears and diminishes the consequences of incomplete recovery, the changes predicted from the combined effects of facilitation and incomplete recovery are much less, and slightly underestimate the AH values at each steady state HA interval. When the effects of fatigue are included to produce an overall prediction based on all rate-dependent properties (solid curve), there is good agreement with experimental data.

DISCUSSION

Lewis and Master (18) first described the functional AV nodal properties now commonly termed recovery, facilitation and fatigue. In a more recent series of studies, Billette has shown that the effects of each of these properties can be isolated using specific pacing protocols (2,4,5,7,8). We now report methods to quantify recovery, facilitation and fatigue, and show that rate-related changes in AV nodal conduction time can be quantitatively attributed to alterations in these three properties.

Comparison with previous studies of recovery, facilitation and fatigue. The curvilinear nature of the recovery process was recognized by Mobitz (23) and Lewis and Master (18). Mobitz used the recovery curve and the concept of the RP-PR relationship to account for Wenckebach periodicity during Type 1 AV block. Exponential functions have been the most commonly used mathematical approximations of the recovery curve (9-11,30,33,37), with time constants of recovery in the same range as reported in the present paper. Our observation that the recovery time constant is not affected by changes in basic cycle length is similar to the findings of Ferrier and Dresel (10). Van der Tweel et al (39) treated the canine atrioventricular node as a periodically perturbed biological oscillator, and used an exponential function with a time constant averaging about 70 msec to characterize the phase-latency curve (analogous to the recovery curve). Other investigators have applied hyperbolic functions to fit the recovery curve (9,32). Chorro et al (9) showed that a direct fit of recovery data to an exponential function was associated with a lesser sum of squared residuals than either of two hyperbolic functions or a linear relationship. On the other hand, the difference was statistically significant only for the linear and one of the

hyperbolic functions, and the exponential was particularly sensitive to error introduced by logarithmic (linear) transformation.

Lewis and Master (18) noted that the leftward shift in the recovery curve resulting from premature cycles reached steady state in less than 6 beats. Billette (4) showed that this effect of premature activation, which he called "facilitation", reaches steady state after one premature cycle. Prior to the present study, no quantitative methods have been put forward to describe this process. We have shown that facilitation results in a parallel leftward shift of the recovery curve (i.e. τ_{rec} and AH_{∞} are unaltered). Furthermore, the magnitude of leftward shift is well-approximated by an exponential function of premature cycle length.

The term "fatigue" was coined by Lewis and Master, who observed that at rates of over 200/min, AV nodal conduction was slowed by up to 10 msec in dogs, even at coupling intervals long enough to allow for full recovery. Ferrier and Dresel (10) showed that, in isolated dog hearts, decreases in basic cycle length resulted in increased AH time of beats with a similar recovery interval. They noted little change over cycle lengths from 800 to 500 msec, but about an 8 msec increase in basal conduction time as cycle length was further decreased to 300 msec. Jenkins and Belardinelli (14) studied AV nodal accomodation in isolated guinea pig hearts. They found that AV node conduction slowing in response to rapid atrial rates consisted of two components: a large first-beat increase in conduction time (corresponding to incomplete recovery), followed by a smaller, secondary phase (corresponding to fatigue) which reached steady state within 20-35 sec. Billette et al (7) studied the functional characteristics of rate-induced fatigue in the isolated rabbit AV node. The latter authors noted a mean of about 12 msec of conduction slowing due to fatigue at rapid rates, with 50% and 90% of maximum

slowing achieved in about 17 and 90 sec respectively. Our observations confirm and extend these previous findings. We found that the fatigue process was well-approximated by an exponential function (Figure 8), and that the time constant of fatigue development (in number of beats) is independent of the HA interval or cycle length of tachycardia (Figure 9). The maximum magnitude of fatigue occurring in our dogs was 15 msec, in line with the observations of previous investigators. All of the changes in the AV recovery curve resulting from fatigue could be attributed to an increase in AH_{∞}, indicating that fatigue can be considered to cause a parallel upward shift of the AV recovery curve (Figure 10). Our results indicate that facilitation and fatigue can be considered rather simply to represent a parallel leftward and a parallel upward shift of the recovery curve respectively.

Comparison with previous models of AV nodal conduction. We predicted steady state AH intervals by using a single equation (eq. 6) incorporating terms representing basal conduction time, recovery, facilitation, and fatigue. The parameters characterizing each functional variable were determined in separate series' of experiments. When the mean parameters were inserted into equation 6, the resulting predictions of rate-dependent changes in AH interval agreed closely with independently obtained experimental data (Figure 11).

Our model represents, to our knowledge, the first attempt to quantify a complete system of rate-dependent AV nodal properties, and to use the resulting mathematical formulation to predict rate-dependent changes in AV node conduction time. The agreement between the predictions of the model and independently-obtained experimental data suggests that the mathematical formulation accurately represents all rate-dependent AV nodal processes functioning under the conditions of our experiments.

Heethaar et al (11) used an empirical representation of the rate and magnitude of AV conduction changes upon altering heart rate to predict AV conduction time of beats produced by random stimulation of the atria of isolated rat hearts. Their model suggests that the time-dependent factors governing AV nodal conduction during random atrial stimulation are analogous to those operating upon abrupt changes in atrial rate. They did not attempt to relate quantitatively the mathematical properties of their model to any specific underlying physiological functions.

Van der Tweel et al (39) showed that the AV nodal conduction of extrasystolic and post-extrasystolic beats fall on the AV recovery curve, which they considered to reflect a modulated biological oscillator. Results are shown from single experiments. Their results for premature extrasystoles are not surprising, since extrasystoles are used to generate the recovery curve. The post-extrasystolic recovery intervals all fall on the flat portion of the recovery curve; agreement might not have been seen for post-extrasystolic beats with shorter coupling intervals, because facilitation would have shifted the recovery curve of the post-extrasystolic beats to the left.

Shrier et al (30) showed that iteration of the AV nodal recovery curve alone would predict Wenckebach periodicity during atrial pacing in man. Their model generated quite different results in individual patients depending on whether the recovery curve used was obtained at a fast or a slow rate. This indicates the existence of important rate-dependent properties other than recovery <u>per se</u>. In fact, we have used a model similar in approach to that of Shrier et al, but incorporating terms to describe the role of facilitation and fatigue, and have achieved much better agreement with observed Wenckebach behaviours (35).

Underlying ionic mechanisms. The cellular and ionic mechanisms of AV nodal recovery have been studied in detail. Paes de Carvalho and de Almeida showed that AV nodal conduction delay tends to occur in midnodal cells (28). Meredith et al (22) demonstrated time-dependent recovery of cellular excitability following full repolarization (underlying "post-repolarization refractoriness") in central nodal (N) cells of isolated rabbit hearts. They related their intracellular findings to the AV node recovery curve. Subsequent detailed microelectrode studies of the AV node have suggested that the conduction delay during premature AV nodal stimulation may be due to electrotonic propagation in the N-NH region, and that both the recovery of source current in the N region and the recovery of excitability in NH cells are critical determinants of the delay (3,6). These properties are in turn likely related to the recovery from inactivation of the slow inward calcium current which underlies phase 0 depolarization and conduction in the AV node (16,41). Consistent with this idea is the similarity between the recovery time constant of AV nodal conduction (50-100 msec) and the reactivation kinetics of L-type calcium currents in isolated canine cardiac Purkinje cells (12) and of slow inward current in multicellular preparations (19).

The mechanisms underlying facilitation and fatigue are much less well-understood. Billette (6) showed that premature activation results in decreased action potential duration of distal nodal cells, which in turn quantitatively accounts for rate-dependent shortening of the AV nodal functional refractory period. Decreased action potential duration would result in a longer diastolic recovery interval for the post-premature beat at any given cycle length, producing a leftward shift in the post-premature recovery curve. In support of this concept, the maximum decrease in action

potential duration reported by Billette is in the same range as the maximum leftward shift of the recovery curve caused by facilitation in our experiments.

Meredith et al (22) showed that rapid pacing-induced fatigue increases the intracellular current threshold of AV nodal cells, and that this change is demonstrable even at long recovery intervals. They did not comment on any concomitant changes in action potential characteristics. Jenkins and Belardinelli (14) noted that an adenosine antagonist reduces AV nodal accomodation during very rapid pacing (cycle length <170 msec) in isolated, perfused guinea pig hearts. This suggests a potential role for adenosine accumulation in the production of AV nodal fatigue, but more detailed studies are necessary before the underlying mechanism(s) of AV nodal fatigue is(are) fully understood.

Limitations of the present study. The recovery variable that we used for analysis was the HA interval, as employed by Billette (2,4,5,7,8), and analogous to the use of the RP interval by Lewis and Master (18) and Mobitz (23). Other workers have challenged the rationale of using the HA recovery variable, and suggested that the AA interval is a more correct index of AV node recovery time. Simson et al (31) showed a changing AH-HA relationship during 4:3 Wenckebach cycles, and argued against the use of the HA interval as a recovery value on this basis. On the other hand, we have shown, using an approach similar to that presented here, that changing degrees of facilitation during Wenckebach cycles can account for the changing AH-HA relationship. Furthermore, Levy et al (17) have shown that, for a given mean atrial cycle length, quite different patterns of atrioventricular conduction can occur depending on whether the ventriculoatrial time is fixed or allowed to vary over consecutive cycles.

The work described in this manuscript was designed to develop quantitative descriptions of recovery, facilitation, and fatigue, and to determine whether the resulting model, which uses HA interval as the recovery variable, can account for rate-dependent changes in AV nodal conduction time. It was not designed as a test of the comparative merits of the HA compared to the AA interval as an index of AV node recovery time. This issue can only be definitively resolved by detailed microelectrode experiments, and it may well be that both AA and HA intervals contribute to the determination of AV nodal properties under different conditions.

Several variables that can potentially alter AV node conduction were not considered in the present model. The site of AV nodal input can affect conduction through the node (1,13,20), and is not considered in our formulation. Our results do not appear to have been affected, perhaps because we stimulated consistently at the same right atrial site. Billette (7) has shown that the site of atrial stimulation does not alter the expression of time-dependent fatigue in the AV node. Changes in AV nodal input could alter the conduction time in a way not accounted for by our model, and would most likely occur as a result of ectopic atrial activations, or very premature beats that block in the primary AV nodal input and obtain access <u>via</u> a secondary input pathway.

Autonomic tone can vary AV nodal conduction, and its influence was eliminated in this study by combined beta adrenergic receptor blockade and vagal division. Alpha adrenergic stimulation does not alter AV nodal conduction (36). We prevented autonomic effects in order to avoid complexities introduced by changes in autonomic balance resulting from rapid pacing, premature stimulation, etc. Autonomic influences can strongly affect

rate-dependent AV nodal properties (26,27), but their potential role must be studied under carefully-controlled conditions to avoid complex interactions.

Potential importance. The model developed in this paper represents, to our knowledge, the first attempt to quantify a complete system of rate-dependent AV nodal properties, and to then apply the resulting equations to predict prospectively rate-dependent changes in AV nodal function. Its success suggests that, at least at steady state during 1:1 atrial pacing, rate-dependent changes in AV node conduction can be entirely explained on the basis of AV nodal recovery, facilitation and fatigue.

The quantitative descriptors of specific properties that we have developed can be a useful tool to investigate the effects of interventions on individual dynamic properties of the AV node. Using this approach, we have shown that vagal stimulation slows AV nodal recovery, attenuates facilitation, and increases fatigue (26). These discrete changes account for the important rate-dependency of the negative dromotropic effects of the vagi on AV nodal conduction (26,40). Conversely, sympathetic stimulation accelerates AV nodal recovery and attenuates fatigue, while leaving facilitation unaltered (27) Interventions which alter AV nodal properties have generally been considered in a static sense, without evaluating the important changes they may produce in the ways that the AV node responds to an altered input rate. Altered dynamic AV nodal properties may be an important mechanism whereby interventions alter nodal conduction. Lewis and Master (18) suggested that vagal stimulation may slow AV nodal recovery, and Ferrier and Dresel (10) found that adrenergic stimulation with epinephrine reduces AV nodal fatigue. Our model allows for such effects to be precisely quantified, and for the relative importance of changes in recovery, facilitation, and fatigue produced by an intervention to be determined.

The approach presented here may potentially allow for detailed quantitative study of rate-dependent AV nodal properties in man. In the dog, fatigue contributed modestly to rate-dependent AV nodal conduction slowing (Figure 11). Incomplete recovery is the most important determinant of conduction slowing, and its impact at any rate is attenuated by the presence of facilitation. It must be remembered that the effect of facilitation is mediated solely by a leftward shift (i.e. attenuation) of incomplete recovery-facilitation does not accelerate baseline conduction per se. Changes in some or all of these variables may be important in accounting for clinical impairments of AV node conduction, an issue that can potentially addressed by applying the methods developed in this manuscript. Changes in rate-dependent properties, eg. via autonomic tone or other neurotransmitters, may be important determinants of the occurrence and/or termination of tachyarrhythmias involving the AV node. Finally, the development of interventions which selectively alter specific rate-dependent properties might be a promising new approach in the treatment of supraventricular tachyarrhythmias.

ACKNOWLEDGEMENTS

The authors thank Lise de Repentigny for typing the manuscript, and Squibb Pharmaceuticals, Canada, for donating the nadolol that we used to produce beta blockade.

REFERENCES

1. Batsford, W.P., M. Akhtar, A.R. Caracta, M.E. Josephson, S.F. Seides, and A.N. Damato. Effect of atrial stimulation site of the electrophysiological properties of the atrioventricular node in man. Circulation 50: 283-292, 1974.

2. Billette, J. Preceding His-atrial interval as a determinant of atrioventricular nodal conduction time in the human and rabbit heart. Am. J. Cardiol. 38: 889-896, 1976.

3. Billette, J, M.J. Janse, and F.J.L. Van Capelle. Cycle length-dependent properties of AV nodal activation in rabbit hearts. Am. J. Physiol. 231: 1129-1139, 1976.

4. Billette, J. Short time constant for rate-dependent changes of atrioventricular conduction in dogs. Am. J. Physiol. 241: H26-H33, 1981.

5. Billette, J., J.P. Gossard, L. Lepanto, and R. Cartier. Common functional origin for simple and complex responses of atrioventricular node in dogs. Am. J. Physiol. 251: H920-H925, 1986.

6. Billette, J. Atrioventricular nodal activation during periodic premature stimulation of the atrium. Am. J. Physiol. 252: H163-H177, 1987.

7. Billette, J., R. Métayer, and M. St-Vincent. Selective functional characteristics of rate-induced fatigue in rabbit atrioventricular node. Circ. Res. 62: 790-799, 1988.

8. Billette, J., and R. Métayer. Origin, domain, and dynamics of rate-induced variations of functional refractory period in rabbit atrioventricular node. Circ. Res. 65: 164-175, 1989.

9. Chorro, F.J., R. Ruiz-Granell, E. Casadan, R. Garcia-Civera, L. Such, and V. Lopez-Merino. Mathematical descriptions of AV nodal function curves in dogs. PACE 11: 679-686, 1988.

10. Ferrier, G.R., and P.E. Dresel. Relationship of the functional refractory period to conduction in the atrioventricular node. Circ. Res. 35: 204-214, 1974.

11. Heethaar, R.M., J.J.D. Van Der Gon, and F.L. Meijler. Mathematical model of A-V conduction in the rat heart. Cardiovasc. Res. 7: 105-114, 1973.

12. Hirano, Y., H.A. Fozzard, and C.T. January. Characteristics of L- and T-type Ca^{2+} currents in canine cardiac Purkinje cells. Am. J. Physiol. 256: H1478-H1492, 1989.

13. Janse, M.J. Influence of the direction of the atrial wave front on A-V nodal transmission in isolated hearts of rabbits. Circ. Rec. 25: 439-449, 1969.

14. Jenkins, J.R., and L. Belardinelli. Atrioventricular nodal accomodation in isolated guinea pig hearts: physiological significance and role of adenosine. Circ. Res. 63: 97-116, 1988.

15. Karpawich, P.P., P.C. Gillette, R.M. Lewis, A. Zinner, and D.G. McNamara. Chronic epicardial His bundle recordings in awake nonsedated dogs: A new method. Am. Heart J. 105: 16-21, 1983.

16. Kokubun, S., M. Nishimura, A. Noma, and H. Irisawa. Membrane currents in the rabbit atrioventricular node cell. Pflügers Arch. 393: 15-22, 1982.

17. Levy, M.N., P.H. Martin, H. Zieske, and D. Adler. Role of positive feedback in the atrioventricular nodal Wenckebach phenomenon. Circ. Res. 34: 697-710, 1974.

18. Lewis, T., and A.M. Master. Observations upon conduction in the mammalian heart: AV conduction. Heart 12: 209-269, 1925.

19. McDonald, T.F. The slow inward current in the heart. Annu. Rev. Physiol. 44: 425-434, 1982.

20. Mazgalev, T., L.S. Dreifus, H. Iinuma, and E.L. Michelson. Effects of the site and timing of atrioventricular nodal input on atrioventricular conduction in the isolated perfused rabbit heart. Circulation 70: 748-759, 1984.

21. Mazgalev, T., L.S. Dreifus, and E.L. Michelson. A new mechanism for atrioventricular nodal gap-vagal modulation of conduction. Circulation 79: 417-430, 1989.

22. Meredith, B.J., C. Mendez, W.J. Mueller, and G.K. Moe. Electrical excitability of atrioventricular nodal cells. Circ. Res. 23: 69-85, 1968.

23. Mobitz, W. Uber die unvollständige störung der erregungs-überleitung zwischen vorhof und kammer des menschlichen herzens. Zeit Gesamte Exp. Med. 41: 180-237, 1924.

24. Moe, G.K., R.W. Childers, and J. Merideth. Appraisal of "supernormal" AV conduction. Circulation 38: 5-28, 1968.

25. Nayebpour, M., M. Talajic, and S. Nattel. Functional analysis of rate-dependent properties of AV node in anesthetized dogs (Abstract). J. Am. Coll. Cardiol. 15: 201A, 1990.

26. Nayebpour, M., M. Talajic, C. Villemaire, and S. Nattel. Vagal modulation of the rate-dependent properties of the AV node. Circ. Res. 1990 (in press).

27. Nayebpour, M., M. Talajic, and S. Nattel. Autonomic modulation of the frequency-dependent properties of the AV node (Abstract). Clin. Invest. Med. 1990 (in press).

28. Paes de Carvalho, A., and D.F. de Almeida. Spread of activity through the atrioventricular node. Circ. Res. 8: 801-809, 1960.

29. Sachs, L. Applied statistics. New York, Springer-Verlag, 1984.

30. Shrier, A., H. Dubarsky, M. Rosengarten, M.R. Guevara, S. Nattel, and L. Glass. Prediction of complex atrioventricular conduction rhythms in humans with use of the atrioventricular nodal recovery curve. Circulation 76: 1196-1205, 1987.

31. Simson, M.B., J.F. Spear, and E.N, Moore. Electrophysiological studies in AV nodal Wenckebach cycles. Am. J. Cardiol. 41: 244-258, 1978.

32. Simson, M.B., J.F. Spear, and E.N. Moore. Stability of an experimental atrioventricular reentrant tachycardia in dogs. Am. J. Physiol. 240: H947-H953, 1981.

33. Talajic, M., and S. Nattel. Frequency-dependent effects of calcium antagonists on atrioventricular conduction and refractoriness: demonstration and characterization in anesthetized dogs. Circulation 74: 1156-1167, 1986.

34. Talajic, M., D. Papadatos, C. Villemaire, M. Nayebpour, and S. Nattel. The antiarrhythmic actions of diltiazem during experimental AV reentrant tachycardias - Relationship to use-dependent calcium channel blocking properties. Circulation 81: 334-342, 1990.

35. Talajic, M., D. Papadatos, L. Glass, C. Villemaire, and S. Nattel. Mechanism of dynamic changes in Wenckebach-type AV block (Abstract). J. Am. Coll. Cardiol. 15: 201A, 1990.

36. Talajic, M., C. Villemaire, and S. Nattel. Electrophysiological effects of α-adrenergic stimulation. PACE 13: 578-582, 1990.

37. Teague, S., S. Collins, D. Wu, P. Denes, K. Rosen, and R. Arzbaecher. A quantitative description of normal AV nodal conduction curve in man. J. Appl. Physiol. 40: 74-78, 1976.

38. Van Capelle, F.J.L., J.C. du Perron, and D. Durrer. Atrioventricular conduction in isolated rat heart. Am. J. Physiol. 221: 284-290, 1971.

39. Van Der Tweel, I., J.N. Herbschleb, C. Borst, and F.L. Meijler. Deterministic model of the canine atrio-ventricular node as a periodically perturbed, biological oscillator. J. Appl. Cardiol. 1: 157-173, 1986.

40. Wallick, D.W., P.J. Martin, Y. Masuda, and M.N. Levy. Effects of autonomic activity and changes in heart rate on atrioventricular conduction. Am. J. Physiol. 243: H523-H527, 1982.

41. Zipes, D.P., and C. Mendez. Action of manganese ions and tetrodotoxin on atrioventricular nodal transmembrane potentials in isolated rabbit hearts. Circ. Res. 32: 447-454, 1973.

Table 1. Quantitative Analysis of Rate-Induced Fatigue on AV Nodal Conduction Time of Premature Beats

	BCL (msec)	HA (msec)	AH_∞ (msec)	τ_{rec} (msec)	HA_{125} (msec)	HA_{125} cor* (msec)
Slow Rate	940±40	866±42	54.8±7	47±6	104±11	104±11
Intermediate Rate	440±21	380±22	61.3±6**	43±7	118±3	110±3
Fast Rate	318±15	234±22	66.4±7**	50±6	116±11	103±13

Abbreviations: BCL = basic cycle length; HA = steady-state HA interval at the basic cycle length; HA_{125} = HA interval corresponding to AH interval of 125 msec (see eq. 2 in text); AH_∞ = AH interval at infinite recovery time according to eq. 1; τ_{rec} = recovery time constant from eq. 1.

* HA_{125} corrected for the magnitude of fatigue, as shown in Fig. 9.

** $p<0.001$ compared to corresponding value at slow rate.

FIGURE LEGENDS

Figure 1. Experimental protocols. Sequences A-D represent the various stimulation protocols used to characterize different functional properties of the AV node. Protocol A shows the last beat at a constant basic cycle length, and one premature (A_1A_2) test cycle. Protocol B was used to characterize AV node facilitation. A series of 15 beats at a cycle length of 1000 msec was followed by a facilitation cycle (A_1A_2) and by a premature test cycle. Protocol C was used to determine the time and rate dependence of the development of fatigue. After 5 minutes of pacing at a cycle length of 1000 msec, a tachycardia with a constant HA interval was initiated, and changes in AH interval were observed. Tachycardias were induced over a wide range of selected HA intervals. Protocol D was used to determine the effects of fatigue on the recovery curve. Thirty beats with a reduced HA interval were followed by a single facilitation-dissipating pause with an H_1A_2 interval equal to the HA interval at the baseline cycle length. The facilitation-dissipating pause was followed by a premature test cycle to evaluate the recovery curve.

Figure 2. Wenckebach cycle lengths (WBCL) were measured about every 20 minutes over the course of each experiment. The constancy of WBCL indicates the stability of the preparation.

Figure 3. Recovery curves at two basic cycle lengths in one experiment.

Figure 4. Recovery curves for activations preceded by a facilitation cycle (Protocol B in Figure 1). As the A_1A_2 (facilitation cycle length) decreases, the recovery curve of A_3 shifts to progressively shorter values of H_2A_3. Top: Examples of 5 recovery curves from one experiment, each fitted with a single exponential relationship. Bottom: The same data are fitted with an exponential curve, but AH_∞ and tau are fixed at mean values obtained from all 10 curves in that experiment. The HA value at which the AH interval was 125 msec (horizontal dashed line) or HA_{125}, was used as an index for the degree of left shift caused by facilitation.

Figure 5. Effects of A_1A_2 interval (facilitation cycle length) on the variables defining recovery curves. HA_{125} decreased with decreasing A_1A_2 intervals, while AH_∞ and τ_{rec} were unchanged. HA_{125} was an exponential function of A_1A_2 interval, as shown by the fitted solid curve. (*p<.05, **p<.01, ***p<.001 vs HA_{125} at the basic cycle length).

Figure 6. Shifts in HA interval as a result of facilitation, plotted against the H_1A_2 interval of the facilitation cycle. ΔHA indicates the decrease in HA_{125} from the value at a cycle length of 1000 msec. The solid line shows the best monoexponential curve fit to observed data.

Figure 7. Changes in the AV recovery curve after 1-4 facilitation cycles. One facilitation cycle shifted the AV recovery curve to the left, relative to a curve at the same basic cycle length without an intervening facilitation cycle (filled circles). Additional facilitation cycles with the same cycle length produced no additional changes in recovery.

Figure 8. Changes in the AH interval after the onset of atrial tachycardia with a constant HA interval. Values are shown as changes in AH interval from the second beat of tachycardia through steady state. Since recovery effects are constant from beat 1 (constant HA), and facilitation effects reach steady state at beat 2, the changes in AH interval (ΔAH) are due completely to AV nodal fatigue. Each set of data was fitted by a simple exponential (solid lines) to calculate the time constant and magnitude of fatigue. Arrow shows the time constant of fatigue at each HA interval.

Figure 9. Top: Magnitude of changes in AH interval due to fatigue at steady state as a function of HA interval and cycle length. Solid line shows exponential curve fit to data. Where error bars are absent, they fall within the range of the symbol. Bottom: Time constant (tau) for the onset of fatigue (τ_{fat} in eq. 4 of text). The rate of tachycardia did not change the time constant of the induction of fatigue.

Figure 10. Effects of rate-induced fatigue on the AV recovery curve. A single facilitation-dissipating cycle was applied prior to the test beat at the fast rate in order to study the selective effects of fatigue on the recovery curve. Fatigue caused an upward shift of the recovery curve (closed diamond). The solid lines are the best fit to the data using eq. 1 of the text. The dashed line shows the recovery curve obtained at the fast rate (fatigue-affected recovery curve), when the magnitude of the upward shift has been subtracted. The close agreement with results at a slow rate suggests that fatigue produces a parallel upward shift of the curve.

Figure 11. Mathematical modeling to identify the relative contribution of each process (recovery, facilitation, and fatigue) to changes in AH interval (ΔAH) over baseline (at BCL 1000 msec) occurring as a result of increases in cardiac rate. As HA interval decreased at the faster rates, both fatigue and recovery components tended to increase AH interval, while facilitation attenuated the effect of recovery, tending to improve conduction. The lines are the predicted values using the mathematical model described in the text. Overall predictions resulting from the combined effects of recovery, facilitation, and fatigue (equation 6) are shown by the solid line, while observed values (mean+SE) are shown by the open circles.

FIGURE 2.1

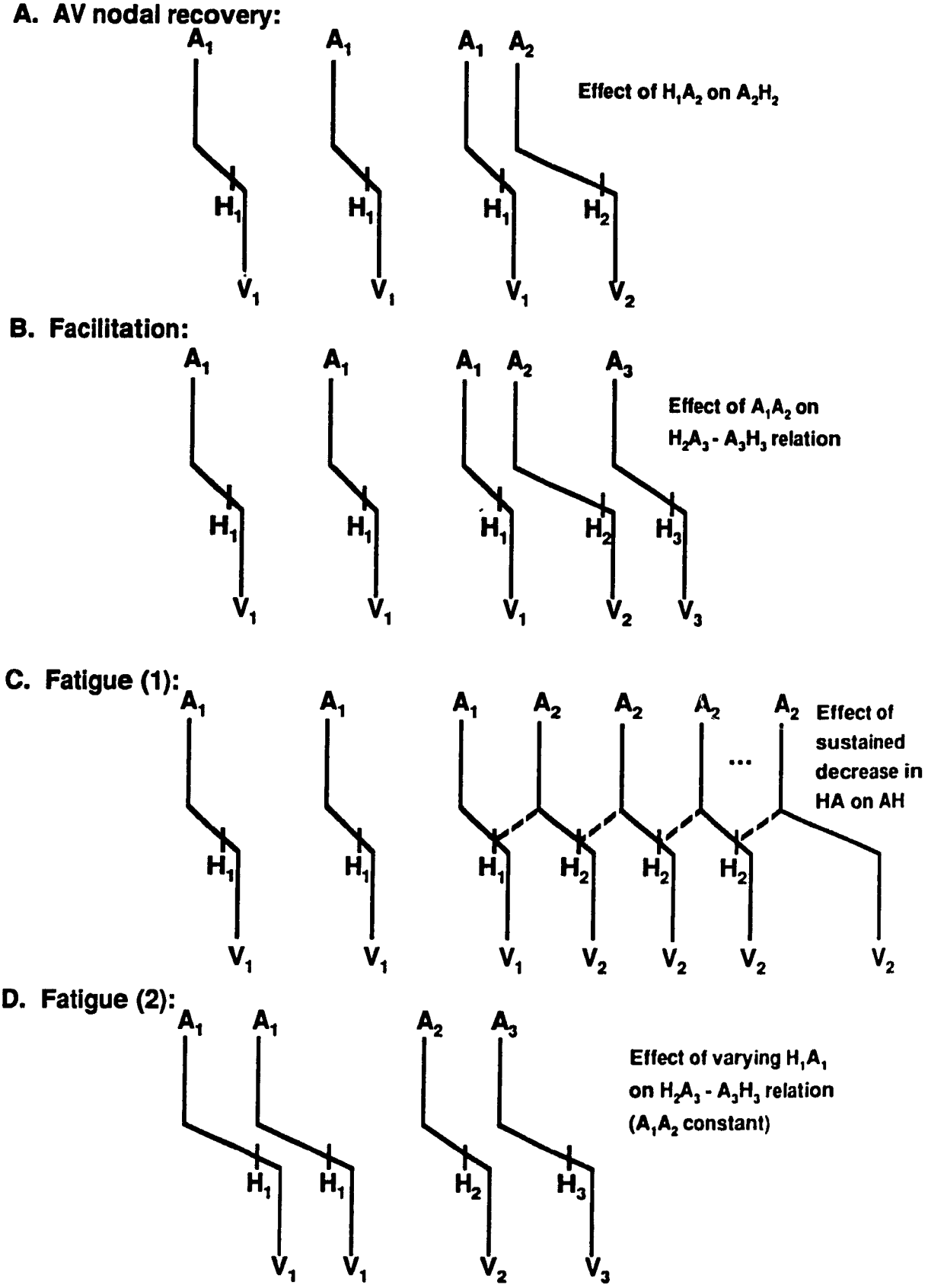
A. AV nodal recovery:
A1
H1
V1
A1
H1
V1
A1 A2
H1 H2
V1 V2
Effect of H1A2 on A2H2
B. Facilitation:
A1
H1
V1
A1
H1
V1
A1 A2 A3
H1 H2 H3
V1 V2 V3
Effect of A1A2 on
H2A3 - A3H3 relation
C. Fatigue (1):
A1
H1
V1
A1
H1
V1
A1 A2 A2 A2 A2
H1 H2 H2 H2
V1 V2 V2 V2 V2
Effect of
sustained
decrease in
HA on AH
D. Fatigue (2):
A1 A1
H1 H1
V1 V1
A2 A3
H2 H3
V2 V3
Effect of varying H1A1
on H2A3 - A3H3 relation
(A1A2 constant)

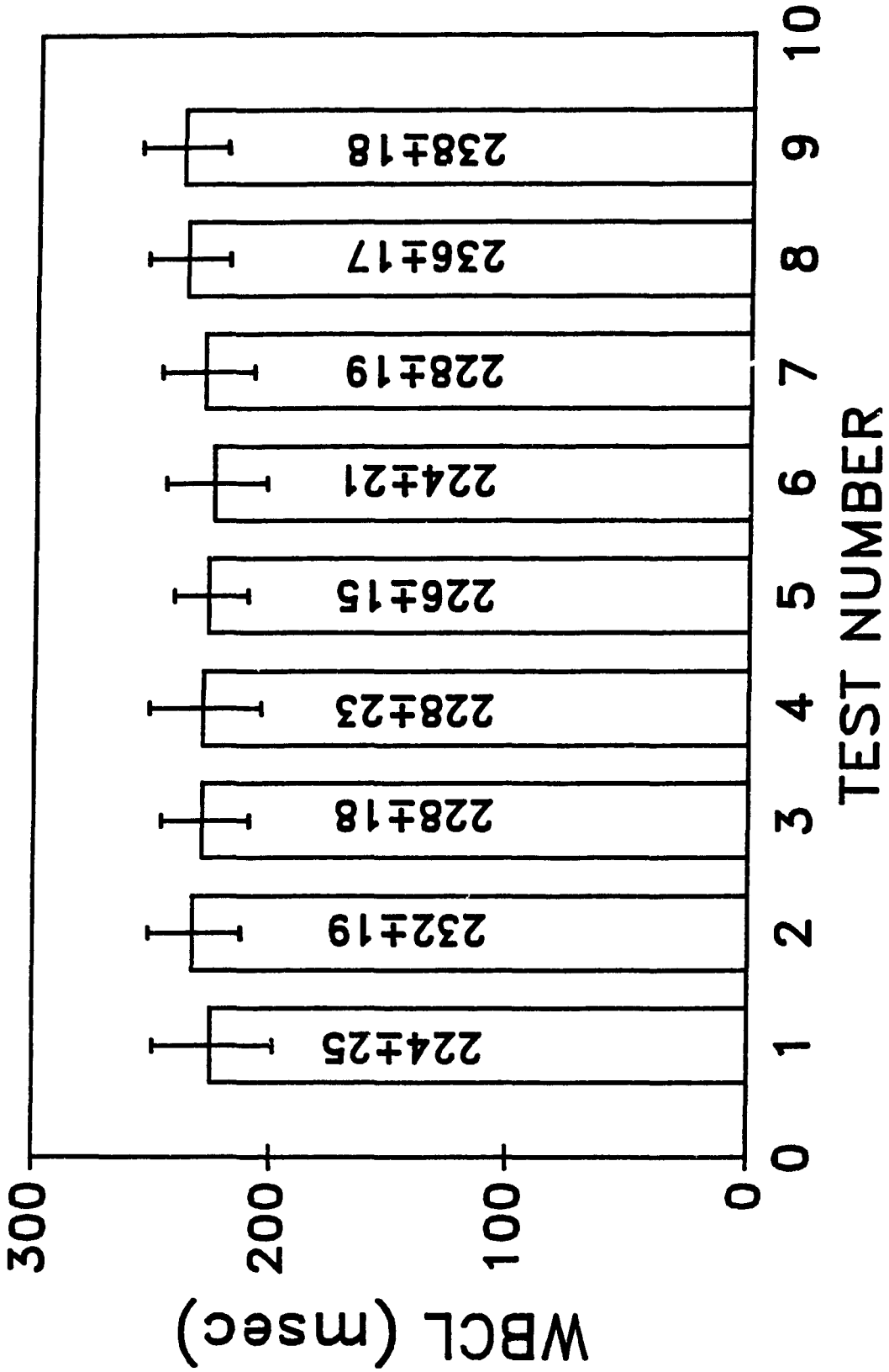
WBCL (msec)
300
200
100
0
0
1
2
3
4
5
6
7
8
9
10
TEST NUMBER
224±25
232±19
228±18
228±23
226±15
224±21
228±19
236±17
238±18

FIGURE 2.2

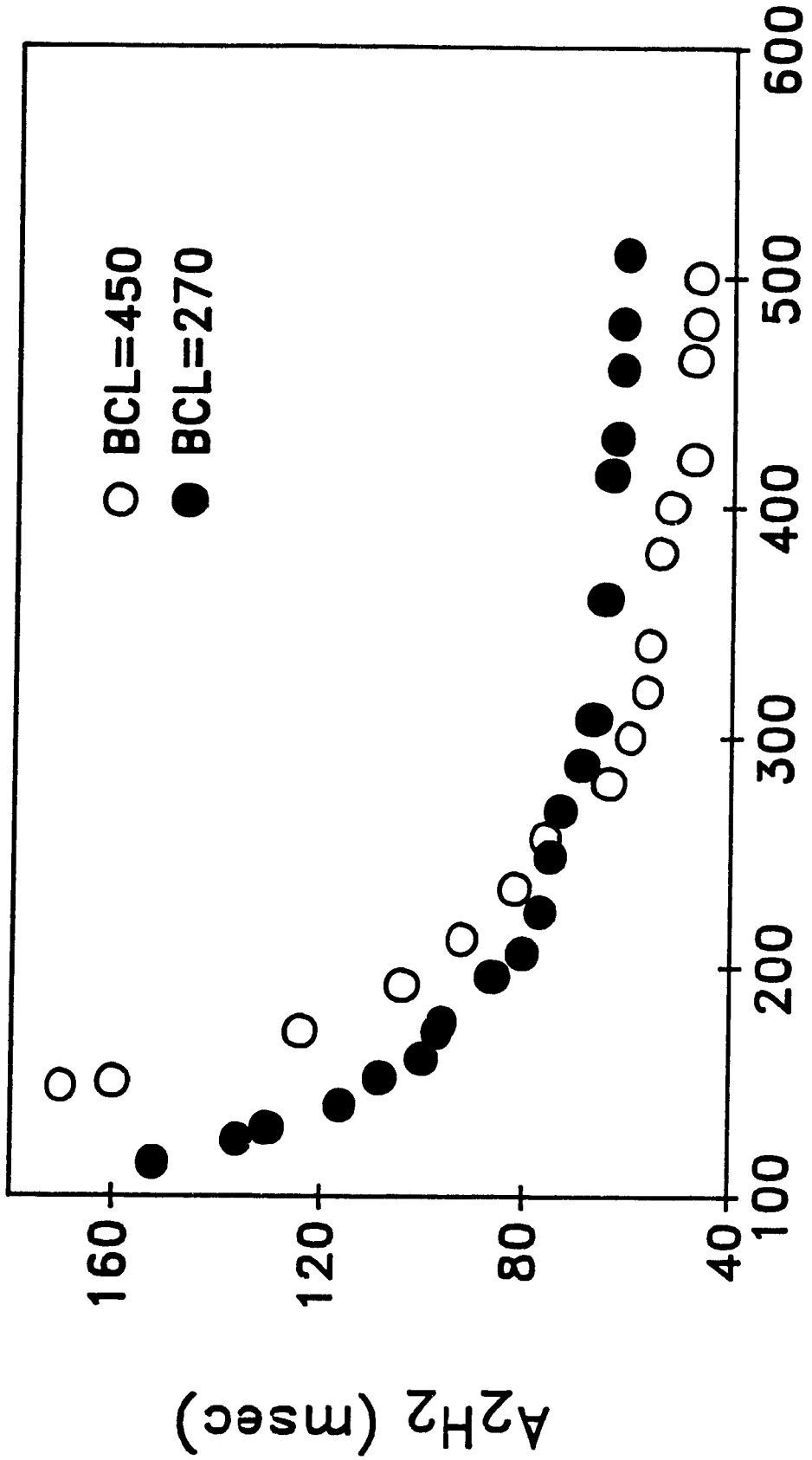
BCL=450
BCL=270
160
120
80
40
100
200
300
400
500
600
A2H2 (msec)
H1A2 (msec)

FIGURE 2.3

FIGURE 2.4

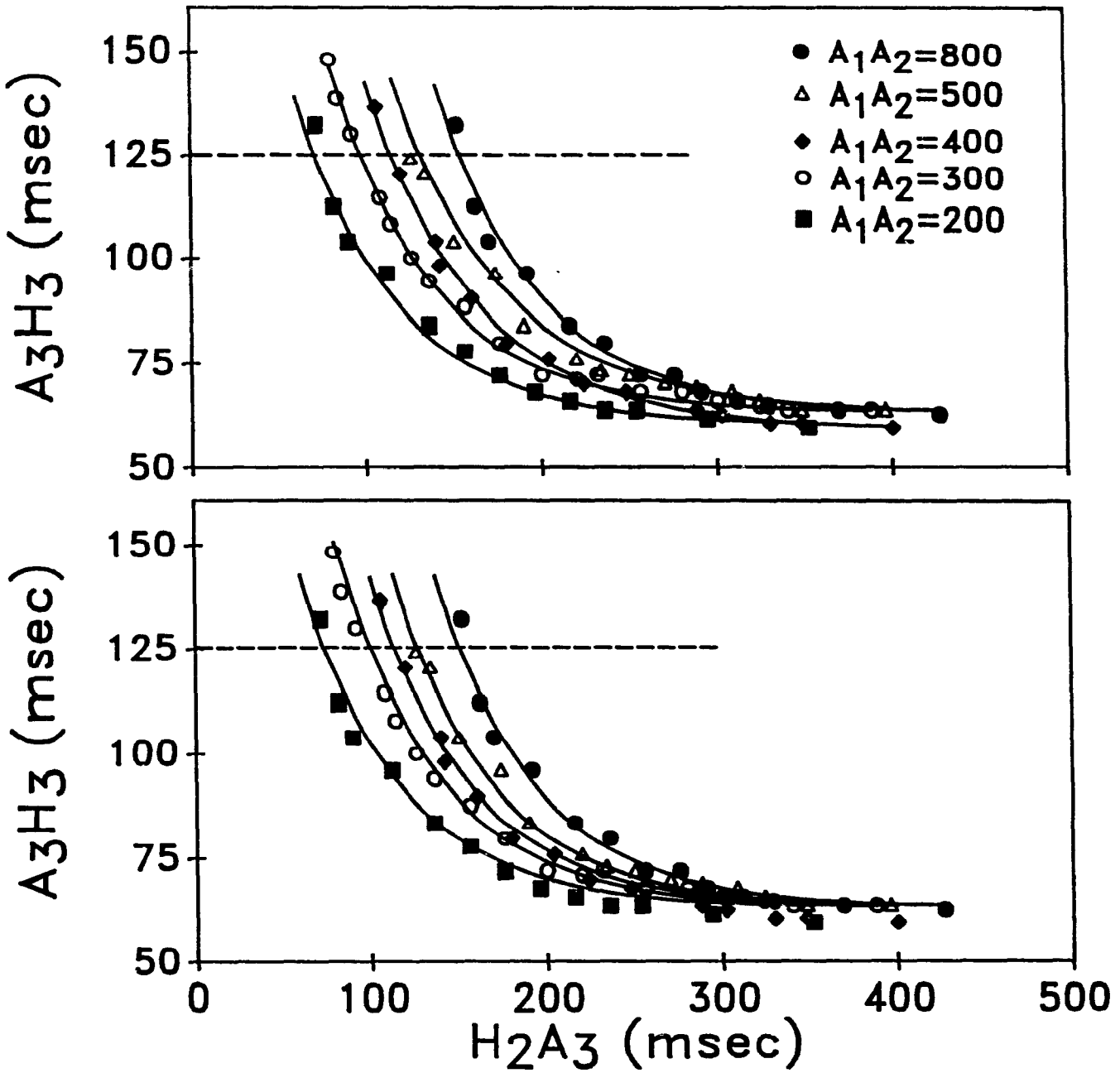
150
125
100
75
50
A3H3 (msec)
A1A2=800
A1A2=500
A1A2=400
A1A2=300
A1A2=200
150
125
100
75
50
A3H3 (msec)
0
100
200
300
400
500
H2A3 (msec)

FIGURE 2.5

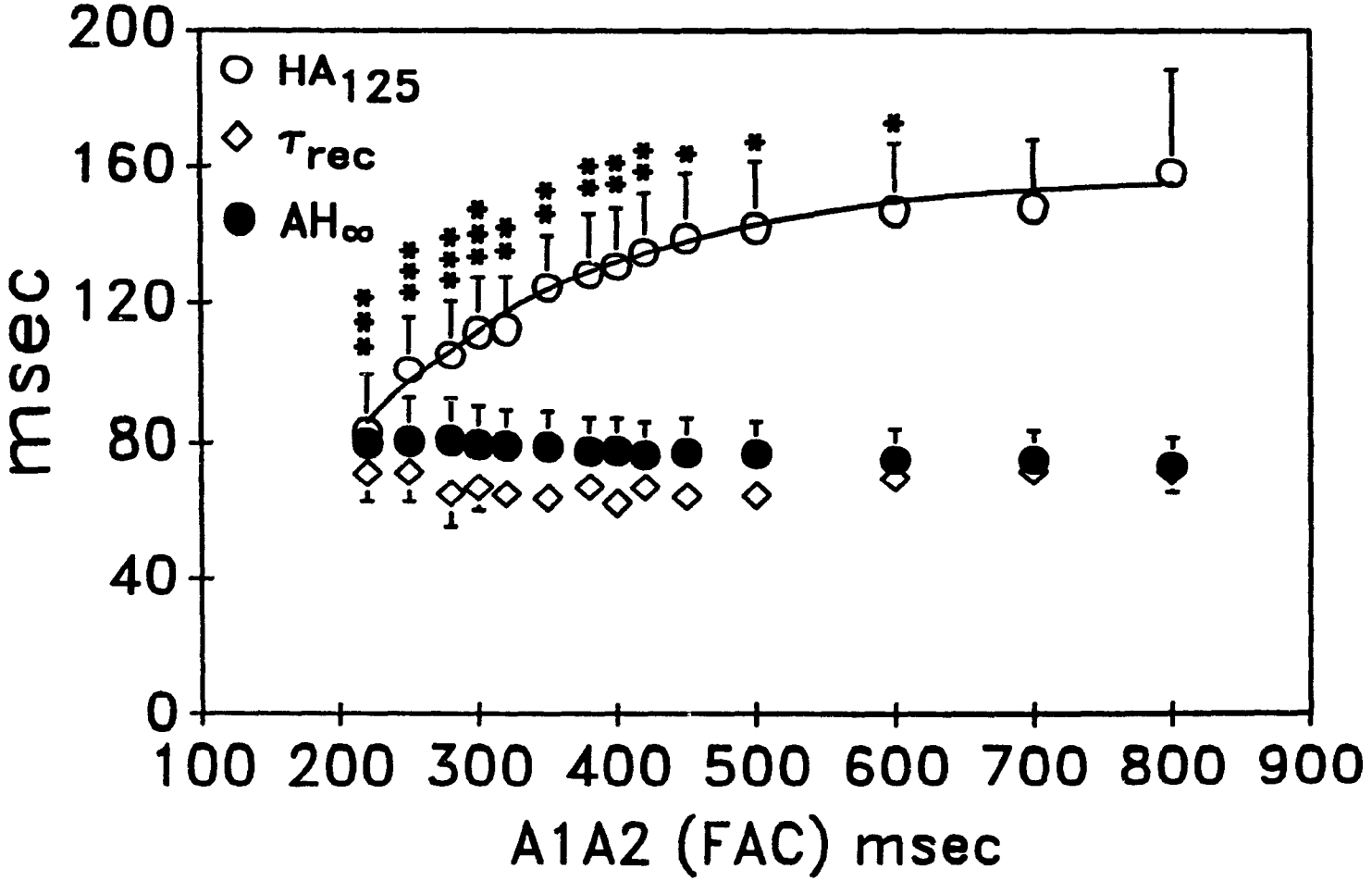
200
160
120
80
40
0
msec
HA125
τrec
AH∞
100 200 300 400 500 600 700 800 900
A1A2 (FAC) msec

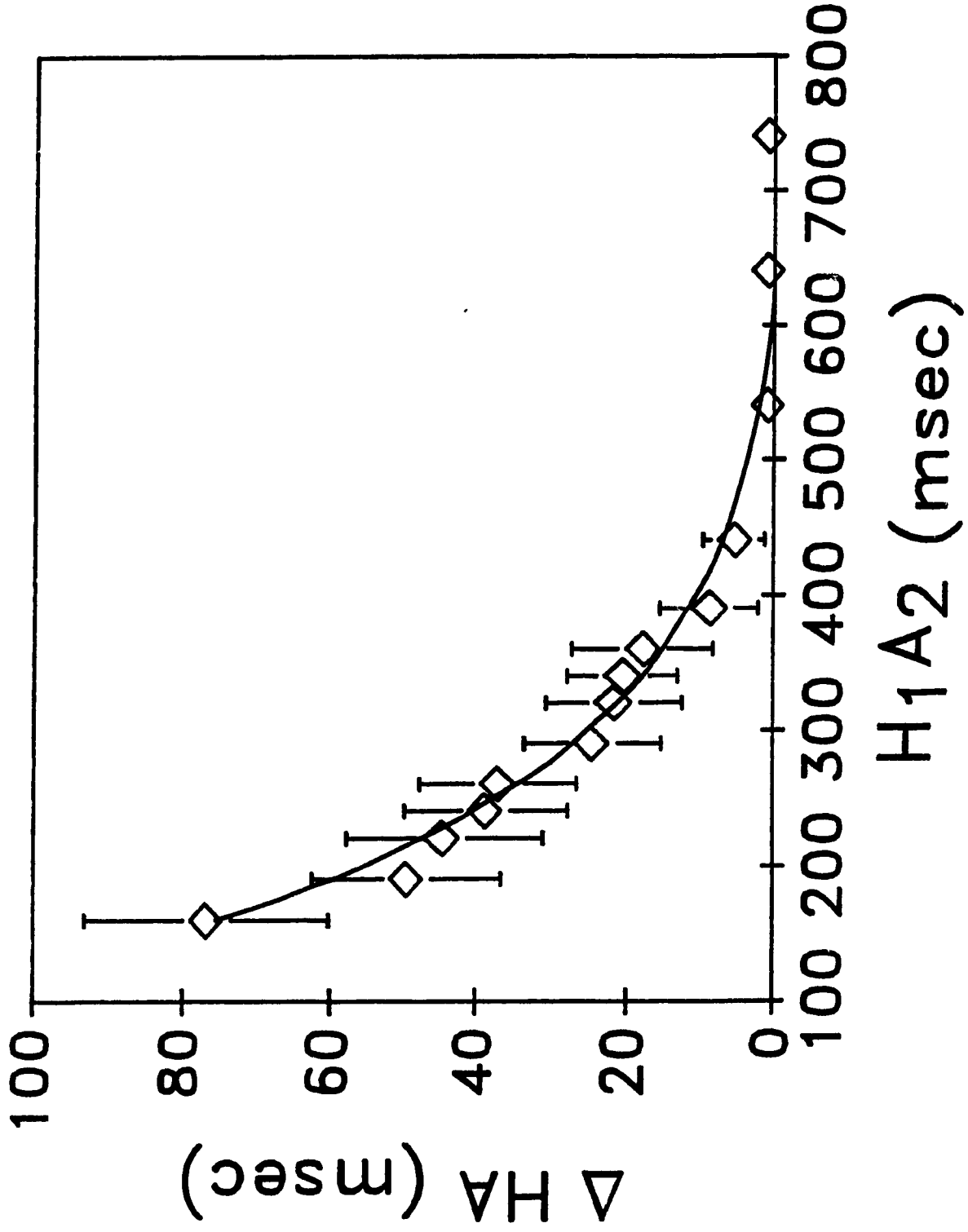
Δ HA (msec)
100
80
60
40
20
0
100 200 300 400 500 600 700 800
H1A2 (msec)

FIGURE 2.6

FIGURE 2.7

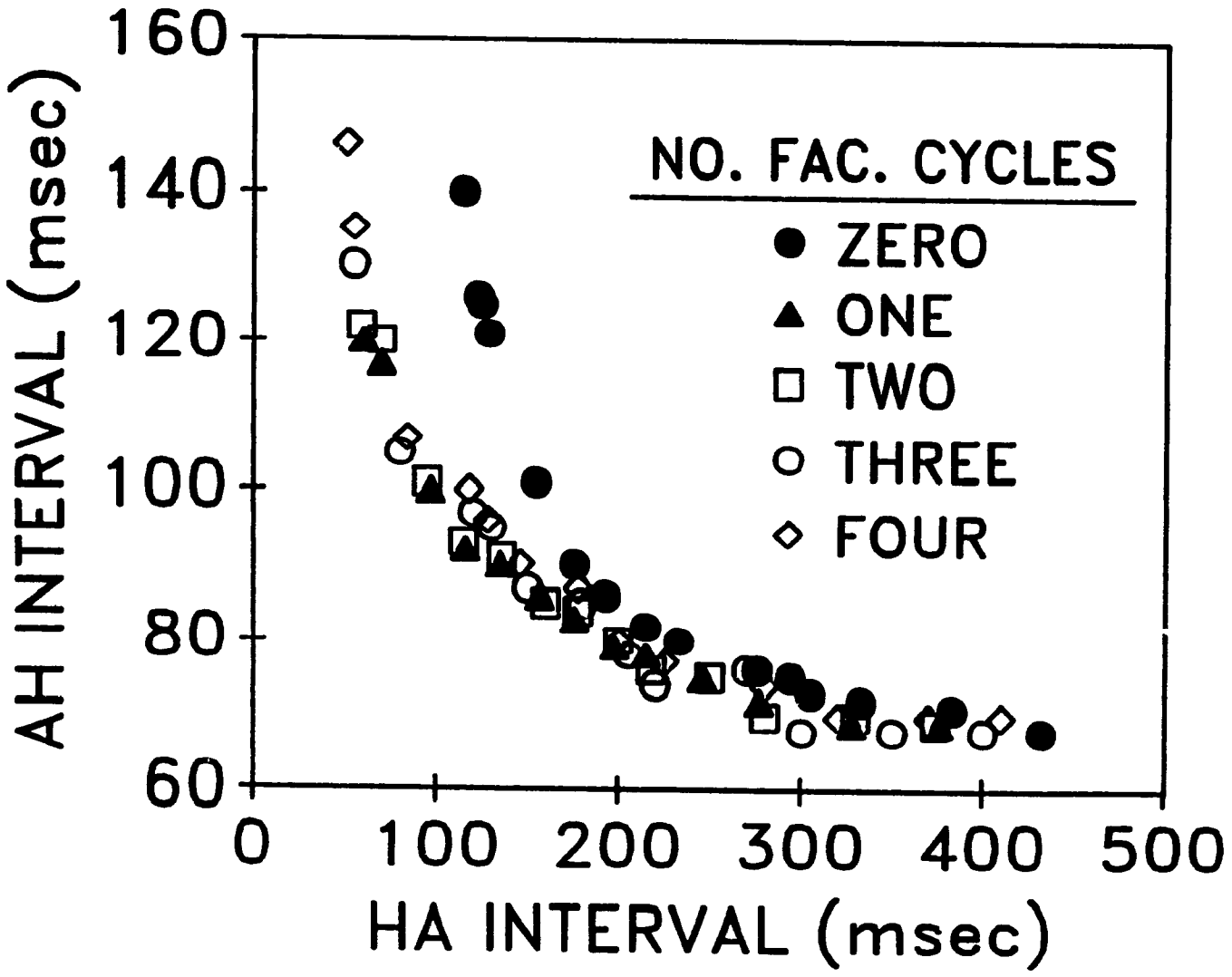
160
140
120
100
80
60
AH INTERVAL (msec)
0
100
200
300
400
500
HA INTERVAL (msec)
NO. FAC. CYCLES
ZERO
ONE
TWO
THREE
FOUR

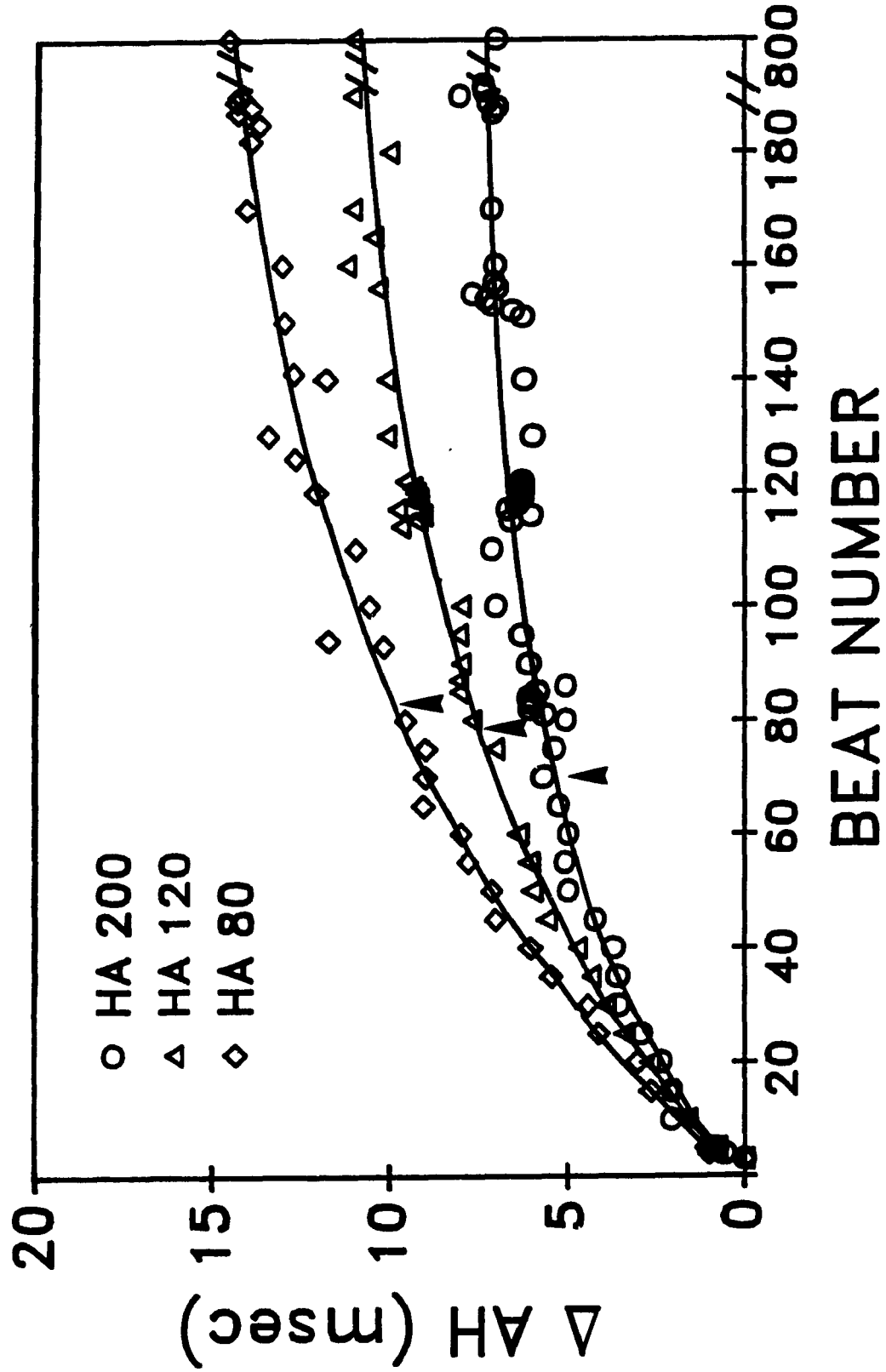
Δ AH (msec)
20
15
10
5
0
20
40
60
80
100
120
140
160
180
800
BEAT NUMBER
HA 200
HA 120
HA 80

FIGURE 2.8

FIGURE 2.9

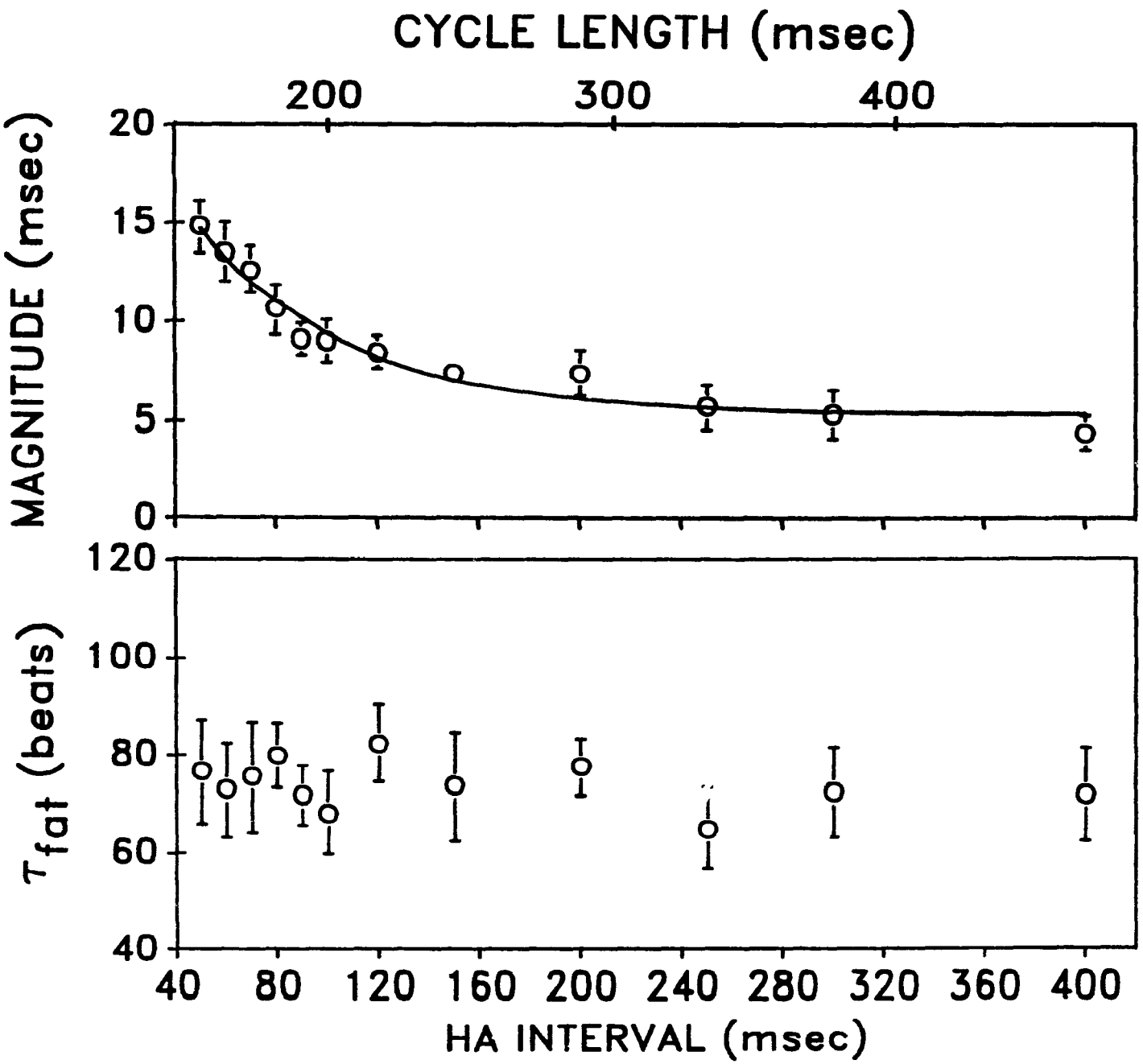
CYCLE LENGTH (msec)
200
300
400
MAGNITUDE (msec)
20
15
10
5
0
120
100
80
60
40
τ_{fat} (beats)
40
80
120
160
200
240
280
320
360
400
HA INTERVAL (msec)

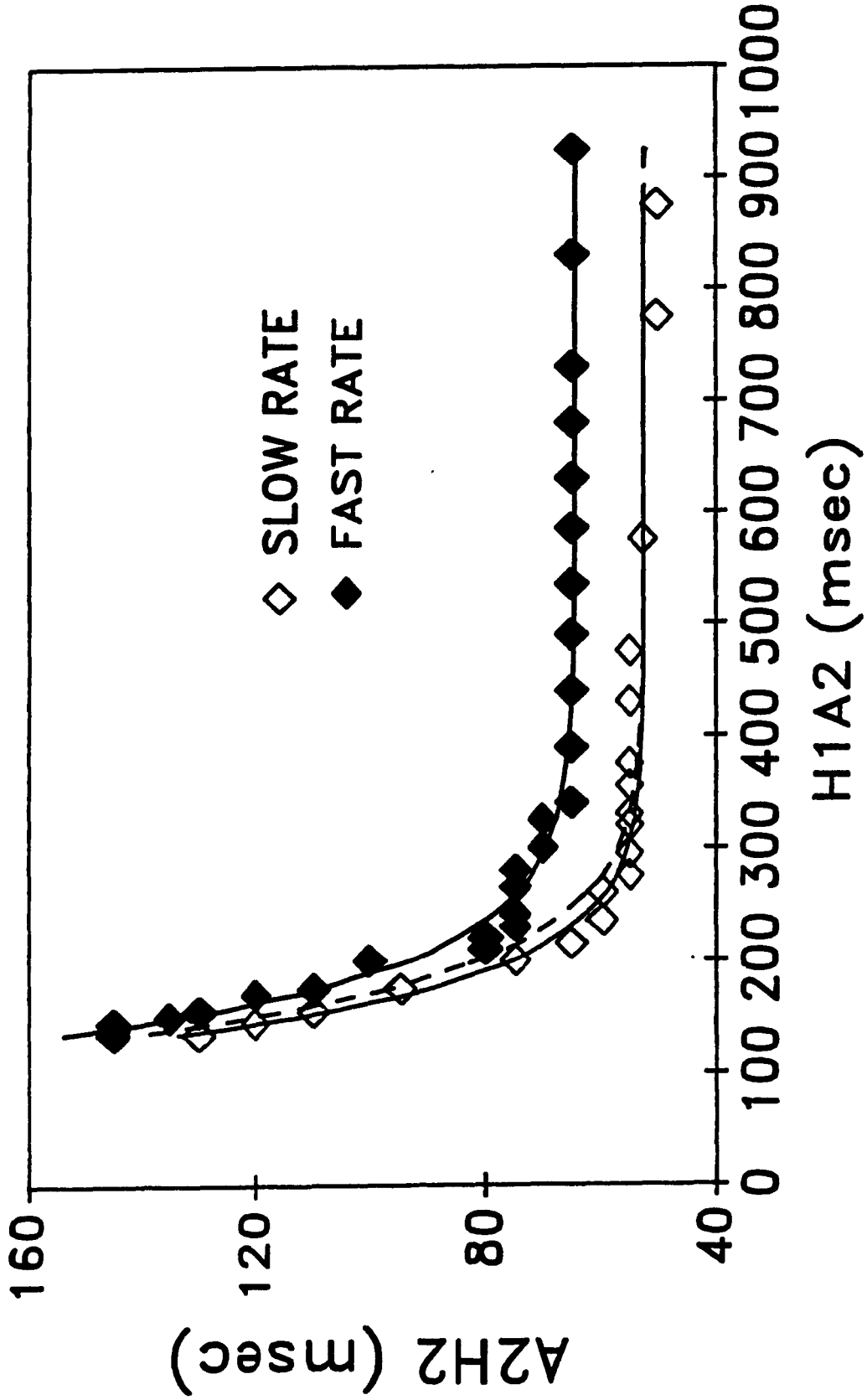
A2H2 (msec)
160
120
80
40
0 100 200 300 400 500 600 700 800 900 1000
H1A2 (msec)
SLOW RATE
FAST RATE

FIGURE 2.10

FIGURE 2.11

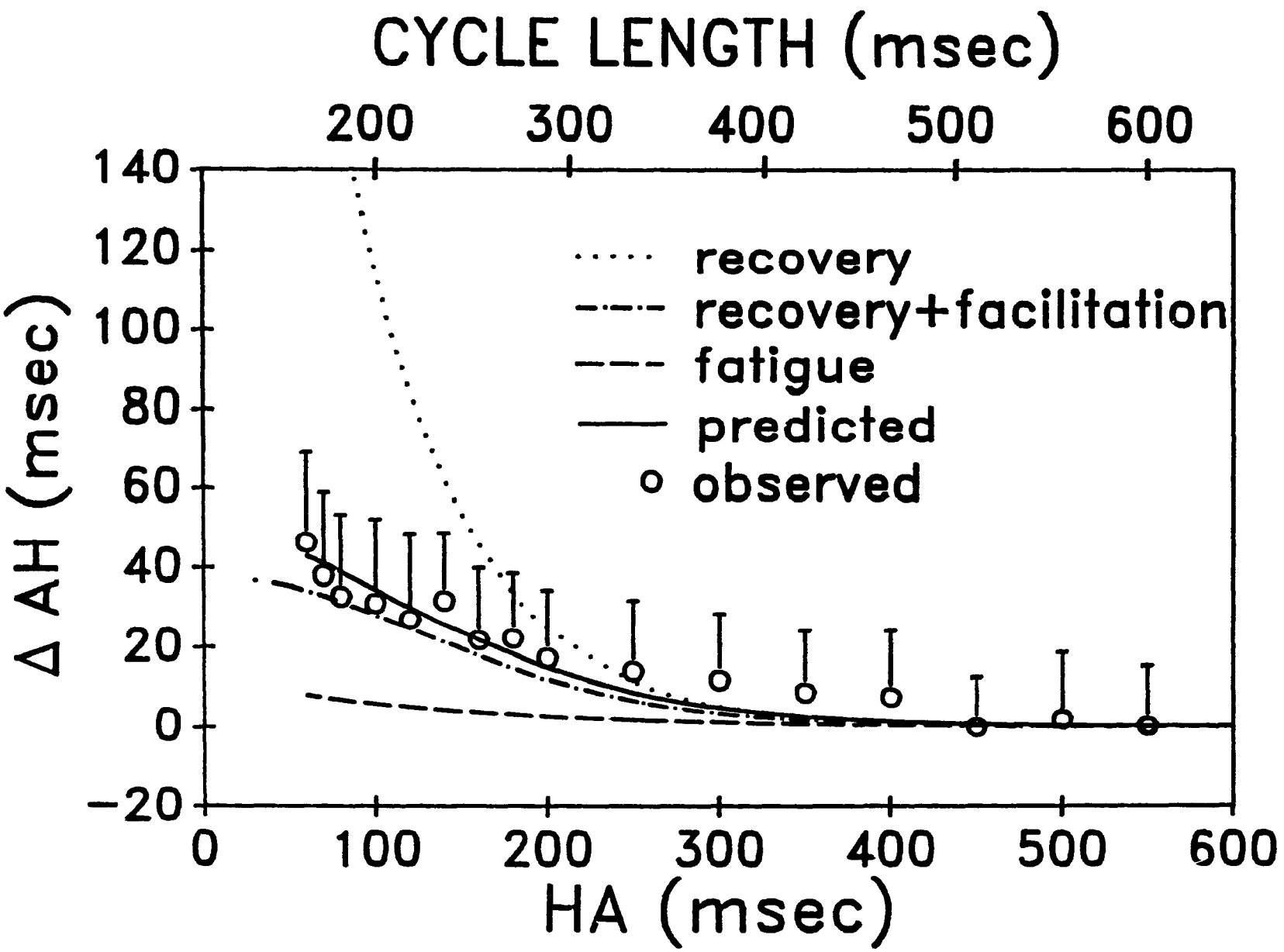
CYCLE LENGTH (msec)
200
300
400
500
600
140
120
100
80
60
40
20
0
−20
Δ AH (msec)
recovery
recovery+facilitation
fatigue
predicted
observed
0
100
200
300
400
500
600
HA (msec)

CHAPTER 3

Vagal Modulation of the Rate-Dependent Properties of the Atrioventricular Node

Vagal Modulation of the Rate-Dependent Properties of the Atrioventricular Node

Mohsen Nayebpour, Mario Talajic, Christine Villemaire, and Stanley Nattel

Vagal effects on atrioventricular (AV) nodal conduction are accentuated by increases in heart rate. To establish the mechanism of these rate-dependent negative dromotropic actions, we studied the properties governing AV nodal adaptation to changes in heart rate in chloralose-anesthetized dogs in the absence and presence of bilateral cervical vagal nerve stimulation (20 Hz, 0.2 msec). Stimulation protocols were applied to evaluate the contributions of changes in AV nodal recovery, facilitation, and fatigue independently of each other. Vagal stimulation slowed AV nodal recovery in a voltage-dependent way, increasing the time constant of recovery (τ_r) from 80±7 to 194±16 msec (mean±SEM, $p<0.01$) at the highest voltage studied. The facilitating effect of a premature (A_2) beat was manifested by a leftward shift of the recovery curve (A_3H_3 versus H_2A_3) of a subsequent A_3 beat. The magnitude of shift depended on the A_1A_2 coupling interval and was reduced by vagal stimulation at all A_1A_2 intervals (maximum shift: control, 63±12 msec; vagus, 24±11 msec; $p<0.01$). When recovery and facilitation were kept constant, abrupt increases in AV nodal activation rate caused a slow ($\tau=75$ beats) increase in AH interval (fatigue). Vagal stimulation increased the magnitude of this process (maximum: control, 11±2 msec; vagus, 27±3 msec; $p<0.001$), without altering its time course. At activation rates comparable to sinus rhythm in humans, vagal stimulation at an intermediate voltage increased the AH interval by 25 msec. As heart rate increased, vagally induced changes in dynamic processes amplified AH prolongation up to fivefold at maximum rate. The role of vagal changes in individual functional properties depended on heart rate, but slowing of recovery was the single most important factor, constituting over 50% of overall vagal action at rapid rates. We conclude that vagal stimulation alters the ways in which the AV node responds to changes in activation rate and that at rapid rates most of the negative dromotropic action of the vagus is due to changes in the AV nodal response to tachycardia. Alterations in rate-dependent AV nodal properties are a novel and potentially important mechanism through which interventions may affect AV nodal conduction. (*Circulation Research* 1990;67:1152-1166)

The atrioventricular (AV) node is unique among electrically conducting cardiac tissues in its sensitivity to changes in heart rate.[1] The frequency-dependent properties of the AV node lead to complex responses to changes in rate,[2-12] which play an important part in protecting the ventricle during atrial fibrillation and flutter[1] and may have a role in the generation and maintenance of reentrant supraventricular arrhythmias.[13-15] Slow recovery of AV nodal conduction after activation is clearly demonstrable[2-12] and must play a major role in determining the response of the AV node to alterations in input rate.

It is clear, however, that the responses of the AV node to a change in cardiac frequency involve processes beyond simple time-dependent recovery after AV nodal activation. Whereas the latter has a rapid time course,[1-19] full adaptation after an abrupt change in atrial rate is much slower and requires up to several minutes.[3,7,19-23] A simple AV recovery model can explain in a gross way patterns of Wenckebach periodicity in dogs[24] and humans,[25] but significant discrepancies remain.[25]

A variety of approaches have been used to characterize the rate-dependent properties of the AV node. The most detailed functional characterization has been achieved by Billette and coworkers.[8,16,18,22,26,27] Using the time from the His bundle spike to the next atrial activation (HA interval) as an index of AV

From the Department of Medicine, Montreal Heart Institute; the Departments of Pharmacology and Therapeutics and Medicine, McGill University; and the Department of Medicine, Université de Montréal, Montreal, Canada.

Supported by the Medical Research Council of Canada, the Quebec Heart Foundation, the Fonds de la Recherche en Santé du Quebec, and the Fonds de Recherche de l'Institut de Cardiologie de Montreal.

Address for reprints: Stanley Nattel, MD, Montreal Heart Institute, 5000 Belanger Street East, Montreal, Quebec H1T 1C8, Canada.

Received November 27, 1989; accepted July 2, 1990.

nodal recovery time, they have analyzed AV nodal function in terms of three distinct properties: recovery, facilitation, and fatigue. Each of these properties can be analyzed independently using selective stimulation protocols.[18,22-26] AV node recovery is defined by the relation between AV nodal conduction time and the preceding HA interval and is most simply studied by measuring the conduction time of extrasystolic AV nodal activations in terms of their prematurity (AH-HA relation). The resulting recovery curve closely approximates a simple exponential.[7,17,25,28-30] When a premature beat is inserted before the test beat, the AH-HA relation is shifted to the left on the HA axis, resulting in faster conduction for a similar HA interval than if there had been no preceding conditioning extrastimulus.[3,8,18] This property has been termed "facilitation," because it results in improved AV nodal conduction.[18,26] Using pacing protocols that maintain a constant level of facilitation and recovery, Billette et al[22] have demonstrated a progressive slowing of AV nodal conduction over several minutes after the onset of tachycardia. This process is unlike recovery and facilitation, which act on a beat-to-beat basis, and has been named AV nodal "fatigue."[20-22] The characterization of these processes has been performed predominantly in vitro, and there is little quantitative information about the response of these properties to interventions that alter AV nodal conduction in vivo.

Vagal tone has an important modulating influence on AV nodal conduction. Increased vagal tone, whether by direct stimulation of vagal nerves[31-36] or through physiological reflexes,[37-40] digitalis,[41,42] pressor agents,[43,44] or acetylcholinesterase inhibitors,[44-46] depresses AV nodal conduction and can be used to treat a variety of supraventricular arrhythmias, including reentrant tachycardias involving the AV node, atrial fibrillation, and atrial flutter.[1,47] Vagal influences on AV nodal conduction are complex and depend on the voltage intensity, frequency, duration, and phase in the cardiac cycle of vagal nerve stimulation.[31-36,48-50] The role of heart rate in modulating vagal actions has been less widely appreciated. Wallick et al[48] noted significant interactions between cardiac frequency and vagal effects on the PR interval. Their observations, along with our own preliminary findings of heart rate-dependent vagal prolongation of AV nodal conduction and refractoriness, suggested that the rate-dependent properties of the AV node can be influenced by vagal stimulation. We therefore undertook the current study to analyze in detail the ability of vagal activity to modulate the functional properties of the AV node. Our specific goals included 1) selectively establishing and characterizing AV nodal recovery, facilitation, and fatigue in an in vivo system; 2) developing mathematical tools by which these properties can be quantified; 3) evaluating the effects of vagal stimulation on each of these properties; and 4) determining the extent to which vagal effects on AV nodal conduction are due to changes in individual functional properties at any given heart rate.

Materials and Methods

General Methods

Mongrel dogs of either sex were anesthetized with morphine (2 mg/kg) and α-chloralose (100 mg/kg i.v.). Catheters were inserted into both femoral veins and arteries and were kept patent with heparinized saline solution (0.9%). Dogs were ventilated via an endotracheal tube by using an animal respirator (Harvard Apparatus, South Natick, Mass.). Tidal volume and respiratory rate were adjusted after measurement of arterial blood gases to ensure adequate oxygenation ($Sao_2 \geq 90\%$) and physiological pH (7.35–7.45). A thoracotomy was performed through the fourth right intercostal space, and the heart was suspended in a pericardial cradle. Body temperature was monitored continuously using a thermistor within the chest cavity and was maintained at 37–38° C by a homeothermic heating blanket.

Bipolar Teflon-coated stainless steel electrodes were inserted into the lateral right atrium and high lateral right ventricle on either side of the AV ring and into the right atrial appendage. A bipolar electrode was inserted epicardially to record a His bundle electrogram.[51] The electrodes located in the atrial appendage and lateral right ventricle were used to record atrial and ventricular electrograms, respectively. The lateral right atrial electrode was used to apply 4-msec square-wave pulses at twice late diastolic threshold, with stimulus timing controlled by a programmable stimulator (Digital Cardiovascular Instruments Inc., Berkeley, Calif.). Electrogram signals were filtered at 30–500 Hz and amplified (Bloom Instruments Ltd., Flying Hills, Pa.) with the output subsequently led into a paper recorder and/or a sensing circuit of the stimulator. A Statham P23 1D transducer (Statham Medical Instruments, Los Angeles, Calif.), electrophysiological amplifiers, and a Mingograf T-16 paper recorder (Siemens-Elema. Ltd., Toronto, Canada) were used to record blood pressure; electrocardiographic leads II and aVR. atrial, His bundle, and ventricular electrograms and stimulus artifacts. Recordings were obtained at a paper speed of 200 mm/sec. resulting in a measurement accuracy of ±2.5 msec. In some experiments, a Mingograf 80 recorder was used at a paper speed of 250 mm/sec.

The sinus node was crushed using a previously described technique[17] to allow for a wide range of pacing rates. β-Blockade was produced with 0.5 mg/kg of intravenous nadolol followed by 0.25 mg/kg every 2 hours. In preliminary studies, this technique produced continuous and stable blockade of cardiac β-adrenergic receptors. The vagus nerves were isolated in the neck, ligated, and divided. A stimulator (model SD9F, Grass Instruments, Inc., Quincy, Mass.) was used to apply bilateral vagal stimulation with a pulse duration of 0.2 msec and frequency of 20

Hz. Voltages (designated V_1, V_2, V_3) were selected in each experiment to produce 33%, 66%, and 100% increases in Wenckebach cycle length (WBCL) relative to control. Mean voltages were V_1=1.9±0.4 V, V_2=3.2±0.5 V, and V_3=3.7±0.4 V. In some experiments, a larger number of stimulation voltages were used to assess the effects of more graded vagal stimulation on AV nodal function.

Experimental Protocols

WBCL was determined under control conditions by decreasing atrial pacing cycle length by 10-msec decrements every 10 beats until second-degree AV block occurred. This was repeated before and after each experimental protocol to ensure stability of AV nodal function during electrophysiological study, both under control conditions and in the presence of vagal stimulation. After each experimental protocol, vagal stimulation was stopped, and WBCL was measured to ensure the stability of the preparation and the reversibility of vagal effects. WBCL was measured at least nine times over the course of each experiment. The intermeasurement SD in each experiment averaged 9.6±0.7 msec, or 4.2±0.5% of the mean WBCL. The maximum variation between any two measurements of WBCL in an individual experiment was 30 msec.

The effective and functional refractory periods of the AV node and atrial effective refractory period were measured with the extrastimulus technique. The effective refractory period of the AV node was defined as the longest atrial (A_1A_2) interval failing to result in a His bundle deflection. The functional refractory period of the AV node was defined as the shortest H_1H_2 output interval resulting from premature atrial stimulation. The atrial effective refractory period was defined as the longest interstimulus (S_1S_2) interval failing to result in a propagated atrial response.

AV nodal conduction was assessed from the His bundle electrogram, with the AH interval defined as the time from the peak after the most rapid deflection in the atrial electrogram of the His bundle electrode to the peak after the most rapid deflection of the His bundle electrogram. The HV interval was defined as the time from bundle of His depolarization (as defined above) to the onset of earliest ventricular activation in the His signal or surface electrocardiographic leads. The HA interval was defined as the time from the peak after the most rapid deflection in the His electrogram to the corresponding peak in the next atrial electrogram in the His recording.

Rate-Dependent Effects of Vagal Stimulation on Atrioventricular Nodal Refractoriness

The effective refractory period of the AV node was measured under steady-state conditions over a wide range of basic cycle lengths (300–1,000 msec). A steady state was achieved by pacing at a given rate for 2 minutes before measurement. After the above measurements were completed under control conditions, the experimental protocol was repeated at different levels of vagal stimulation.

Quantitative Assessment of Functional Rate-Dependent Properties of the Atrioventricular Node

Specific stimulation protocols and analysis techniques were used to quantify selected functional AV nodal properties before and after vagal stimulation. The three basic properties of AV nodal recovery, facilitation, and fatigue were characterized as follows.

Effects of vagal stimulation on atrioventricular nodal recovery. A constant basic cycle length (S_1S_1 interval) was used, and the effect of changes in recovery interval on AV nodal conduction was determined. A single premature or delayed stimulus (S_2) was introduced after every 15 basic stimuli, and a curve relating A_2H_2 (AV nodal conduction time of the test impulse) to the H_1A_2 interval was established. The H_1A_2-A_2H_2 relation was determined at two basic cycle lengths (at a cycle length 50 msec above the WBCL and at a cycle length of 600 msec). A number of investigators have found this relation to be exponential.[7,25,29–32] We therefore used monoexponential curve-fitting techniques (see below) to characterize the AV nodal recovery curve before and after vagal stimulation.

Vagal effects on facilitation resulting from premature stimulation. Premature atrial activation (A_2) results in a leftward shift of the AV nodal recovery curve (as defined above) for a subsequent A_3 impulse.[3,8,18] This process has been termed facilitation and reaches steady state after one cycle at a new rate.[18] We studied this process by pacing at a fixed S_1S_1 cycle length for at least 5 minutes. A premature atrial impulse (S_2) was then introduced to produce a selected A_1A_2 "facilitation cycle" after every 15 basic stimuli. A test impulse (S_3) was then applied after each S_2, and the AV node response to S_3 was monitored to generate an H_2A_3-A_3H_3 recovery curve. The latter curve was studied over a wide range of A_1A_2 facilitation cycle lengths (FCLs) with A_1A_2 varied from 800 to 20 msec greater than the refractory period of the AV nodal conduction system.

Each H_2A_3-A_3H_3 recovery curve was fitted by a monoexponential model. As FCL was shortened, the recovery curve of A_3 shifted gradually to the left in a parallel fashion. The degree of leftward shift was found to be an exponential function of FCL. We evaluated vagal effects on facilitation by directly comparing the degree of leftward shift of the A_3 recovery curve at each FCL before and after vagal stimulation, as well as by assessing the effects of vagal stimulation on the relation between the leftward shift and FCL.

Characterization of vagal effects on rate-induced fatigue in the atrioventricular node. A slow process of AV nodal conduction slowing, which is independent of AV nodal recovery and facilitation, can be demonstrated after abrupt increases in atrial rate.[16,22] To study the magnitude and rate of this process, we used

a sensing and pacing circuit to sense each ventricular activation and pace the right atrium with a given VA interval. Because the HV interval was measured and remained constant throughout each experiment, this allowed us to initiate a tachycardia with a given HA interval and to maintain the HA interval constant throughout the tachycardia.

The onset of fatigue was studied over a wide range of HA intervals under control conditions and then during vagal stimulation. An average of 10 HA intervals was studied under each condition. After tachycardia was initiated at a given HA interval, it was maintained for at least 5 minutes to ensure that steady-state conditions had been achieved. A period of recovery of at least 5 minutes was allowed for dissipation of fatigue before the next test run. During each tachycardia, the AH interval increased as a first-order function of beat number. Exponential curve fitting was used to determine the time constant and magnitude of fatigue at any HA interval. Because the HA interval was constant throughout the tachycardia, changes in recovery (as defined above) should not alter the AH from the first beat of the tachycardia through steady-state conditions. Billette[18] showed that facilitation reaches steady state by the second beat of a tachycardia with a constant HA interval,[18] and we verified that this was the case under both control and vagal stimulation conditions in our dogs. Therefore, the magnitude of AH interval change from beat 2 of the tachycardia to steady-state conditions (as determined from the best-fit exponential curve) should be an accurate index of the fatigue process that is independent of both recovery and facilitation.

The magnitude of fatigue was also assessed in a different way under control and vagal conditions. We determined the AV nodal recovery curve as described above under steady-state conditions at a slow rate. We then increased the rate, and when steady-state conditions were achieved, introduced after every 15 beats a pause (S') with a preceding H_1A' interval equal to the HA interval at the slow rate. As shown by Billette et al,[22] this is sufficient to completely dissipate the facilitation resulting from rapid pacing, without altering the degree of fatigue. We then determined the recovery curve of a beat resulting from an S_2 by measuring the A_2H_2 interval as a function of the preceding $H'A_2$ interval. This recovery curve should reflect the effects of fatigue alone.[22] These measurements were made using the same HA values for the slow and fast rates under both control and vagal conditions in each experiment.

Data Analysis

Results are reported as the mean±SEM. Multiple comparisons between control and vagal stimulation data were made by two-way analysis of variance with Scheffe contrasts.[52] Comparisons between only two groups of experimental data were made with Student's *t* test. Two-tailed tests were used for all statistical comparisons, and a probability of 5% or less was taken to indicate statistical significance. Exponential curve fitting was performed using Marquardt's technique on an IBM AT compatible computer.

To ascertain that the effects of vagal stimulation on AV nodal function that we studied were due to stimulation of muscarinic cholinergic receptors, vagal stimulation was applied before and after atropine in three experiments. The voltages for bilateral vagal stimulation with 0.2-msec square-wave pulses at 20 Hz required to produce 30–200% increases in WBCL were determined. Atropine (1 mg i.v.) was given, and vagal stimulation was repeated at the previously determined voltage levels. In all experiments, vagal stimulation after atropine had no effect on WBCL, indicating that the effects of vagal stimulation on AV nodal conduction were due to stimulation of muscarinic cholinergic receptors.

Five experiments were performed to determine vagal effects as a function of steady-state rate, and five were performed to measure vagal effects on the AV nodal recovery curve.. At least three levels of vagal stimulation were studied in those experiments. Because of the complexity of experiments used to study facilitation and fatigue, only one vagal stimulation voltage (V_2) was used in each experiment. Facilitation was studied in eight dogs, and fatigue was studied in 10 dogs, with fatigue kinetics studied in eight of these and the fatigue-induced recovery curve shift evaluated in five (three dogs underwent both fatigue protocols). All animal care techniques followed the recommendations of the Canadian Council on Animal Care, and research protocols were approved by the Animal Care Committee of the Montreal Heart Institute.

Results

General Effects of Vagal Stimulation

Vagal nerve stimulation increased WBCL, AV conduction time, AV nodal effective refractory period, and AV nodal functional refractory period in a voltage-dependent manner (Table 1). The effect of vagal stimulation to increase WBCL was the same before and after each experimental protocol, indicating that the effects of vagal stimulation were constant (Figure 1). After vagal stimulation was stopped, WBCL rapidly returned to control values, indicating that the effects of vagal stimulation were reversible and that underlying AV nodal function did not change over the course of each experiment.

Rate-Dependent Effects of Vagal Stimulation on Atrioventricular Nodal Refractoriness

Vagal stimulation increased the AV nodal effective refractory period in a rate-dependent way (Figure 2). Under control conditions, atrial refractoriness was generally greater than AV nodal effective refractory period. The values that we obtained for the nodal effective refractory period are therefore an upper limit for true AV nodal effective refractory period under control conditions. These values decreased

TABLE 1. Electrophysiological Variables Before and After Vagal Stimulation

	WBCL (msec)		Voltage	AVFRP	AVERP	AERP	BP
	Prestudy	Poststudy	intensity (V)	(msec)	(msec)	(msec)	(mm Hg)
Control	200±11	205±9	...	258±10	150±7	150±7	138±8/86±5
V_1	270±9*	265±10*	1.9±0.3	285±23	190±15	140±4	134±3/89±8
V_2	332±7*	335±9*	3.1±0.4	330±15†	260±11‡	130±4	134±4/94±3
V_3	435±6*	432±5*	3.7±0.3	407±28*	355±36*	132±8	129±6/92±3

Values are mean±SEM. Prestudy values are the values measured at the beginning of each experimental protocol, and poststudy values are the values measured at the end of the experimental protocol. Atrial refractoriness was limiting under control conditions in all experiments; therefore, the value listed for effective refractory period of the atrioventricular node (AVERP) is an upper limit established by the atrial refractory period. WBCL, Wenckebach cycle length; AVFRP, functional refractory period of the atrioventricular node measured at a basic cycle length of 500 msec; AERP, atrial effective refractory period; BP, arterial blood pressure; V_1, V_2, V_3, voltage to increase WBCL by 33%, 66%, and 100%, respectively, in each experiment.

*$p<0.001$ compared with corresponding control value.
†$p<0.05$ compared with corresponding control value.
‡$p<0.01$ compared with corresponding control value.

with decreasing cycle length. After vagal stimulation, AV conducting system refractoriness was determined by the refractory period of the AV node, and the AV nodal effective refractory period showed significant increases as pacing cycle length was reduced. Vagal stimulation resulted in rate-dependent changes in the steady-state AH interval, with vagally induced increases in the AH interval becoming larger as pacing cycle length decreased (Figure 2).

Characterization of Atrioventricular Nodal Functional Properties and the Effects of Vagal Stimulation

An example of one experiment relating A_2H_2 to H_1A_2 interval under control conditions and after vagal stimulation is shown in Figure 3. Under control conditions, A_2H_2 was constant over a wide range of recovery time (greater than 300 msec). With further decreases in recovery time (H_1A_2 interval), there was a rapid increase in A_2H_2 until refractoriness was encountered. In the presence of vagal stimulation, the AV nodal recovery curve was shifted to the right and upward. The degree and magnitude of this shift depended on the voltage used to stimulate the vagal nerves. Not only did vagal stimulation increase the AH interval at long H_1A_2 intervals, indicating a tonic effect, but it also slowed AV nodal recovery, as shown by a decreased slope of the recovery curve. Each AV nodal recovery curve was fitted by nonlinear curve fitting to an equation of the form

$$AH_t = AH_\infty + A \cdot \exp(-t/\tau_r) \quad (1)$$

where AH_t is the AH interval at an HA interval of t, AH_∞ is AH after an infinitely long recovery time, A is the difference between the AH interval for HA=0 and AH_∞, and τ_r is the recovery time constant. The

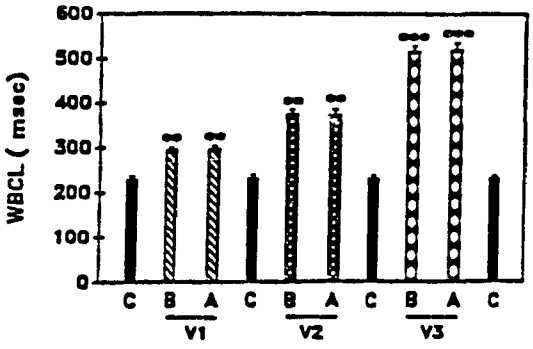

FIGURE 1. *Voltage-dependent effects of vagal stimulation on Wenckebach cycle length (WBCL). WBCL was measured during vagal stimulation before (B) and right after (A) each experimental protocol. Vagal stimulation increased WBCL in a voltage-dependent fashion. After each period of vagal stimulation, WBCL in the absence of vagal stimulation (C) returned to control values. V1, V2, and V3, increasing voltage intensities as defined in the text. **p<0.01, ***p<0.001, compared with control by paired t test.*

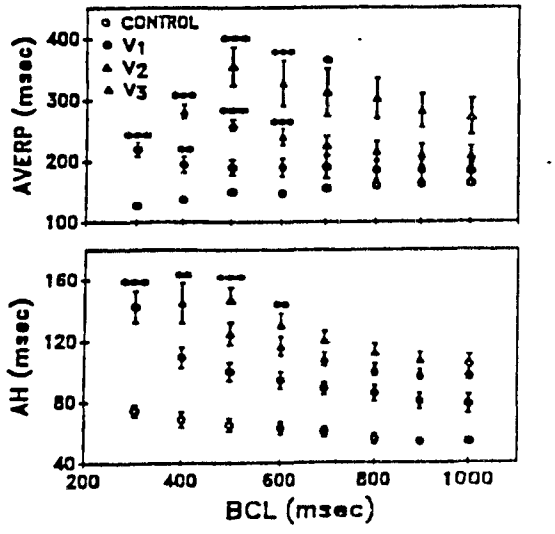

FIGURE 2. *Effective refractory period of the atrioventricular node (AVERP)* (top panel) *and steady-state AH interval* (bottom panel) *under control conditions and during vagal stimulation at progressively higher voltages (V_1, V_2, V_3). *p<0.05, **p<0.01, ***p<0.001, compared with vagal effects at a cycle length (BCL) of 1,000 msec at the same voltage intensity.*

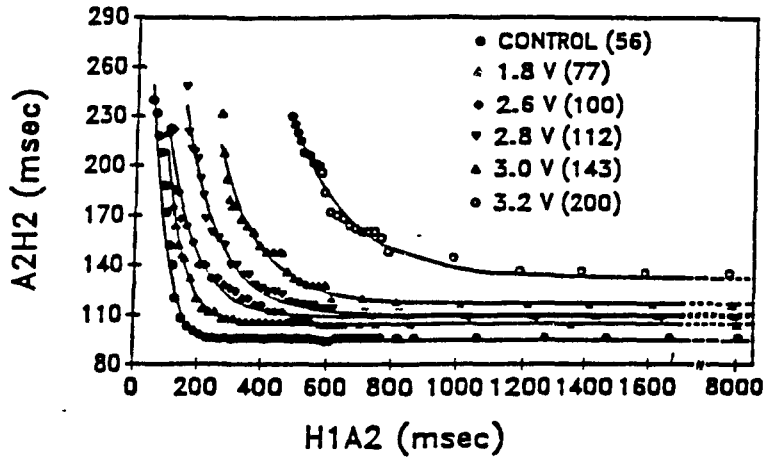

FIGURE 3. *Relation between atrioventricular conduction time (AH interval) and recovery time (HA interval) under control conditions and in the presence of vagal stimulation at five different voltages (shown after symbols) in a representative experiment. Atrioventricular recovery curves were fitted by a nonlinear curve-fitting technique. The time constant of each recovery curve is shown in parentheses after each symbol legend.*

mean correlation coefficients for the fits were 0.993 with an SD of 0.005. Time constants were found to be independent of basic cycle length, so results for the standard cycle length of 600 msec were used for all comparisons. As shown in Figure 3, vagal stimulation produced a voltage-dependent increase in the recovery time constant in this experiment. Figure 4 shows the average recovery time constants for the standard voltages (V_1, V_2, V_3) in all experiments used to study recovery. Vagal stimulation significantly increased the time course of recovery in a voltage-dependent fashion.

Effects of Vagal Stimulation on Atrioventricular Nodal Facilitation

Single atrial premature beats (A_2) shifted the recovery curve in response to a subsequent A_3 complex to the left in a fashion that depended on the A_1A_2 interval (FCL). Figure 5 (top panel) shows raw data from a series of recovery curves obtained with varying facilitation (A_1A_2) cycle lengths. The best-fit exponential curves to the same data are also shown. Because these curves were shifted to the left in a parallel fashion, the degree of shift can be quantified by determining the HA interval for any given AH interval. We determined the HA interval corresponding to an AH value of 125 msec for the recovery curve at each FCL. This was designated the "HA_{125}" and is indicated by the intersection between the horizontal dashed line and the recovery curve at each FCL in Figure 5.

The data in the bottom panel of Figure 5 were obtained during vagal stimulation in the same exper-

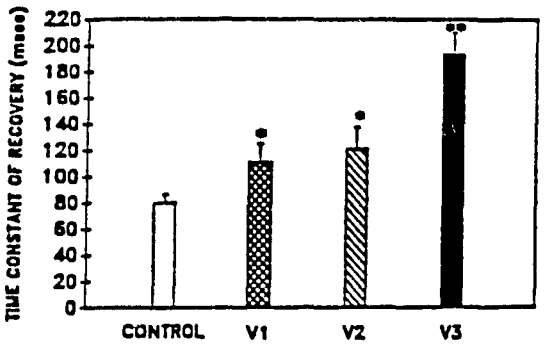

FIGURE 4. *Changes in recovery time constant resulting from vagal stimulation at progressively larger voltages (V1, V2, V3). *$p<0.05$, **$p<0.01$, compared with control.*

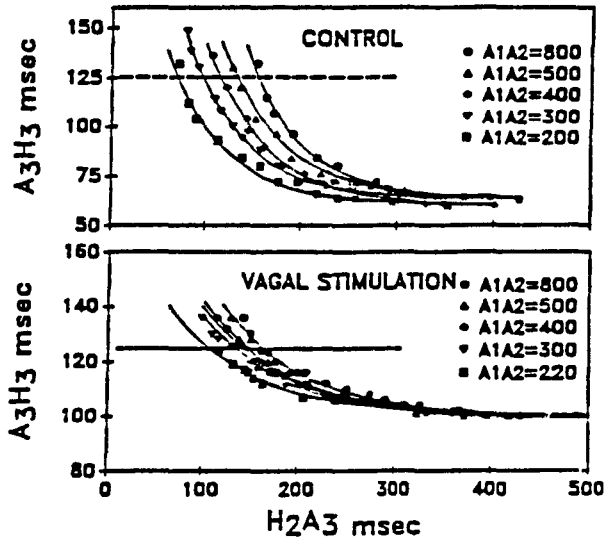

FIGURE 5. *Recovery curves for activations preceded by an interpolated beat (A_2) over a range of A_1A_2 coupling intervals. As the A_1A_2 interval decreases, the recovery curve of A_3 shifts to progressively shorter values of H_2A_3. In the experiment shown, as well as all others, vagal stimulation* (bottom panel) *resulted in a smaller facilitation-induced shift in the recovery curve than present under control conditions* (top panel). *Each recovery curve was fitted with a single exponential relation, shown by the solid lines. The HA value at which the AH interval was 125 msec (horizontal dashed line), or HA_{125}, was used as an index for the degree of leftward shift caused by premature stimulation. Vagal stimulation reduced the change in HA_{125} caused by facilitation. In each experiment, complete A_3H_3-A_2H_3 recovery curves were obtained at 10 A_1A_2 intervals, under both control and vagal conditions. Only five curves are shown for each in this figure for the sake of clarity.*

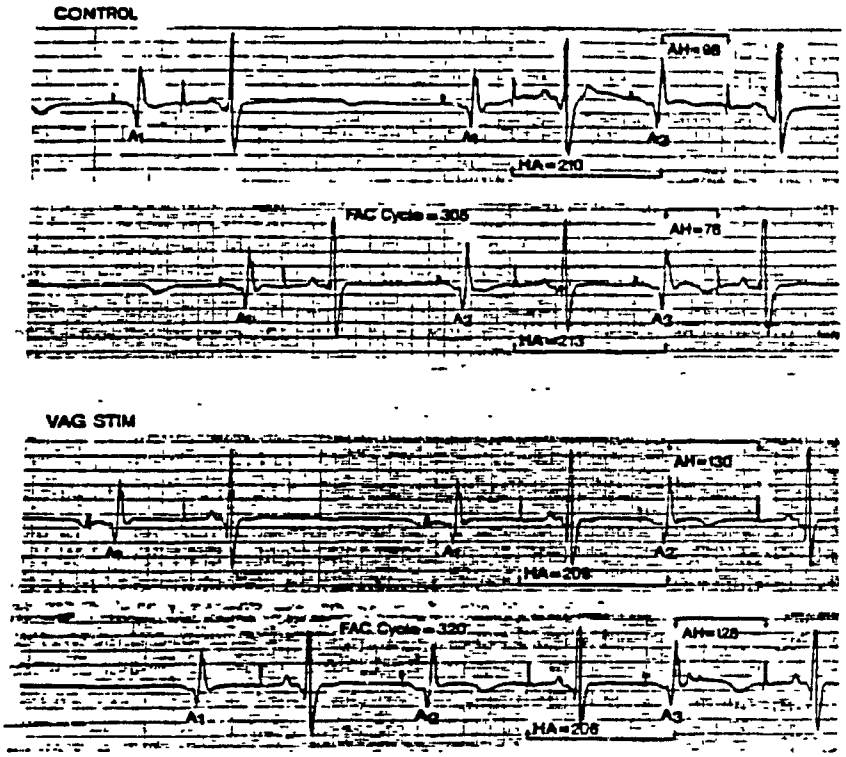

FIGURE 6. *Analog data from a representative experiment showing the AH interval corresponding to a premature activation with a given HA time (upper tracing for each set) and the shortening in AH for a similar HA interval when preceded by an intervening facilitation (FAC) cycle (lower tracing for each set).* Top panels *Results under control conditions* Bottom panels *Results in the presence of vagal stimulation. Because of a poor sinus node crush, basic cycle length was 450 msec in this experiment. Recording speed, 250 mm/sec.*

iment. Vagal stimulation reduced the amount of leftward shift resulting from facilitation over a similar range of A_1A_2 intervals. Changes in FCL produced much less alteration in HA_{125} in the presence of vagal stimulation than under control conditions. An illustrative example of the effect of vagal stimulation on AV nodal facilitation is presented in Figure 6.

To obtain a quantitative estimate of HA_{125} at each FCL in each experiment, we solved for t in Equation 1 at an AH_t value of 125 with values of A, AH_∞, and τ_r obtained from nonlinear curve fitting of each recovery curve. Figure 7 shows the mean values of HA_{125}, τ_r, and AH_∞ as a function of FCL under control conditions (top panel) and in the presence of vagal stimulation (bottom panel). An identical range of values for FCL was studied under both conditions. Under either condition, AH_∞ and τ_r were unchanged by changing FCL, as shown by the hatched and open bars, respectively, confirming that facilitation caused a parallel leftward shift of the recovery curve. Under control conditions (top panel), HA_{125} decreased significantly as FCL decreased. In the presence of vagal stimulation (bottom panel), τ_r and AH_∞ were increased relative to control values but were not significantly changed by changes in FCL. HA_{125} was greater in the presence of vagal stimulation, reflecting the rightward shift of the recovery curves, and showed much less change with changing FCL than under control conditions.

To further quantify the leftward shift of recovery curves caused by facilitation, we related changes in HA_{125} from those at a basic cycle length of 800 msec (Δ HA) to the FCL and found it to be well fitted (mean $r=0.98\pm0.01$) by the relation

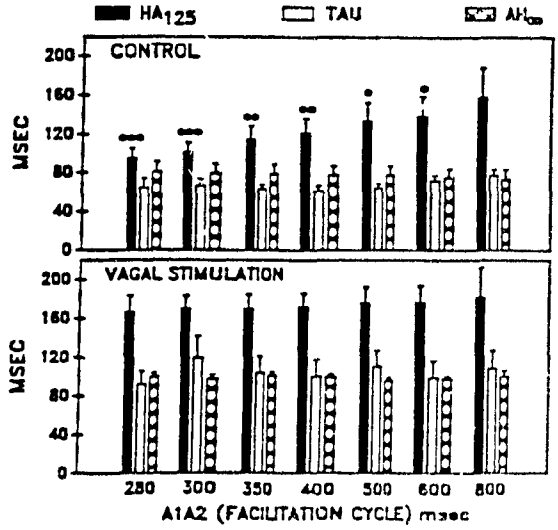

FIGURE 7. *Defining variables for recovery curves preceded by facilitation cycles of varying duration. While AH_∞ and the recovery time constant (tau) were unchanged by facilitation, indicating parallel curve shift, HA_{125} (the HA value at which the AH interval was 125 msec) decreased with decreasing facilitation cycle length under control conditions* *p<0.05, **p<0.01, ***p<0.001, *compared with corresponding values at A_1A_2 of 800 msec.* Top panel: *Control values* Bottom panel: *Vagal stimulation increased all three variables, and premature stimulation produced small decreases in HA_{125} in the presence of vagal stimulation.*

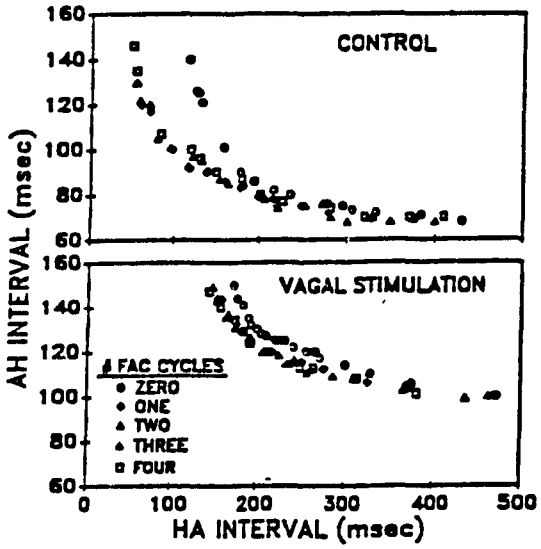

FIGURE 8. *Changes in the atrioventricular recovery curve after one to four facilitation (FAC) cycles. One facilitation cycle shifted the atrioventricular recovery curve to the left, relative to curve at the same basic cycle length without an intervening facilitation cycle* (○). *Additional facilitation cycles at the same cycle length as the first produced no additional changes in the recovery curve either under control conditions* (top panel) *or in the presence of vagal stimulation* (bottom panel).

$$\Delta HA_{fac} = \Delta HA_{max} \exp(-FCL/\tau_{fac}) \qquad (2)$$

where ΔHA_{fac} is HA_{125} at a given FCL minus HA_{125} at a basic cycle length of 800 msec, and τ_{fac} is a characteristic time constant. The maximum facilitation observed over a corresponding range of cycle lengths decreased from 63±12 msec under control conditions to 24±11 msec under vagal stimulation ($p<0.05$). On the other hand, vagal stimulation did not significantly alter τ_{fac}, which averaged 148±18 msec under control conditions and 207±22 msec in the presence of vagal stimulation.

Under both control conditions and vagal stimulation, the leftward shift of the recovery curve was maximal after one premature cycle (Figure 8). No further changes in the position of the AV nodal recovery curve were seen when the recovery curve was tested after two or more premature cycles.

Effect of Vagal Stimulation on Atrioventricular Nodal Fatigue

When a tachycardia was initiated at a constant HA interval, AV nodal conduction time slowly increased over the next several minutes (Figure 9). The magnitude of conduction slowing was greater for tachycardias with shorter HA intervals, that is, faster rates. Vagal stimulation enhanced the magnitude of conduction slowing produced by tachycardia at any given HA interval (Figure 9, bottom panel). Under both control and vagal conditions, the development of AV nodal fatigue was well fitted by a monoexponential relation (solid curves in Figure 9) of the form

$$\Delta AH_n = \Delta AH[1-\exp(-n/\tau_{fat})] \qquad (3)$$

where ΔAH_n is the increase in AH caused by fatigue at beat n of the tachycardia, ΔAH is the total increase in AH attributable to fatigue at steady state, and τ_{fat} is the time constant for the onset of fatigue. To control for recovery and facilitation, all changes in AH interval during tachycardia are calculated in relation to the AH of the second beat of the tachycardia. Both ΔAH and τ_{fat} were calculated for tachycardias at each HA interval studied in each experiment. The mean corre-

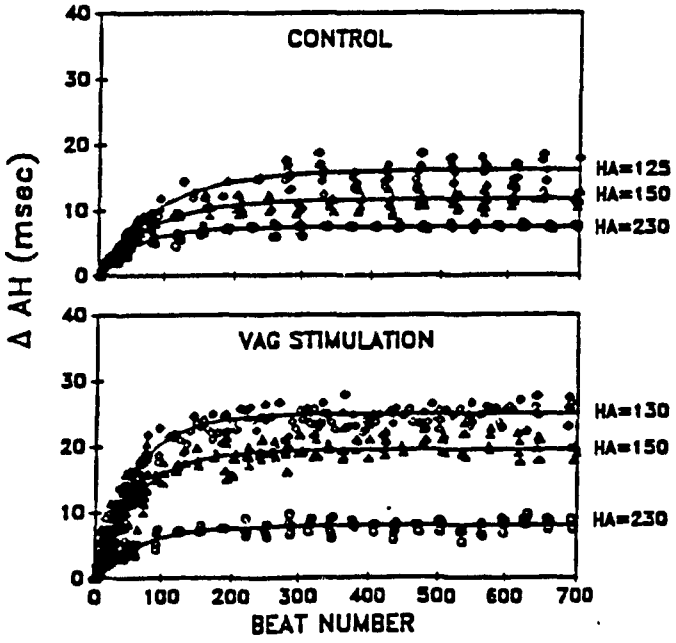

FIGURE 9. *Changes in AH interval after the onset of atrial tachycardia with a constant HA interval. Values are shown from beat 2 through steady state. Because recovery effects are constant from beat 1 (constant HA) and facilitation effects reach steady state at beat 2, the changes in AH interval shown are due completely to atrioventricular nodal fatigue. Each curve was fitted by a simple exponential (solid lines).*

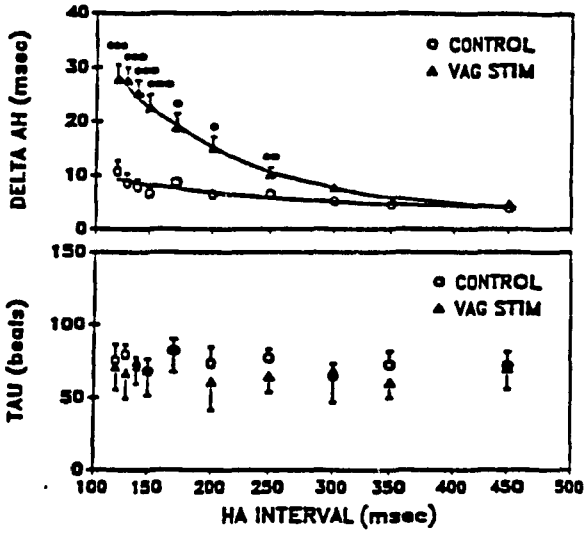

FIGURE 10. Top panel: *Change in AH interval caused by fatigue at steady state (delta AH) as a function of HA interval.* $^{*}p<0.05$, $^{**}p<0.01$, $^{***}p<0.001$, *for difference between vagal stimulation (VAG STIM) and control values at a given HA interval. Solid lines show exponential curve fits to data. Where error bars are absent, they fall within the range of the symbol.* Bottom panel: *Time constant (tau) for onset of fatigue (τ_{fat} in Equation 3 of text). Neither changes in HA interval nor vagal stimulation altered the time course of fatigue.*

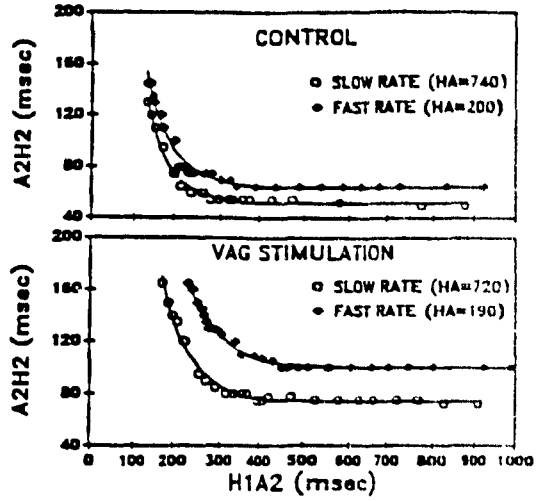

FIGURE 11. *Results from a typical experiment showing the effects of fatigue on the atroventricular recovery curve. A single facilitation-dissipating cycle before the test beat was applied at the fast rate to study the effects of fatigue alone on the recovery curve. Fatigue caused a parallel upward shift of the recovery curve* (top panel), *an effect greatly accentuated by vagal (VAG) stimulation* (bottom panel).

lation coefficient between the best-fit curves and experimental data was 0.93±0.01, an excellent correlation considering the small magnitude of fatigue (less than or equal to 5 msec) at long HA intervals.

Figure 10 shows mean data for Δ AH and τ_{fat} as a function of the HA interval of tachycardia, both under control conditions and in the presence of vagal stimulation. The time constant for the onset of fatigue (bottom panel) was similar for tachycardias over a wide range of HA intervals and was not altered by vagal stimulation. The magnitude of AH increase (top panel) resulting from fatigue, on the other hand, depended on the HA interval and was significantly increased in the presence of vagal stimulation. The magnitude of AH change caused by fatigue at any steady-state HA interval (ΔAH_{HA}) could be expressed as

$$\Delta AH_{HA} = \Delta AH_{max} \exp(-K \cdot HA) + C \qquad (4)$$

where ΔAH_{max} is Δ AH at HA of 0, and K and C are constants obtained by nonlinear least-squares regression. The curves resulting from data obtained under both control and vagal conditions are shown by the solid lines in the top of Figure 10.

The ability of vagal stimulation to augment AV nodal fatigue was independently confirmed by methods illustrated in Figure 11. Under control conditions, an AV nodal recovery curve was obtained at a long steady-state HA interval. Fatigue was then induced by 5 minutes of pacing at a much shorter HA interval. A single facilitation-dissipating cycle, with an HA equal to the baseline long HA interval, was then introduced after every 15 beats, and the recovery curve of a subsequent test beat was evaluated. As shown by Billette et al,[22] the parallel upward shift in the resulting AV nodal recovery curve is an index of fatigue independent of both recovery and facilitation. The same protocol was repeated in each experiment in the presence of vagal stimulation, with recovery curves obtained at the same basic HA intervals as under control conditions. The degree of shift in the recovery curve was greater in each case in the presence of vagal stimulation. A quantitative estimate was obtained by fitting each recovery curve to an equation of the form of Equation 1 (curve fits for the data in Figure 11 are shown by the solid lines) and subtracting AH_s at the slow rate from AH_f at the fast rate. This index of fatigue-induced shift in the recovery curve averaged 7±1 msec under control conditions and 18±2 msec ($p<0.01$) in the presence of vagal stimulation. These values agree well with changes in the AH interval measured by analyzing kinetics of fatigue (Figure 10) over a corresponding range of HA intervals.

Analysis of the Heart Rate–Dependent Role of Vagal Effects on Recovery, Facilitation, and Fatigue

Because vagal stimulation alters a variety of rate-dependent AV nodal properties, the effects of vagal stimulation should be a dynamic function of heart rate. The predicted increase in AH interval caused by vagal stimulation at any given HA interval can be broken down into four components: 1) a tonic com-

ponent (ΔAH_t), 2) an increase caused by the delay in recovery (ΔAH_{rec}), 3) an increase caused by a decreased magnitude of facilitation (ΔAH_{fac}), and 4) an increase caused by an augmentation of fatigue (ΔAH_{fat}). These can be stated mathematically at any HA interval as follows (where subscripts V and C represent values under vagal and control conditions, respectively):

$$\Delta AH_t = AH_{sC} - AH_{sV}$$

(from Equation 1, at a basic cycle length of 1 second for each)

$$\Delta AH_{rec} = A_V \exp(-HA/\tau_V) - A_C \exp(-HA/\tau_C)$$

where τ_V and τ_C are τ_r for vagal and control conditions (from Equation 1)

$$\Delta AH_{fac} = A_V \exp[-(HA + \Delta HA_{facV})/\tau_V] - A_C \exp[-(HA + \Delta HA_{facC})/\tau_C] - \Delta AH_{rec}$$

(from Equations 1 and 2)

$$\Delta AH_{fat} = \Delta AH_{maxV} \exp(-K_V \cdot HA) + C_V - \Delta AH_{maxC} \exp(-K_C \cdot HA) - C_C$$

(from Equation 4).

The accurate calculation of each of the determining constants governing all three processes (recovery, facilitation, and fatigue) simultaneously under both control and vagal conditions is too time consuming for any single experiment. To estimate the contribution of these processes to the rate-dependent effects of vagal stimulation, we used mean values obtained from the results of all experiments used to study each process to get overall estimates of AH_s, A, τ_r, ΔHA_{max}, τ_{fac}, ΔAH_{max}, K, and C under control conditions and in the presence of vagal stimulation (of intensity V_2). The predicted changes in AH interval resulting from vagally induced changes in recovery, fatigue, and facilitation are shown as a function of the steady-state HA interval in Figure 12. At long HA intervals, vagal stimulation increases the AH interval by about 25 msec, an effect that is not altered by rate-dependent processes until an HA interval of about 500 msec. As the HA interval is decreased further, alterations in dynamic processes increase considerably. At the shortest HA interval analyzed (120 msec), changes in dynamic processes have resulted in an over fivefold amplification of vagal effect. At short steady-state recovery intervals, over half of the vagal action on the AV node is due to slowing in recovery, with the remaining effect caused by a decrease in facilitation, increase in fatigue, and tonic increase in AH_s, in approximately equal proportions. The results of three individual experiments in which the effects of vagal stimulation could be examined over a wide range of HA intervals are superimposed on the graph of changes predicted from mean changes in dynamic processes. The results of these individual experiments show qualitative agreement with the predictions of the model.

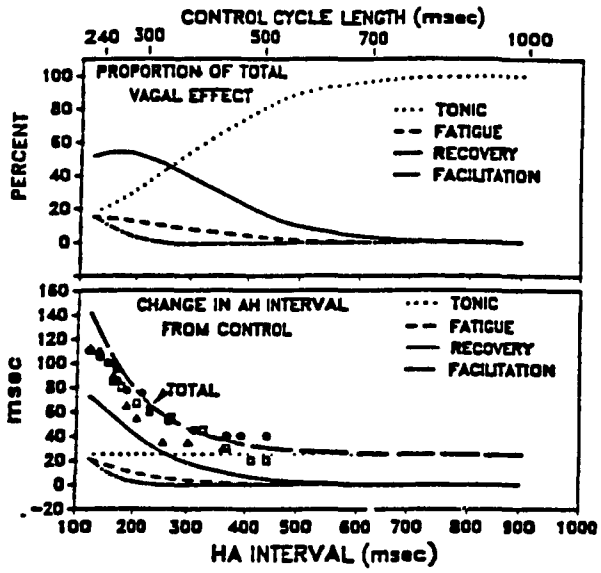

FIGURE 12. Bottom panel: *Changes in AH interval resulting from vagal effects on recovery, facilitation, and fatigue, based on the mathematical model described in the text. The sum of all three effects was used to predict total change in AH interval resulting from vagal stimulation at V_2, as a function of steady-state HA interval and control cycle length. Each set of symbols shows results from an individual experiment, which are in good agreement with predictions of the model.* Top panel: *Because of the varying importance of vagal effects on each time-dependent atrioventricular nodal function at different steady-state HA intervals, the total vagal effect was composed of a rate-dependent combination of changes in time-dependent and time-independent actions.*

Discussion

The current findings indicate that vagal stimulation slows AV nodal conduction in both time-independent and time-dependent ways. The latter result from changes in intrinsic AV nodal functional responses to altered activation rate. Depending on cardiac rate, the frequency-dependent component can constitute from 0% to 80% of the overall vagal effect on the AV node and can amplify vagal effects at rapid rates severalfold compared with effects at slow rates.

Comparison to Previous Analyses of Rate-Dependent Atrioventricular Nodal Properties

Since the classic studies of Mobitz[2] and Lewis and Master,[3] many investigators have studied the changes in AV nodal conduction of premature beats. Both hyperbolic[11,30,53] and exponential[7,17,25,28–30] functions have been used to fit the AV nodal recovery curve, with the exponential model apparently providing a better fit.[30] We used an exponential model to fit AV nodal recovery curves and obtained time constants of recovery similar to those previously observed.[7,17,25,28–30]

The maximum shift in the AV nodal recovery curve caused by facilitation was somewhat greater in our experiments than in previous work.[18] This is probably due to the much wider range of atrial rates that we

were able to study in chloralose-anesthetized dogs with crushed sinus nodes compared with dogs with intact sinus nodes anesthetized with pentobarbital.[18] The maximum magnitude of fatigue in our dogs averaged 11 msec (Figure 9), which was quite similar to values of 11–12.5 msec in the isolated rabbit AV node noted by Billette et al.[22] There are no previous mathematical models of the rate dependence of facilitation and fatigue with which to compare our findings.

Little previous work has been done on the effects of vagal stimulation on the accommodation of the AV node to rate change. The AV nodal recovery curves observed by Lewis and Master[3] after vagal stimulation show a slightly slower recovery process, noted but not quantified by the authors. Wallick and coworkers[48] found that vagal effects interacted significantly with heart rate in determining AV conduction changes, but underlying mechanisms were not explored. Narula and Runge[20] observed an attenuation of slow AV nodal accommodation by atropine, perhaps related to the effects of vagal tone on AV nodal fatigue that we noted. Jenkins and Belardinelli[23] noted no change in the AV nodal accommodation to rate of isolated guinea pig hearts after atropine administration. This is not necessarily in conflict with our findings, because the rate of acetylcholine release in isolated hearts without central nervous input is likely to be quite low in the absence of direct nerve stimulation.

Role of Vagal Alterations in Atrioventricular Nodal Kinetic Properties

All three kinetic properties of the AV node (recovery, facilitation, and fatigue) were altered by vagal stimulation. Vagal stimulation slowed recovery (Figures 3 and 4), so that recovery was incomplete for a longer period after AV nodal activation. At rates associated with HA intervals greater than 500 msec, changes in recovery had little effect on conduction. However, as the HA interval shortened, less complete recovery became an increasingly important factor, constituting over 50% of the overall vagal effect at rapid rates (Figure 12). The extent of facilitation was reduced by vagal stimulation, while the magnitude of fatigue was enhanced. The former effect reduced the leftward shift in the recovery curve that results from short cycles and favors conduction at rapid rates (Figures 5–7), while the latter effect increases the slowly developing component of AV nodal conduction impairment during sustained tachycardia (Figure 9). Both of these phenomena are most important at short HA intervals (Figure 12). Changes in each kinetic property contribute to the overall frequency-dependent effects of vagal stimulation, with the amount of conduction slowing attributable to each depending on the steady-state HA interval (Figure 12).

Possible Mechanisms of Vagal Effects on Recovery, Facilitation, and Fatigue

Little information is available regarding the underlying ionic mechanisms of the rate-sensitive properties of the AV node. The time constant of the AV nodal recovery curve (60–80 msec) is in the same range as the time constant of recovery of L-type calcium currents in isolated canine cardiac Purkinje cells[54] and for slow inward current in multicellular preparations.[55] It is quite likely that the time dependent recovery of AV nodal conduction is related to the recovery of L-type calcium channels from their inactivation during the preceding action potential. Whether other mechanisms, such as the time dependent inactivation of outward currents activated during the preceding plateau, also contribute is unknown.

The cellular processes governing AV nodal facilitation and fatigue are largely unknown. Premature stimulation shortens action potential duration in the distal AV node[56] and could cause a leftward shift in the subsequent AH-HA relation by increasing the diastolic recovery time preceding beats at any given coupling interval. Adenosine accumulation has been shown to contribute to AV nodal fatigue in the isolated guinea pig heart at rates in excess of 400 beats/min and in the presence of hypoxia.[23] The contribution of adenosine to AV nodal fatigue at more physiological AV nodal activation rates appears to be insignificant,[23] and no other clear determining mechanisms have been identified.

The release of acetylcholine from vagal nerve endings reduces the upstroke velocity, amplitude, and duration of AV nodal action potentials.[57–59] Acetylcholine at physiological concentrations decreases net slow inward current in atrial[60,61] and AV nodal[62] tissues by increasing an acetylcholine-dependent outward current rather than by directly reducing slow inward current. This acetylcholine-dependent potassium current shows time-dependent relaxation after repolarization.[62] This could result in a time-dependent component of AV nodal recovery with a different time course from that of calcium current reactivation and might explain the change in recovery time constants we noted during vagal stimulation. The abbreviation of AV nodal action potentials caused by acetylcholine[58,59] may attenuate the action potential shortening resulting from rate increases, possibly accounting for the decreased facilitation that we saw in the presence of vagal stimulation. Reduced atrial action potential duration shortening with rate increases was noted in response to vagal stimulation by Mubagwa and Carmeliet.[63] They attributed this finding to a larger repolarizing current during rapid stimulation, resulting in a diminished influence from a given quantity of acetylcholine-induced outward current. Potential mechanisms by which vagal stimulation enhances fatigue remain totally speculative. Because AV nodal fatigue is demonstrable in the presence of atropine,[26] acetylcholine release cannot be the sole mechanism underlying fatigue. Vagal

stimulation might cause a rate-dependent process with a time course similar to fatigue or may simply enhance the underlying fatigue mechanism. The unchanged time constant of fatigue (Figure 10) in the presence of vagal stimulation favors the latter possibility. The significance of other actions of vagal stimulation, such as changes in the pattern of atrial input,[34] in altering the kinetic response of the AV node remains to be determined.

Limitations of the Current Model

Rapid (200-Hz) field stimulation of vagal nerve endings results in hyperpolarization of the AV node, but the response fades to a steady state over time.[64] Similar time-related desensitization has been reported during exposure to large concentrations of acetylcholine.[63,65] We measured WBCL just before and just after each experimental protocol (Figure 1) to ensure that vagal effects were constant during the protocol. After each protocol, vagal stimulation was discontinued, and WBCL was verified to assure that underlying control conditions were constant. The stability of vagal effects in our experiments may have been due to a lack of desensitization because of our stimulation frequency (20 Hz). Alternatively, because desensitization is rapid and is followed by a new steady-state effect,[63-65] we may have missed a brief initial period of greater effect. In any case, vagal actions were constant throughout each experimental protocol, and desensitization, if present at all, did not alter our results.

Under resting conditions, vagal discharge rate is not constant but varies with the phase of respiration, resulting in cyclical changes in AV nodal conduction.[66,67] Spontaneous vagal activity in vivo may occur in repetitive bursts of activity,[68] and the timing of a single burst of vagal activity is an important determinant of the resulting conduction changes.[50] On the other hand, continuous vagal firing at frequencies up to 40 Hz has been recorded under physiological conditions augmenting vagal output.[69] We elected to stimulate the vagi continuously at a constant frequency, varying stimulation intensity to produce a desired effect. In this way, we achieved a constant action over time and were able to study vagally induced changes in the functional properties of the AV node in a controlled fashion. It would be of interest to study the effects of single and repetitive bursts of vagal stimulation on discrete rate-dependent aspects of AV nodal function.

We used the HA interval as an index of AV nodal recovery time to characterize rate-dependent properties of the AV node. Because most of the slowing in AV nodal conduction during premature stimulation occurs in the N-NH region, with little delay proximal to the N zone and distal to the NH area,[4,56] this approach has some underlying justification. Levy et al[24] have also provided evidence for the necessity of considering the interval from ventricular to atrial activation in assessing AV nodal recovery. Many investigators have analyzed changes in AV nodal conduction in terms of the preceding AA interval (or cycle length). It is not within the scope of the techniques that we used to address the relative merits of these approaches. The changes in the recovery curve that result from vagal stimulation are not altered by the recovery time index used, because transformation of AH versus HA curves to AH versus AA curves simply requires the addition of a constant value (the steady-state AH interval) to each HA value on the horizontal axis. Similarly, the qualitative nature of vagal effects on AV nodal fatigue are not altered by changing the index of recovery time. On the other hand, AV nodal facilitation is a process that is demonstrable only when the HA interval is used as the index of recovery time. Billette and Métayer have shown that this approach resolves a number of previously confusing rate-dependent properties of the AV node's functional refractory period.[16] Studies of the effects of acetylcholine on action potential duration restitution in the distal AV node would be valuable in resolving the nature and possible mechanisms of vagal effects on AV nodal facilitation.

Significance of Findings

Vagal input plays a major role in modulating AV nodal properties, and changes in vagal tone (whether spontaneous or the result of treatment) are important in the occurrence and termination of both tachyarrhythmias and bradyarrhythmias. We have shown that vagal actions are a dynamic function of heart rate as a result of vagally induced alterations in the functional properties of the AV node. The augmentation by tachycardia of refractoriness changes caused by vagal stimulation (Figure 2) could result in enhanced antiarrhythmic actions of the vagus during supraventricular tachyarrhythmias. This type of selective action has previously been shown to underlie beneficial responses to calcium antagonist drugs during atrial fibrillation[70] and AV reentrant tachycardias.[71] Calcium antagonists produce rate-dependent changes in AV nodal function by virtue of state-dependent calcium channel blockade,[17] a mechanism that does not apply to the effects of vagal stimulation. Nonetheless, the potential clinical importance of tachycardia-dependent AV nodal depressant properties applies equally to both.

The effects of interventions on the AV node are generally evaluated in terms of steady-state changes in a measure of AV nodal conduction—AH or PR interval, or AV conduction time. Few studies have considered the frequency-dependent actions of such interventions, and such analysis has been generally qualitative. We have shown that vagal stimulation alters discrete rate-dependent functional properties of the AV node. Vagally induced changes in functional properties resulted in a fivefold magnification of AV nodal conduction slowing at rapid rates (Figure 12). Changes in AV nodal recovery, facilitation, and fatigue accounted for a total of 80% of overall vagal conduction slowing at rates associated with an HA interval of 150 msec.

This novel approach to analyzing the effects of interventions on the AV node, resting on many recent advances in AV node physiology, provides the basis for new insights into pharmacological control of AV nodal function. Rate-dependent responses to vagal augmentation may explain why doses of digitalis that produce modest changes in AV nodal function during sinus rhythm may significantly slow the ventricular response to atrial fibrillation and prevent reentrant tachycardias involving the AV node. For example, Wu et al[72] found that digitalis prevented the induction of sustained AV node reentrant tachycardia in five patients, but echoes were totally prevented in only one. In four of five patients, either single echoes or short runs of tachycardia with spontaneous termination were seen, consistent with changes in rate-dependent AV nodal responses. Kosowsky and coworkers[73] found that digitalis increased the PR interval by a mean of 7% at heart rates of 60–80 beats/min but by 17% at heart rates of 120–160 beats/min. Purinergic agonists such as adenosine and ATP are being used increasingly to treat patients with paroxysmal supraventricular tachycardias.[74,75] Jenkins and Belardinelli[23] showed that the effects of endogenous adenosine on the AV node are most demonstrable at rapid activation rates. Increased adenosine production in the face of oxygen supply and demand mismatching clearly played a role in the effects that they showed at rapid rates. However, changes in AV nodal functional properties may also contribute importantly, both to the frequency-dependent actions of endogenous adenosine and to the clinical response to exogenous purinergic agonists. Further study of the manipulation of rate-dependent AV nodal properties could lead to important pharmacological advances. Agents that purely altered rate-dependent properties could have minimal effects during sinus rhythm and yet produce therapeutically effective AV nodal depression during the rapid activation of supraventricular tachyarrhythmias.

We have shown that changes in vagal input importantly modify the rate-dependent properties of the AV node. While corresponding information is not available regarding adrenergic effects, β-adrenergic stimulation has been found to accelerate the recovery from inactivation of calcium-dependent action potentials.[76] Furthermore, adrenergic stimulation can reduce the effects of fatigue on the AV node.[7] These findings imply that autonomic regulation of AV nodal conduction is not a static function of the pattern of autonomic input but is a dynamic property changing with changes in cardiac rate and rhythm. The effects of autonomic interventions must therefore be understood in terms of changes in the way the AV node adapts to altered activation rate. Furthermore, any investigators using in vivo studies for evaluating rate-dependent AV nodal properties must consider the autonomic state during study and the potential changes in properties that may result from autonomic reflex responses to pacing, the stress of the intervention, etc. Such considerations will be essential if detailed analysis of the AV node's functional properties is to be extended to humans.

This is the first study, to our knowledge, that analyzes the effects of an intervention on the various rate-dependent properties of the AV node. Using specific pacing protocols, we have defined the changes that occur in each of the discrete functional properties of the AV node as a result of vagal stimulation. Furthermore, we have shown that the sum of vagally induced changes in these properties accounts for the rate-dependent actions of the vagus and that the role of changes in each property is a dynamic function of heart rate. This method of analysis may prove to be very valuable in studying the effects of other interventions on the AV node and in evaluating specific aspects of AV nodal function in patients with abnormal AV nodal properties causing tachyarrhythmias or bradyarrhythmias.

Acknowledgments

The authors thank Lise de Repentigny for typing the manuscript, Nancy Turmel for technical assistance, and Squibb Pharmaceuticals, Montreal, Canada, for supplying nadolol.

References

1. Childers R: The AV node: Normal and abnormal physiology. *Prog Cardiovasc Dis* 1977;19:361–384
2. Mobitz W: Über die unvollständige Störung der Erregungsüberleitung zwischen Vorhof und Kammer des menschlichen Herzens. *Z Gesamte Exp Med* 1924;41:180–237
3. Lewis T, Master AM: Observations upon conduction in the mammalian heart: AV conduction. *Heart* 1925,12:209–269
4. Billette J, Janse MJ, Van Capelle FJL: Cycle length–dependent properties of AV nodal activation in rabbit hearts. *Am J Physiol* 1976;231:1129–1139
5. Loeb JM, deTarnowsky JM, Warner MR, Whitson CC. Dynamic interactions between heart rate and atrioventricular conduction. *Am J Physiol* 1985;249 H505–H511
6. Van Capelle FJL, du Perron JC, Durrer D: Atrioventricular conduction in isolated rat heart. *Am J Physiol* 1971,221: 284–290
7. Ferrier GR, Dresel PE. Relationship of the functional refractory period to conduction in the atrioventricular node. *Circ Res* 1974;35:204–214
8. Billette J: Preceding His-atrial interval as a determinant of atrioventricular nodal conduction time in the human and rabbit heart. *Am J Cardiol* 1976,38:889–896
9. Moe GK, Childers RW, Merideth J. Appraisal of "supernormal" AV conduction. *Circulation* 1968,38:5–28
10. Simson MB, Spear JF, Moore EN: Electrophysiological studies in AV nodal Wenckebach cycles. *Am J Cardiol* 1978,41: 244–258
11. Simson MB, Spear JF, Moore EN: Stability of an experimental atrioventricular reentrant tachycardia in dogs. *Am J Physiol* 1981,240:H947–H953
12. Mazgalev T, Dreifus LS, Inuma H, Michelson EL: Effects of the site and timing of atrioventricular nodal input on atrioventricular conduction in the isolated perfused rabbit heart. *Circulation* 1984;70:748–759
13. Moe GK, Preston JB, Burlington H. Physiologic evidence for a dual A-V transmission system. *Circ Res* 1956,4 357–375
14. Denes P, Wu D, Dhingra R, Chuquimia R, Rosen KM Demonstration of dual A-V nodal pathways in patients with paroxysmal supraventricular tachycardia. *Circulation* 1973,48 549–555

15. Josephson ME, Kastor JA: Supraventricular tachycardia: Mechanisms and management. *Ann Intern Med* 1977;87: 346–358
16. Billette J, Métayer R: Origin, domain, and dynamics of rate-induced variations of functional refractory period in rabbit atrioventricular node. *Circ Res* 1989;65:164–175
17. Talajic M, Nattel S: Frequency-dependent effects of calcium antagonists on atrioventricular conduction and refractoriness: Demonstration and characterization in anesthetized dogs. *Circulation* 1986;74:1156–1167
18. Billette J: Short time constant for rate-dependent changes of atrioventricular conduction in dogs. *Am J Physiol* 1981;241: H26–H33
19. Merideth J, Mendez C, Mueller WJ, Moe GK: Electrical excitability of atrioventricular nodal cells. *Circ Res* 1968;23: 69–85
20. Narula OS, Runge M: Accommodation of A-V nodal conduction and fatigue phenomenon in the His-Purkinje system, in Wellens HJJ, Lie KI, Janse MJ (eds): *The Conduction System of the Heart.* Philadelphia, Lea & Febiger, 1976, pp 529–544
21. Loeb JM, deTarnowsky JM, Whitson CC, Warner MR: Atrioventricular nodal accommodation: Rate- and time-dependent effects. *Am J Physiol* 1987;252:H578–584
22. Billette J, Métayer R, St-Vincent M: Selective functional characteristics of rate-induced fatigue in rabbit atrioventricular node. *Circ Res* 1988;62:790–799
23. Jenkins JR, Belardinelli L: Atrioventricular nodal accommodation in isolated guinea pig hearts: Physiological significance and role of adenosine. *Circ Res* 1988;63:97–116
24. Levy MN, Martin PJ, Zieske H, Adler D: Role of positive feedback in the atrioventricular nodal Wenckebach phenomenon. *Circ Res* 1974;34:697–710
25. Shiner A, Dubarsky H, Rosengarten M, Guevara MR, Nattel S, Glass L: Prediction of complex atrioventricular conduction rhythms in humans with use of the atrioventricular nodal recovery curve. *Circulation* 1987;76:1196–1205
26. Billette J, Gossard JP, Lepanto L, Cartier R: Common functional origin for simple and complex responses of atrioventricular node in dogs. *Am J Physiol* 1986;251:H920–H925
27. Billette J, St-Vincent M: Functional origin of rate-induced changes in atrioventricular nodal conduction time of premature beats in the rabbit. *Can J Physiol* 1987;65:2329–2337
28. Heethaar RM, Van Der Gon JJD, Meijler FL: Mathematical model of A-V conduction in the rat heart. *Cardiovasc Res* 1973;7:105–114
29. Teague S, Collins S, Wu D, Denes P, Rosen K, Arzbaecher R: A quantitative description of normal AV nodal conduction curve in man. *J Appl Physiol* 1976;40:74–78
30. Chorro FJ, Ruiz-Granell R, Casadan E, Garcia-Civera R, Such L, Lopez-Merino V: Mathematical descriptions of AV nodal function curves in dogs. *PACE* 1988;11:679–686
31. Levy MN, Zieske H: Autonomic control of cardiac pacemaker activity and atrioventricular transmission. *J Appl Physiol* 1969; 27:465–470
32. Spear JF, Moore EN: Influence of brief vagal and stellate nerve stimulation on pacemaker activity and conduction within the atrioventricular conduction system of the dog. *Circ Res* 1973;32:27–41
33. Martin P: Secondary AV conduction responses during tonic vagal stimulation. *Am J Physiol* 1983;245:H584–H591
34. Mazgalev T, Dreifus LS, Michelson EL, Pelleg A: Effect of postganglionic vagal stimulation on the organization of atrioventricular nodal conduction in isolated rabbit heart tissue. *Circulation* 1986;74:869–880
35. Inoue H, Zipes DP: Changes in atrial and ventricular refractoriness and in atrioventricular nodal conduction produced by combinations of vagal and sympathetic stimulation that result in a constant spontaneous sinus cycle length. *Circ Res* 1987; 60:942–951
36. Meijler FL, Janse M: Morphology and electrophysiology of the mammalian atrioventricular node. *Physiol Rev* 1988;68: 608–647
37. Cohn AE, Fraser RF: Paroxysmal tachycardia and the effect of stimulation of the vagus nerves by pressure. *Heart* 1913;14: 93–108
38. Klein HO, Hoffman BF: Cessation of paroxysmal supraventricular tachycardias by parasympathomimetic interventions. *Ann Intern Med* 1974;81:48–50
39. Josephson ME, Seides SE, Batsford WB, Caracta AR, Damato AN, Kastor JA: The effects of carotid sinus pressure in re-entry paroxysmal supraventricular tachycardia. *Am Heart J* 1974;88:694–697
40. Lown B, Levine SA: The carotid sinus: clinical value of its stimulation. *Circulation* 1961;23:766–789
41. Schaal SF, Sugimoto T, Wallace AG, Sealy WC: Effects of digitalis on the functional refractory period of the AV node: Studies in awake dogs with and without cardiac denervation. *Cardiovasc Res* 1968;4:356–359
42. Goodman DJ, Rossen RM, Cannom DS, Rider AK, Harrison DC: Effect of digoxin on atrioventricular conduction. *Circulation* 1975;51:251–256
43. Youmans WB, Goodman MJ, Gould J: Neosynephrine in treatment of paroxysmal supraventricular tachycardia. *Am Heart J* 1949;37:359–373
44. Chotkowski LA, Powell CP, Radcliffe RL: Methoxamine hydrochloride in the treatment of paroxysmal supraventricular tachycardia. *N Engl J Med* 1954;250:674–676
45. Moss AJ, Aledort LM: Use of edrophonium (Tensilon) in the evaluation of supraventricular tachycardia. *Am J Cardiol* 1966; 17:58–62
46. Cantwell JD, Dawson JE, Fletcher GF: Supraventricular tachyarrhythmias: Treatment with edrophonium. *Arch Intern Med* 1972;130:221–224
47. Waxman MB, Wald RW, Sharma AD, Huerta F, Cameron DA: Vagal techniques for termination of paroxysmal supraventricular tachycardia. *Am J Cardiol* 1980;46:655–664
48. Wallick DW, Martin PJ, Masuda Y, Levy MN: Effects of autonomic activity and changes in heart rate on atrioventricular conduction. *Am J Physiol* 1982;243:H523–H527
49. Levy MN, Martin PJ, Iano T, Zieske H: Effects of single vagal stimuli on heart rate and atrioventricular conduction. *Am J Physiol* 1970;218:1256–1262
50. Mazgalev T, Dreifus LS, Michelson EL: A new mechanism for atrioventricular nodal gap–vagal modulation of conduction. *Circulation* 1989;79:417–430
51. Karpawich PP, Gillette PC, Lewis RM, Zinner A, McNamara DG: Chronic epicardial His bundle recordings in awake nonsedated dogs: A new method. *Am Heart J* 1983;105:16–21
52. Sachs L: *Applied Statistics.* New York, Springer-Verlag New York, Inc, 1984
53. Simson MB, Spear J, Moore EN: The relationship between atrioventricular nodal refractoriness and the functional refractory period in the dog. *Circ Res* 1979;44:121–126
54. Hirano Y, Fozzard HA, January CT: Characteristics of L- and T-type Ca^{2+} currents in canine cardiac Purkinje cells. *Am J Physiol* 1989;256:H1478–H1492
55. McDonald TF: The slow inward current in the heart. *Annu Rev Physiol* 1982;44:425–434
56. Billette J: Atrioventricular nodal activation during periodic premature stimulation of the atrium. *Am J Physiol* 1987;252: H163–H177
57. Cranefield PF, Hoffman BF, de Carvalho AP: Effects of acetylcholine on single fibers of the atrioventricular node. *Circ Res* 1959;7:19–23
58. West TC, Toda N: Response of the A-V node of the rabbit to stimulation of intracardiac cholinergic nerves. *Circ Res* 1967; 20:18–31
59. Mazgalev T, Dreifus LS, Michelson EL, Pelleg A: Vagally induced hyperpolarization in atrioventricular node. *Am J Physiol* 1986;251:H631–H643
60. Ten Eick R, Nawrath H, McDonald TF, Trautwein W: On the mechanism of the negative inotropic effect of acetylcholine. *Pflugers Arch* 1976;361:207–213
61. Iijima T, Irisawa H, Kameyama M: Membrane currents and their modification by acetylcholine in isolated single atrial cells of the guinea-pig. *J Physiol* (Lond) 1985;359:485–501

62. Nishimura M, Habuchi Y, Hiromasa S, Watanabe Y: Ionic basis of depressed automaticity and conduction by acetylcholine in rabbit AV node. *Am J Physiol* 1988;255:H7–H14
63. Mubagwa K, Carmeliet E: Effects of acetylcholine on electrophysiological properties of rabbit cardiac Purkinje fibers. *Circ Res* 1983;53:740–751
64. Salata JJ, Jalife J: "Fade" of hyperpolarizing responses to vagal stimulation at the sinoatrial and atrioventricular nodes of the rabbit heart. *Circ Res* 1985;56:718–727
65. Baumgarten CM, Singer DH, Fozzard HA: Intra- and extracellular potassium activities, acetylcholine and resting potential in guinea pig atria. *Circ Res* 1984;54:65–73
66. Warner MR, Loeb JM: Beat-by-beat modulation of AV conduction: I. Heart rate and respiratory influences. *Am J Physiol* 1986;251:H1126–H1133
67. Warner MR, deTarnowsky JM, Whitson CC, Loeb JM: Beat-by-beat modulation of AV conduction: II. Autonomic neural mechanisms. *Am J Physiol* 1986;251:H1134–H1142
68. Iriuchijima J, Kumada M: Activity of single vagal fibers efferent to the heart. *Jpn J Physiol* 1964;14:479–487
69. Kunze DL: Reflex discharge patterns of cardiac vagal efferent fibres. *J Physiol* (Lond) 1972;222:1–15
70. Talajic M, Navebpour M, Jing W, Nattel S: Frequency-dependent effects of diltiazem on the atrioventricular node during experimental atrial fibrillation. *Circulation* 1989;80:380–389
71. Talajic M, Papadatos D, Villemaire C, Navebpour M, Nattel S: Antiarrhythmic actions of diltiazem during experimental atrioventricular reentrant tachycardias. Importance of use-dependent calcium channel–blocking properties. *Circulation* 1990;81:334–342
72. Wu D, Wyndham C, Amat-Y-Leon F, Denes P, Dhingra RC, Rosen KM: The effects of ouabain on induction of atrioventricular nodal re-entrant paroxysmal supraventricular tachycardia. *Circulation* 1975;52:201–207
73. Kosowsky BD, Haft JI, Lau SH, Stein E, Damato AN: The effects of digitalis on atrioventricular conduction in man. *Am Heart J* 1968;75:736–742
74. DiMarco JP, Sellers TD, Lerman BB, Greenberg ML, Berne RM, Belardinelli L: Diagnostic and therapeutic use of adenosine in patients with supraventricular tachyarrhythmias. *J Am Coll Cardiol* 1985;6:417–425
75. Belhassen B, Glick A, Laniado S: Comparative clinical and electrophysiologic effects of adenosine triphosphate and verapamil on paroxysmal reciprocating junctional tachycardia. *Circulation* 1988;77:795–805
76. Tsuji Y, Inoue D, Pappano AJ: β-Adrenoceptor agonist accelerates recovery from inactivation of calcium-dependent action potentials. *J Mol Cell Cardiol* 1985;17:517–521

KEY WORDS • AV node • vagus • electrophysiology • arrhythmias • calcium channels

CHAPTER 4

The Effects of Beta Adrenergic Receptor Stimulation and Blockade on Rate-Dependent AV Node Properties

The Effects of Beta Adrenergic Receptor Stimulation and Blockade on Rate-dependent AV Node Properties

Mohsen Nayebpour, Mario Talajic, and Stanley Nattel

Short Title: Beta Adrenergic Effects on Rate-dependence of AV Node.

Submitted to Circulation Research, November 22, 1990.

Key Words: AV conduction - Arrhythmias, atrial - ECG - Calcium channels - Sympathetic nervous system - AV block - Isoproterenol.

From the Department of Medicine, Montreal Heart Institute, the Departments of Pharmacology and Therapeutics and Medicine, McGill University, and the Department of Medicine, University of Montreal, Montreal, Canada.

Supported by operating grants from the Medical Research Council of Canada, the Quebec Heart Foundation, and the Fonds de Recherche de l'Institut de Cardiologie de Montréal. Dr. Talajic is a Research Scholar of the Canadian Heart Foundation. Dr. Nattel is a recipient of the Nordic-Fonds de la Recherche en Santé du Québec Research Scholarship.

Address for reprints: Stanley Nattel, M.D., Montreal Heart Institute, 5000 Belanger Street East, Montreal, Quebec, CANADA H1T 1C8.
Tel: (514) 376-3330. FAX: (514) 376-1355.

Abstract

Recent work has shown that alterations in the dynamic AV nodal response to changes in heart rate can significantly modify AV nodal function. The present study was designed to evaluate the nature and potential importance of sympathetic regulation of the rate-dependent properties of the AV node. Selective stimulation protocols and mathematical formulations were used to quantify independently AV nodal recovery, facilitation, and fatigue in 7 morphine-chloralose anesthetized dogs. Vagal effects were prevented by bilateral vagal transection and intravenous atropine, and the sinus node was crushed to allow for a broader range of pacing cycle lengths. Beta blockade increased the recovery time constant (τ_r) for the conduction of premature test beats from 43±5 msec (control, M±SE) to 69±4 msec ($p<.001$), while isoproterenol slightly decreased τ_r to 35±2 msec (NS). In addition, beta blockade significantly increased the amount of rate-dependent AV nodal fatigue from 7±1 msec (control) to 17±2 msec ($p<.001$) at the fastest rates tested. Neither isoproterenol nor beta blockade altered AV nodal facilitation. A mathematical model incorporating quantitative indices of AV nodal function accounted accurately for tachycardia-dependent increases in AH interval, which were enhanced by beta blockade and reduced by isoproterenol. Furthermore, this model showed that beta adrenergic effects were importantly increased by increasing heart rate, with the majority of the rate-dependent action being due to changes in the time course of AV nodal recovery. We conclude that the degree of beta adrenergic stimulation importantly alters the way in which the AV node responds to changes in heart rate. The effects of sympathetic stimulation on the AV nodal response to tachycardia are opposite to those of

vagal stimulation, indicating that the dynamic properties of the AV node are under mutual regulation by both limbs of the autonomic nervous system. This constitutes a novel mechanism of regulation of AV nodal function which is potentially of both physiologic and clinical significance.

AV nodal function determines the occurrence and consequences of a wide variety of cardiac arrhythmias. The likelihood of intranodal AV block, AV node reentrant tachycardia, and orthodromic tachycardia in association with an accessory pathway, as well as the clinical consequences of atrial fibrillation and flutter, are highly related to the conduction and refractoriness properties of the AV node.[1,2] The ability of the AV node to respond to an atrial input with a propagated response is, in turn, related in a complex fashion to the activation history of the AV node.[3-13]

A variety of approaches have been used to study the processes underlying the rate-dependent properties of the AV node. The conduction of a premature impulse through the AV node is slowed increasingly as its coupling interval decreases.[3-10,12-21] This phenomenon has been attributed to incomplete AV nodal recovery, and has a time constant in the range of 50-100 msec.[8,12,18-21] On the other hand, an abrupt and sustained increase in activation frequency results in a gradual slowing of AV nodal conduction requiring minutes to reach steady state.[4,8,11,22-25] This "fatigue" process is associated with a decrease in AV nodal excitability,[22] and cannot be explained solely on the basis of incomplete recovery of excitability after activation.[22] Single premature AV nodal activations (A_2) shift the recovery curve of a subsequent A_3 beat (A_3V_3 vs V_2A_3 or A_3H_3 vs H_2A_3) to the left on the recovery time axis.[4,16,18] This results in a decrease in the time-dependent slowing of premature activations at any given recovery interval, and has been called AV nodal "facilitation". Billette and co-workers have shown that the properties of recovery, fatigue and facilitation can be characterized independently using specific stimulation protocols.[13,18,24]

The degree of sympathetic stimulation is known to be an important regulator of AV nodal function. Beta adrenergic stimulation, whether via direct activation of the sympathetic innervation of the heart[26-28] or by the exogenous administration of adrenergic agonists,[8,29,30] accelerates AV nodal conduction. Baroreflex control of the heart results in enhanced sympathetic input and accelerates AV conduction in situations that increase heart rate.[31,32] The autonomic adjustments to upright posture facilitate the induction of sustained AV node reentrant tachycardia,[33] and groups of patients have been identified who have known AV node reentrant tachycardia but in whom programmed stimulation fails to induce the clinical tachycardia unless intravenous isoproterenol is infused.[34-36] Beta blockade slows AV nodal conduction,[37] and can prevent the induction[38,39] and clinical occurrence[39-41] of sustained AV nodal reentry. The sympathetic nervous system thus plays an important role in regulating AV nodal function and determining the occurrence and manifestations of supraventricular arrhythmias.

The dependence of AV nodal function on heart rate and autonomic tone are well-known, but the interactions between the two are poorly understood. We have recently shown that changes in the AV node response to heart rate are an important mechanism of vagal action.[42] There is evidence that changes in sympathetic tone may also influence AV nodal accomodation to heart rate. Wallick et al showed that heart rate influences the effect of sympathetic nerve stimulation on AV nodal conduction in dogs,[28] and Prystowsky and Page have provided evidence for a similar interaction between heart rate and sympathetic effects in man.[43] We have developed mathematical approaches to the quantification of individual AV nodal properties,[44] and have shown that these approaches can account for both rate-dependent changes in AV nodal

conduction time[44] and for the rate-dependent effects of the vagus nerve on AV conduction.[42] The present study was designed to assess the possibility that sympathetic stimulation alters AV nodal conduction by changing the ways in which the AV node adapts to heart rate. Specific goals were (1) to evaluate whether beta-adrenergic stimulation or blockade alter basic rate-dependent properties like AV nodal recovery, facilitation or fatigue and (2) to determine the extent to which such changes account for sympathetically-mediated alterations in AV nodal conduction as a function of heart rate.

Methods

General Methods

Mongrel dogs of either sex were anesthetized with morphine (2 mg/kg) and α-chloralose (100 mg/kg i.v.). Catheters were inserted into both femoral veins and arteries and were kept patent with heparinized saline solution (0.9%). Dogs were ventilated via an endotracheal tube using a Harvard animal respirator. Tidal volume and respiratory rate were adjusted after measurement of arterial blood gases to ensure adequate oxygenation (SaO_2 ≥90%) and physiologic pH (7.35 to 7.45). A thoracotomy was performed through the fourth right intercostal space and the heart was suspended in a pericardial cradle. Body temperature was monitored continuously using a thermistor within the chest cavity and was maintained at 37-38°C by a homeothermic heating blanket.

Bipolar Teflon-coated stainless steel electrodes were inserted into the lateral right atrium and high lateral right ventricle on either side of the atrioventricular ring, and into the right atrial appendage. A bipolar electrode was inserted epicardially to record a His bundle electrogram.[45]

The electrodes located in the atrial appendage and lateral right ventricle were used to record atrial and ventricular electrograms respectively. The lateral right atrial electrode was used to apply 4 msec square-wave pulses at twice late diastolic threshold, with stimulus timing controlled by a programmable stimulator (Digital Cardiovascular Instruments Inc., Berkeley, CA). Electrogram signals were filtered at 30-500 Hz and amplified (Bloom Instruments Ltd, Flying Hills, PA) with the amplified output subsequently led into a paper recorder and/or a sensing circuit of the stimulator. A Statham P23 1D transducer (Statham Medical Instruments, Los Angeles, CA), electrophysiologic amplifiers and a Mingograf T-16 paper recorder (Siemens-Elema, Ltd., Toronto, Ont.) were used to record blood pressure, electrocardiographic leads II and aVR, atrial, His bundle and ventricular electrograms, and stimulus artifacts. Recordings were obtained at a paper speed of 200 mm/sec, resulting in a measurement accuracy of ±2.5 msec.

The sinus node was crushed using a previously described technique[19] to allow for a wide range of pacing rates. The vagus nerves were isolated in the neck, ligated, and divided. Atropine was given as an initial intravenous bolus of 1 mg, followed by 0.5 mg every 2 hours. We have shown previously that this produces sustained muscarinic receptor blockade.[46]

Measurement of Electrophysiologic Variables

Wenckebach cycle length (WBCL) was determined under control conditions by decreasing atrial pacing cycle length by 10 msec decrements every 10 beats until second degree AV block occurred. The effective refractory period of the AV node (AVERP) and atrial effective refractory period (AERP) were measured with the extrastimulus technique. The AVERP was defined as the longest atrial

(A_1A_2) interval failing to result in a His bundle deflection. The AERP was defined as the longest interstimulus (S_1S_2) interval failing to result in a propagated atrial response.

Atrioventricular conduction was assessed from the His bundle electrogram, with the AH interval defined as the time from the peak following the most rapid deflection in the atrial electrogram of the His bundle electrode to the peak following the most rapid deflection of the His bundle electrogram. The HV interval was defined as the time from bundle of His depolarization (as defined above) to the onset of earliest ventricular activation in the His signal. The HA interval was defined as the time from the peak following the most rapid deflection in the His electrogram to the corresponding peak in the next atrial electrogram in the His recording.

Quantitative Assessment of Functional Rate-dependent Properties of the AV Node

Specific stimulation protocols and analysis techniques were used to quantify selected functional AV nodal properties before and after vagal stimulation. The three basic properties of AV nodal recovery, facilitation, and fatigue were characterized as previously described in detail.[42] A brief summary follows:

1. <u>AV node recovery</u>. The atrium was paced at a basic cycle length (S_1S_1) of 500 msec and a single premature or delayed stimulus (S_2) was introduced after every 15 basic stimuli. The relationship between A_2H_2 (AV nodal conduction time of the test impulse) to H_1A_2 interval was established, and the resulting data fitted to a single exponential relation.

2. AV nodal facilitation. The atrium was paced at a constant basic cycle length of 500 msec. A premature atrial impulse (S_2) was introduced to produce a selected A_1A_2 "facilitation cycle" after every 15 basic stimuli. A test impulse (S_3) was then applied after each S_2, and the AV node response to S_3 was monitored to generate an H_2A_3-A_3H_3 recovery curve. The latter curve was studied at 7 values of (A_1A_2) facilitation cycle lengths (FCL) between 500 msec and 20 msec greater than the refractory period of the AV conduction system.

Each H_2A_3-A_3H_3 recovery curve was fitted by a monoexponential model and the H_2A_3 value at which the A_3H_3 interval is 125 msec (to be referred to as the "HA_{125}") was calculated for each curve. The HA_{125} is an index of the position of the curve on the horizontal axis. Changes in HA_{125} reflect the magnitude of parallel leftward shift in the recovery curve resulting from facilitation, and are well-fitted by an exponential function of FCL.[42]

3. AV nodal fatigue. A sensing and pacing circuit were used to sense each ventricular activation and pace the right atrium with a given VA interval. Since the HV interval remained constant throughout each experiment, this allowed us to initiate a tachycardia with a given HA interval and to maintain the HA interval constant throughout the tachycardia. Tachycardia was initiated abruptly and maintained for five minutes, with the atrial cycle length prior to tachycardia set at 500 msec by using an activation-inhibited demand pacemaker at a rate of 120/min. After five minutes of tachycardia, the sense-pace circuit was closed, and five minutes at the baseline cycle length (500 msec) were allowed for recovery before initiating tachycardia with a different HA interval. Fatigue was studied at a total of 7 HA intervals in

each experiment. The onset of fatigue is well-approximated by a monoexponential function of beat number,[42] and nonlinear curve fitting was used to characterize the appearance of fatigue for each tachycardia.

Experimental Protocol

AV nodal recovery, fatigue and facilitation were characterized under control conditions as described above. Steady-state values for AH interval were determined over a wide range of cycle lengths, with five minutes of pacing at each cycle length used to ensure steady-state conditions. WBCL was measured before and after each experimental protocol to confirm the stability of each preparation. Isoproterenol was then infused *via* an infusion pump (EDCO Scientific Inc., Model 848, Chapel Hill, NC) at a rate of 2-5 µg/min. The rate of isoproterenol infusion was selected to produce a 20-30 msec decrease in WBCL, and the infusion rate was then kept constant in a given dog. Three dogs received an infusion of 2 µg/min, and four others an infusion of 5 µg/min. Thirty minutes after the onset of isoproterenol infusion, the measurements obtained under control conditions were repeated. Isoproterenol was then discontinued, and 20 min allowed for a return to baseline. When WBCL had returned to control values as determined by five consecutive measurements, 0.5 mg/kg of nadolol was given. We have shown previously that this results in sustained beta blockade for over two hours. Twenty minutes later, all measurements were repeated.

Data Analysis

Results are reported as the mean±SE. Comparisons between multiple groups were made by two-way analysis of variance with Scheffé contrasts.[47]

Comparisons between two groups of experimental data only were made with Student's t-test. Two-tailed tests were used for all statistical comparisons and a probability of 5% or less was taken to indicate statistical significance. Exponential curve fitting was performed using Marquardt's technique on an IBM AT compatible computer. A total of seven dogs were studied, with complete experimental protocols performed in all animals.

Results

General Effects of Beta Receptor Stimulation and Blockade

Beta receptor stimulation with isoproterenol accelerated AV nodal conduction, and decreased atrial effective refractory period and WBCL (Table 1). Beta blockade had the opposite effects. AVERP was not measurable in most experiments because it was less than AERP, ie. premature beats early enough to encounter AV nodal refractoriness could not be initiated in the atrium. Isoproterenol reduced diastolic arterial pressure and tended to increase systolic pressure, while beta blockade significantly reduced both systolic and diastolic pressure. The stability of the preparation is indicated by the consistent values of WBCL obtained at the beginning, midpoint, and end of each experimental protocol (Fig. 1). A high baseline level of adrenergic stimulation in this open-chest preparation is suggested by the generally larger effect of beta blockade than of beta adrenergic stimulation.

Changes in AV Nodal Recovery

Typical AV recovery curves under control conditions, in the presence of isoproterenol, and after nadolol are shown in Figure 2. Isoproterenol decreased, and beta blockade increased, the AH intervals associated with

coupling intervals long enough to allow for complete recovery. Beta blockade resulted in a slower time course of recovery (ie. longer time constant, as shown by the arrow in Fig. 2), while isoproterenol slightly accelerated recovery. The mean recovery time constant averaged 43±5 msec under control conditions, compared to 69±4 msec ($p<.001$) after beta blockade and 35±2 msec (p=NS) in the presence of isoproterenol.

AV Nodal Facilitation

A premature AV nodal activation resulted in leftward shift of the AV nodal recovery curve for a subsequent beat, as shown by data from a typical experiment in Figure 3. The magnitude of leftward shift for a given coupling interval was similar under all 3 conditions. In order to analyze changes in facilitation, each AV recovery curve was fitted to the equation

$$AH_{HA} = AH_{\infty} + A \exp(-HA/\tau_{rec}) \qquad \text{(eq. 1)}$$

Where AH_{HA} = AH interval at a given HA interval, AH_{∞} = AH interval after full recovery (corresponding to an infinitely long recovery time), A and τ_{rec} are constants. Since facilitation corresponds to a parallel leftward shift of the recovery curve, the magnitude of shift was quantified by calculating the HA time associated with an AH interval of 125 msec for each curve, or HA_{125}.

As shown in Figure 4, the HA_{125} decreased with decreased A_1A_2 interval (FCL) under all 3 conditions. HA_{125} values were greater in the presence of beta blockade, indicating that lesser degrees of prematurity of the test (A_3) impulse were needed to attain an AH of 125 msec than under control conditions. The opposite occurred in the presence of isoproterenol - the test beat had to be more premature (ie. at a smaller HA interval) in order

to prolong the AH to 125 msec. The slowing effect of beta blockade on recovery is indicated by significantly greater recovery time constants (τ_{rec}) compared to control, while isoproterenol changed recovery in the opposite direction. Isoproterenol also accelerated basal AV nodal conduction, as shown by AH_{∞}, while beta blockade had the opposite effect. In contrast to the reduction in HA_{125} resulting from decreased FCL under each experimental condition, neither AH_{∞} nor τ_{rec} were significantly affected by FCL. This confirms the parallel nature of recovery curve shifts resulting from facilitation.

Decreases in HA_{125} produced by a premature beat at any FCL relative to the value at the basic cycle length of 500 msec (ΔHA) are an index of the magnitude of facilitating effect at that FCL. As shown in Figure 5, this index of the magnitude of facilitation was not significantly altered by beta adrenergic stimulation or blockade. Changes in HA interval at any FCL can be fitted to an equation of the form

$$\Delta HA = K\exp(-FCL \cdot B) \qquad \text{(eq. 2)}$$

where K is a constant equal to the (theoretical) change in HA interval at a FCL of 0, and B is a rate constant. The mean values of K and B were unaltered by beta adrenergic stimulation and blockade (Table 2), indicating that the level of sympathetic tone did not alter AV nodal facilitation. Values of HA_{125} predicted by this analysis are shown by the dotted curves in Figure 4. The parallel nature of these curves indicate the lack of any changes in facilitation as a result of varying beta adrenergic tone.

AV Nodal Fatigue

The initiation of a tachycardia with a constant HA interval results in AH prolongation over the subsequent 200 beats. Since HA is constant, this

gradual increase in AH interval cannot be due to changes in AV nodal recovery. Facilitation reaches steady state within one cycle of tachycardia.[16,42] Therefore, further changes in AH interval are due to AV nodal fatigue. Figure 6 shows the time course of changes in AH interval from beat 2 of the tachycardia until a steady state has been achieved in a representative experiment. For each tachycardia, changes in AH interval were well-fitted by an exponential relation of the form

$$\Delta AH_n = \Delta AH_{ss}[1 - \exp(-n/\tau_{fat})] \qquad \text{(eq. 3)}$$

where ΔAH_n = change in AH interval due to fatigue for the n^{th} beat, ΔAH_{ss} = steady-state change in AH interval due to fatigue, and τ_{fat} = a time constant. The solid lines in Figure 6 show the best-fit curves to data from 3 tachycardias under each condition. A total of 7 tachycardias were studied in each experiment.

In the experiment illustrated in Figure 6, beta blockade increased the magnitude of fatigue (ΔAH_{ss}). This was a general finding in all experiments, as shown by the mean data in Figure 7. The time constant for fatigue onset (τ_{fat}) did not appear to be affected by sympathetic tone, averaging 65±7 beats under control conditions, 84±18 in the presence of isoproterenol, and 47±4 beats after beta blockade (p=NS). The magnitude of AH change due to fatigue at any steady-state HA interval (ΔAH_{HA}) was found to be an exponential function of HA, of the form

$$\Delta AH_{HA} = \Delta AH_{max} \exp(-D \cdot HA) + C \qquad \text{(eq. 4)}$$

where ΔAH_{max}, C, and D are constants obtained by nonlinear curve fitting. The dashed lines in Figure 7 show fits to the mean data using equation 4 for each condition.

Role of Changes in Rate-dependent Properties

The basic AV recovery equation (eq. 1 above) describes the effect of coupling interval on AV nodal conduction, but does not consider the role of facilitation or fatigue. It fails, therefore, to account fully for AV node conduction changes in response to circumstances in which the level of facilitation or fatigue is changing.[9,12,48] During sustained rate changes, alterations in both facilitation and fatigue occur. To evaluate the role of sympathetic modulation of AV nodal properties at different heart rates, it is necessary to analyze the contribution of sympathetic changes in all 3 rate-dependent AV nodal properties.

We have previously shown[48] that the contribution of facilitation and fatigue can be incorporated into the basic AV nodal recovery equation 1. Facilitation is incorporated by considering HA in equation 1 to be modulated by the preceding cycle length (according to eq. 2), and AH_{∞} is adjusted to account for the effect of fatigue described by equation 4. Accordingly, equation 1 can be rewritten as:

$$AH_{HA} = P + A \exp(-Q/\tau_{rec}) \qquad \text{(eq. 5)}$$

where $P = AH'_{\infty} + \Delta AH_{HA}$, for $AH'_{\infty} = AH_{\infty}$ at a cycle length of 500 msec, and ΔAH_{HA} is as defined in equation 4 above; and $Q = HA + \Delta HA$, for ΔHA as defined in equation 2 above.

Data in each experiment was used to calculate the constants AH'_{∞}, A, τ_{rec}, K, B, ΔAH_{max}, C, and D as defined above. The mean constants for all experiments are shown in Table 2. These mean constants were substituted into the corresponding equations to obtain estimates for any steady state HA interval of the predicted effects of incomplete recovery alone (from eq. 1), of recovery modified by facilitation (according to eq. 2), of fatigue alone

(eq. 4), and of all 3 processes functioning simultaneously (eq. 5). Values at each cycle length were subtracted from those at a BCL of 500 msec, to provide an estimate of rate-dependent slowing at any cycle length due to the influence of each process.

The resulting curves for all experimental conditions are shown in Figure 8. Isoproterenol decreases the effect of incomplete recovery, while beta blockade enhances it, in addition to increasing the effect of fatigue. These changes result in reduced rate-dependent conduction slowing in the presence of isoproterenol, and increased rate-dependent conduction slowing in the presence of beta blockade. Experimental data showing the magnitude of AH prolongation at each basic cycle length (open boxes and error bars) agrees well with the predictions of the above analysis.

In order to further analyze the role of changes in rate-dependent properties, we determined the magnitude of AV conduction change attributable to sympathetically-mediated changes in recovery and fatigue. AH intervals in the presence of isoproterenol were compared to those in the presence of beta blockade, in order to contrast findings associated with a constant, enhanced level of beta adrenergic stimulation with those in the absence of beta-mediated effects. As shown in Figure 9, beta adrenergic stimulation results in a decrease in AH interval, which becomes more marked as cycle length (or HA interval) decreases. Predicted changes (from the approach described above) are shown by the solid curve, and agree well with experimental data. The mathematical analysis allows us to attribute the observed AH reduction to changes in underlying AV nodal properties. At cycle lengths >500 ms, all of the AH reduction caused by isoproterenol is attributable to a time-independent (tonic) action. As cycle length is

reduced, the acceleration of recovery produced by sympathetic stimulation becomes important, and accounts for over half of the acceleration in conduction resulting from sympathetic stimulation at rapid rates. While a reduction of fatigue may also play a role at very rapid rates, it is predominantly the change in AV nodal recovery that accounts for the rate-dependent effects of sympathetic stimulation on AV node conduction.

Discussion

We have shown that the degree of beta adrenergic tone can importantly alter the ways in which the AV node responds to changes in input pattern. The net effect of sympathetic stimulation is to reduce the conduction slowing effect of increases in heart rate, while beta blockade enhances the negative dromotropic effect of supraventricular tachycardia.

Comparison With Previous Studies of Sympathetic Effects on the AV Node

As reviewed in the Introduction, sympathetic nerve stimulation,[26-28] exogenous beta agonists,[8,29,30] and baroreflex-mediated increases in sympathetic tone[31,32] all enhance AV node conduction by causing beta adrenergic receptor activation. Ferrier and Dresel showed that basal AV nodal conduction time at rapid rates is reduced by the infusion of epinephrine,[8] suggesting that adrenergic stimulation reduces the extent of AV nodal fatigue associated with tachycardia. Wallick et al[28] showed that the acceleration of AV conduction caused by sympathetic nerve stimulation depends on the paced atrial rate, and is magnified by tachycardia. The AH interval shortening produced by isoproterenol infusion in man similarly depends on the atrial activation rate.[49]

While the above observations suggest an interaction between adrenergic tone and rate-dependent AV nodal properties, the precise nature of this interaction has not been determined. In an extensive series of studies, Billette and co-workers[5,13,16,18,24,50] have shown that the properties of AV nodal recovery, facilitation, and fatigue can be studied independently using selective stimulation protocols. We have developed mathematical techniques to quantify these properties,[42,44,46,48] and in the present study have applied these methods to analyse the effects of sympathetic stimulation and blockade.

Beta blockade substantially increased the amount of rate-dependent fatigue, in agreement with the observations of Ferrier and Dresel.[8] In addition, beta blockade slowed the recovery of AV nodal conduction following preceding activation. Beta receptor stimulation had the opposite effects, tending to reduce the conduction slowing effects of rate increases. In general, the changes produced by beta blockade were larger than those resulting from beta adrenergic stimulation, probably reflecting the high level of resting sympathetic tone in this open-chest, anesthetized preparation. Neither beta blockade nor isoproterenol appeared to affect AV nodal facilitation.

Autonomic Regulation of Rate-dependent AV Nodal Properties

In the present study, we have found that beta adrenergic stimulation attenuates rate-dependent AV nodal conduction changes. We have previously reported that vagal stimulation accentuates rate-dependent conduction slowing in the AV node.[42] Figure 10 shows the amount of rate-dependent AH prolongation (as a percent change from the AH value at a cycle length of 500 msec) as a function of pacing cycle length under 3 conditions: 1) control; 2) beta adrenergic stimulation with isoproterenol; and 3) enhanced vagal

tone. Values in the presence of isoproterenol were derived from data presented in the current manuscript. Results representing the effects of enhanced vagal tone were obtained by analyzing data obtained in a previous study[42] for which this specific analysis was not previously performed. Control values correspond to an absence of autonomic effects in the presence of nadolol and bilateral surgical vagotomy. Control data was available from both the present study and the previous investigation of vagal stimulation. Since control data did not differ significantly between the studies, control results from both studies were combined for presentation in Figure 9.

Rate-dependent AV nodal conduction slowing manifested as statistically significant increases in AH interval as cycle length shortened. Vagal stimulation resulted in larger increases in AV nodal conduction time, and these changes became statistically significant at longer basic cycle lengths than under control conditions. Isoproterenol had the opposite effect, greatly attenuating the increases in AH interval as cycle length shortened. These observations are similar to those presented in a schematic figure by Prystowsky and Page,[43] and suggest that the rate-dependent behaviour of the AV node is under reciprocal control of both limbs of the autonomic nervous system.

Our results indicate that beta adrenergic tone modulates the rate-dependent AV nodal properties of recovery and fatigue, without changing facilitation. As shown in Figure 8, increases in AH interval with decreases in cycle length are fully attributable to the participation of recovery, facilitation and fatigue over a wide range of sympathetic tone. Vagal stimulation alters AV nodal accommodation by increasing AV nodal fatigue and slowing recovery, effects opposite to those of sympathetic stimulation.[42] Vagal effects are

not due to simple antagonism of adrenergic actions,[51] because they occur in the presence of continuous beta adrenergic receptor blockade under both control and vagal stimulation conditions.[42] Furthermore, while neither isoproterenol nor beta blockade altered facilitation in the present study, vagal stimulation markedly attenuates AV nodal facilitation.[42]

Possible Ionic Mechanisms of Adrenergic Effects on AV Nodal Recovery and Fatigue

The precise ionic mechanisms of AV nodal recovery and fatigue remain unknown. It is likely that AV nodal recovery is related to the time required for reactivation of L-type calcium channels.[42,46,48] Beta adrenergic stimulation accelerates the recovery of slow channel action potentials,[52] and promotes reactivation of calcium current in single guinea-pig ventricular myocytes.[53] An acceleration of the recovery of calcium current from inactivation is thus a probable explanation of the more rapid recovery of AV nodal conduction upon beta adrenergic stimulation. Acetylcholine slows calcium current repriming,[53] which may account for the retardation of AV nodal recovery resulting from vagal stimulation.[42]

AV nodal fatigue may be related to ion accumulation or depletion, metabolic dysfunction, or electrogenic transport mechanisms. Adenosine release may contribute to AV nodal fatigue under certain circumstances.[25] If extracellular potassium accumulation plays a role in AV nodal fatigue, it is possible that the ability of beta adrenergic stimulation to stimulate Na^+, K^+-ATP'ase activity[54,55] accounts for its fatigue-attenuating properties.

Potential Limitations of our Findings

We studied three levels of adrenergic tone in our dogs: resting basal tone

in an open-chest, anesthetized preparation; a constantly-increased level of beta adrenergic receptor stimulation resulting from continuous isoproterenol infusion; and the absence of beta adrenergic stimulation resulting from beta blockade with nadolol. We have not examined the complex changes in rate-dependent AV nodal properties that may occur with continuously changing levels of sympathetic activity.[56,57] While such studies would have been interesting, they are beyond the scope of the present manuscript. Direct membrane actions of beta blockers can be a complicating factor in electrophysiologic studies. Nadolol, however, is devoid of any direct membrane actions[58] and all of its effects observed in this study can be safely attributed to beta adrenergic receptor blockade.

The site of AV nodal input can modify AV nodal conduction,[59-61] and was not considered in the analysis presented here. In the present study, the initial site of atrial activation was kept constant by atrial activation, and changes in AV nodal conduction were well-explained by our mathematical treatment (Figure 9). If adrenergic stimulation altered the site of atrial pacemaker activity, as can occur under some experimental conditions,[62] changes in AV nodal conduction not accounted for by our model could result.

We used the HA interval as an index of AV nodal recovery time. The relative merits of the HA interval and the AA interval as indices of AV nodal recovery period have been disputed, and resolution of this issue is beyond the capability of the methods used in this study. Levy et al have shown that changes in HA interval can importantly affect AV nodal conduction at a constant cycle length,[6] and Billette has reported that consideration of the HA interval can explain previously poorly-understood properties of AV nodal functional refractoriness.[63] Using the HA interval as a recovery index, we

have developed a relatively straightforward mathematical analysis which can be used to quantify individual AV nodal properties and to study their response to interventions. Furthermore, this analysis accounts well for steady-state AV nodal conduction at different rates,[46] for complex Wenckebach-type behaviours,[48] and for the effects of vagal[42] and sympathetic stimulation (present study) on rate-dependent AV nodal conduction.

Potential Significance

Autonomic influences are well-known to regulate AV nodal conduction. Our findings indicate that modulation of the AV nodal response to rate change constitutes an important mechanism of such influences. This mechanism would serve an important physiological function, by tending to maintain 1:1 AV nodal conduction in the presence of physiologic tachycardias resulting from heightened sympathetic and reduced parasympathetic tone.

Changes in rate-dependent AV nodal properties may contribute importantly to the effects of beta adrenergic receptor stimulation and blockade on cardiac arrhythmias. The acceleration of AV nodal recovery that results from sympathetic stimulation at least partially accounts for its ability to abbreviate AV nodal refractoriness.[33,35,36] In combination with a reduction in AV nodal fatigue resulting from tachycardia, accelerated recovery from preceding activation may explain the facilitating effect of sympathetic activation on the induction and spontaneous occurrence of AV node reentry.[33,35,36] Converse actions may account for the prevention of AV nodal reentry by beta blockers.[38,39] The ability of beta blockade to increase AV nodal fatigue may account for the ability of beta blockade to convert sustained AV node reentrant tachycardias to non-sustained arrhythmias.[38]

Conclusions

We have shown that the degree of beta adrenergic receptor activation modulates discrete rate-dependent properties of the AV node. These actions decrease AV nodal conduction slowing by tachycardia when sympathetic tone is high, and increase the negative dromotropic effects of tachycardia in the presence of beta adrenergic receptor blockade. The accomodation properties of the AV node are under reciprocal control of both limbs of the autonomic nervous system, and constitute a heretofore little-recognized aspect of autonomic regulation of AV nodal function. Further work needs to be done to clarify the underlying mechanisms of dynamic AV nodal properties, and of autonomic effects on them.

Acknowledgments

The authors thank Lise de Repentigny for typing the manuscript, Nancy Turmel and Christine Villemaire for technical help, and Squibb Pharmaceuticals (Can.) for supplying the nadolol used to produce beta blockade.

References

1. Zipes DP: Specific arrhythmias - diagnosis and treatment, in Braunwald E (ed); Heart Disease, Third Edition. Philadelphia, W.B. Saunders Co, 1988, pp 658-716
2. Josephson ME, Buxton AE, Marchlinksi FE: The tachyarrhythmias, in Braunwald E, Isselbacker KJ, Petersdorff RG, Wilson JD, Martin JB, Fauci AS (eds): Harrison's Principles of Internal Medicine, Eleventh Edition. New York, McGraw-Hill Book Co., 1987, pp 923-937
3. Mobitz W: Uber die unvollständige störung der erregungs-überleitung zwischen vorhof und kammer des menschlichen herzens. Zeit Gesamte Exp Med 1924;41:180-237
4. Lewis T, Master AM: Observations upon conduction in the mammalian heart: AV conduction. Heart 1925:12:209-269
5. Billette J, Janse MJ, Van Capelle FJL: Cycle length-dependent properties of AV nodal activation in rabbit hearts. Am J Physiol 1976;231:1129-1139
6. Levy MN, Martin PH, Zieske H, Adler D: Role of positive feedback in the atrioventricular nodal Wenckebach phenomenon. Circ Res 1974;34:697-710
7. Van Capelle FJL, du Perron JC, Durrer D: Atrioventricular conduction in isolated rat heart. Am J Physiol 1971;221:284-290
8. Ferrier GR, Dresel PE: Relationship of the functional refractory period to conduction in the atrioventricular node. Circ Res 1974;35:204-214
9. Simson MB, Spear JF, Moore EN: Electrophysiological studies in AV nodal Wenckebach cycles. Am J Cardiol 1978;41:244-258
10. Mazgalev T, Dreifus LS, Iinuma H, Michelson EL: Effects of the site and timing of atrioventricular nodal input on atrioventricular conduction in the isolated perfused rabbit heart. Circulation 1984;70:748-759

11. Loeb JM, deTarnowsky JM, Whitson CC, Warner MR: Atrioventricular nodal accommodation: rate- and time-dependent effects. Am J Physiol 1987;252:H578-H584

12. Shrier A, Dubarsky H, Rosengarten M, Guevara MR, Nattel S, Glass L: Prediction of complex atrioventricular conduction rhythms in humans with use of the atrioventricular nodal recovery curve. Circulation 1987;76:1196-1205

13. Billette J, Gossard JP, Lepanto L, Cartier R: Common functional origin for simple and complex responses of atrioventricular node in dogs. Am J Physiol 1986;251:H920-H925

14. Moe GK, Preston JB, Burlington H: Physiologic evidence for a dual A-V transmission system. Circ Res 1956;IV:357-375

15. Denes P, Wu D, Dhingra R, Chuquimia R, Rosen KM: Demonstration of dual A-V nodal pathways in patients with paroxysmal supraventricular tachycardia. Circulation 1973;48:549-555

16. Billette J: Preceding His-atrial interval as a determinant of atrioventricular nodal conduction time in the human and rabbit heart. Am J Cardiol 1976;38:889-896

17. Simson MB, Spear JF, Moore EN: Stability of an experimental atrioventricular reentrant tachycardia in dogs. Am J Physiol 1981;240:H947-H953

18. Billette J: Short time constant for rate-dependent changes of atrioventricular conduction in dogs. Am J Physiol 1981;241:H26-H33

19. Talajic M, Nattel S: Frequency-dependent effects of calcium antagonists on atrioventricular conduction and refractoriness: demonstration and characterization in anesthetized dogs. Circulation 1986;74:1156-1167

20. Teague S, Collins S, Wu D, Denes P, Rosen K, Arzbaecher R: A quantitative description of normal AV nodal conduction curve in man. J Appl Physiol 1976;40:74-78

21. Chorro FJ, Ruiz-Granell R, Casadan E, Garcia-Civera R, Such L, Lopez-Merino V: Mathematical descriptions of AV nodal function curves in dogs. PACE 1988;11:679-686

22. Meredith BJ, Mendez C, Mueller WJ, Moe GK: Electrical excitability of atrioventricular nodal cells. Circ Res 1968;23:69-85

23. Narula OS, Runge M: Accommodation of A-V nodal conduction and fatigue phenomenon in the His-Purkinje system, in Wellens HJJ, Lie KI, Janse MJ (eds); The Conduction System of the Heart. Philadelphia, Lea & Febiger, 1976

24. Billette J, Métayer R, St-Vincent M: Selective functional characteristics of rate-induced fatigue in rabbit atrioventricular node. Circ Res 1988;62:790-799

25. Jenkins JR, Belardinelli L: Atrioventricular nodal accommodation in isolated guinea pig hearts: physiological significance and role of adenosine. Circ Res 1988;63:97-116

26. Rothberger DJ, Winterberg H: Ueber die Beziehung der Herznerven zur Automatischen Reizerzeugung und zum Ploetzlechen Herztode. Arch ges Physiol 1911;141:343-377

27. Spear JF, Moore EN: Influence of brief vagal and stellate nerve stimulation on pacemaker activity and conduction within the atrioventricular conduction system of the dog. Circ Res 1973;32:27-41

28. Wallick DW, Martin PJ, Masuda Y, Levy MN: Effects of autonomic activity and changes in heart rate on atrioventricular conduction. Am J Physiol 1982;243:H523-H527

29. Lister JW, Stein E, Kosowsky BD, Lau SH, Damato AN: Atrioventricular conduction in man. Am J Cardiol 1965;16:516-523

30. Wallace AG, Troyer WG, Lesage MA, Zotti EF: Electrophysiologic effects of isoproterenol and beta blocking agents in awake dogs. Circ Res 1966;18:140-148

31. O'Toole MF, Wurster RD, Phillips JG, Randall WC: Parallel baroreceptor control of sinoatrial rate and atrioventricular conduction. Am J Physiol 1984;246:H149-H153

32. Warner MR, Loeb JM: Reflex regulation of atrioventricular conduction. Am J Physiol 1987;252:H1077-H1085

33. Mann DE, Reiter MJ: Effects of upright posture on atrioventricular nodal reentry and dual atrioventricular nodal pathways. Am J Cardiol 1988;62:408-412

34. Hariman RJ, Gomes JAC, El-Sherif N: Catecholamine-dependent atrioventricular nodal reentrant tachycardia. Circulation 1983;67:681-686

35. Brownstein SL, Hopson RC, Martins JB, Aschoff AM, Olshansky B, Constantin L, Kienzle MG: Usefulness of isoproterenol in facilitating atrioventricular nodal reentry tachycardia during electrophysiologic testing. Am J Cardiol 1988;61:1037-1041

36. Huycke EC, Lai WT, Nguyen NX, Keung EC, Sung RJ: Role of intravenous isoproterenol in the electrophysiologic induction of atrioventricular node reentrant tachycardia in patients with dual atrioventricular node pathways. Am J Cardiol 1989;64:1131-1137

37. Priola DV: Effects of beta receptor stimulation and blockade on A-V nodal and bundle branch conduction in the canine heart. Am J Cardiol 1973;31:35-40

38. Wu D, Denes P, Dhingra R, Khan A, Rosen KM: The effects of propranolol on induction of A-V nodal reentrant paroxysmal tachycardia. Circulation 1974;50:665-677

39. Bauernfeind RA, Wyndham CR, Dhingra RC, Swiryn SP, Palileo E, Strasberg B, Rosen KM: Serial electrophysiologic testing of multiple drugs in patients with atrioventricular nodal reentrant paroxysmal tachycardia. Circulation 1980;62:1341-1349

40. Sung RJ, Tai DY, Svinarich JT: Beta-adrenoceptor blockade: Electrophysiology and antiarrhythmic mechanisms. Am Heart J 1984;108:1115-1120

41. Seides SF, Josephson ME, Batsford WP, Weisfogel GM, Lau SH, Damato AN: The electrophysiology of propranolol in man. Am Heart J 1974;88:733-741

42. Nayebpour M, Talajic M, Villemaire C, Nattel S: Vagal modulation of the rate-dependent properties of the atrioventricular node. Circ Res 1990;67:1152-1166

43. Prystowsky EN, Page RL: Electrophysiology and autonomic influences of the human atrioventricular node, in Mazgalev T, Dreifus LS, Michelson EL (eds): Electrophysiology of the Sinoatrial and Atrioventricular Nodes. Prog Clin Biol Res 1988;275:259-277. New York, Alan R. Liss, Inc.

44. Nayebpour M, Talajic M, Nattel S: Functional analysis of rate-dependent properties of AV node in anesthetized dogs (abstract). J Am Coll Cardiol 1990;15:201A

45. Karpawich PP, Gillette PC, Lewis RM, Zinner A, McNamara DG: Chronic epicardial His bundle recordings in awake nonsedated dogs: a new method. Am Heart J 1983;105:16-21

46. Nayebpour M, Talajic M, Jing W, Nattel S: Autonomic modulation of the frequency-dependent actions of diltiazem on the atrioventricular node in anesthetized dogs. J Pharmacol Exp Ther 1990;253:353-361

47. Sachs L: Applied Statistics. New York, Springer-Verlag, 1984

48. Talajic M, Papadatos D, Glass L, Villemaire C, Nattel S: Mechanism of dynamic changes in Wenckebach-type AV block (abstract). J Am Coll Cardiol 1990;15:201A

49. Kammerling JM, Miles WM, Prystowsky EN: Effects of graded isoproterenol infusions on human cardiac electrophysiologic properties. Circulation 1985;72(Suppl III):III-252

50. Billette J, St-Vincent M: Functional origin of rate-induced changes in atrioventricular nodal conduction time of premature beats in the rabbit. Can J Physiol 1987;65:2329-2337

51. Inoue H, Zipes DR: Changes in atrial and ventricular refractoriness and in atrioventricular nodal conduction produced by combinations of vagal and sympathetic stimulation that result in a constant spontaneous sinus cycle length. Circ Res 1987;60:942-951

52. Tsuji Y, Inoue D, Pappano AJ: β-adrenoceptor agonist accelerates recovery from inactivation of calcium-dependent action potentials. J Mol Cell Cardiol 1985;17:517-521

53. Shimoni Y, Spindler AJ, Noble D: The control of calcium current reactivation by catecholamines and acetylcholine in single guinea-pig ventricular myocytes. Proc R Soc Lond 1987;230:267-278

54. Chae SW, Wang DY, Gong QY, Lee CO: Effect of norepinephrine on Na^+-K^+ pump and Na^+ influx in sheep cardiac Purkinje fibers. Am J Physiol 1990;258:C713-C722

55. Diacono J, Diétrich J, Lajoix H: Opposite effects of adrenaline and ouabain on the resting potential of rat atrial cells. Life Sci 1986;39:2541-2550

56. Warner MR, Loeb JM: Beat-by-beat modulation of AV conduction. I. Heart rate and respiratory influences. Am J Physiol 1986;251:H1126-H1133

57. Warner MR, deTarnowsky JM, Whitson CC, Loeb JM: Beat-by-beat modulation of AV conduction. II. Autonomic neural mechanisms. Am J Physiol 1986;251:H1134-H1142

58. Weiner N: Drugs that inhibit adrenergic nerves and block adrenergic receptors, in Goodman Gilman A, Goodman LS, Rall TW, Murad F (eds): Goodman and Gilman's, The Pharmacologic Basis of Therapeutics, Seventh edition. New York, MacMillan Publishing Co., 1985, pp 194.

59. Batsford WP, Akhtar M, Caracta AR, Josephson ME, Seides SF, Damato AN: Effect of atrial stimulation site of the electrophysiological properties of the atrioventricular node in man. Circulation 1974;50:283-292

60. Janse MJ: Influence of the direction of the atrial wave front on A-V nodal transmission in isolated hearts of rabbits. Circ Res 1969;25:439-449

61. Mazgalev T, Dreifus LS, Iinuma H, Michelson EL: Effects of the site and timing of atrioventricular nodal input on atrioventricular conduction in the isolated perfused rabbit heart. Circulation 1984;70:748-759

62. Priola DV, Randall WC: Alterations in cardiac synchrony induced by the cardiac sympathetic nerves. Circ Res 1964;15:463-472

63. Billette J, Métayer R: Origin, domain, and dynamics of rate-induced variations of functional refractory period in rabbit atrioventricular node. Circ Res 1989;65:164-175

Table 1. Effects of Isoproterenol and Beta Adrenergic Receptor Blockade.

	WBCL (ms)	AERP (ms)	AH (ms)	Blood pressure (mmHg)
Control	167±8.8	132±6	57±5	136±7 / 89±5
Isoproterenol	146±10**	122±5	47±3*	142±10 / 69±5*
β-blocked	242±15***	161±10**	92±6***	103±7***/ 73±6*

Abbreviations: WBCL = Wenckebach cycle length; AERP = atrial effective refractory period; AH = AH interval.
All measurements other than WBCL were obtained at a basic cycle length of 500 msec.
* $p<.05$; ** $p<.01$; *** $p<.001$ compared to control.

Table 2. Mean Values of Constants Characterizing AV Nodal Recovery, Facilitation and Fatigue in 7 Dogs.

	Control	Isoproterenol	β-blocked	Units
AH'_{∞}†	54±5	45±4*	85±7***	msec
A	1.5±.3	1.0±.3	0.6±.1	sec
τ_{rec}	43±5	35±2	69±4***	msec
K	317±59	425±114	395±128	msec
B	0.009±.002	0.010±.002	0.009±.003	$msec^{-1}$
ΔAH_{max}	12±1	18±4	24±2**	msec
C	-1±1	0±1	-2±1	msec
D	0.008±.002	0.014±.003	0.006±.001	$msec^{-1}$

† Abbreviations are defined in equations 1,2,4 and 5 of the text. AH'_{∞}, A and τ_{rec} were obtained by fitting recovery data at a cycle length of 500 msec to equation 1 for each experiment, and averaging the values obtained in all 7 experiments. K and B were obtained by fitting facilitation data in each experiment to equation 2. ΔAH_{max}, C and D were obtained by fitting fatigue data from each experiment to equation 4, as shown for the mean data in Figure 7.

* $p<.05$, ** $p<.01$, *** $p<.001$ compared to corresponding control value.

Figure Legends

Figure 1. Wenckebach cycle length (WBCL) at the beginning (1), middle (2), and end (3) of electrophysiologic study protocols under control, isoproterenol (ISO) and β-blocked conditions. C= value after discontinuation of isoproterenol and prior to nadolol administration. (Results are mean±SE).

Figure 2. AV recovery curves from a representative experiment, with the best exponential curve fits, shown by the solid lines, and time constants indicated by arrows.

Figure 3. Recovery curves for a test atrial beat (A_3) preceded by a variety of A_1A_2 (facilitation) cycle lengths in a representative experiment. As the A_1A_2 decreased, the AV nodal recovery curve of the A_3 beat shifted progressively to the left. The solid lines are best-fit exponentials to the raw data shown.

Figure 4. Values of the HA interval corresponding to an AH value of 125 msec (HA_{125}), the AH interval after full recovery (AH_∞), and recovery time constant (τ_{rec}) as a function of A_1A_2 (facilitation) cycle length (FCL). Results were obtained by fitting recovery data (of the type shown in Figure 3), for an A_3 test beat to the equation $AH_n = AH_\infty + A \exp(-HA/\tau_{rec})$, at each FCL. HA_{125} was obtained by using the best-fit values of AH_∞, A, and τ_{rec} for each curve to solve for the HA corresponding to an AH of 125 msec. * $p<.05$, ** $p<.01$, *** $p<.001$ compared to control at the same FCL.

Figure 5. Changes in HA_{125} from value at 500 msec (ΔHA) as a function of facilitation cycle length (FCL). Values are mean±SE for all 7 dogs under each condition. Differences in ΔHA between conditions were not statistically significant at any FCL.

Figure 6. Changes in AH interval (ΔAH) as a function of beat number after the onset of tachycardia in a representative experiment. Solid lines show best-fit exponential curves. The time course of AH prolongation was similar under all 3 conditions, but its magnitude for a given HA interval was greatest in the presence of beta blockade, least in the presence of isoproterenol, and intermediate under control conditions.

Figure 7. Magnitude of fatigue (ΔAH at steady state) for tachycardias with HA intervals shown. Results (mean±SE) were obtained from curve fits to the type of data presented in Figure 6. Dashed curves represent best-fit exponentials to mean data. ** $p<.01$, *** $p<.001$ compared to control values.

Figure 8. Predicted rate-dependent changes in AH interval due to incomplete recovery, recovery modified by facilitation, and fatigue as a function of basic cycle length (BCL). Mean characterizing constants determined experimentally (Table 2) were substituted into equations 1, 2, and 4 respectively (see text) to obtain predictions shown. Changes due to recovery and facilitation were added to those resulting from fatigue to obtain the total predicted rate-dependent AH prolongation (solid lines). The latter are in close agreement with experimentally-observed values (mean±SE).

Figure 9. Top: Reductions in AH interval resulting from beta adrenergic stimulation. Values in the presence of isoproterenol were compared to values in the absence of beta adrenergic stimulation (beta blockade). The mathematical model presented in the text was used to estimate the reduction in AH interval due to beta-mediated acceleration of recovery and attenuation of fatigue for any steady-state HA interval. These were added to the time-independent (tonic) change in AH interval resulting from isoproterenol, in order to predict the total AH interval reductions produced by beta adrenergic stimulation. The latter are in close agreement with experimental observations. Bottom: Proportion of total β-adrenergic effect on AH interval due to tonic actions and changes in recovery and fatigue, at each HA interval.

Figure 10. Rate-dependent increases in AH interval as a function of basic cycle length in the presence of isoproterenol, vagal stimulation, and control conditions (beta blockade and bilateral vagal transection). Vagal results were obtained by a new analysis of data obtained in a previous study.[42] * $p<.05$, ** $p<.01$, *** $p<.001$ compared to AH value under the same conditions at a cycle length of 500 msec (statistics performed using raw AH interval data).

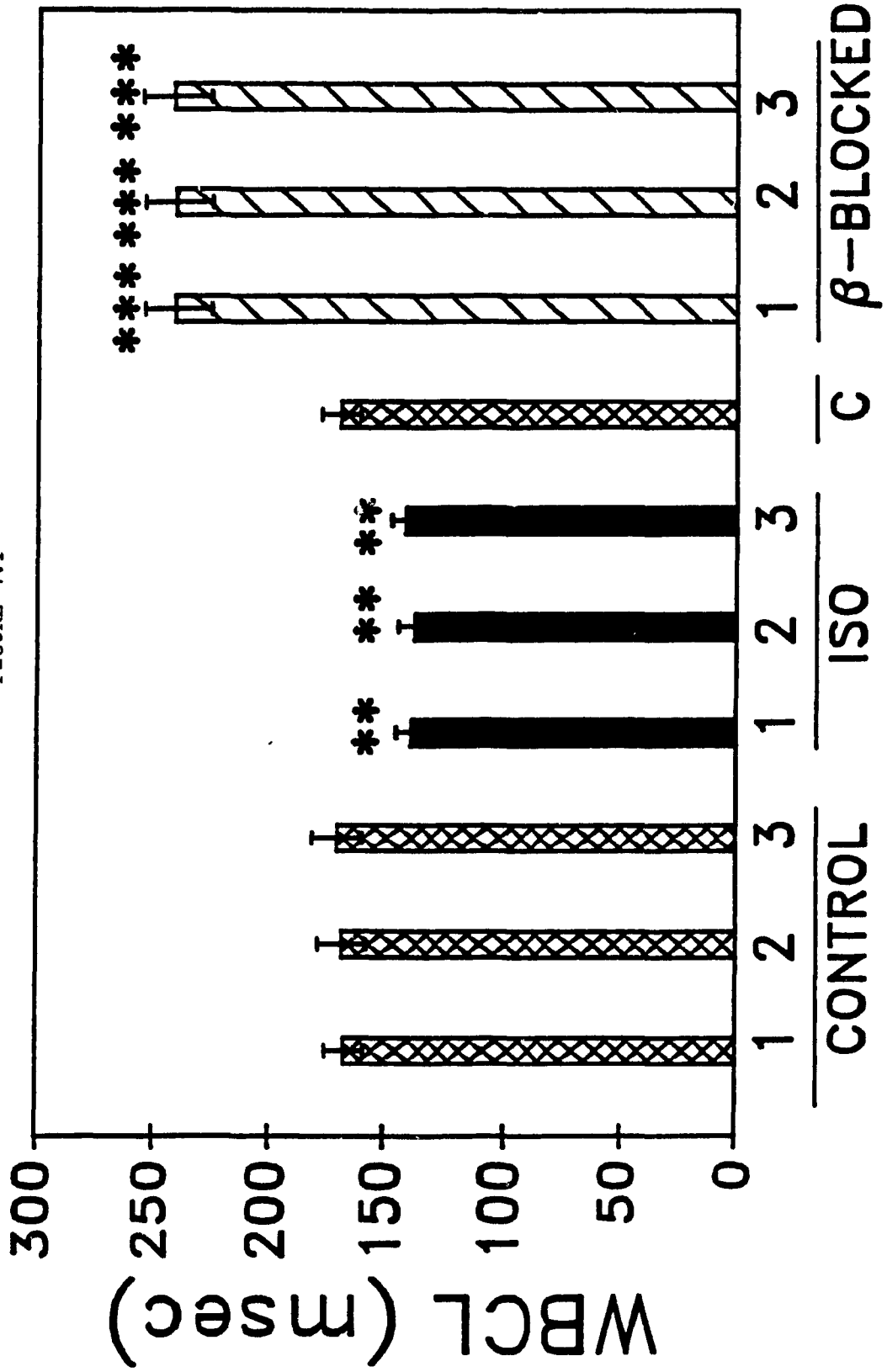
WBCL (msec)
300
250
200
150
100
50
0
1 2 3
CONTROL
1 2 3
ISO
C
1 2 3
β-BLOCKED
**
**
**
****
****
****

FIGURE 4.1

FIGURE 4.2

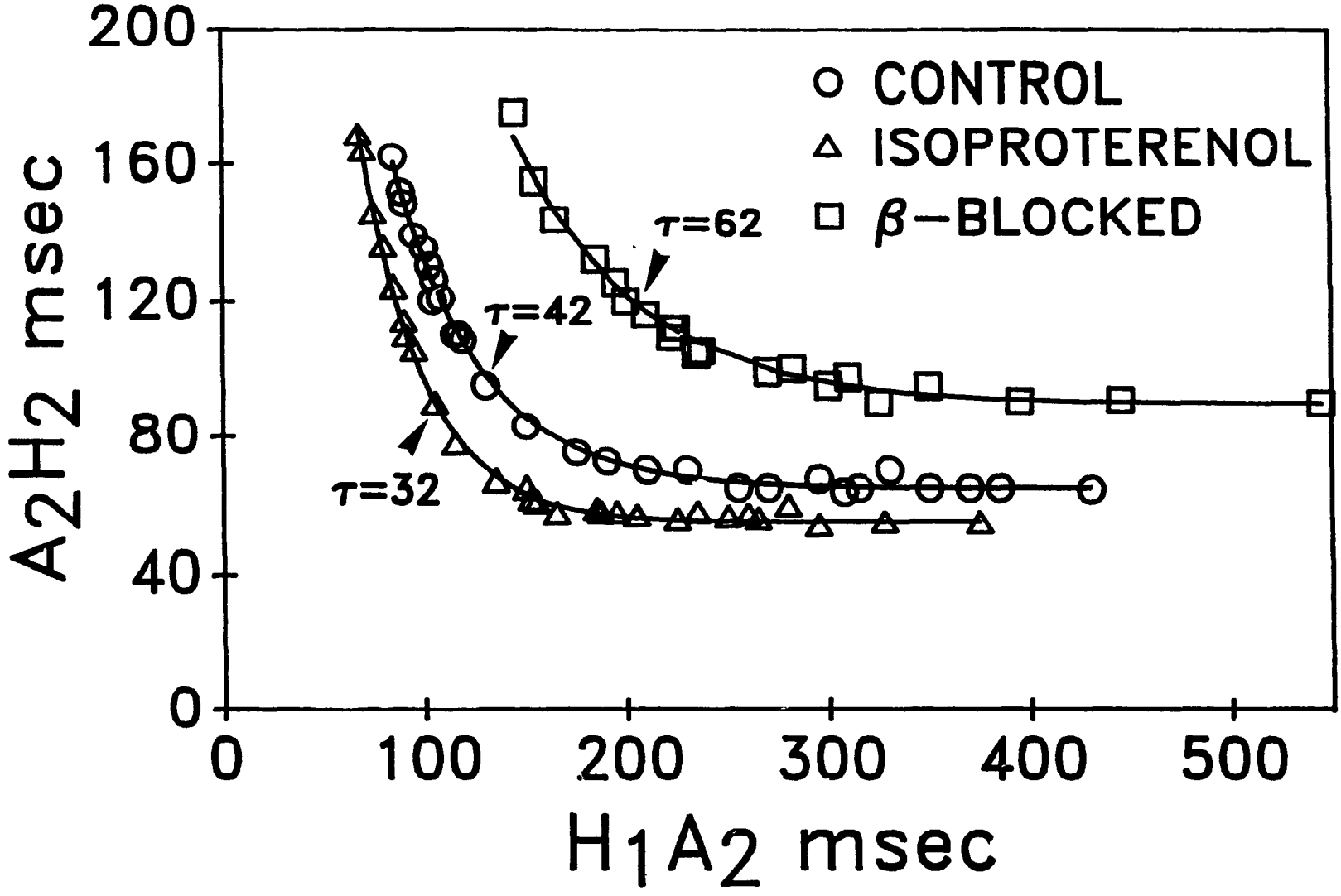
200
160
120
80
40
0
A2H2 msec
0
100
200
300
400
500
H1A2 msec
CONTROL
ISOPROTERENOL
β−BLOCKED
τ=62
τ=42
τ=32

FIGURE 4.3

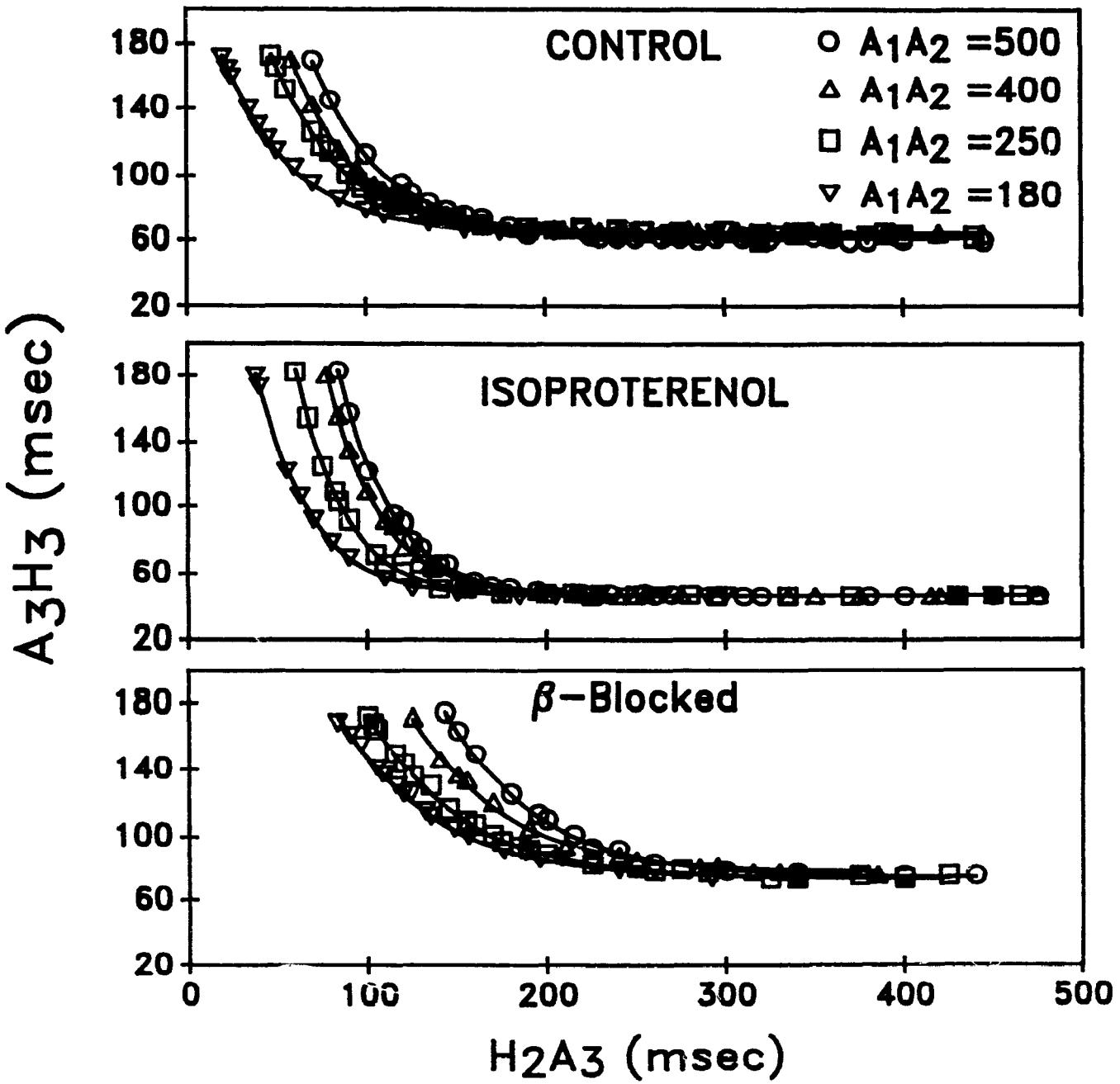
CONTROL
ISOPROTERENOL
β–Blocked
A1A2 =500
A1A2 =400
A1A2 =250
A1A2 =180
A3H3 (msec)
H2A3 (msec)
180
140
100
60
20
0
100
200
300
400
500

FIGURE 4.4

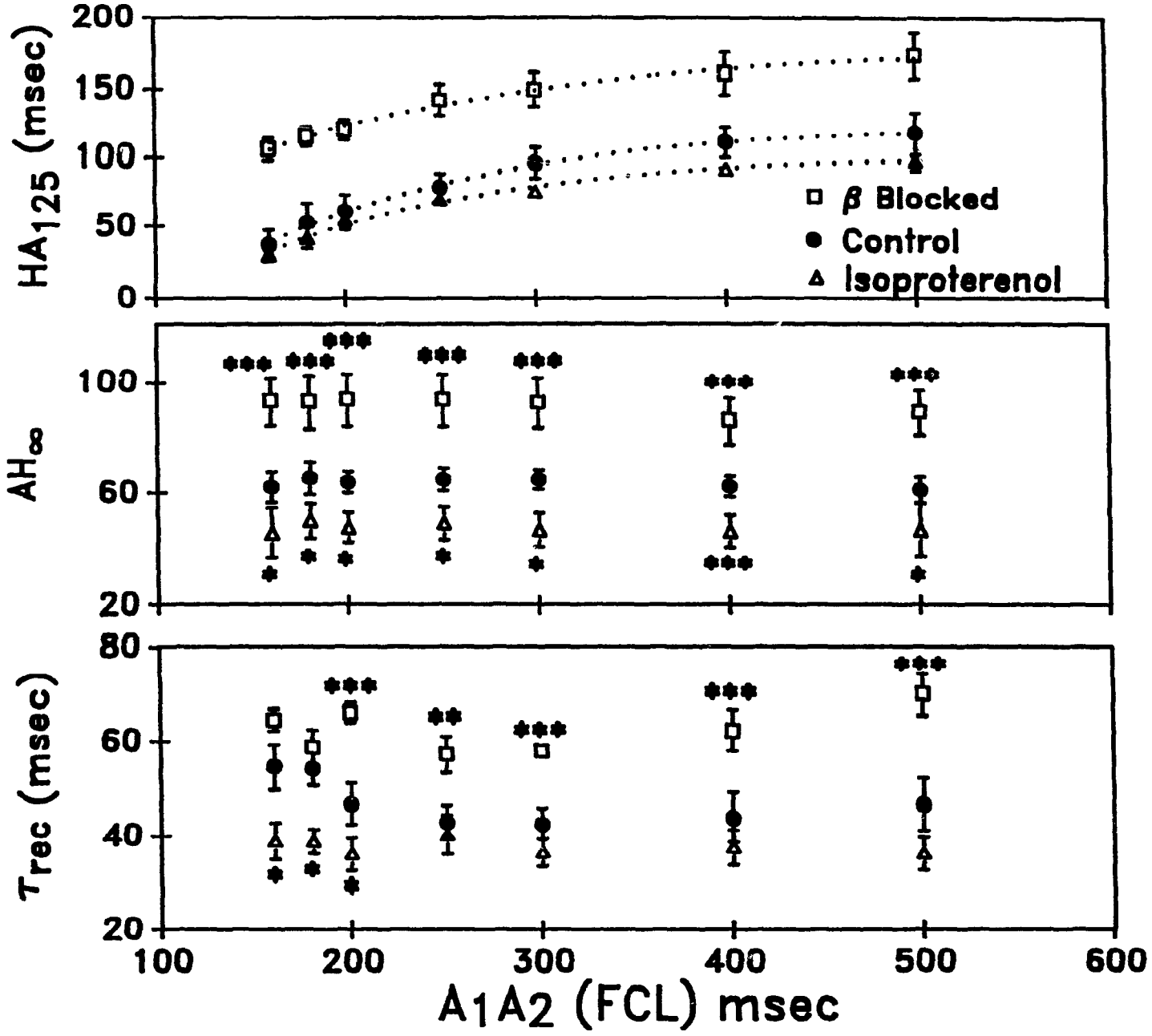
HA125 (msec)
200
150
100
50
0
β Blocked
Control
Isoproterenol
AH8
100
60
20
Trec (msec)
80
60
40
20
100
200
300
400
500
600
A1A2 (FCL) msec

FIGURE 4.5

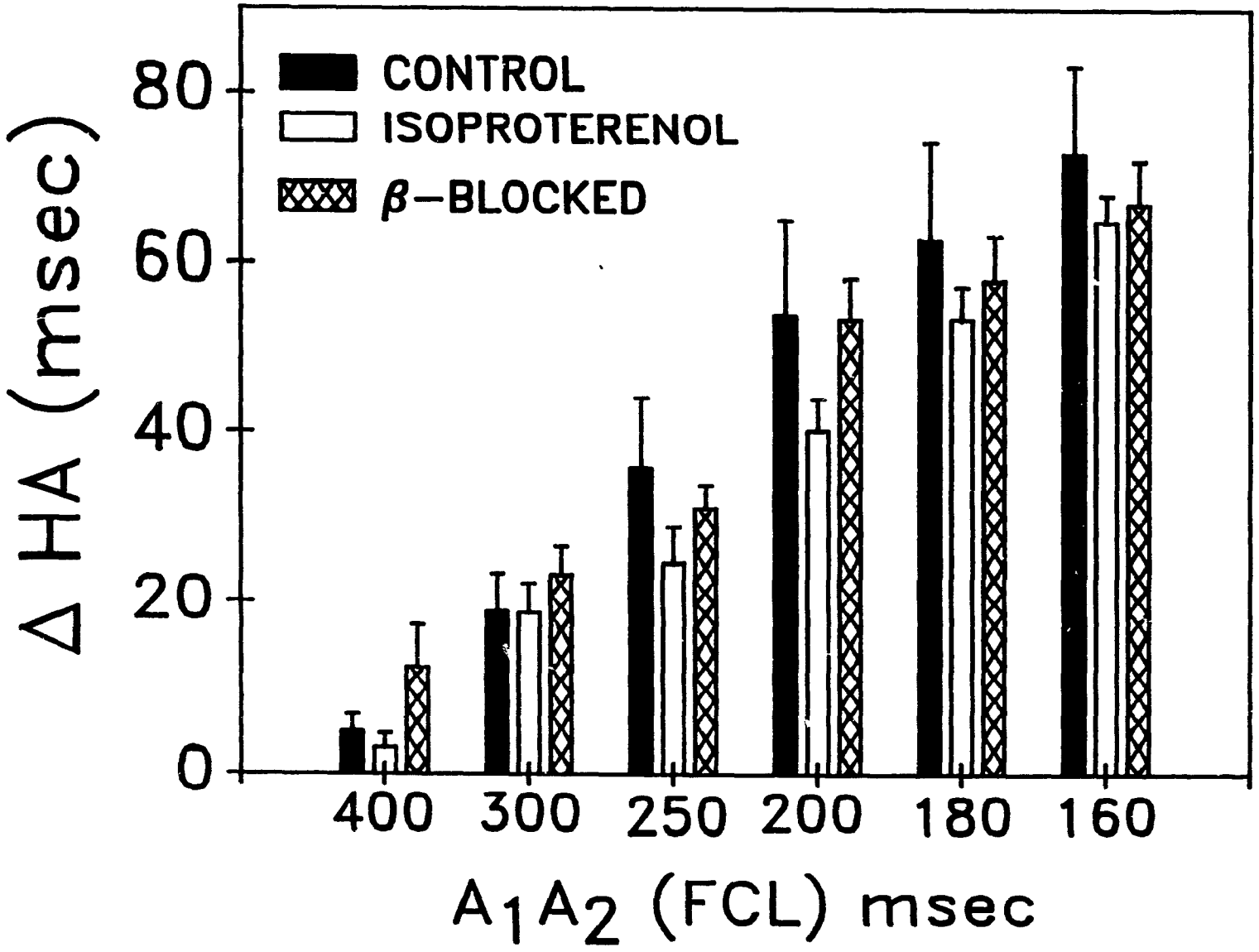
CONTROL
ISOPROTERENOL
β–BLOCKED
Δ HA (msec)
80
60
40
20
0
400
300
250
200
180
160
A1A2 (FCL) msec

FIGURE 4.6

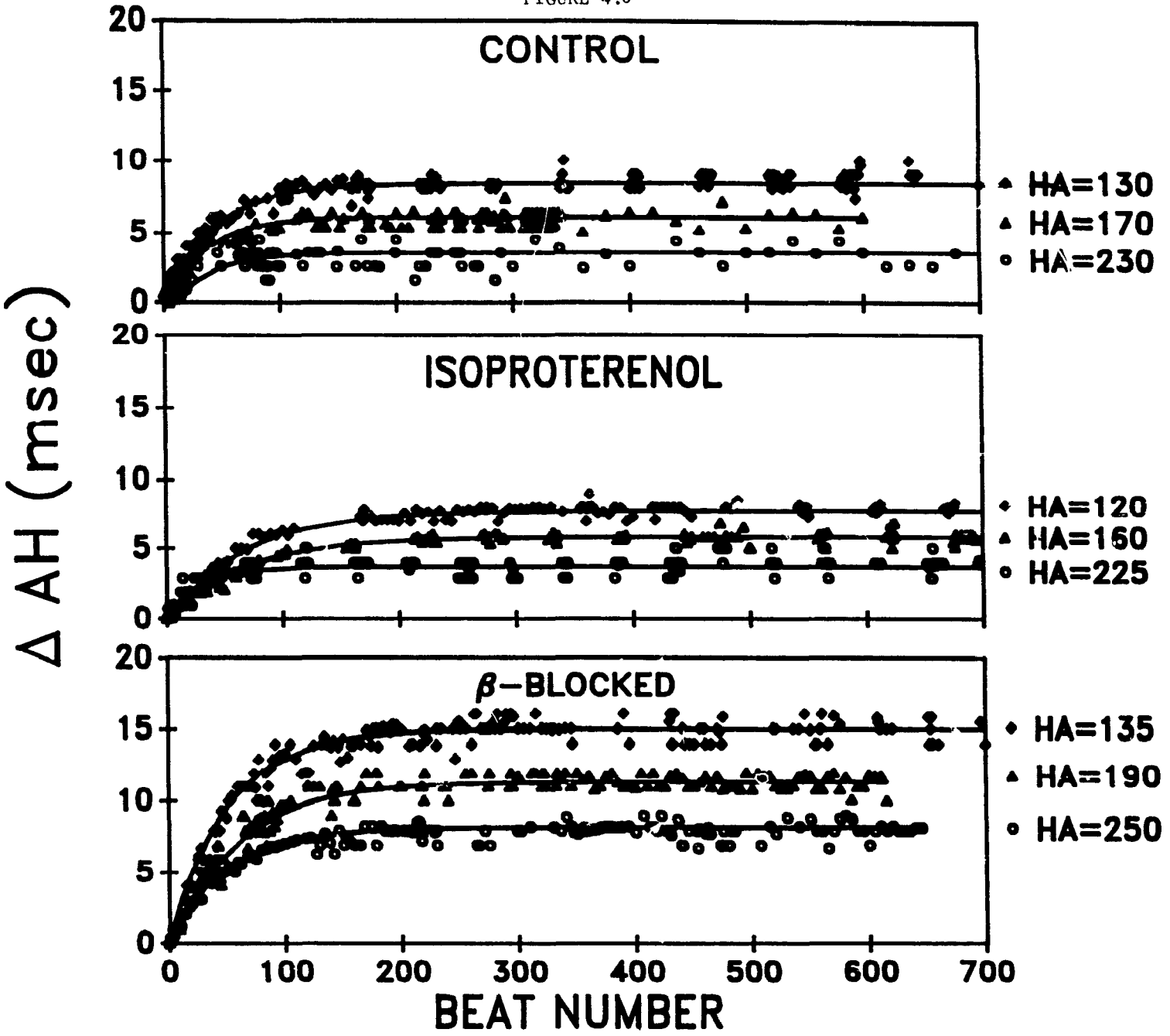
CONTROL
ISOPROTERENOL
β–BLOCKED
Δ AH (msec)
BEAT NUMBER
0
5
10
15
20
100
200
300
400
500
600
700
HA=130
HA=170
HA=230
HA=120
HA=160
HA=225
HA=135
HA=190
HA=250

FIGURE 4.7

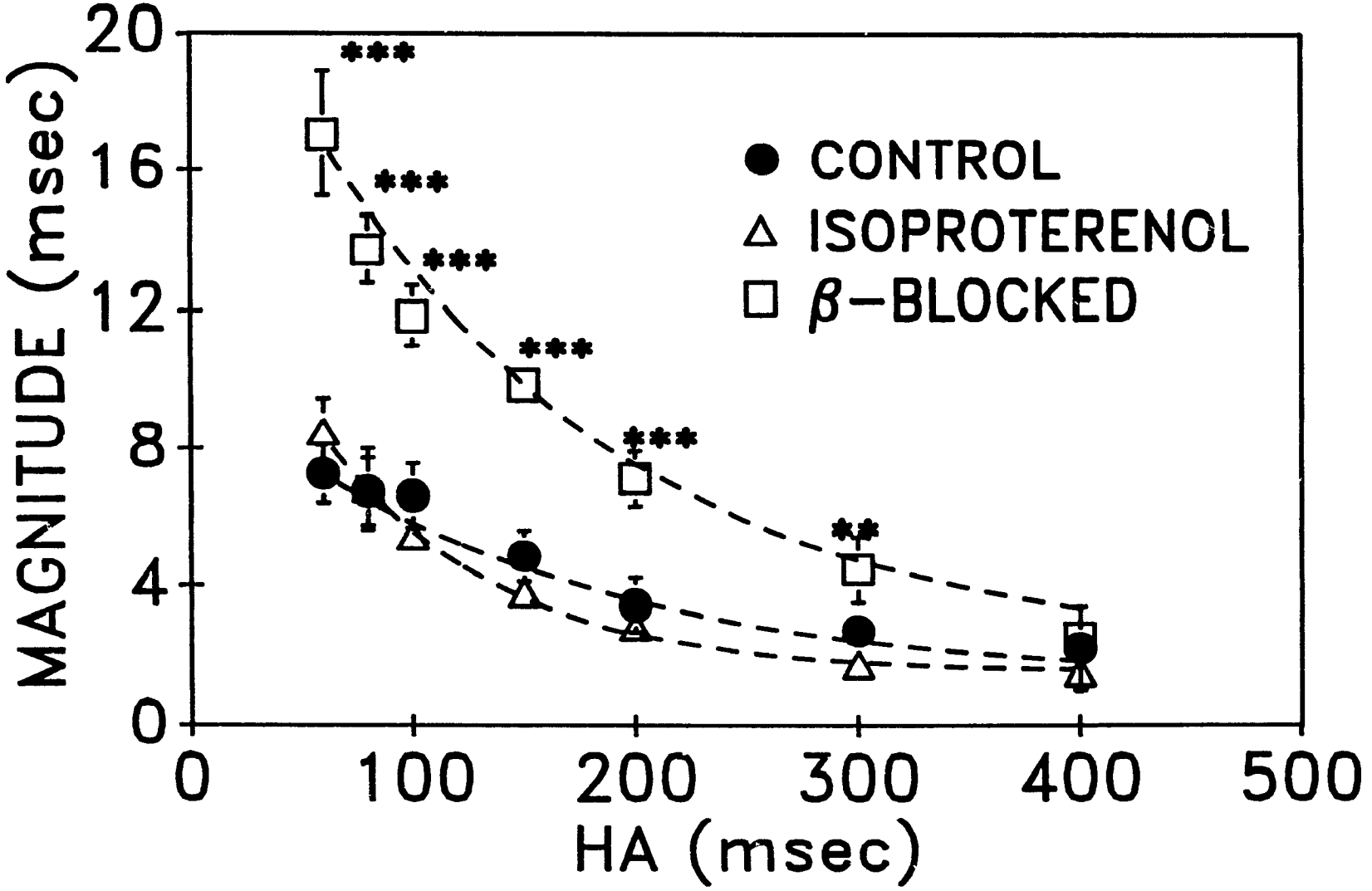
MAGNITUDE (msec)
20
16
12
8
4
0
0
100
200
300
400
500
HA (msec)
***
***
***
***
***
**
CONTROL
ISOPROTERENOL
β–BLOCKED

FIGURE 4.8

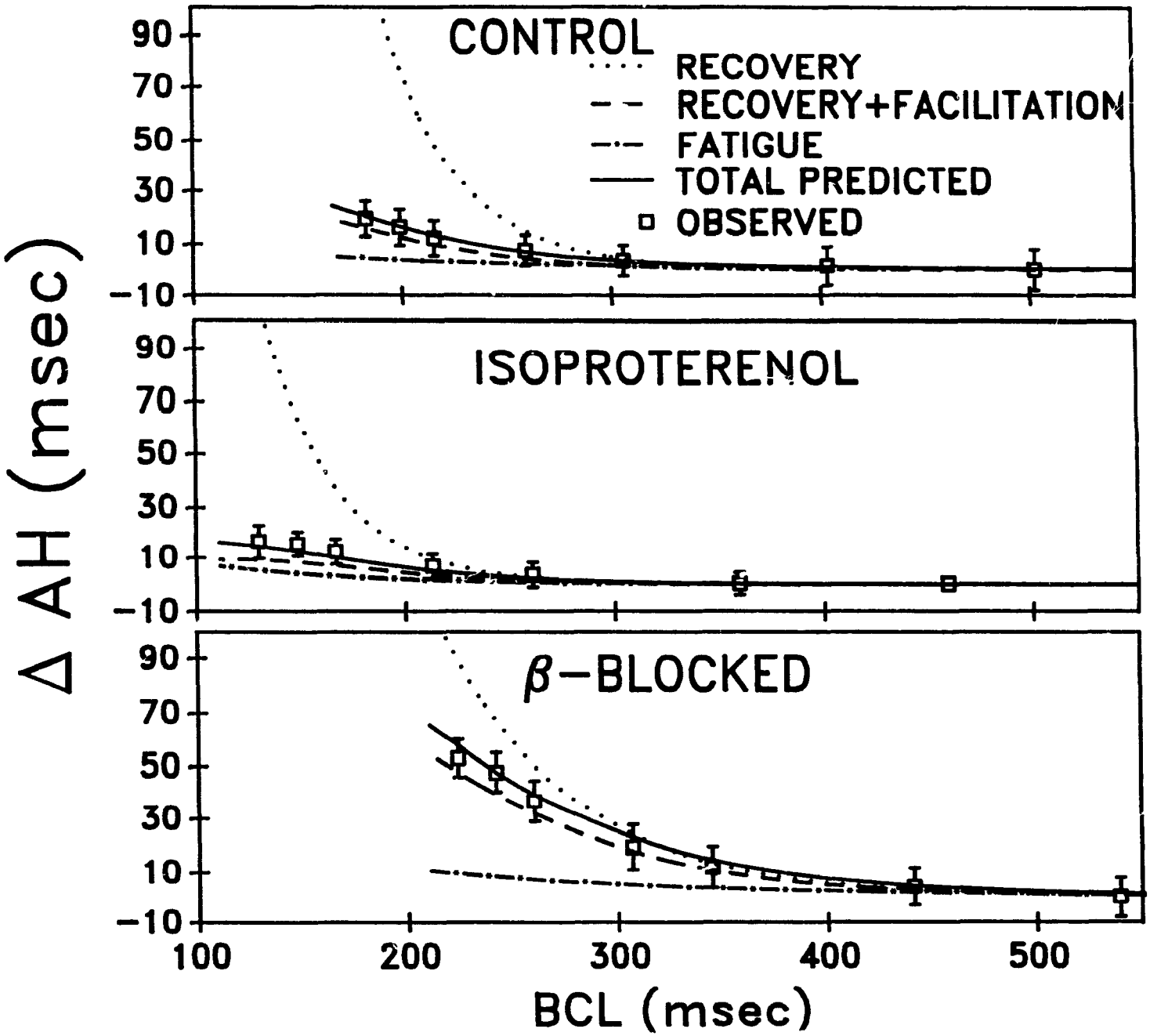
CONTROL
RECOVERY
RECOVERY+FACILITATION
FATIGUE
TOTAL PREDICTED
OBSERVED
ISOPROTERENOL
β−BLOCKED
Δ AH (msec)
BCL (msec)
90
70
50
30
10
−10
100
200
300
400
500

FIGURE 4.9

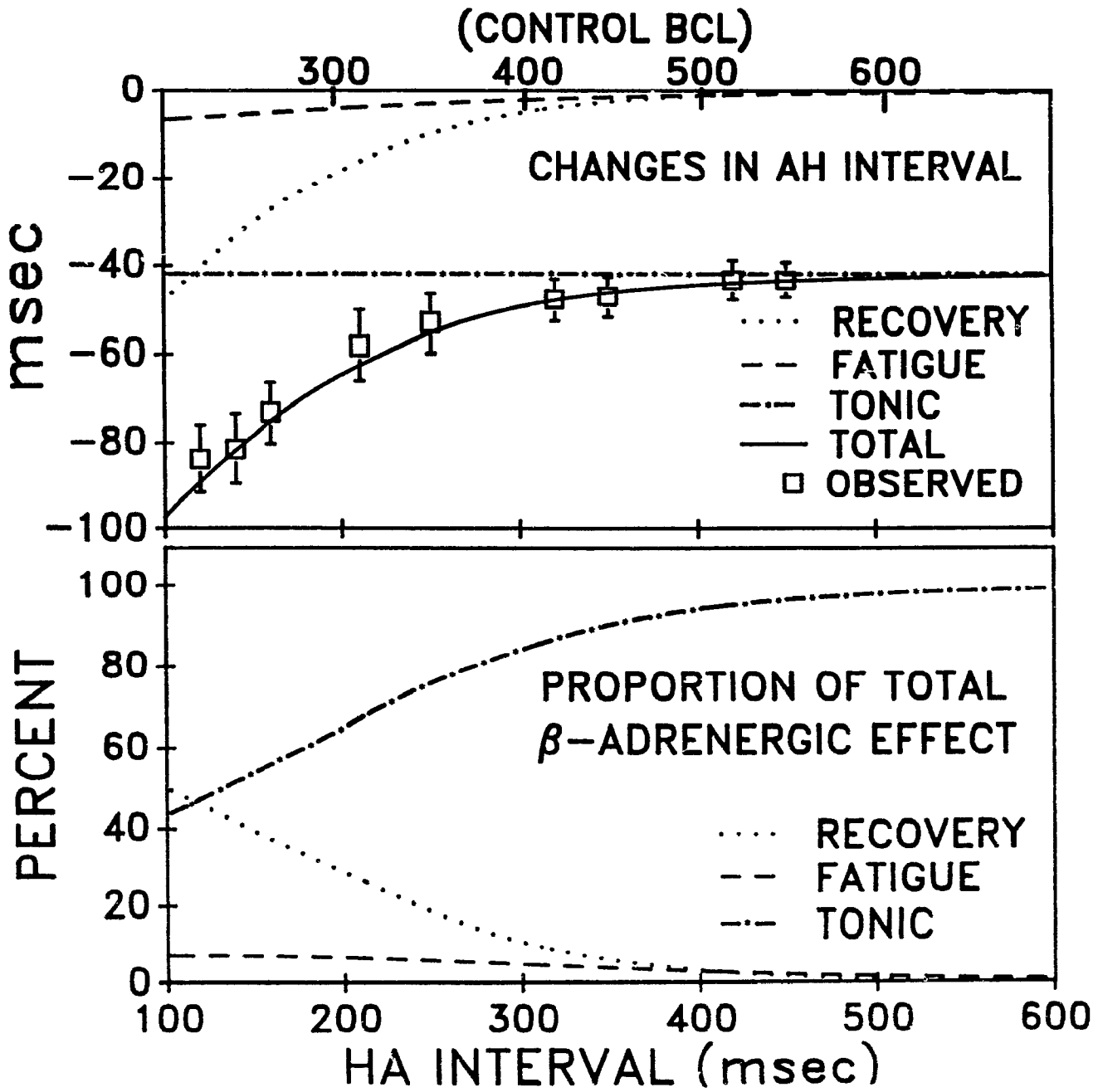
(CONTROL BCL)
300
400
500
600
0
-20
-40
-60
-80
-100
msec
CHANGES IN AH INTERVAL
RECOVERY
FATIGUE
TONIC
TOTAL
OBSERVED
100
80
60
40
20
0
PERCENT
PROPORTION OF TOTAL
β-ADRENERGIC EFFECT
RECOVERY
FATIGUE
TONIC
100
200
300
400
500
600
HA INTERVAL (msec)

FIGURE 4.10

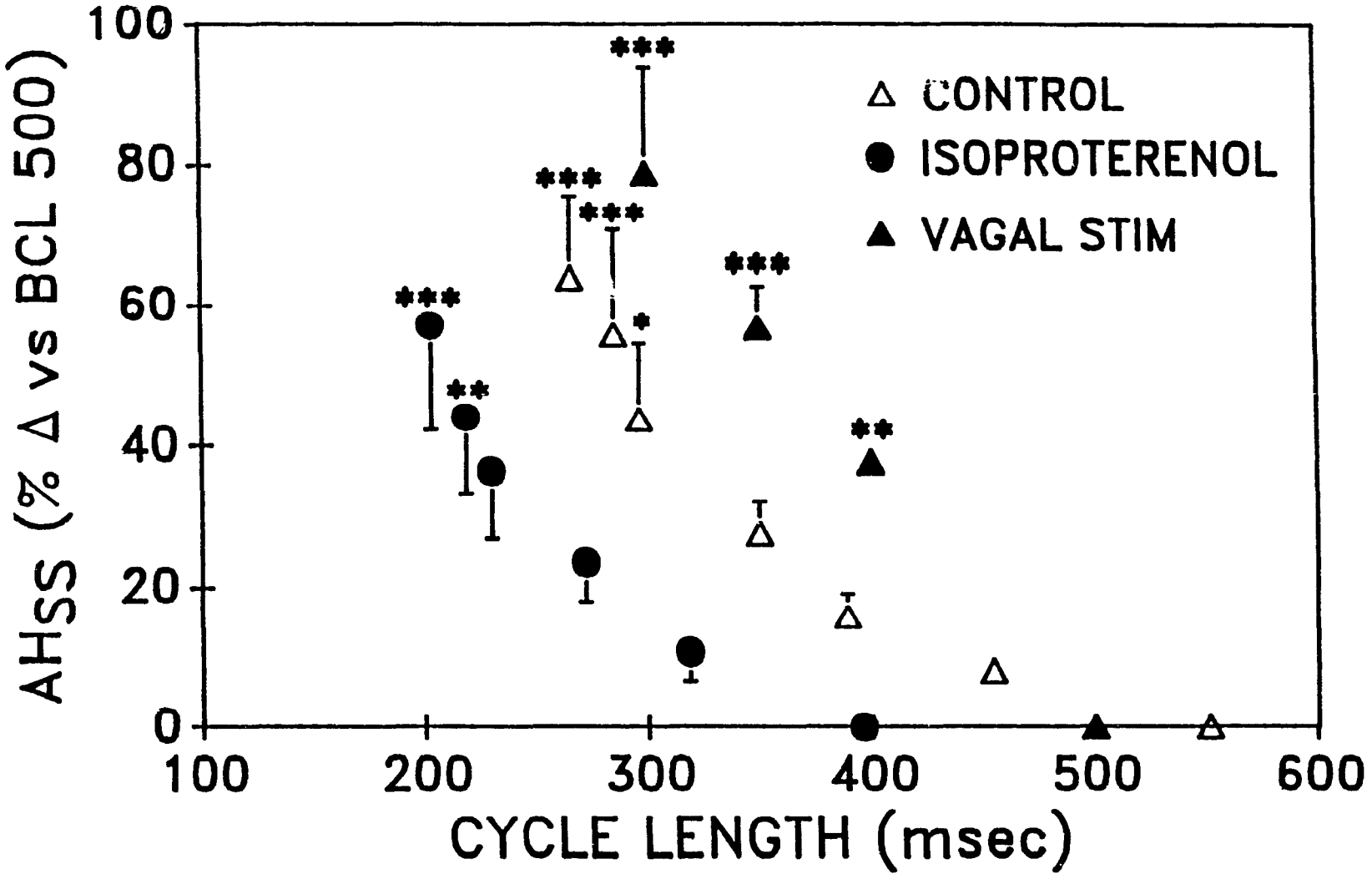
100
80
60
40
20
0
AHSS (% Δ vs BCL 500)
100
200
300
400
500
600
CYCLE LENGTH (msec)
CONTROL
ISOPROTERENOL
VAGAL STIM
***
***
***
***
*
***
**
**

CHAPTER 3

Frequency-Dependent Effects of Diltiazem on the Atrioventricular Node During Experimental Atrial Fibrillation

Frequency-Dependent Effects of Diltiazem on the Atrioventricular Node During Experimental Atrial Fibrillation

Mario Talajic, MD, Mohsen Nayebpour, PharmD,
Wuhua Jing, MD, and Stanley Nattel, MD

Calcium channel blockers depress atrioventricular (AV) nodal properties in vivo in a frequency-dependent manner, suggesting that selective drug action during supraventricular arrhythmias may result from use-dependent properties. The present study was designed to examine whether or not the rate-dependent actions of diltiazem account for its therapeutic effects during atrial fibrillation. The determinants of the ventricular response to atrial fibrillation (concealed AV nodal conduction and AV node functional refractory period, AVFRP) were evaluated at multiple cycle lengths (with extrastimulus techniques) and during electrically induced atrial fibrillation (with indirect indexes from RR interval histograms) in anesthetized dogs. In the presence of diltiazem, AVFRP increased progressively relative to control as rate accelerated. At cycle lengths comparable to sinus rhythm in humans, AVFRP increased 10%, 17%, and 32% after doses 1, 2, and 3 of diltiazem, respectively. Drug-induced increases in AVFRP were greater at basic cycle lengths just above the Wenckebach point (17%, 48%, and 81%) and were maximal during atrial fibrillation (39%, 86%, and 154% increases for doses 1, 2, and 3, respectively). Diltiazem also increased the AV conduction system effective refractory period in a frequency-dependent manner without affecting the atrial effective refractory period, thereby increasing the potential zone of concealment into the AV node. Frequency-dependent increases in the zone of concealment were produced by diltiazem and were associated with marked increases in the standard deviation of RR interval histograms during atrial fibrillation (257%, 526%, and 923% increases after doses 1, 2, and 3, respectively). The combination of rate-dependent increases in AVFRP and zone of concealment resulted in a marked amplification of diltiazem's effects during atrial fibrillation, with mean RR interval increases (88%, 200%, and 300% after doses 1, 2, and 3, respectively) that were 8–10 fold greater than increases in AVFRP at cycle lengths comparable to sinus rhythm in humans. We conclude that diltiazem's frequency-dependent effects lead to highly selective depression of AV nodal function during atrial fibrillation. (*Circulation* 1989;80:380–389)

Electrophysiologic and negative inotropic effects of calcium channel blockers are dependent on underlying heart rate.[1-3] Prior in vitro studies have shown that maximal depression of slow inward current occurs at faster driving frequencies and with activations ending shorter diastolic intervals.[4-8] We have recently shown that verapamil, diltiazem, and nifedipine slow atrioventricular (AV) nodal conduction and prolong AV nodal refractoriness in vivo in a frequency-dependent manner and that the time course of recovery of AV conduction slowing is specific to the drug studied.[9] On the basis of these observations, we hypothesized that these agents would have more profound effects on AV nodal properties during supraventricular tachyarrhythmias than during sinus rhythm. This would lead to desirable selectivity in their action during the very arrhythmias for which they are used. However, this hypothesis has not been directly tested in either spontaneous or experimentally induced arrhythmias.

Atrial fibrillation is an example of a supraventricular arrhythmia for which use-dependent drug effects

From the Departments of Medicine, Montreal Heart Institute and University of Montreal, and the Departments of Pharmacology and Medicine, McGill University, Montreal, Quebec, Canada.

Supported by the Quebec Heart Foundation, the Medical Research Council of Canada, Fonds de la Recherche en Santé du Quebec, Fonds de Recherche de l'Institut de Cardiologie de Montreal, and Nordic Laboratories, Canada. M.T. is a Scholar of the Canadian Heart Foundation.

Address for correspondence: Dr. Mario Talajic, Montreal Heart Institute, 5000 Belanger Street East, Montreal, Quebec, Canada H1T 1C8.

Received October 24, 1988; revision accepted April 4, 1989.

may be particularly important in determining efficacy, because atrial impulses at rates of 400–600/min result in a high input rate to the AV node.[10] Verapamil and diltiazem have been effective in controlling the ventricular rate during this arrhythmia.[11–15] The determinants of the ventricular response during atrial fibrillation include the functional refractory period of the AV node (AVFRP) and concealed AV nodal conduction resulting from intranodal impulse block.[16–20] Preferential salutary effects of calcium channel blockers during atrial fibrillation could be produced by rate-dependent changes in either AVFRP or the degree of concealed conduction in the AV node.

The purpose of this study was to examine the effects of diltiazem on the ventricular response during experimental atrial fibrillation and to relate these effects to rate-related changes in functional refractoriness and concealed AV nodal conduction to determine the clinical relevance of frequency-dependent drug actions.

Methods

General

Mongrel dogs of either sex were anesthetized with morphine (2 mg/kg s.c.) and α-chloralose (100 mg/kg i.v.). Catheters were inserted into both femoral veins and arteries and were kept patent with heparinized saline (0.9%). Dogs were ventilated through an endotracheal tube with a Harvard animal respirator (South Natick, Massachusetts). Tidal volume and respiratory rate were adjusted after measurement of arterial blood gases to ensure adequate oxygenation ($Sao_2 \geq 90\%$) and physiologic pH (7.35 to 7.45). A thoracotomy was performed through the fourth right intercostal space. After suspension of the heart in a pericardial cradle, two bipolar Teflon-coated stainless steel electrodes were inserted into the right atrial appendage for recording and stimulation. Body temperature was monitored continuously with a thermistor within the chest cavity and was maintained at 37–38° C by a homeothermic heating blanket. A Statham P23 ID transducer (Cleveland, Ohio), electrophysiologic amplifiers, and a paper recorder (Siemens Mingograf 80, Sweden) were used to record blood pressure, electrocardiographic leads II and aV_R, a right atrial electrogram, and stimulus artifacts. Stimulation was applied with 4-msec square-wave impulses at twice late diastolic threshold. The sinus node was crushed to allow for a wide range of pacing rates.

All dogs were autonomically blocked to measure direct drug effects without contamination by autonomic reflex changes. Vagal effects were prevented by surgical division of the cervical vagi followed by intravenous administration of 1 mg atropine. β-Blockade was produced by administration of 0.5 mg/kg atenolol. Repeated doses of atropine (0.5 mg) and atenolol (0.25 mg/kg) were administered hourly. This regimen has previously produced sustained autonomic blockade.[9,21]

Experimental Protocol

Experiments were conducted to assess 1) the frequency-dependent effects of diltiazem on AV nodal refractoriness during atrial pacing and induced atrial fibrillation (eight dogs) and 2) the frequency-dependent effects of diltiazem on concealed AV nodal conduction (four additional dogs).

Atrioventricular nodal refractoriness (atrial pacing and atrial fibrillation). Wenckebach cycle length was determined under control conditions by decreasing atrial pacing cycle length by 10 msec decrements until second-degree AV block occurred. This was repeated before and after each experimental protocol to ensure stability of AV nodal function during electrophysiologic study under control conditions and during each drug infusion. The functional refractory period of the AV conduction system (AVFRP) was determined by introducing single premature stimuli (S_2) after 20 basic (S_1) stimuli. The resulting V_1V_2 interval was measured, and a curve relating V_1V_2 to the S_1S_2 interval was established. The AVFRP was defined as the shortest V_1V_2 resulting from premature atrial stimulation. This process was repeated at multiple basic cycle lengths (S_1S_1) ranging from 300 to 1,000 msec. The effective refractory period of the AV conduction system (AVERP) was defined as the longest A_1A_2 failing to result in a propagated ventricular response and was determined at the same cycle lengths. The atrial effective refractory period (AERP) was also determined at a pacing cycle length of 600 msec.

After determination of the AERP, AVERP, and AVFRP, atrial fibrillation was induced by continuous atrial stimulation at 10–50 Hz.[17,22] In each experiment, atrial pacing cycle length was adjusted until the resultant ventricular response was consistently irregular. Pacing-induced atrial fibrillation was confirmed in each case by observing irregular atrial activity in the electrocardiographic and intracardiac recordings and by the persistence of spontaneous atrial fibrillation lasting between several seconds and several minutes after the interruption of pacing. Two minutes after induction of atrial fibrillation, a continuous electrocardiographic recording lasting 5–10 minutes was obtained. Because AV nodal conduction slowing in the presence of diltiazem requires time to reach steady state during pacing at any given rate,[9] all determinations of refractoriness during steady-state pacing or atrial fibrillation were preceded by pacing for 2 minutes.

After control measurements were completed, incremental doses of diltiazem were infused intravenously, and the experimental protocol was repeated. The dosing regimens used were developed in previously published experiments[9] and were designed to result in steady-state concentrations spanning the range of concentrations observed after therapeutic doses of diltiazem in humans. The elec-

TABLE 1. Diltiazem Doses, Resulting Plasma Concentrations, and Electrophysiologic Effects

	Dose		Plasma concentration (ng/mg)		Wenckebach CL (msec)		AVERP	AERP*
	Loading (μg/kg)	Maintenance (μg/kg/min)	Before	After	Before	After	(msec)	(msec)
Dose 1								
Control	—	—	—	—	224±33	214±33	189±16	157±6
Drug	200	3.0	30±16	28±14	268±40†	279±52†	278±76	153±21
Dose 2								
Control	—	—	—	—	211±27	210±28	187±27	155±27
Drug	400	7.0	63±8	70±14	404±67†	419±94†	306±85†	158±26
Dose 3								
Control	—	—	—	—	200±31	194±23	198±39	175±29
Drug	800	15.0	210±51	207±68	514±127‡	494±111‡	385±104†	175±17

Results are shown for five experiments after dose 1, eight after dose 2, and five after dose 3. The loading dose was given over 10 minutes, after which the maintenance dose was begun. Electrophysiologic study was begun 10 minutes after the end of the loading dose. Results of plasma concentration determination and Wenckebach cycle length before and after electrophysiologic protocol are shown.

AVERP, AERP, effective refractory periods of the atrioventricular conduction system and atrium, respectively (measured at a cycle length of 600 msec).

*Results for AERP were obtained in 3, 6, and 4 experiments after doses 1, 2, and 3, respectively.

†$p<0.05$, ‡$p<0.01$ vs. control.

trophysiologic study was repeated 10 minutes after completion of each loading dose. Before and after each experimental protocol, blood samples were obtained during the maintenance drug infusion, for subsequent measurement of plasma diltiazem concentrations. The loading and maintenance doses used and the resulting plasma concentrations are listed in Table 1.

Concealed atrioventricular nodal conduction. Concealed conduction was assessed in four animals by modifications of previously described methods.[23,24] The right atrial appendage was paced at a constant basic cycle length. Single premature atrial stimuli (S_2) were introduced after 20 basic stimuli (S_1S_1). The resulting S_2V_2 interval was measured and used as an index of AV nodal conduction time. This was plotted against S_1S_2 and is referred to as the AV node recovery curve. The atrial and AV conduction system effective refractory periods were also determined at the same basic cycle length during the determination of the AV node recovery curve. This was performed under control conditions and after diltiazem administration. The protocol was then repeated after interpolating a nonconducted atrial impulse (S') between the last beat of the basic drive (S_1) and the test stimulus (S_2). Coupling intervals were chosen so that S' resulted in atrial activation but was blocked in the AV node (i.e., S_1S' exceeded the atrial effective refractory period but was less than the AVERP). AVERP was determined throughout a range of S_1S' intervals, with S_1S' increased by 10-msec increments (from 30 msec beyond AERP to 10 msec below the AVERP of S_1). In this way, the zone between the AERP and AVERP was scanned with the interpolated atrial stimulus during repeated determinations of AVERP. An S' that fails to penetrate into the AV node should have no measurable effect on the node, whereas an S' that penetrates nodal tissue without exiting (i.e., is concealed) will make it more difficult for a subsequent S_2 to propagate, thereby increasing AVERP.[23] A 10-msec or greater increase in the AVERP of S_1 after introduction of the interpolated nonconducted atrial impulse (S') was taken to indicate concealed conduction of S' into the AV node. The zone of concealment was defined as the range of S_1S' intervals causing concealment.[22,23] Zone of concealment was measured at basic cycle lengths ranging from 500 to 1,000 msec. During the control state, AVERP uncommonly exceeded AERP by more than 30 msec, indicating lack of a potential zone of concealed AV conduction by the definition established. Because of the complexity and prolonged duration of the protocol to evaluate AV nodal concealment, all measurements were performed after infusion of a single dose (dose 2) of diltiazem (Table 1).

Data Analysis

Electrophysiologic recordings during refractory period determinations were made at 250 mm/sec, and continuous recordings during atrial fibrillation were made at 50 mm/sec. All measurements were made with a digitizing tablet coupled to an IBM compatible microcomputer by commercially available software (Sigmascan, Jandel Scientific, Corte Madera, California). During determination of AVERP under control conditions, refractoriness of atrial tissue was sometimes limiting,[25] and thus, the value obtained for AVERP was an upper limit only. After infusion of diltiazem, AVERP always exceeded AERP.

Consecutive RR intervals during induced atrial fibrillation were measured, and RR interval histograms were constructed.[19] A minimum of 500 ventricular complexes were analyzed during each period of atrial fibrillation. The mean, minimum, and standard deviation of RR intervals were calculated for each histogram. The minimum RR interval during atrial fibrillation was used as an index of the func-

tional refractory period of the AV node during atrial fibrillation.[10,19,26]

Group data are presented as the mean±SD. Multiple comparisons between control and experimental group means were made by two-way analysis of variance with Scheffé's test or by the unpaired *t* test with Bonferroni's correction.[27] Two-tailed tests were used for all statistical comparisons, and a probability of 5% or less was considered as significant.

The range of cycle lengths that could be studied was limited by the Wenckebach cycle length and spontaneous automaticity, which determined the shortest and longest pacing cycle length, respectively, under any experimental condition. Because the range of cycle lengths studied varied between experiments, we analyzed results in terms of the longest and shortest cycle length in each experiment during each drug infusion. Results in the presence of diltiazem were compared with results under control conditions at the same cycle length within each experiment. Effects of a given infusion at the longest cycle in each experiment were then grouped for statistical analysis as were effects at the shortest cycle length.

Plasma diltiazem concentration was measured by reverse-phase high-performance liquid chromatography (HPLC). Plasma samples (0.5 ml) were extracted with 0.1 ml 1N hydrochloric acid, into 2.5 ml dichloromethane to which 15 μl internal standard solution (16 μg/ml L-8040, kindly supplied by Ayerst Laboratories, Montreal, Canada) had been added. After it had been thoroughly mixed, the solution was dried under nitrogen gas and reconstituted with 45 μl mobile phase (95% methanol in water, with 0.3 ml/l glacial acetic acid and 2 g/l octanesulfonic acid). The resulting solution was injected onto a 5-μ ODS column (Chromatography Sciences, Montreal, Canada). Diltiazem was detected by a Waters ultraviolet absorbance meter at a wave length of 237 nm. The retention times for diltiazem and internal standard were 6 and 7.5 minutes, respectively, at a flow rate of 2.5 ml/min. All samples were assayed in duplicate, and a three-point standard curve was obtained in control plasma for each assay run.

Results

Plasma Concentrations of Diltiazem and Resulting Electrophysiologic Effects

Administration of incremental doses of diltiazem resulted in stable plasma concentrations ranging from 28±14 to 210±51 ng/ml (Table 1). Wenckebach cycle length and AVERP were prolonged in a concentration-dependent manner after drug infusion (Table 1). No changes in AERP were observed. Drug effects, as reflected by Wenckebach cycle length, were stable during each experimental protocol, with less than 10% variation during each drug infusion.

Effects of Diltiazem on the Ventricular Response During Experimental Atrial Fibrillation

Rapid atrial stimulation induced atrial fibrillation that was continuous during stimulation and lasted for a variable length of time after cessation of pacing in all experiments. Atrial fibrillation persisted spontaneously for more than 5 minutes after pacing in three experiments. The characteristics of the ventricular response to atrial fibrillation were similar in these studies during continuous electrical stimulation compared with values during subsequent spontaneous fibrillation as indicated by mean RR interval (211±31 during stimulation and 221±38 msec after), minimum RR interval (132±27 and 147±38 msec), and standard deviation of RR intervals (40±8 and 48±40 msec). A representative example of RR interval histograms of atrial fibrillation during and after continuous pacing is shown in Figure 1.

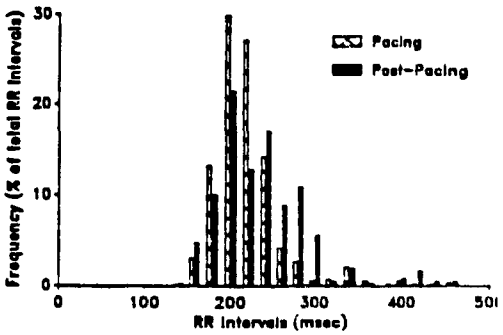

FIGURE 1. *RR interval histograms during atrial fibrillation induced by continuous electrical stimulation (hatched bars) and during subsequent spontaneous fibrillation (closed bars) in a representative experiment. Frequency of measured RR intervals during atrial fibrillation (expressed as a percentage of total number of complexes) is plotted for 20-msec ranges of RR intervals. In both cases, unimodal distributions that were skewed to the right were observed. Mean RR, minimum RR, and standard deviation of RR complexes were similar (212, 139, and 49 msec during continuous pacing; 245, 139, and 90 msec during postpacing atrial fibrillation).*

After the infusion of diltiazem, the RR interval histogram recorded during atrial fibrillation was shifted to the right with an increase in the minimum RR interval (index for AVFRP during atrial fibrillation) and the mean ventricular response (mean RR interval) (Figure 2). The mean ventricular response was substantially slowed by the drug (Table 2). The shape of the RR interval histogram was also altered by the administration of diltiazem. In all cases, the range of RR intervals increased markedly so that the mean RR interval was prolonged to a greater extent than the minimum RR interval recorded (Figure 2). This "splaying out" of the RR interval histogram corresponded to a concentration-dependent increase in the standard deviation of histograms after drug administration (Table 2).

Effects of Diltiazem on Atrioventricular Functional Refractory Period

Figure 3 illustrates a representative experiment in which the relation between AVFRP and atrial rate

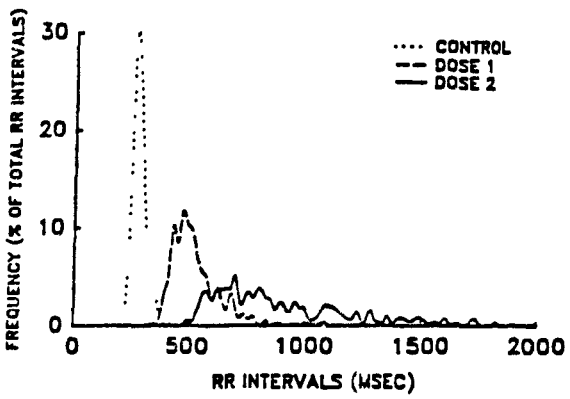

FIGURE 2. *Plot of distribution of RR intervals recorded during experimental atrial fibrillation before and after infusion of diltiazem in a representative experiment (doses 1 and 2; dose 3 not given). Frequency of measured RR intervals during atrial fibrillation (expressed as a percentage of the total number of complexes) is plotted for 20-msec ranges of RR intervals. Administration of diltiazem resulted in a shift of the RR interval histogram to the right as well as a change in the shape of the histogram. A dose-dependent increase in the standard deviation of RR intervals (33, 111, and 357 msec, for control, dose 1, and dose 2, respectively) was associated with a progressive splaying out to the right of the RR interval histograms. As a result, the mean RR interval prolonged more than did the minimum RR interval during atrial fibrillation (mean RR interval of 270, 524, and 919 msec; minimum RR interval of 209, 337, and 496 msec, for control, dose 1, and dose 2, respectively).*

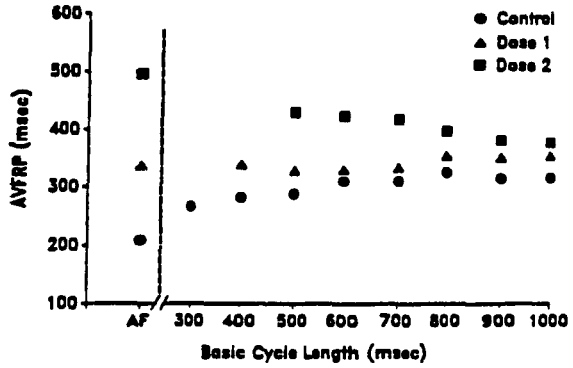

FIGURE 3. *Plot of atrioventricular functional refractory period (AVFRP) measured directly during atrial pacing (right of the dashed line) or indirectly as minimum RR interval during induced atrial fibrillation (AF) in a representative experiment (doses 1 and 2; dose 3 not given in this experiment). Under control conditions, AVFRP decreased as cycle length decreased, and the minimum AVFRP was recorded during atrial fibrillation. After diltiazem administration, small increases in AVFRP were noted at long cycle lengths. As the basic cycle length decreased, changes in AVFRP relative to control resulting from diltiazem increased. Maximal increases in AVFRP were produced during induced atrial fibrillation.*

was examined before and after drug infusion. The minimum RR interval during pacing-induced atrial fibrillation under control and drug conditions is also shown. Under control conditions, AVFRP decreased consistently at shorter cycle lengths, and the shortest AVFRP (minimum RR interval) was observed during atrial fibrillation in all experiments. After the infusion of diltiazem, AVFRP was increased at all cycle lengths. In contrast to control observations, AVFRP did not decrease (e.g., dose 1, Figure 3) or increased (dose 2, Figure 3) as pacing cycle length decreased. Drug responses were evaluated at long cycle lengths (mean rates of 60–70 beats/min) and at short cycle lengths (mean rates of 111–160 beats/min) for all experiments. Table 2 summarizes the changes in AVFRP observed during atrial pacing at

TABLE 2. **Effects of Diltiazem on Experimental Atrial Fibrillation and Atrioventricular Refractory Period During Atrial Pacing**

	Atrial fibrillation				AVFRP (msec)					
	Mean RR		SD		AF (Min RR)		S-BCL		L-BCL	
Dose 1										
Control	293±58		46±19		216±47		265±39		333±66	
Drug	538±232	(88%)	178±143	(257%)	298±81	(39%)	313±65	(17%)	368±83	(10%)
Dose 2										
Control	293±62		51±19		208±45		274±33		323±47	
Drug	*882±447	(200%)	*302±212	(526%)	**387±123	(86%)	***408±69	(48%)	378±72	(17%)
Dose 3										
Control	275±72		47±22		187±50		270±31		313±18	
Drug	**1,058±207	(300%)	***425±56	(923%)	***461±75	(154%)	**491±94	(81%)	414±72	(32%)

Results shown are for four experiments after dose 1, eight experiments after dose 2, and five experiments after dose 3. Matching control data (obtained at identical cycle lengths in the case of AVFRP at S-BCL and L-BCL) are displayed with posttreatment values. Percent change over control are shown in parentheses. Cycle lengths at which AVFRP at S-BCL was obtained averaged 375±50, 463±52, and 540±114 msec, for doses 1, 2, and 3, respectively. Corresponding cycle lengths at which AVFRP at L-BCL was obtained averaged 825±126, 863±160, and 1,000±0 msec. Mean±SD of raw data is expressed in msec.

Mean RR, mean RR interval during electrically induced atrial fibrillation; SD, standard deviation of RR intervals from the mean value during atrial fibrillation; AVFRP, functional refractory period of the atrioventricular conduction system, measured indirectly during atrial fibrillation (AF) as the minimum RR interval (Min RR) observed, during pacing at the shortest basic cycle length obtainable (S-BCL) and during pacing at the longest basic cycle length possible (L-BCL).

*$p<0.05$, **$p<0.01$, ***$p<0.001$ vs. control values.

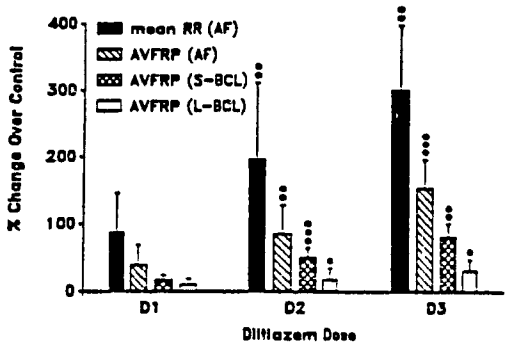

FIGURE 4. *Histogram of mean percent change in atrioventricular functional refractory period (AVFRP, open or hatched bars), and mean ventricular response rate during atrial fibrillation (mean RR, solid bars) for doses 1, 2, and 3 of diltiazem. Changes in AVFRP were measured directly at the longest basic cycle length available (L-BCL), shortest basic cycle length available (S-BCL), and indirectly (as minimum RR interval) during atrial fibrillation (AF). Matched control cycle lengths were used to calculate the percent change for measurements at L-BCL and S-BCL. Dose-dependent increases in AVFRP (under all pacing conditions) and mean ventricular response during AF were noted. Drug-induced changes in AVFRP increased progressively as activation rate was increased from L-BCL to S-BCL to atrial fibrillation. Increases in mean RR interval during atrial fibrillation were, in turn, larger than the corresponding increases in AVFRP. Results shown are from four experiments after dose 1, eight experiments after dose 2, and five experiments after dose 3 of diltiazem.* $^{*}p<0.05$; $^{**}p<0.01$; $^{***}p<0.001$ *drug vs. control.*

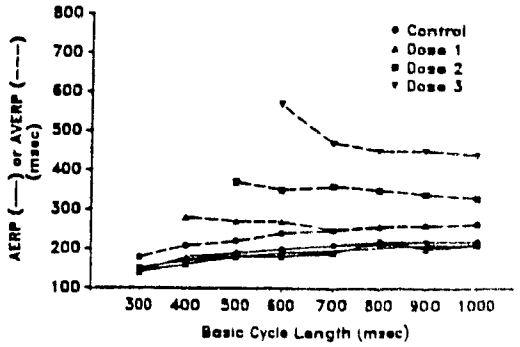

FIGURE 5. *Plot of representative experiment displaying atrial (AERP) and atrioventricular (AVERP) effective refractory periods as a function of cycle length before and after three doses of diltiazem. AERP was not changed by the administration of diltiazem, whereas dose-dependent increases in AVERP were observed. Drug-induced increases in AVERP depended on atrial stimulation rate, and larger changes were observed at shorter cycle lengths.*

the shortest and longest pacing cycle lengths available and the changes in minimum RR interval during atrial fibrillation. After dose 1 of diltiazem, a mean increase of 10% in AVFRP over control was observed at the longest cycle length studied, whereas a 39% increase in minimum RR interval (index for AVFRP) was noted during experimental atrial fibrillation. Similar rate-dependent increases in AVFRP were observed after doses 2 and 3. Although the longest absolute values of AVFRP after drug administration were noted during pacing at the shortest pacing cycle length, larger percent increases in minimum RR interval during atrial fibrillation were observed at all doses (Table 2, Figure 4).

The relation between diltiazem's effects on mean ventricular response and AVFRP are displayed in Figure 4. The increase in mean ventricular response produced by diltiazem during atrial fibrillation was much larger than the drug's effect on AVFRP at long cycle lengths, and the former effect averaged 8.9, 10.9, and 9.4 times larger than the latter effect for doses 1, 2, and 3, respectively. Frequency-dependent increases in AVFRP accounted for approximately one half of the 10-fold increase in drug effect observed during atrial fibrillation (3.9–4.8 fold increases in AVFRP). The remainder of drug effect on mean ventricular response during atrial fibrillation was accounted for by an increase in concealed AV nodal conduction as reflected by an increase in the standard deviation of RR interval histograms (Table 2).

Effects of Diltiazem on Concealed Atrioventricular Nodal Conduction

The potential zone of concealment, during which nonconducted atrial impulses can penetrate the AV node and cause subsequent impulse delay or block, is defined by the difference between AERP and AVERP at any given cycle length. Figure 5 illustrates a representative experiment in which AERP and AVERP were determined at multiple cycle lengths before and after infusion of diltiazem. Before drug administration, this potential zone was small (<30 msec) at all cycle lengths tested. After diltiazem, frequency-dependent increases in AVERP, without changes in AERP were noted. Thus, the potential zone of concealment was increased by diltiazem in a frequency-dependent fashion because of increases in AVERP. A representative experiment in which this zone was scanned with interpolated atrial stimuli is shown in Figure 6. Under control conditions at a cycle length of 500 msec, AV conduction time of test stimuli was exponentially related to the test stimulus coupling interval (S_1S_2). After drug infusion, the relation between AV conduction time and S_1S_2 was shifted upward and to the right. Introduction of concealed atrial extrastimuli (S') caused a further parallel horizontal shift of the AV nodal recovery curve. Earlier concealed atrial extrastimuli shifted the recovery curve to a lesser extent than did later concealed atrial extrastimuli.

In all four experiments, concealment was documented to occur in the presence of diltiazem (dose 2) at all S_1S' intervals greater than the AERP and

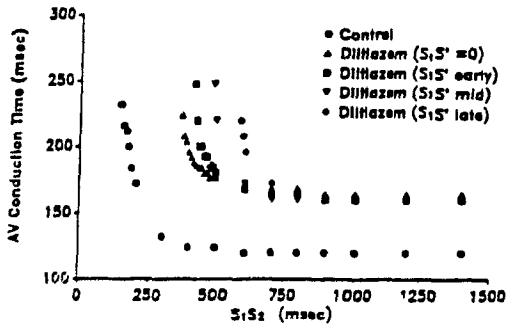

FIGURE 6. *Plot of atrioventricular conduction time as a function of atrial coupling interval (S_1S_2) in the absence and presence of concealed atrial extrastimuli in a typical experiment. Under control conditions with a basic cycle length of 500 msec, AV conduction time was exponentially related to S_1S_2. After diltiazem administration, in the absence of an interpolated atrial extrastimulus ($S_1S'=0$), the curve was shifted upward and to the right. Interpolation of nonconducted atrial stimuli (S') between the last beat of the basic train (S_1) and the test stimulus (S_2) resulted in a further shift of the curve to the right (i.e., concealed conduction). Concealed atrial stimuli with a coupling interval 30 msec greater than atrial effective refractory period (S_1S' early) displaced the curve to a lesser extent than did concealed atrial extrastimuli at a coupling interval 10 msec shorter than atrioventricular effective refractory period (S_1S' late) or atrial extrastimuli with an intermediate coupling interval (S_1S' mid).*

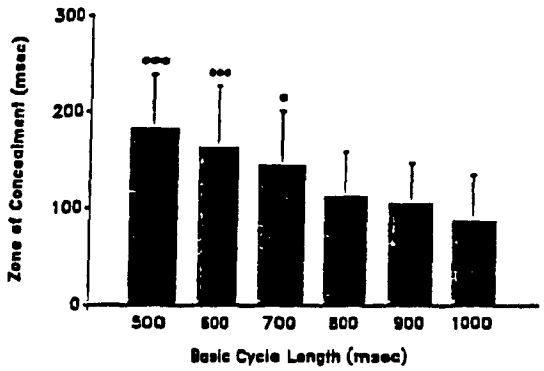

FIGURE 7. *Histogram of zone of concealment as a function of cycle length in the presence of diltiazem. At each cycle length, zone of concealment was directly measured by determining the range of intervals during which an atrial stimulus interpolated between the last beat of the basic drive (S_1) and a test stimulus (S_2) caused the atrioventricular nodal effective refractory period (determined with S_2) to increase by a minimum of 10 msec. Larger zones of concealment were observed at shorter cycle lengths. *p<0.05, ***p<0.001, relative to values obtained at basic cycle length of 1,000 msec. Values shown represent mean data for four experiments.*

less than the AVERP. However, the length of the zone during which atrial impulses were concealed depended on underlying heart rate, and larger zones were observed at shorter cycle lengths (Figure 7).

Discussion

Understanding of antiarrhythmic drug action has improved with the appreciation that cardiac frequency is an important modulator of drug action and that important differences in frequency-dependent properties exist within a specific class of drugs. These concepts have been incorporated into recent models of antiarrhythmic drug action.[28,29] Although frequency-dependent effects on cardiac conduction and refractoriness in vivo have been documented, their importance in determining antiarrhythmic efficacy has not been adequately addressed.

We have previously demonstrated that calcium channel blockers have important frequency-dependent effects on AV nodal conduction and refractoriness.[9] Because atrial fibrillation results in a very fast input rate into the AV node, rapid AV nodal activation in the presence of calcium channel blockers should result in increased block of inward calcium current and a slower ventricular response rate. This would lead to enhancement of antiarrhythmic drug effects by the very tachyarrhythmias for which these drugs are used and would lead to desirable selectivity of drug action. We found that diltiazem's actions during atrial fibrillation were disproportional to its effects at cycle lengths comparable to resting sinus rhythm. Progressive amplification by increases in atrial rate led to maximal effects during atrial fibrillation.

Although several models have been proposed to account for the ventricular response to atrial fibrillation,[16-20,22,30-40] our results can be understood by the classic mechanisms proposed by Langendorf[16] and extended by others.[17-20,22,36] It is assumed that rapid, irregular atrial impulses penetrate the AV node with variable strength from multiple directions. The resulting ventricular response is determined by two factors: 1) the functional refractory period of the AV node,[19,26,30] which constrains the maximum exit rate from the AV node, and 2) the role of concealed AV nodal responses.[16,17,22] Our results suggest that the beneficial effects of diltiazem during atrial fibrillation are secondary to increases in both the AVFRP and the impairment in AV nodal conduction resulting from concealed AV nodal responses. Moreover, these effects on AV nodal properties were markedly dependent on stimulation rate, implying that frequency-dependent drug-receptor interactions may be responsible for maximizing drug effects during tachyarrhythmias.

We found that the percentage by which diltiazem increased AVFRP became progressively larger as atrial rate increased and that the largest percent increases were observed during atrial fibrillation. The rate dependence of AVFRP in the presence of diltiazem was the opposite of that described in the absence of drug[41-44] (as confirmed by our control

observations). The AVFRP is not a pure index of AV nodal refractoriness. It is directly related to the coupling interval at which the slope of the AV recovery curve (AH plotted against A_1A_2) equals unity.[43] Thus, increases in the AVERP, which shift the AV recovery curve to longer atrial coupling intervals, lead to increases in the AVFRP. In addition, AVFRP is inversely related to the conduction time of A_1 and directly related to the conduction time of A_2 during extrastimulus testing.[43,44] Nonetheless, AVFRP remains a useful measure clinically and conceptually because it equals the minimum coupling interval at which impulses can exit from the AV node, and as such, AVFRP constrains the maximum ventricular rate that can occur during rapid atrial rhythms. In addition, Billette[45] showed that the functional refractory period is determined by the action potential duration of cells within the distal portion of the AV node.

We used the minimum RR interval observed during atrial fibrillation as an index of the AVFRP during this arrhythmia. Although the minimum RR interval is not a direct measure of the functional refractory period, it is directly proportional to the AVFRP measured by the extrastimulus technique,[19] and it correlates with the mean ventricular response during experimental atrial fibrillation.[20] Because the percentage by which diltiazem increased AVFRP rose progressively during accelerations in atrial pacing associated with 1:1 AV conduction, we would expect that at least comparable increases would be observed during atrial fibrillation, when AV nodal activations are more frequent. The increases in minimum RR interval observed during atrial fibrillation are consistent with this interpretation.

Diltiazem-induced increases in the minimum RR interval during atrial fibrillation accounted for approximately one half of the observed slowing of the mean ventricular response during atrial fibrillation. Several observations suggested that rate-related increases in concealed AV nodal conduction were at least as important to diltiazem's beneficial effects. All atrial activations failing to conduct to the ventricles in the presence of the drug caused AV nodal delay of subsequent atrial impulses. Zone of concealment was therefore determined at any cycle length by the difference between the AERP and AVERP. Because diltiazem increased the AVERP in a rate-dependent fashion, without altering atrial refractoriness, it caused a rate-related increase in the difference between AERP and AVERP, and consequently zone of concealment.

The width of the RR interval histograms during atrial fibrillation increased consistently after the administration of diltiazem, implying increases in the quantity of AV node concealment during atrial fibrillation. Similar changes in the RR interval histogram during atrial fibrillation have been observed during oral diltiazem therapy in patients with chronic atrial fibrillation.[14] Increases in the amount of concealed conduction, suggested by the observed changes in the RR interval histograms, could be due to a change in the atrial input frequency into the AV node (so that more impulses are likely to fall during zone of concealment), or to an increase in zone of concealment itself. Thiesen and coworkers[14] suggested that diltiazem alters the input into the AV node during atrial fibrillation. However, diltiazem did not alter atrial refractoriness in our dogs, and in previous studies, we showed that atrial conduction is also unaffected by diltiazem.[7] Because the properties of atrial fibrillation are determined by atrial conduction velocity and refractoriness and because diltiazem affects neither of these variables in autonomically blocked dogs, it is unlikely that the atrial input pattern during atrial fibrillation was altered by diltiazem in our dogs. These considerations, coupled with direct observations of zone of concealment during atrial pacing, are consistent with the hypothesis that the increases in AV nodal concealment produced by diltiazem during atrial fibrillation result from an increase in the concealment zone due to rate-dependent increases in AVERP.

Frequency-dependent increases in AV nodal refractoriness and concealment led to dramatic amplification of diltiazem's effects during atrial fibrillation. The amplification of drug effect by tachycardia is likely related to the preferential binding of diltiazem to AV nodal calcium channels that occurs during depolarization and is followed by drug unbinding after repolarization.[29] At slower rates (e.g., in sinus rhythm) diastolic time is longer, allowing more drug unbinding and less AV nodal depression. However, during atrial fibrillation, frequent AV nodal activation limits the recovery time available between impulses, leading to an accumulation of diltiazem binding and enhanced drug effects. This activation increases the AVFRP, increasing the minimum output interval that the AV node can support, and this also increases the AVERP, increasing the number of impulses that block in the AV node and that leave it in a state of increased refractoriness (concealed conduction).

Potential Limitations

Our model of atrial fibrillation was designed to simulate the chaotic, rapid input into the AV node that occurs during atrial fibrillation in humans. It was not intended to simulate the areas of slowed atrial conduction and increased heterogeneity of atrial refractoriness that may be responsible for spontaneous initiation and maintenance of the arrhythmia. Reservations about the applicability of observations concerning electrically induced atrial fibrillation to the spontaneous arrhythmia have been made.[46] In addition, we did not obtain autocorrelograms during atrial fibrillation, therefore, periods of regularization of RR intervals may have occurred without recognition. However, the structure of RR interval histograms recorded in our experiments were unimodal and skewed to the right as previously reported in spontaneous atrial fibrillation in

humans.[14,32,34,36,38] In addition, the characteristics of atrial fibrillation during continuous stimulation were similar to those of atrial fibrillation that persisted after pacing in those experiments in which the arrhythmia persisted long enough to allow analysis. Furthermore, the changes in RR interval histograms that we observed after the administration of diltiazem were very similar to those reported after oral therapy in humans.[14,47]

Intravenous diltiazem does not affect intra-atrial conduction time or the HV interval.[9] We have also shown that changes in the AV conduction time that occur in response to premature stimulation in this model occur exclusively as a result of changes in the AH interval, while HV times remain constant.[9] Moreover, during experimental and spontaneous atrial fibrillation,[17,48] all impulses activating the His bundle lead to ventricular activation, justifying the use of ventricular activation as an exit marker of the AV node. Thus, although His bundle electrograms were not used in these experiments, this does not present a major problem in interpreting the results.

These experiments were performed in autonomically blocked dogs to eliminate variability in AV conduction resulting from autonomic reflex responses to the vasodilating effects of diltiazem and to varying pacing protocols. In autonomically intact animals, we have made preliminary observations that suggest that autonomic reflexes blunt the magnitude of the effect observed at any concentration of diltiazem but that the rate dependence of drug actions are unaffected.[49]

Conclusion

In conclusion, diltiazem exerts its beneficial effects during atrial fibrillation by increasing AVFRP and the tendency of atrial impulses to manifest concealed conduction in the AV node. Both of these effects are amplified by increases in atrial rate. As a result of these frequency-dependent drug interactions, diltiazem selectively depresses AV nodal function during atrial fibrillation, and results in much smaller effects at rates corresponding to sinus rhythm in humans. This explains why doses of diltiazem in humans that have very minor effects on AV conduction during sinus rhythm can produce important and clinically useful reductions in the ventricular response rate during atrial fibrillation. These observations are consistent with the expected clinical consequences of recent models of antiarrhythmic drug action.[28,29]

Acknowledgments

We thank Randi Elituv-Feder, Carol Matthews, and Christine Villemaire for their excellent technical assistance and Lise de Repentigny for typing the manuscript. Diltiazem was generously supplied by Nordic Laboratories.

References

1. Wit AL, Cranefield PF: Effect of verapamil on the sinoatrial and atrioventricular nodes of the rabbit and the mechanism by which it arrests reentrant atrioventricular nodal tachycardia. *Circ Res* 1974;35:413–425
2. McCans JL, Lindenmeyer GE, Munson RG, Evans RW, Schwartz A: A dissociation of positive staircase (Bowditch) from ouabain-induced positive inotropism: Use of verapamil. *Circ Res* 1974;35:439–447
3. Bayer R, Hennekes R, Kaufmann R, Mannhold R: Inotropic and electrophysiological actions of verapamil and D600 in mammalian myocardium: I. Pattern of inotropic effects of the racemic compounds. *Naunyn-Schmiedebergs Arch Pharmacol* 1975;290:49–68
4. Ehara T, Kaufmann R: The voltage- and time-dependent effects of (−)-verapamil on the slow inward current in isolated cat ventricular myocardium. *J Pharmacol Exp Ther* 1978;207:49–55
5. McDonald TF, Pelzer D, Trautwein W: On the mechanism of slow calcium channel block in heart. *Pflugers Arch* 1980; 385:175–179
6. Kanaya S, Katzung BG: Effects of diltiazem on transmembrane potential and current of right ventricular papillary muscle of ferrets. *J Pharmacol Exp Ther* 1984;228:245–251
7. Tung L, Morad M: Voltage- and frequency-dependent block of diltiazem on the slow inward current and generation of tension in frog ventricular muscle. *Pflugers Arch* 1983; 398:189–198
8. Lee KS, Tsien RW: Mechanism of calcium channel blockade by verapamil, D600, diltiazem and nitrendipine in single dialysed heart cells. *Nature* 1983;302:790–794
9. Talajic M, Nattel S: Frequency-dependent effects of calcium antagonists on atrioventricular conduction and refractoriness: Demonstration and characterization in anesthetized dogs. *Circulation* 1986;74:1156–1167
10. Fillette F, Fontaine G: Ventricular response in atrial fibrillation: Effects of AV nodal refractory periods, atrioventricular block, and preexcitation syndromes, in Surawicz B, Reddy CP, Prystowsky EN (eds): *Tachycardias*. Boston, Martinus Nijhoff Publishing, 1984, pp 245–257
11. Schwartz JB, Keefe D, Kates RE, Kirsten E, Harrison DC: Acute and chronic pharmacodynamic interaction of verapamil and digoxin in atrial fibrillation. *Circulation* 1982; 65:1163–1170
12. Klein HO, Kaplinsky E: Verapamil and digoxin: Their respective effects on atrial fibrillation and their interaction. *Am J Cardiol* 1982;50:894–900
13. Roth A, Harrison E, Mitani G, Cohen J, Rahimtoola SH, Elkayam U: Efficacy and safety of medium- and high-dose diltiazem alone and in combination with digoxin for control of heart rate at rest and during exercise in patients with chronic atrial fibrillation. *Circulation* 1986;73:316–324
14. Thiesen K, Haufe M, Peters J, Thiesen F, Jahrmarker H: Effect of the calcium antagonist, diltiazem, on atrioventricular conduction in chronic atrial fibrillation. *Am J Cardiol* 1985;55:98–102
15. Steinberg JS, Katz RJ, Bren GB, Buff LA, Varghese PJ: Efficacy of oral diltiazem to control ventricular response in chronic atrial fibrillation at rest and during exercise. *J Am Coll Cardiol* 1987;9:405–411
16. Langendorf R, Pick A, Katz LN: Ventricular response in atrial fibrillation: Role of concealed conduction in the AV junction. *Circulation* 1965;32:69–75
17. Moore EN: Observations on concealed conduction in atrial fibrillation. *Circ Res* 1967;21:201–208
18. Mazgalev T, Dreifus LS, Bianchi J, Michelson EL: Atrioventricular nodal conduction during atrial fibrillation in rabbit heart. *Am J Physiol* 1982;243:H754–H760
19. Billette J, Nadeau RA, Roberge F: Relation between the minimum RR interval during atrial fibrillation and the functional refractory period of the AV junction. *Cardiovasc Res* 1974;8:347–351

20. Billette J, Roberge FA, Nadeau RA: Role of the atrioventricular junction in determining the ventricular response to atrial fibrillation *Can J Physiol Pharmacol* 1975,53.575–585
21. Nattel S, Elituv-Feder R, Matthews C, Nayebpour M, Talajic M: The concentration dependence of class III and beta-blocking effects of sotalol in anesthetized dogs *J Am Coll Cardiol* 1989,13 1190–1194
22. Moe GK, Abildskov JA Observations on the ventricular dysrhythmia associated with atrial fibrillation in the dog heart. *Circ Res* 1964,14 447–460
23. Moe GK, Abildskov JA, Mendez C An experimental study of concealed conduction. *Am Heart J* 1964,67.338–356
24. Wu D, Denes P, Dhingra RC, Wyndham CR, Rosen KM Quantification of human atrioventricular nodal concealed conduction utilizing $S_1S_2S_3$ stimulation. *Circ Res* 1976, 39:659–665
25. Ferrier GR. Dresel PE. Role of the atrium in determining the functional and effective refractory period and the conductivity of the atrioventricular transmission system. *Circ Res* 1973;33:375–385
26. Rowland E, Curry P, Fox K, Krikler D Relation between atrioventricular pathways and ventricular response during atrial fibrillation and flutter *Br Heart J* 1981;45 83–87
27. Sachs L. *Applied Statistics* New York, Springer Verlag, 1984
28. Grant AO, Starmer CF, Strauss HC Antiarrhythmic drug action—Blockade of the inward sodium current *Circ Res* 1984;55.427–439
29. Hondeghem LM, Katzung BG Antiarrhythmic agents· The modulated receptor mechanism of action of sodium and calcium channel-blocking drugs. *Annu Rev Pharmacol Toxicol* 1984;24 387–423
30. Soderstrom N· What is the reason for the ventricular arrhythmia in cases of auricular fibrillation? *Am Heart J* 1950, 40·212–223
31. Braunstein JR, Franke EK Autocorrelation of ventricular response in atrial fibrillation. *Circ Res* 1961,9 300–304
32. Horan LG, Kistler JC Study of ventricular response in atrial fibrillation. *Circ Res* 1961,9 305–311
33. Ten Hoopen M. Ventricular response in atrial fibrillation A model based on retarded excitation. *Circ Res* 1966,19 911–916
34. Goldstein RE, Barnett GO A statistical study of the ventricular irregularity of atrial fibrillation. *Comput Biomed Res* 1967,1.146–161
35. Yamada K, Okajima M, Hori K, Fujino T, Muraki H, Hishida H, Kobayashi T On the genesis of the absolute ventricular arrhythmia associated with atrial fibrillation. *Circ Res* 1968;22.707–715
36. Bootsma BK, Hoelen AJ, Strackee J, Meijler FL Analysis of RR intervals in patients with atrial fibrillation at rest and during exercise *Circulation* 1970,41 783–794
37. Cohen RJ, Berger RD, Dushane TT A quantitative model for the ventricular response during atrial fibrillation *IEEE Trans Biomed Eng* 1983,30 769–780
38. Hashida E, Tasaki T Considerations on the nature of irregularity of RR intervals and the function of the atrioventricular node in atrial fibrillation in man based on time series analysis *Jpn Heart J* 1984,25 669–687
39. Wittkampf FHM, de Jongste MJ, Lie HI, Meijler FL The effect of right ventricular pacing on ventricular rhythm during atrial fibrillation *J Am Coll Cardiol* 1988,11 539–545
40. Dreifus LS, Mazgalev T "Atrial paralysis" Does it explain the irregular ventricular rate during atrial fibrillation? *J Am Coll Cardiol* 1988,11 546–547
41. Mendez C, Gruhzit CC, Moe GK Influence of cycle length upon refractory period of auricles, ventricles, and AV node in the dog *Am J Physiol* 1956,184 287–295
42. Cagin NA, Kunstadt D, Levitt B The influence of cycle length on the effective and functional refractory period of the human AV node. *Angiology* 1976,27 468–474
43. Simson MB, Spear J, Moore EN The relationship between atrioventricular nodal refractoriness and the functional refractory period in the dog *Circ Res* 1979,44 121–126
44. Ferrier GR, Dresel PE. Relationship of the functional refractory period to conduction in the atrioventricular node *Circ Res* 1974,35 204–214
45. Billette J Atrioventricular nodal activation during periodic premature stimulation of the atrium *Am J Physiol* 1987, 21 H163–H177
46 Strackee J, Hoelen AJ, Zimmerman NE, Meijler FL Artificial atrial fibrillation in the dog An artifact? *Circ Res* 1971, 28 441–445
47. Shenasa M, Kus T, Fromer M, LeBlanc RA, Dubuc M, Nadeau M Effect of intravenous and oral calcium antagonists (diltiazem and verapamil) on sustenance of atrial fibrillation *Am J Cardiol* 1988,62 403–407
48 Lau SH, Damato AN, Berkowitz WD, Patton RD A study of atrioventricular conduction in atrial fibrillation and flutter in man using His bundle recordings *Circulation* 1969,40 71–78
49. Nayebpour M, Talajic M, Jing W, Nattel S Modulation of diltiazem's frequency-dependent effects on atrial fibrillation by autonomic tone (abstract) *Clin Invest Med* 1988,11 D54

KEY WORDS • diltiazem • atrial fibrillation • frequency dependent effects • atrioventricular node • antiarrhythmia agents

CHAPTER 6

Antiarrhythmic Actions of Diltiazem During Experimental Atrioventricular Reentrant Tachycardias

Importance of Use-Dependent Calcium Channel-Blocking Properties

Antiarrhythmic Actions of Diltiazem During Experimental Atrioventricular Reentrant Tachycardias

Importance of Use-Dependent Calcium Channel-Blocking Properties

Mario Talajic, MD, Demetrios Papadatos, BSc, Christine Villemaire, BSc, Mohsen Nayebpour, PharmD, and Stanley Nattel, MD

The purpose of this study was to determine if the known frequency-dependent effects of diltiazem on inward calcium current result in selective actions during supraventricular tachycardia. These effects were evaluated by use of an experimental model of orthodromic atrioventricular reentrant tachycardia (AVRT). AVRT was induced in 15 dogs over a wide range of retrograde conduction times before and after two doses of diltiazem. Diltiazem produced a tachycardia-related suppression of atrioventricular nodal conduction resulting in greater efficacy for faster than for slower AVRTs. The degree of slowing for tachycardias that remained inducible after diltiazem administration was greater for AVRTs with a rapid initial rate (dose 1, 29%; dose 2, 40%) than for slower AVRTs (dose 1, 11%, $p<0.01$; dose 2, 18%, $p<0.001$). Rate-dependent AVRT slowing occurred because of a time-dependent phase of AH interval prolongation after the onset of tachycardia, which was observed only after diltiazem administration. To further clarify the mechanism of diltiazem's selective actions against faster tachycardias, its effects on the minimum pathway for reentry, or wavelength, were examined in four dogs. The ratio of refractory period to revolution time (RP/RT), an index of wavelength, was measured for each AVRT before and after diltiazem administration. Diltiazem increased the positive slope of the relation between RP/RT and the AVRT rate threefold compared with control ($p<0.05$). This rate-dependent effect prevented AVRT when RP/RT became greater than unity. In conclusion, rate-dependent atrioventricular node depression by diltiazem results in greater tachycardia slowing and higher rates of termination during atrioventricular reentrant tachycardias with faster initial rates and shorter retrograde conduction intervals. (*Circulation* 1990:81:334–342)

Recent understanding of antiarrhythmic drug action has improved with the appreciation that increases in cardiac frequency enhance the effects of antiarrhythmic agents. This property, known as frequency dependence, has been well characterized in vitro for most sodium and calcium channel blockers.[1-3] The in vivo consequences of frequency dependence, particularly relating to antiarrhythmic or proarrhythmic drug properties, are less well defined.[3] We have previously shown that diltiazem alters atrioventricular (AV) nodal properties in vivo in a frequency-dependent manner and have suggested that this might result in selective effects during supraventricular arrhythmias.[4] In a subsequent study, we found that rapid AV nodal input, which occurs during atrial fibrillation, amplifies diltiazem's effects on both AV nodal functional refractory period and concealed AV nodal conduction.[5] Much greater slowing of the mean ventricular response during atrial fibrillation occurs than would be expected based on effects during sinus rhythm.

Diltiazem is also effective for paroxysmal supraventricular tachycardia.[6-12] Because reentry that incor-

From the Department of Medicine, Montreal Heart Institute, University of Montreal and the Departments of Pharmacology and Therapeutics and Medicine, McGill University, Montreal, Quebec, Canada.

Supported by the Quebec Heart Foundation, the Medical Research Council of Canada, the Fonds de Recherche en Sante du Québec, the Fonds de Recherche de l'Institut de Cardiologie de Montreal and Nordic Laboratories, Canada. M.T is a Scholar of the Canadian Heart Foundation.

Address for correspondence: M Talajic, MD, Montreal Heart Institute, 5000 Belanger Street East, Montreal, Quebec, H1T 1C8, Canada.

Received June 15, 1989, revision accepted August 29, 1989

porates the AV node is the presumed mechanism for most paroxysmal supraventricular tachycardia.[13,14] changes in the balance between AV node refractoriness and AV nodal conduction are critical in determining whether a tachycardia can be sustained. One approach to the analysis of reentrant rhythms, which considers relative changes in conduction and refractoriness, is the examination of drug-induced changes in tachycardia wavelength.[15–19] The wavelength of a reentrant tachycardia (λ) is the distance traveled by the reentrant impulse during one refractory period. If the length of the potential reentrant circuit is shorter than λ, the excitation wavefront will enter refractory tissue and become extinguished.[15–17]

The purpose of this study was to determine if the known frequency-dependent effects of diltiazem on inward calcium current result in selective actions during paroxysmal supraventricular tachycardia. These effects were evaluated by use of an experimental model of orthodromic AV reentrant tachycardia (AVRT) in which the properties of the retrograde limb of the reentrant circuit could be controlled experimentally.[20–23] The consequences of frequency-dependent calcium channel blockade were examined by studying the effects of diltiazem on dynamic and steady-state AVRT properties and by indirectly evaluating the rate-dependent effects of diltiazem on tachycardia wavelength. A preliminary communication of these results has been presented in abstract form.[24]

Methods

Fifteen mongrel dogs were anesthetized with 2 mg/kg s.c. morphine and 100 mg/kg i.v. α-chloralose. Femoral arterial and venous catheters were inserted and were kept patent with heparinized saline solution. Dogs were ventilated by means of an endotracheal tube with an animal respirator (Harvard Apparatus, South Natick, Massachusetts). Respiratory parameters were adjusted to ensure adequate oxygenation ($SaO_2 \geq 90\%$) and physiologic pH (7.35–7.45). A thoracotomy was performed through the fourth right intercostal space, and the heart was suspended in a pericardial cradle. Bipolar Teflon-coated stainless steel electrodes were inserted into the lateral right atrium and high lateral right ventricle on either side of the atrioventricular ring and into the right atrial appendage. A bipolar electrode was inserted epicardially to record a His bundle electrogram by previously described techniques.[4] The electrodes located in the atrial appendage and lateral right ventricle were used to record atrial and ventricular electrograms, respectively. All stimulation was applied with 4-msec square-wave impulses at twice late-diastolic threshold. Body temperature was monitored by a thermistor within the chest cavity and was maintained at 37–38° C by a homeothermic heating blanket. A Statham P23 ID transducer (Cleveland, Ohio), electrophysiologic amplifiers, and a paper recorder (model T16, Siemens Mingograf, Sweden) were used to record blood pressure, electrocardiographic leads II and aVR, atrial, His bundle and ventricular electrograms, and stimulus artifacts.

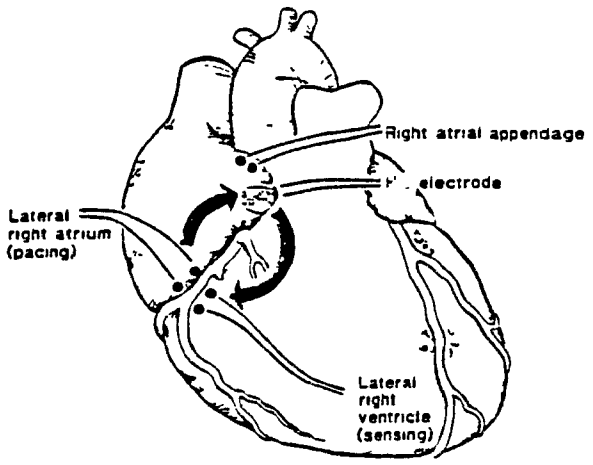

FIGURE 1. *Schematic drawing of experimental atrioventricular reentrant tachycardia. A sensing and pacing circuit was used to detect local ventricular activation at the right ventricular bipolar electrode and to pace the right atrium by means of the lateral right atrial electrode after a preselected delay (VA interval). A sustained reentrant tachycardia (indicated by the arrow) resulted by using the atrioventricular node as the anterograde limb and the pacemaker circuit as the retrograde limb.*

All dogs were autonomically blocked to measure direct drug effects and to avoid the reflex autonomic changes associated with tachycardia or diltiazem administration. Vagal effects were prevented by surgical division of the cervical vagi followed by intravenous administration of 1 mg atropine. β-blockade was produced by administration of 0.5 mg/kg nadolol. Repeated doses of 0.5 mg atropine and 0.25 mg/kg nadolol were administered every 2 hours. Pilot studies showed that this regimen produced sustained autonomic blockade.

Experimental Protocol

Wenckebach cycle length was determined under control conditions by decreasing atrial pacing cycle length by 10-msec decrements until second-degree AV block occurred. This procedure was repeated before and after each experimental protocol to ensure the stability of AV nodal function during the electrophysiologic study.

AVRT was induced experimentally by modifications of previously described methods.[20–23] A sensing and pacing circuit was used to detect ventricular activation at the right ventricular bipolar electrode and to pace the right atrium by means of the lateral right atrial electrode after a preselected delay (VA interval). This reentrant atrial impulse was conducted to the ventricles by means of the normal atrioventricular conducting system and was again detected by the lateral right ventricular electrode. As a result, a sustained reentrant tachycardia using the AV node as the anterograde limb and the pacemaker circuit as the retrograde limb was initiated and

maintained for each selected VA interval (Figure 1). This tachycardia has a fixed retrograde conduction time and mimics the characteristics of orthodromic AVRT mediated by an accessory pathway in humans. Tachycardia was induced at a selected VA interval by engaging the pacing circuit, was maintained for 2 minutes, and was then terminated by turning off the circuit. This procedure was followed by a 1-minute rest period. The protocol was repeated with a variety of VA intervals between 10 and 300 msec. An average of eight AVRTs were induced in each dog; each VA was studied before and after diltiazem administration. The VA interval in this study was the time between the peak of the right ventricular electrogram recorded at a site adjacent to the AV ring and the onset of the atrial stimulus artifact. Corresponding VA intervals measured from the earliest recorded ventricular activation to the earliest atrial activation (as calculated clinically) are 40–50 msec longer. Thus, the range of VA intervals tested in the current study span the range of intervals observed clinically.[25,26]

After control measurements were completed, incremental doses of diltiazem hydrochloride (prepared from pure crystalline powder and physiologic saline) were infused intravenously. The experimental protocol was repeated 10 minutes after the completion of each loading dose. The dosing regimens were developed in prior studies[4,5] and consisted of a loading infusion (0.2 mg/kg i.v. for dose 1 and 0.4 mg/kg for dose 2) administered over 10 minutes, followed by a continuous maintenance infusion (0.003 mg/kg/min for dose 1 and 0.007 mg/kg/min for dose 2). The doses selected were intended to produce steady-state concentrations spanning the range observed during oral diltiazem therapy in man.[9,11] Because of the duration of the experimental protocol needed, only one dose of diltiazem (dose 1) was evaluated in experiments assessing tachycardia wavelength. Blood samples were obtained just before and after each experimental protocol for subsequent measurement of plasma diltiazem concentration by high-performance liquid chromatography.[5] After the experimental protocol had been completed, dogs were killed with lethal doses of pentobarbital. The experimental protocol was reviewed and approved by the hospital animal care committee and internal review board, and all experiments were conducted according to the guidelines of the Canadian Council on animal care.

Data Analysis

Diltiazem effects on dynamic and steady-state characteristics of AVRT were evaluated in 11 dogs (five after both doses of diltiazem, three after dose 1 only, and three after dose 2 only). An additional four dogs were used for analysis of drug-induced changes in tachycardia wavelength.

All electrogram and electrocardiographic recordings were obtained at 200 mm/sec. The His bundle electrogram was stable throughout the duration of nine of 15 experiments. In each of these nine experiments, the AH interval was measured from the onset of the atrial electrogram in the His recording to the upstroke of the His bundle potential. Because all changes in AV conduction time occurring during premature stimulation or during tachycardia were found to occur in the AH interval alone, with HV intervals remaining constant, AV intervals were used in the remaining experiments as an index of AV nodal conduction time. Results obtained in experiments in which AH interval was analyzed did not differ from those obtained in experiments in which AV interval was used. All measurements were made with a digitizing tablet and commercial software (Jandel Scientific, Corte Madeira, California) coupled to an IBM-AT–compatible microcomputer. Measurement accuracy was ±2.5 msec.

AVRTs were classified as sustained if they persisted for 2 minutes, at which time steady-state values of AH (AH_{ss}) and cycle length (CL_{ss}) were measured. Dynamic changes were evaluated by plotting AH interval as a function of beat number after the onset of tachycardia for each VA interval. Changes in AH interval (ΔAH) after tachycardia onset were fitted to a monoexponential function of beat number (bn) by use of Marquardt's technique (Stargraphics Statistical Graphics, Rockville, Maryland). The time constant of change in AH interval (τ) was determined for each fitted curve by use of the resulting equation: $\Delta AH = \Delta AH_{max} \cdot \exp(-bn/\tau)$, where ΔAH_{max} is maximum change in AH interval.

Wavelength (λ) Analysis

λ of a reentrant circuit is equal to the product of average conduction velocity (CV) and the longest refractory period of the circuit (RP)[17]:

$$\lambda = CV \cdot RP \quad (1)$$

Mean conduction velocity is given by the length of the reentrant circuit (L) divided by the revolution time of the tachycardia (RT).

$$CV = L/RT \quad (2)$$

During sustained tachycardia, the RT equals the tachycardia cycle length. After substituting Equation 2 into Equation 1 and rearranging terms:

$$\lambda/L = RP/RT \quad (3)$$

The relation between the minimum path length to sustain reentry (λ) and the actual anatomic path length (L) can therefore be expressed as the ratio RP/RT. Tachycardia can only be sustained if the path length is greater than the wavelength, that is, if λ/L is less than one. RP was determined for each sustained AVRT in four dogs by measuring the effective RP of the AV conducting system (by the extrastimulus technique)[27] at a cycle length equal to CL_{ss} during AVRT. RT was determined by measuring CL_{ss} during AVRT. The RP/RT ratio was calculated and plotted as a function of tachycardia rate before and after administration of diltiazem. The relation between RP/RT and tachycardia rate was fitted by linear

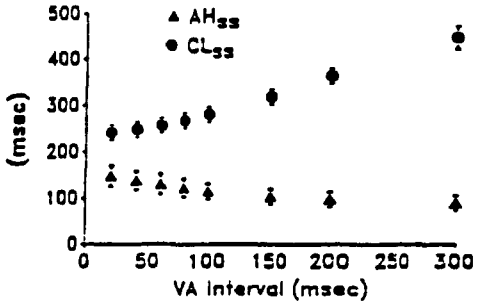

FIGURE 2. *Plot of control steady-state cycle length (CL_{ss}) and AH interval (AH_{ss}) as a function of retrograde conduction time (VA interval). The mean of 11 control experiments are shown. Multiple atrioventricular reentrant tachycardias were induced in each experiment by varying VA interval. Reductions in VA interval led to decreases in mean CL_{ss} and increases in AH_{ss}.*

least-squares regression[25] for each set of control or drug data in each experiment. AV reentry in patients with accessory pathways involves impulse conduction through five distinct cardiac tissues with differing conduction velocities and refractory periods.[29] During the present experiments, tachycardia termination was always due to atrial or AV nodal refractoriness. Therefore, the RP of the proximal AV conduction system (atrium or AV node) was limiting in the ability to sustain tachycardia and was used in λ calculations.

Statistical Methods

Results are reported as mean±SD. Comparisons between control and drug data were made by the paired Student's *t* test with the Bonferroni correction when indicated.[28] Comparisons between multiple experimental groups were made by the unpaired Student's *t* test with the Bonferroni correction. Two-tailed tests were used for all comparisons, and $p<0.05$ was taken to indicate statistical significance.

Results

Properties of AVRT Under Control Conditions

Under control conditions, AVRTs at shorter VA intervals (corresponding to retrograde pathways with faster retrograde conduction times) were faster, as shown in Figure 2. The relation between VA interval and CL_{ss} was not linear because of increases in AH_{ss} at shorter VA intervals, which partially offset the decreases in retrograde conduction time (Figure 2). No changes in intra-atrial or intraventricular conduction time occurred during AVRT. Atrial refractoriness prevented tachycardia induction at shorter VA intervals under control conditions (mean, 34±26 msec). Delayed termination of tachycardia was not observed under control conditions; if the pacing circuit was able to capture the atrium, sustained tachycardia always resulted.

Pharmacologic Actions of Diltiazem

Diltiazem administration resulted in concentration-dependent increases in Wenckebach cycle length (Table 1). Drug effects were stable over the course of each infusion, with less than 10% variation between values of Wenckebach cycle length measured before and after each experimental protocol.

TABLE 1. **Steady-State Characteristics of Atrioventricular Reentrant Tachycardia Before and After Diltiazem Administration**

	Dose 1		Dose 2	
Plasma concentration (ng/ml)	52±29		141±85	
Wenckebach cycle length (msec)				
Control	226±21		219±16	
Drug	347±65*		425±25*	
CL_{ss}				
Slow AVRT (beats/min)				
Control	442±22	(11%)	439±22	(18%)
Drug	490±42†		518±23*	
Fast AVRT (beats/min)				
Control	291±53	(29%)‡	334±59	(40%)§
Drug	375±77*		459±43*	
AH_{ss}				
Slow AVRT (beats/min)				
Control	87±15	(63%)	91±18	(97%)
Drug	140±27*		172±26*	
Fast AVRT (beats/min)				
Control	111±26	(85%)‖	103±16	(128%)‡
Drug	200±29*		231±31*	

The properties of atrioventricular reentrant tachycardias (AVRTs) remaining sustained after diltiazem administration are shown. The AVRTs occurring at the shortest retrograde conduction time that resulted in sustained tachycardia under both control and drug conditions were defined as fast AVRTs; AVRTs at the longest retrograde conduction time studied under both control and drug conditions were defined as slow AVRTs. The mean rate of slow and fast AVRT under control conditions was 136±9 and 211±35 beats/min for dose 1 data and 137±7 and 184±30 beats/min for dose 2 data. Results are reported as mean±SD for matched control and drug data with percent change in parentheses. Results of plasma concentration and Wenckebach cycle length represent averages of values obtained before and after the experimental protocol.

CL_{ss} and AH_{ss}, steady-state cycle length and AH interval, respectively, of AVRT.

*$p<0.001$, †$p<0.01$ for drug vs. control.

‡$p<0.001$, §$p<0.01$. ‖$p<0.05$ for percent change occurring during fast AVRT compared with percent change during slow AVRT.

Effects of Diltiazem on the Steady-State Characteristics of AVRT

Diltiazem slowed AVRT. AVRTs that were faster under control conditions were slowed to a greater extent than AVRTs with an initially slow rate. Figure 3 shows tachycardia CL_{ss} (top panel) and AH_{ss} (bottom panel) as a function of VA interval before and after diltiazem administration, in a typical experiment. Diltiazem increased the cycle length of AVRT in a dose-dependent manner, with all changes in cycle length caused by AH interval prolongation. Drug-induced increases in AH_{ss} and CL_{ss} were greater for faster tachycardias, that is, those induced with

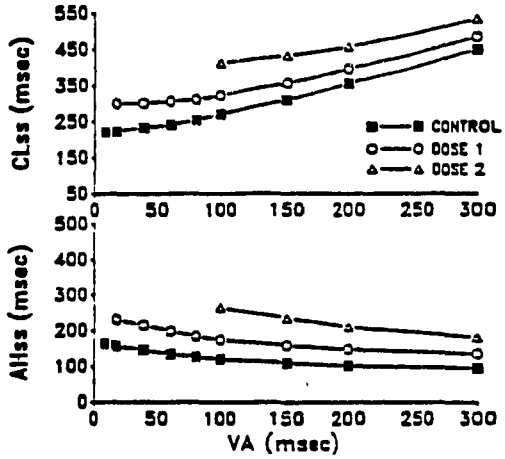

FIGURE 3. *Plots of diltiazem-induced changes in steady-state cycle length (CL_{ss}) and AH interval (AH_{ss}) as a function of retrograde conduction time (VA) in a representative experiment. Sustained atrioventricular reentrant tachycardia was suppressed by dose 1 of diltiazem at VA intervals less than 20 msec and by dose 2 at VA intervals less than 100 msec. Diltiazem caused dose-dependent increases in AH_{ss} and CL_{ss} during atrioventricular reentrant tachycardias that remained inducible after drug administration and that were more prominent at shorter VA intervals.*

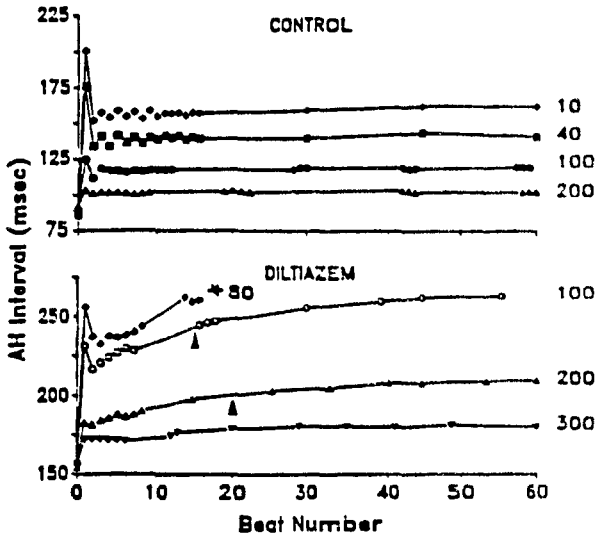

FIGURE 4. *Plots showing dynamic changes in AH interval after the onset of atrioventricular reentrant tachycardia before and after diltiazem in a representative experiment. The retrograde conduction time (VA interval) of each AVRT is indicated at the right of each curve. Under control conditions* (top panel), *the AH interval increased to a maximum with the first beat of tachycardia at all VA intervals tested. Oscillations of AH interval were noted during the initial first through third beats of atrioventricular reentrant tachycardia at shorter VA intervals, but little change in AH interval was noted thereafter. After diltiazem administration* (bottom panel), *a new time-dependent phase of AV conduction slowing appeared after the onset of atrioventricular reentrant tachycardia. This phase followed a monoexponential time course. The time constants for atrioventricular reentrant tachycardias with VA intervals of 200 and 100 msec are indicated by arrows and equal 20 and 17 beats, respectively. This time-dependent phase after tachycardia onset led to delayed tachycardia termination (*) at short VA intervals (80 msec in this experiment).*

shorter VA intervals. In this experiment, the cycle length of an AVRT at a VA interval of 300 msec (control AVRT rate, 134 beats/min) increased 85 msec after dose 2 of diltiazem, whereas at a VA interval of 100 msec (control AVRT rate, 222 beats/min) the corresponding cycle length increase was 141 msec.

Mean CL_{ss} and AH_{ss} measured during sustained AVRT are displayed in Table 1. Only results of AVRTs that remained sustained after diltiazem administration are shown. Results obtained for the slowest control AVRT in each experiment have been grouped together (slow AVRT, mean 136 and 137 beats/min for doses 1 and 2, respectively), as have the results for the fastest control AVRT (fast AVRT, mean 211 and 184 beats/min for doses 1 and 2, respectively). Overall, diltiazem's tachycardia slowing effect was about twice as great for fast AVRTs compared with slow AVRTs.

Dynamic Changes in AV Conduction During AVRT

To examine potential mechanisms of selective drug action during AVRT, beat-to-beat changes in AH interval before and after diltiazem administration were examined as shown in Figure 4. Under control conditions (top panel), the AH interval increased to a maximum with the first beat of tachycardia. Oscillations of AH interval occurred during the initial first through third beats of AVRT at shorter VA intervals as previously described,[23] but little change in AH interval was noted thereafter. After diltiazem administration (bottom panel), a new phase of AV conduction slowing with an exponential time course appeared after the onset of tachycardia.

To quantify the magnitude of this phase, the difference between AH_{ss} and the AH interval of beat 3 (AH_3) was calculated for each sustained tachycardia in each experiment. AH_3 was chosen as a reference to avoid the confounding influence of AH oscillations occurring at the onset of tachycardia. Mean data for all experiments are shown in Figure 5. Prominent rate- and dose-dependent increases in the magnitude of time-dependent conduction slowing were recorded after diltiazem administration in contrast to their absence under control conditions. The additional AV conduction slowing occurring after tachycardia onset in the presence of diltiazem resulted in tachycardia termination at shorter VA intervals (e.g., see results at VA=80 msec, bottom panel, Figure 4).

The time constants for the onset of AH prolongation are indicated by arrows in Figure 4. The correlation coefficients for the nonlinear monoexponential curve fits of this data averaged 0.96±0.02 for 19 sets

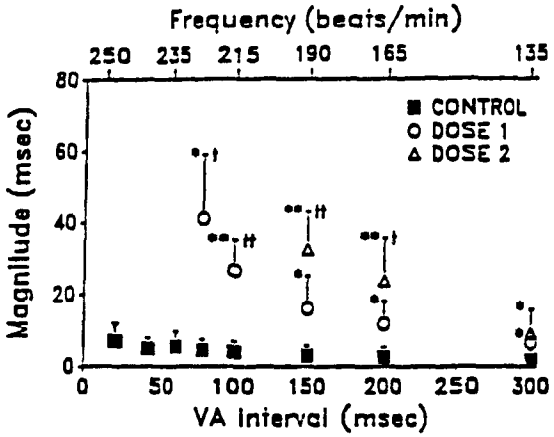

FIGURE 5. *Plot of magnitude of time-dependent phase of atrioventricular conduction slowing after tachycardia onset (defined as the difference between steady-state AH interval and the AH interval of beat 3 of tachycardia. AH_{ss}–AH_3). Magnitude is plotted as a function of retrograde conduction time (VA interval, bottom axis) and mean control atrioventricular reentrant tachycardia rate obtained at that VA interval (top axis). Nonsignificant increases in AH_{ss}–AH_3 were observed under control conditions. After diltiazem, dose-dependent increases in AH_{ss}–AH_3 were observed, which increased at shorter VA intervals. *p<0.05 and **p<0.01 for drug vs. control. †p<0.05 and ††p<0.01 for drug value vs. drug value obtained at VA interval of 300 msec.*

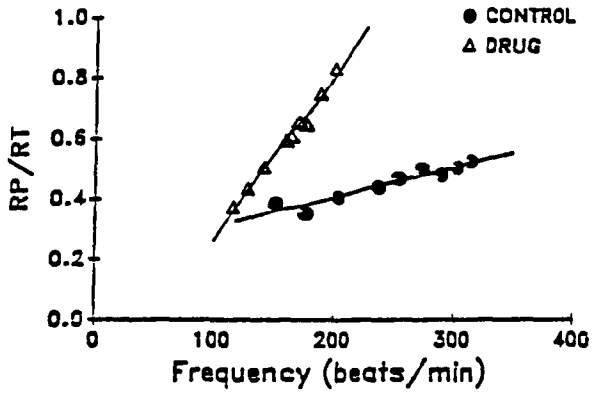

FIGURE 6. *Plot of ratio of refractory period (RP) to revolution time (RT) before and after dose 1 of diltiazem as a function of atrioventricular reentrant tachycardia rate in a representative experiment. Each point represents RP/RT measured during a single atrioventricular reentrant tachycardia, and the solid lines represent best-fit lines by least-squares regression of the RP/RT–atrioventricular reentrant tachycardia rate relation. Based on theoretical considerations presented in the text, changes in RP/RT should be proportioned to changes to tachycardia wavelength. In this experiment, the slope of the regression line was five times as steep in the presence of diltiazem, indicating much greater heart rate dependence of RP/RT than under control conditions.*

of data obtained during dose 1 and 0.98±0.01 for 17 sets of dose 2 data. The time constant of the time-dependent AV conduction slowing was concentration dependent and averaged 29±3 beats after dose 1 of diltiazem and 17±4 beats after dose 2 ($p<0.05$ vs. time constant of dose 1).

Effects of Diltiazem on Wavelength of AVRT

Diltiazem prevented reentrant tachycardias by causing frequency-dependent increases in λ during AVRT in each experiment. Figure 6 shows results obtained in a representative experiment before and after dose 1 of diltiazem. Under both conditions, RP/RT increased as tachycardia rate increased. However, diltiazem strongly increased the slope of this relation, resulting in larger values of RP/RT for tachycardias of equal rate. The slope of the RP/RT versus AVRT rate relation averaged 0.0027±0.0015 under control conditions and 0.0068±0.0017 after diltiazem therapy ($p<0.05$). Correlation coefficients averaged 0.97±0.02 for control data and 0.99±0.01 for drug data. According to the theory developed above, RP/RT should equal λ/L, and when this ratio exceeds unity, the tachycardia should not sustain itself. This was, in fact, seen; no tachycardias could be sustained for cycle lengths at which predicted RP/RT was greater than 1.

Efficacy of Diltiazem Against AVRT

As a result of rate-dependent increases in λ of AVRT, diltiazem prevented AVRTs with faster control rates more often than slower AVRTs (Figure 7). Dose-dependent increases in efficacy were observed during faster AVRTs, such that the drug was uniformly effective at VA intervals equal to or less than 20 msec after dose 1 (mean control rate, 250 beats/min) and VA intervals equal to or less than 80 msec

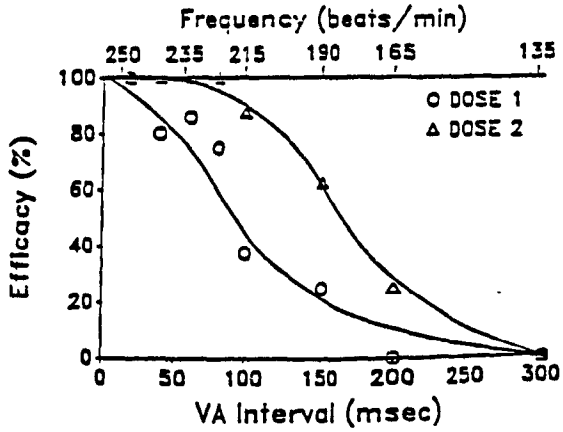

FIGURE 7. *Plot of efficacy of diltiazem for atrioventricular reentrant tachycardia as a function of retrograde conduction time (VA interval, bottom axis) and mean control atrioventricular reentrant tachycardia rate (top axis). The efficacy of diltiazem was strongly dependent on both dose and control atrioventricular reentrant tachycardia properties (i.e., rate as determined by VA interval). Uniform efficacy was observed at VA intervals of less than 20 msec after dose 1 and at VA intervals of less than 80 msec after dose 2.*

after dose 2 (mean control rate, 224 beats/min). Diltiazem was ineffective for very slow AVRTs.

Discussion

The present study was designed to evaluate the importance of frequency-dependent properties of diltiazem in determining drug efficacy against AVRT. These experiments have demonstrated that diltiazem causes greater slowing of faster AVRT as a result of a time-dependent phase of AH interval prolongation, observed only after diltiazem administration. Furthermore, diltiazem-induced increases in AV nodal refractoriness prevailed over AV nodal conduction slowing and led to rate-dependent increases in λ. These increases in λ caused selective termination of faster tachycardias.

Classically, antiarrhythmic drugs are characterized by their effects on cardiac conduction and refractoriness. The analysis of λ allows for quantification of the balance between changes in conduction velocity and refractoriness as they affect the ability to sustain reentry. It is possible that at certain heart rates or drug concentrations, diltiazem-induced changes in refractoriness may not be sufficiently large to counteract drug-induced conduction slowing and could perpetuate AVRT, albeit at a slower rate.[30] In such a case, decreases in λ would be expected. These were not observed in the current study, perhaps because conduction through the AV node constitutes only a part of the overall revolution time during AVRT, the remaining portions of which are unaltered by calcium channel blockade. The concept of λ analysis has recently been used to explain the occurrence of reentrant atrial rhythms in isolated preparations and in intact animals.[18,19] Rensma and coworkers[19] concluded that λ analysis was a more reliable index in predicting the response of reentrant arrhythmias to drug therapy than either CV or RP alone. Furthermore, Feld and colleagues[31,32] have demonstrated that successful therapy for experimental atrial flutter occurs more frequently with agents that increase atrial refractoriness with minimal effects on atrial conduction, conditions associated with an increased λ.

Mechanism of Effects

The mechanism of selective drug effects on rapid AVRT is likely to be twofold. First, under control conditions, tachycardias with shorter retrograde conduction intervals were faster and had longer AH intervals indicating that the reentering wavefront penetrated the AV node anterogradely during its relative RP. Agents that increase AV nodal refractoriness (such as diltiazem) would be expected to suppress such tachycardias more easily, since the AV node is already partially refractory before therapy. Second, the rate-dependent binding of diltiazem to calcium channels is enhanced during faster tachycardias. Evidence for this was found by studying the time-dependent changes in AH interval after tachycardia onset (Figures 4 and 5). The magnitude of this process was dose dependent, whereas its time course was similar to that reported for the onset of diltiazem-induced block of slow inward current in vitro[33–36] and of diltiazem-induced AV conduction slowing in vivo.[4] The time constant of change in AH interval was smaller at a larger dose, as expected from prior studies of antiarrhythmic drug binding.[37,38] The enhancement of calcium channel blockade by tachycardia is related to preferential binding of diltiazem to calcium channels during depolarization, followed by drug unbinding after repolarization (diastole).[1–3] During sinus rhythm, the number of depolarizations during a given interval is less and diastolic time is greater than during tachycardia; these conditions allow less drug binding and less AV nodal depression. During faster tachycardias, that is, those with shorter retrograde conduction times, frequent AV nodal activation increases binding and limits the recovery time between activations; these conditions lead to an accumulation of receptor-bound diltiazem and enhanced drug effects.

Potential Limitations

We evaluated the ratio of λ to L (using the RP/RT ratio) before and after diltiazem; thus, λ was not measured directly. However, the activation sequence (and presumably L) was constant in each experiment, so that changes in RP/RT occurring after diltiazem administration or changes in tachycardia rate were a result of changes in λ alone. Autonomically blocked animals were used to address the direct mechanisms of drug action. Because of this, some caution is warranted before applying our results to clinical tachycardias in which autonomic responses to tachycardias occur.[39] However, Ellenbogen et al[40] have shown that verapamil causes frequency-dependent increases in AH interval in autonomically intact patients. Furthermore, we[41] have shown that the frequency dependence of the effects of diltiazem is unchanged in dogs with intact autonomic tone.

Clinical Consequences

Our results suggest that frequency-dependent effects of calcium channel blockers should cause selective effects during spontaneous AVRTs in humans. This selectivity of action would allow for a low risk of adverse effects during sinus rhythm for a drug dose that effectively prevents (or terminates) tachycardia. Despite having potent antiarrhythmic effects, diltiazem is generally well tolerated and rarely causes resting AV conduction disturbances.[42] Roy et al[10] reported that intravenous diltiazem caused small increases in AH interval during sinus rhythm but much larger increases during supraventricular tachycardia induced in the same patients.

The current study suggests that initial tachycardia characteristics may be important in determining whether diltiazem is an effective therapy. Verapamil, another rate-dependent calcium channel blocker,[4] is more efficacious in children with faster AVRTs and shorter VA intervals than in those with slower

AVRTs.[43] In addition, verapamil is considerably more efficacious than propranolol despite causing comparable AV nodal conduction slowing during sinus rhythm.[43] Because the different efficacy of the agents are not due to differences in AV conduction slowing during sinus rhythm, verapamil's rate-dependent effects during tachycardia may account for its superiority over propranolol.

The model of reentrant supraventricular tachycardia that we used simulated reentry involving an accessory bypass tract as the retrograde limb. Although one cannot extrapolate directly from our observations to supraventricular tachycardias due to reentry confined to the AV node, it is quite possible that the rate-dependent effects of calcium antagonists would play a similar role in preventing or terminating AV node reentry.

Acknowledgments

The authors would like to thank Nancy Turmel and Carol Matthews for excellent technical help and Léna Dumais and Luce Bégin for secretarial assistance. Diltiazem was generously supplied by Nordic Laboratories, Montreal, Quebec, and nadolol was provided by Squibb Canada, Montreal, Quebec.

References

1. Hondeghem LM, Katzung BG. Antiarrhythmic agents: The modulated receptor mechanism of action of sodium and calcium channel-blocking drugs. *Annu Rev Pharmacol Toxicol* 1984;24:387–423
2. Grant AO, Starmer CF, Strauss HC. Antiarrhythmic drug action—Blockade of the inward sodium current. *Circ Res* 1984;55:427–439
3. Hondegnem LM: Antiarrhythmic agents: Modulated receptor applications *Circulation* 1987;75:514–520
4. Talajic M, Nattel S. Frequency-dependent effects of calcium antagonists on atrioventricular conduction and refractoriness: Demonstration and characterization in anesthetized dogs. *Circulation* 1986;74:1156–1167
5. Talajic M, Naveopour M, Jing W, Nattel S: Frequency-dependent effects of diltiazem on the AV node during experimental atrial fibrillation. *Circulation* 1989;80:380–389
6. Rozanski JJ, Zaman L, Castellanos A. Electrophysiologic effects of diltiazem hydrochloride on supraventricular tachycardia. *Am J Cardiol* 1982;49:621–628
7. Betriu A, Chaitman BR, Bourassa MG, Brevers G, Scholl JM, Bruneau P, Gagne P, Chabot M: Beneficial effect of intravenous diltiazem in the acute management of paroxysmal supraventricular tachyarrhythmias. *Circulation* 1983;67:88–94
8. Rowland E, McKenna WJ, Gülker H, Krikler DM. The comparative effects of diltiazem and verapamil on atrioventricular conduction and atrioventricular reentry tachycardia. *Circ Res* 1983;52(suppl I):I-163–I-168
9. Yeh SJ, Kou HC, Lin FC, Hung JS, Wu D: Effects of oral diltiazem in paroxysmal supraventricular tachycardia. *Am J Cardiol* 1983;52:271–278
10. Roy D, Marchand E, Chabot M, Gagné P, Waters DD, Bourassa MG. Electrophysiologic effects of intravenous diltiazem in patients with recurrent supraventricular tachycardias *Can J Cardiol* 1985;1:302–305
11. Shenasa M, Fromer M, Faugere G, Nadeau R, Leblanc RA, Lambert C, Sadr-Ameli MA. Efficacy and safety of intravenous and oral diltiazem for Wolff-Parkinson-White syndrome. *Am J Cardiol* 1987;59:301–306
12. Huycke EC, Sung RJ, Dias VC, Milstein S, Hariman RJ, Platia EV, the Multicenter Diltiazem PSVT Study Group: Intravenous diltiazem for termination of reentrant supraventricular tachycardia. A placebo-controlled, randomized, double-blind, multicenter study. *J Am Coll Cardiol* 1989;13:538–544
13. Wellens HJJ, Brugada P: Mechanisms of supraventricular tachycardia. *Am J Cardiol* 1988;62:10D–15D
14. Klein GJ, Sharma AD, Yee R, Guiraudon GM: Classification of supraventricular tachycardias. *Am J Cardiol* 1987; 60:27D–31D
15. Mines GR: On dynamic equilibrium in the heart. *J Physiol* (Lond) 1913;46:349–383
16. Lewis T: *The Mechanism and Graphic Registration of the Heart Beat*, ed 3. London, Shaw & Sons, 1925
17. Wiener N, Rosenblueth A. The mathematical formulation of the problem of conduction of impulses in a network of connected excitable elements, specifically in cardiac muscle. *Arch Inst Cardiol Mex* 1946;16:205–265
18. Smeets JLRM, Allessie MA, Lammers WJEP, Bonke FIM, Hollen J: The wavelength of the cardiac impulse and reentrant arrhythmias in isolated rabbit atrium. *Circ Res* 1986;58:96–108
19. Rensma PL, Allessie MA, Lammers WJEP, Bonke FIM, Schalij MJ: Length of excitation wave and susceptibility to reentrant atrial arrhythmias in normal conscious dogs. *Circ Res* 1988;62:395–410
20. Moore EN, Spear JF, Boineau JP: Electrophysiologic studies on preexcitation in the dog using an electronically simulated atrioventricular bypass tract. *Circ Res* 1972;31:174–185
21. Simson MB, Spear JF, Moore EN: Stability of an experimental atrioventricular reentrant tachycardia in dogs. *Am J Physiol* 1981;240:H947–H953
22. Teague S, Denes P, Amat-y-Leon F, Rosen K: Effect of anomalous pathway location on rate of canine experimental A-V reentrant tachycardia. *Am J Physiol* 1977;233:H44–H49
23. Talajic M, Papadatos D, Villemaire C, Nattel S: Mechanism and significance of cycle length alternans during supraventricular tachycardia (abstract). *J Am Coll Cardiol* 1989;13:185A
24. Papadatos D, Talajic M, Villemaire C, Nattel S: Retrograde conduction properties determine rate-dependent efficacy of diltiazem for AV reentrant tachycardia (abstract). *J Am Coll Cardiol* 1989;13:251A
25. Benditt DG, Pritchett ELC, Smith WM, Gallagher JJ: Ventriculoatrial intervals: Diagnostic use in paroxysmal supraventricular tachycardia. *Ann Intern Med* 1979;91:161–166
26. Brugada P, Farre J, Green M, Heddle B, Roy D, Wellens HJJ: Observations in patients with supraventricular tachycardia having a P-R interval shorter than the R-P interval. Differentiation between atrial tachycardia and reciprocating atrioventricular tachycardia using an accessory pathway with long conduction times. *Am Heart J* 1984;107:556–570
27. Josephson ME, Seides SF: *Clinical Cardiac Electrophysiology: Techniques and Interpretations*. Philadelphia, Lea & Febiger, 1979, p 41
28. Sachs L: *Applied Statistics*. New York, Springer-Verlag, Inc. 1984
29. Dugernier T, Brugada P, Lemery R, Chenex E, Wellens HJJ: Application of the wavelength concept to circus movement tachycardia (abstract). *Circulation* 1986;74(suppl II):II-259
30. Talano JV, Tommaso C: Slow channel calcium antagonists in the treatment of supraventricular tachycardia. *Prog Cardiovasc Dis* 1982;25:141–156
31. Feld GK, Venkatesh N, Singh BN: Pharmacologic conversion and suppression of experimental canine atrial flutter: Differing effects of *d*-sotalol, quinidine, and lidocaine and significance of changes in refractoriness and conduction. *Circulation* 1986; 74:197–204
32. Feld GK, Venkatesh N, Singh BN: Effects of *N*-acetylprocainamide and recainam in the pharmacologic conversion and suppression of experimental canine atrial flutter: Significance of changes in refractoriness and conduction. *J Cardiovasc Pharmacol* 1988;11:573–580
33. Kanaya S, Katzung BG: Effects of diltiazem on transmembrane potential and current of right ventricular papillary muscle of ferrets. *J Pharmacol Exp Ther* 1984;228:245–251
34. Uehara A, Hume JR: Interactions of organic calcium channel antagonists with calcium channels in single frog atrial cells. *J Gen Physiol* 1985;85:621–647

35. Lee KS, Tsien RW: Mechanism of calcium channel blockade by verapamil, D600, diltiazem and nitrendipine in single dialysed heart cells. *Nature* 1983;302:790–794
36. Tung L, Morad M: Voltage and frequency-dependent block of diltiazem on the slow inward current and generation of tension in frog ventricular muscle. *Pflugers Arch* 1983;398:189–198
37. Hondeghem LM, Katzung BG. Time- and voltage-dependent interactions of antiarrhythmic drugs with cardiac sodium channels. *Biochem Biophys Acta* 1977;472 373–398
38. Starmer CF, Keer RB: Simulation of use-dependent uptake of ion channel blocking agents by excitable memoranes. *IEEE Trans Biomed Eng* 1985;32:770–774
39. Waxman MB, Wald RW, Cameron D: Interactions between the autonomic nervous system and tachycardias in man. *Cardiol Clin* 1983;1:143–185
40. Ellenbogen KA, German LD, O'Callaghan WG, Colavita PG, Marchese AC, Gilbert MR, Strauss HC: Frequency-dependent effects of verapamil on atrioventricular nodal conduction in man. *Circulation* 1985;72:344–352
41. Navebpour M, Talajic M, Jing W, Nattel S: Modulation of diltiazem's frequency-dependent effects on atrial fibrillation by autonomic tone (abstract). *Clin Invest Med* 1988;11:D54
42. Winniford MD, Hillis LD: Calcium antagonists in patients with cardiovascular disease. Current perspectives. *Medicine* 1985;64:61–73
43. Silberbach M, Dunnigan A, Benson DW Jr: Effect of intravenous propranolol or verapamil on infant orthodromic reciprocating tachycardia. *Am J Cardiol* 1989;63:438–442

KEY WORDS • diltiazem • supraventricular tachycardia • accessory pathways • antiarrhythmia agents

CHAPTER I

Autonomic Modulation of the Frequency-Dependent Actions of Diltiazem on the Atrioventricular Node in Anesthetized Dogs

0022-3565/90/2531 0353$02 00/0
THE JOURNAL OF PHARMACOLOGY AND EXPERIMENTAL THERAPEUTICS

VOL 253 No
Printed in U.S.A.

Autonomic Modulation of the Frequency-Dependent Actions of Diltiazem on the Atrioventricular Node in Anesthetized Dogs[1]

MOHSEN NAYEBPOUR, MARIO TALAJIC,[2] WUHUA JING and STANLEY NATTEL

Department of Medicine, Montreal Heart Institute (M N , M T , S N), the Departments of Pharmacology and Therapeutics, and Medicine McGill University (M N , W J , S N), and the Department of Medicine, Universite de Montreal (M T), Montreal, Quebec, Canada

Accepted for publication January 3, 1990

ABSTRACT

Calcium antagonists have rate-dependent effects on atrioventricular node refractoriness in autonomically blocked dogs Autonomic reflexes can attenuate diltiazem s actions and could alter their frequency-dependence. We evaluated the effects of four steady-state drug concentrations in each of seven dogs with intact autonomic tone, six with muscarinic blockade (atropine) and eight with combined muscarinic and *beta* adrenergic blockade. Diltiazem depressed atrioventricular nodal function less in autonomically intact dogs than in the other two groups. The concentration-response relationship for increases in Wenckebach cycle length (compared to intact dogs) was twice as steep among dogs with muscarinic blockade ($P < .001$) and three times as steep with combined blockade ($P < .001$). For an equal dose of diltiazem, the slope of drug-induced refractory period prolongation *vs* pacing cycle length was similar (−0 20 ± 0 11%/msec, mean ± S.D) in intact dogs compared to atropinized dogs (−0 21 ± 0 10%/msec) and dogs with combined blockade (−0 24 ± 0 14%/msec) Amplification of diltiazem s actions by the rapid atrial rate during atrial fibrillation was associated with increases in mean RR interval which were 8 3 times as large as changes in refractory period produced by the drug at slow heart rates We conclude: 1) autonomic reflexes reduce diltiazem's effect for any given plasma concentration, 2) changes in vagal tone can play an important role in the autonomic response to diltiazem, and 3) despite altering the magnitude of diltiazem s effects, autonomic mechanisms do not prevent frequency-dependent drug action Preserved rate-dependent actions despite intact autonomic reflexes would allow for selective suppression of atrioventricular nodal function by diltiazem during supraventricular tachyarrhythmias in humans, as shown previously in the presence of autonomic blockade in experimental animals

Calcium antagonists produce a rate-dependent blockade of calcium inward current (Ehara *et al.*, 1978, McDonald *et al.*, 1980; Lee and Tsien, 1983, Tung and Morad, 1983; Kanaya and Katzung, 1984). AV node conduction slowing produced by calcium channel blockers in anesthetized, autonomically blocked dogs is interval-dependent, with a time dependency of drug action that parallels the kinetics of slow channel blockade *in vitro* (Talajic and Nattel, 1986) The rate-dependent effects of verapamil and diltiazem on AV node refractoriness (Talajic and Nattel, 1986) suggest that these agents should have selective depressant actions on AV nodal conduction during supraventricular tachyarrhythmias, with much less effect during sinus rhythm. We have shown that, in autonomically blocked dogs, diltiazem decreases the ventricular response rate during atrial fibrillation by 8 to 10 times as much as it increases AV node refractory period during sinus rhythm (Talajic *et al.*, 1989).

This type of frequency-dependent drug action could explain how doses of diltiazem that do not greatly alter AV conduction during sinus rhythm (Shenasa *et al.*, 1987) can importantly slow the ventricular response rate during atrial fibrillation (Theisen *et al.*, 1985) or prevent the induction of paroxysmal supraventricular tachycardia (Shenasa *et al.*, 1987, Yeh *et al.* 1983) One problem in extrapolating from previous animal observations (Talajic and Nattel, 1986, Talajic *et al.* 1989, 1990) to clinical situations is the potential modulating role of autonomic reflexes All of the available calcium antagonists are peripheral vasodilators, and cause reflex sympathetic activation which tends to offset their direct actions (Serruys *et al.*, 1985 Dodek and Ruedy, 1983, Singh *et al.*, 1983) Although supraventricular tachyarrhythmias increase the rate-dependent effects of calcium antagonists on the AV node, they could also

Received for publication September 28, 1989
[1] This work was supported by operating grants from the Medical Research Council of Canada, the Quebec Heart Foundation, the Fonds de Recherche de l'Institut de Cardiologie de Montreal and Nordic Pharmaceuticals, Canada Ltd
[2] A research scholar of the Canadian Heart Foundation

ABBREVIATIONS: AV, atrioventricular; WBCL, Wenckebach cycle length; AVERP atrioventricular system effective refractory period AVFRP AV node functional refractory period, AERP, atrial effective refractory period AVCT, atrioventricular conduction time, SBCL, shortest atrial cycle length with 1 1 AV nodal conduction at a given diltiazem dose in each dog, LBCL, longest atrial cycle length with 1 1 AV nodal conduction at a given diltiazem dose in each dog

result in increased sympathetic activation which would increase calcium currents (Brown and Yatani, 1986), and could blunt or eliminate the rate-dependent enhancement of drug action.

The present experiments were designed to evaluate the ways in which intact autonomic tone modifies the actions of diltiazem on the AV node, during regular paced atrial rhythms and in the presence of electrically induced atrial fibrillation. We studied the role of the autonomic nervous system by determining the response to diltiazem in dogs with *beta* adrenergic and *muscarinic receptor* blockade, and comparing this response to results in autonomically intact dogs. In addition, the specific importance of vagal reflexes was evaluated by comparing the response of intact dogs to that of dogs treated with i.v. atropine to block muscarinic cholinergic receptors. Our results indicate an important role for rate-dependent diltiazem actions on the AV node in the presence of intact autonomic reflex mechanisms.

Methods

General methods. Mongrel dogs of either sex were anesthetized with morphine (2 mg/kg s.c.) and α-chloralose (100 mg/kg i.v.). Catheters were inserted into both femoral veins and arteries and were kept patent with heparinized saline solution (0.9%). Dogs were ventilated *via* an endotracheal tube using a Harvard animal respirator. Tidal volume and respiratory rate were adjusted after measurement of arterial blood gases to ensure adequate oxygenation (arterial oxygen saturation ≥ 90%) and physiologic pH (7.35 to 7.45). Blood gas measurements were repeated intermittently during the experiment to ensure that they remained in the physiologic range. A thoracotomy was performed through the 4th right intercostal space. Two bipolar Teflon-coated stainless-steel electrodes were inserted into the right atrial appendage for recording and stimulation. Body temperature was maintained at 37–38°C by a homeothermic heating blanket. A Statham P23 ID transducer, electrophysiologic amplifiers and a paper recorder (Siemens Mingograf 80) were used to record blood pressure, electrocardiographic leads II and aVR, a right atrial electrogram, and stimulus artifacts. Stimulation was applied using 4-msec square-wave impulses at twice late diastolic current threshold. The sinus node was crushed to allow for a wide range of pacing rates.

Measurement of electrophysiologic variables. WBCL was measured by decreasing atrial pacing cycle length by 10-msec decrements every 20 sec until second degree AV block occurred. The effective and functional refractory periods (AVERP and AVFRP, respectively) of the AV conducting system and the AERP were measured using the extrastimulus technique and standard definitions (Talajic *et al.*, 1989). AVCT was defined as the interval from the onset of atrial activation in the atrial electrogram until the onset of ventricular activation on the surface ECG. Atrial fibrillation was produced by maintained atrial stimulation at 10 to 20 Hz. The presence of atrial fibrillation was identified by grossly irregular atrial activity, as recorded by the atrial electrode and a similarly irregular ventricular response. In addition, the presence of atrial fibrillation was confirmed by a period of spontaneous atrial fibrillation, lasting from several seconds to minutes, which persisted after electrical stimulation was stopped. We have shown previously that the properties of electrically induced atrial fibrillation are very similar in terms of the AVFRP, mean RR and S.D. of the RR (as determined from RR response histograms) to those of spontaneous fibrillation in a given animal (Talajic *et al.*, 1989).

Pacing-induced atrial fibrillation was maintained for at least 5 min in each experiment. RR intervals during atrial fibrillation were measured in order to analyze the ventricular response, using approximately 500 RR intervals for each study period. RR intervals were measured using a commercially available digitizing pad and software (Sigmascan, Jandel Scientific, Corte Madera, CA) interfaced with an IBM compatible microcomputer. RR interval analysis was begun 2 min after the onset of atrial fibrillation, because of the time required to achieve steady-state rate-dependent effects of diltiazem (Talajic and Nattel, 1986).

Assessment of autonomic influences. The modulation of diltiazem's effects by autonomic tone was studied by comparing the drug's actions in three groups of dogs: 1) seven dogs with intact autonomic nervous systems (referred to in this manuscript as "intact dogs"); 2) six dogs with muscarinic cholinergic blockade ("vagally blocked"); and 3) eight dogs with combined *beta* adrenergic and muscarinic blockade ("autonomically blocked"). Muscarinic blockade was achieved by administering an initial dose of 1 mg of atropine i.v., followed by 0.5 mg of atropine hourly. *Beta* blockade was produced with 0.5 mg/kg of arenolol i.v., followed by 0.25 mg/kg each hour. These techniques have been shown to produce continuous and stable blockade of cardiac muscarinic (Talajic and Nattel, 1986) and *beta* adrenergic (Nattel *et al.*, 1989a) receptors. *Alpha* adrenergic blockade was not used because preliminary studies showed that neither stimulation of cardiac *alpha*-1 adrenergic receptors (with phenylephrine) nor their blockade (with prazosin) alter AERP, AVCT, AVERP, AVFRP or WBCL (Villemaire *et al.*, 1989).

Experimental protocol. Under control conditions, AERP, AVCT, AVERP and AVFRP were measured over a range of atrial basic cycle lengths from just above the WBCL to just below the automatic cycle length. At least 2 min were allowed to pass after changing the pacing cycle length before making any measurements. WBCL was determined, and atrial fibrillation was then induced. Electrocardiographic recordings were obtained at 250 mm/sec to determine AVFRP, and at 50 mm/sec during atrial fibrillation.

Diltiazem was infused according to the protocol shown in table 1. Ten minutes after the end of each loading dose, the measurements made under control conditions were repeated. WBCL was measured before and after each electrophysiologic study, to ascertain the stability of drug effects over the study interval. Data are presented for doses that produced measurable drug effects without excessive toxicity, *i.e.*, doses 3 and 4 for intact dogs, 2 to 4 for vagally blocked dogs and 1 to 3 for autonomically blocked dogs.

Data analysis. Frequency histograms were constructed for the ventricular response to atrial fibrillation during each study period. The minimum RR interval during atrial fibrillation was obtained, as an index of AVFRP during atrial fibrillation (Billette *et al.*, 1974). The S.D. of RR intervals was calculated, as a reflection of the amount of concealed conduction into the AV node during atrial fibrillation (Billette *et al.*, 1975). Plasma diltiazem concentrations were measured before and after each study using previously described high-performance liquid chromatography methods (Talajic and Nattel, 1986; Talajic *et al.*, 1989).

Repeated measures were compared to the same control value using analysis of variance with Scheffe contrasts (Sachs, 1984). All measurements were made under the same conditions of autonomic tone in any given dog, *i.e.*, values in the presence of diltiazem in autonomically or vagally blocked dogs were compared to prediltiazem control values after the establishment of autonomic or vagal blockade in the same animal. Comparisons between only two groups of data were made by Student's *t* test (Sachs, 1984). Comparisons among all three groups of dogs were made by unpaired *t* test with a Bonferroni correction (Sachs, 1984). The significance of differences between the slopes of regression lines was determined by linear least-squares regression followed by a *t* test between the regressions (Goldstein, 1964). Group data are presented in this manuscript as the mean ± S.D. A P value of less than .05 was taken to indicate statistical significance.

Results

Relationship between diltiazem dose, plasma concentration and electrophysiological effects. Vagal blockade decreased WBCL and AVERP, reflecting abbreviated AV nodal retractoriness. Combined *beta* adrenergic and muscarinic blockade had the opposite effect. Because of intergroup variability

before blockade, the control values of the various groups of dogs postblockade did not necessarily differ from each other as expected based on the effects of vagal and *beta* blockade (table 1). The infusion regimens produced stable plasma concentrations and electrophysiological effects (as measured by WBCL) during each drug infusion. Diltiazem increased indices of AV node function (WBCL and AVERP) in a dose-dependent fashion, without altering AERP. The effects of diltiazem were qualitatively similar in all groups of dogs, but occurred at smaller doses in vagally blocked dogs than in autonomically intact dogs, and at smaller doses still in autonomically blocked dogs. This difference was not due to changes in diltiazem pharmacokinetics resulting from altered autonomic tone, because the plasma concentrations produced by a given dose regimen were similar in all three groups of dogs.

Figure 1 shows a concentration-response analysis for the effects of diltiazem on WBCL in the three groups of dogs. Within each group, there is a highly significant correlation between effects on WBCL and plasma drug concentration. The slopes of the concentration-response relationships are, however, quite different. Among vagally blocked dogs, the slope (0.40) is about twice the slope of intact dogs (0.22, $P < .001$). The slope among autonomically blocked dogs (0.62) is about 3 times the slope of intact dogs, and is significantly steeper than the slope of vagally blocked or intact dogs ($P < .01$, $P < .001$, respectively). This indicates that diltiazem increases WBCL about twice as much in vagally blocked dogs, and 3 times as much in autonomically blocked dogs, compared to intact animals with the same plasma concentration.

Rate-dependent drug effects on AV refractoriness. Changes in AV refractoriness produced by diltiazem depended on the rate of AV nodal activation. Figure 2 shows the relationship between diltiazem-induced increases in AVERP and steady-state cycle length during 1:1 atrial pacing. Each value represents the change produced by diltiazem relative to drug-free control values in the same dog at the same cycle length. In all three groups of dogs, increases in heart rate produced substantial and statistically significant increases in drug effect. The magnitude of the effect of a given dose depended on background autonomic tone, with a given dose producing the largest effect in autonomically blocked dogs, the smallest effect in intact dogs and an intermediate effect in vagally blocked dogs. Nonetheless, the pattern of cycle-length dependence was similar in all three groups of dogs, with substantially greater drug action as cycle length decreased. In each experiment, the change in AVERP produced by diltiazem was strongly determined by cycle length. The slope of the relationship between AVERP changes and cycle length was similar for a given diltiazem dose for all three groups of dogs (table 2). This indicates that the frequency dependence of this effect of diltiazem was not altered substantially by different patterns of background autonomic tone, despite large changes in the overall magnitude of effect.

In order to analyze further the role of rate-dependent changes in AV node refractoriness during atrial fibrillation, we studied the effects of diltiazem on AVFRP. The functional refractory period determines, and is indicated by, the minimum output interval from the AV nodal system. As such, it is important in governing the ventricular response to atrial fibrillation, and is related to refractory properties in the distal AV node (Billette, 1987). During 1:1 atrial pacing, the rate-dependent pattern of diltiazem-induced changes in AVFRP was similar to that of AVERP. The range of cycle lengths that could be studied was different for different doses of diltiazem, as a result of drug-induced increases in Wenckebach cycle length. We therefore compared drug effects on AVFRP at the shortest cycle length attainable during each dose (SBCL) with effects on AVFRP at the longest cycle length (LBCL) possible for that dose. Although SBCL and LBCL differed between animals and among different doses in the same animal, changes were always expressed relative to control at the same cycle length. Furthermore, comparisons were always made between paired values for LBCL and SBCL at the same dose in the same dog, and were therefore valid despite interdose and interanimal variability. As shown in figure 3, diltiazem increased AVFRP substantially more at short pacing cycle lengths than at long cycle lengths.

TABLE 1

Diltiazem dose regimens, plasma concentrations and resulting electrophysiological effects

All values are shown as the mean ± S.D. Loading and maintenance doses were 0.2 mg/kg, 0.003 mg/kg·min^{-1} (Dose 1), 0.4 mg/kg, 0.007 mg/kg·min^{-1} (Dose 2), 0.8 mg/kg, 0.015 mg/kg·min^{-1} (Dose 3), and 0.10 mg/kg, 0.020 mg/kg·min^{-1} (Dose 4). All loading doses were given over 10 min and were immediately followed by the maintenance infusion. Electrophysiological study was begun 10 min later. In intact and vagally blocked dogs no significant effects occurred during Doses 1 and 2 and Dose 1, respectively, so complete electrophysiological studies were not performed during these infusions.

	Diltiazem Conc		WBCL (msec)		AVERP	AERP	BP
	Prestudy	Poststudy	Prestudy	Poststudy			
	mg/ml		*msec*		*msec*	*msec*	*mm Hg*
			Autonomically intact dogs (n = 7)				
Control			161 ± 13	160 ± 12	160 ± 12	100 ± 8	151 ± 17/87 ± 10
Dose 3	198 ± 55	169 ± 47	293 ± 75**	293 ± 70**	248 ± 84	102 ± 13	152 ± 35/87 ± 13
Dose 4	459 ± 73	514 ± 119	427 ± 38***	415 ± 40***	280 ± 47**	113 ± 15	138 ± 17/79 ± 11
			Vagally blocked dogs (n = 6)				
Control			172 ± 16	172 ± 16	171 ± 25	128 ± 15	158 ± 19/103 ± 24
Dose 2	117 ± 38	86 ± 19	282 ± 37**	300 ± 35**	260 ± 92	135 ± 10	154 ± 20/104 ± 15
Dose 3	263 ± 45	187 ± 30	418 ± 51***	407 ± 40***	338 ± 90**	140 ± 13	143 ± 26/86 ± 18
Dose 4	606 ± 108	526 ± 102	560 ± 98***	558 ± 97***	483 ± 98***	145 ± 8	148 ± 25/71 ± 12
			Autonomically blocked dogs (n = 8)				
Control			214 ± 33	214 ± 32	187 ± 27	155 ± 27	141 ± 27/83 ± 22
Dose 1	30 ± 16	28 ± 15	268 ± 39**	279 ± 51**	278 ± 76	153 ± 21	155 ± 8/80 ± 9
Dose 2	77 ± 26	70 ± 14	404 ± 67***	419 ± 93***	306 ± 85***	158 ± 24	140 ± 14/88 ± 13
Dose 3	195 ± 86	210 ± 51	514 ± 127***	494 ± 111***	384 ± 116**	175 ± 27	151 ± 28/90 ± 26

*$P < .05$ **$P < .01$ ***$P < .001$ compared to corresponding control value

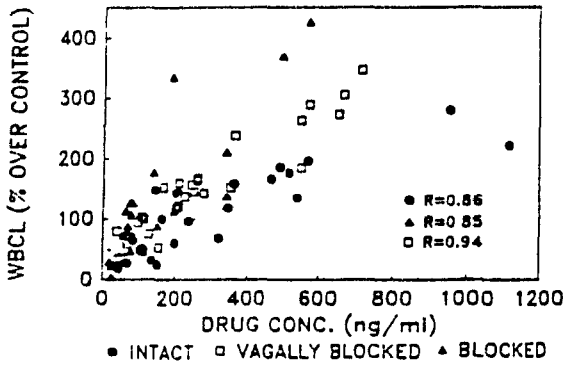

Fig. 1. Concentration (CONC)-response curves for diltiazem-induced increases in WBCL. The slope of the relationship was significantly steeper in vagally blocked dogs (0.40%/ng ml^{-1}) than in autonomically intact dogs (0.21%/ng ml^{-1}, $P < .001$), indicating that changes in vagal tone attenuate this effect of diltiazem in intact dogs. Among autonomically blocked dogs, the slope (0.62%/ng ml^{-1}) was significantly steeper than among vagally blocked dogs ($P < .01$) or intact dogs ($P < .001$), indicating that *beta* adrenergic receptor stimulation also contributes importantly to the reflex attenuation of diltiazem's actions in sympathetically intact dogs.

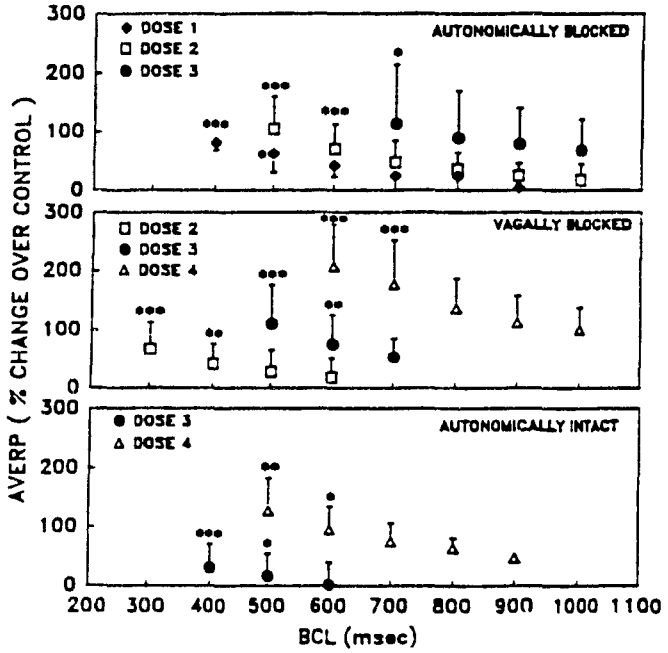

Fig. 2. Rate-dependent changes in the AVERP produced by diltiazem. Values are shown as a percentage of change compared to the predrug control value at the same cycle length. *$P < .05$, **$P < .01$, ***$P < .001$ compared to the effect of diltiazem at the longest cycle length available for a given drug dose in a given set of dogs. BCL, basic cycle length.

The shortest RR interval during atrial fibrillation indicates the shortest output cycle from the AV node during that arrhythmia, and is an index of AVFRP during atrial fibrillation (Billette *et al.*, 1974). Diltiazem produced large increases in the shortest RR interval during atrial fibrillation in all three groups of dogs. The magnitude by which AVFRP during atrial fibrillation increased was greater than the changes in AVFRP during fixed-rate atrial pacing at short and long cycle lengths (fig. 3).

Rate-dependent effects on AV conduction. Diltiazem increased AVCT in a rate-dependent fashion (fig. 4). Rate-dependence of action was seen in all three groups of dogs. Data over the same cycle length range (500–800 msec) was available for doses with similar effects in all groups, dose 2 in autonomically blocked dogs, dose 3 for vagally blocked dogs and dose 4 for intact animals. The slopes of the regression lines relating changes in AVCT to basic cycle length over this range in each experiment averaged -0.08 ± 0.03%/msec for intact dogs, -0.12 ± 0.06%/mec for vagally blocked dogs and -0.07 ± 0.02%/msec for autonomically blocked dogs. There were no significant differences in slopes among groups.

Changes in the ventricular response to atrial fibrillation produced by diltiazem. Diltiazem produced dose-related increases in the mean RR interval during atrial fibrillation in all groups of dogs (table 3). These increases in mean RR interval were 8.3 times as large (range 4–14.7 times) as increases in functional refractory period at long pacing cycle lengths. The mean value of long cycle lengths ranged from 650 ± 129 to 867 ± 52 msec, making them comparable to the mean resting sinus cycle length in humans.

Changes in the mean RR interval were substantially larger for a given dose among autonomically blocked dogs than among autonomically intact or vagally blocked dogs. The potential mechanism of this difference can be appreciated by examining RR interval histograms during atrial fibrillation, as illustrated by the results from one animal in each group as shown in figure 5. With increasing doses of diltiazem, the shortest RR interval during atrial fibrillation (the left-sided limit of each histogram) increased in all three groups of dogs, although larger doses were needed to achieve the same effect on the shortest RR among vagally blocked dogs compared to autonomically blocked animals, and larger doses still among intact animals. In addition, there was a "splaying out" of RR intervals in the presence of diltiazem in all dogs. The overall form of the histogram was splayed out more among autonomically blocked dogs than among intact or vagally blocked dogs, even at doses that produced a comparable increase in the shortest RR interval. This splaying out of the RR interval histogram indicates an increase in the number of atrial impulses consecutively concealed in the AV node (Moe and Abildskov, 1964), and can be described quantitatively by the S.D. of the RR interval distribution (Billette *et al.*, 1975). As indicated in table 3, the S.D. of RR intervals was increased more by a given dose of diltiazem among autonomically blocked dogs than among intact or vagally blocked dogs. The percentage increase in S.D. was significantly larger for dose 2 among autonomically blocked dogs than among vagally blocked dogs ($P < .05$, unpaired t test) and for dose 3 for autonomically blocked than both intact and vagally blocked dogs ($P < .05$ for each, unpaired t test with Bonferroni correction). There were no statistically significant differences between autonomically intact and vagally blocked dogs in the response of RR interval S.D.s.

Discussion

The specific goals of this study were to determine: 1) whether autonomic reflex activity blunts or eliminates the rate-dependent effects of diltiazem; 2) the potential role of changes in vagal tone in the autonomic reflex response to diltiazem; and 3) the ways in which the frequency-dependent effects of diltiazem on the AV node are modulated by the presence of background autonomic reflexes. In addressing these issues, we have obtained information that allows for a deeper understanding of the electrophysiological and antiarrhythmic effects of this widely used drug.

TABLE 2

Relationship between drug-induced changes in AVERP and cycle length

	Slope (−%/msec)*			Correlation Coefficient*		
	Intact	Vagal block	Blocked	Intact	Vagal block	Blocked
Dose 1			0 11 ± 0 03			0 89 ± 0 03
2		0 12 ± 0 02	0 13 ± 0 06		0 93 ± 0 05	0 92 ± 0 04
3	0 20 ± 0 11	0 21 ± 0 10	0 24 ± 0 14	0 91 ± 0 04	0 94 ± 0 04	0 94 ± 0 05
4	0 22 ± 0 09	0.30 ± 0 13		0 96 ± 0 05	0 96 ± 0 02	

*The results shown are the mean slope (±S D) and correlation coefficient for the relationship between drug-induced increases in AVERP and pacing cycle length as determined from data in each experiment There were no significant differences in slope (indicating the rate-dependence of drug action) between groups of dogs at any dose

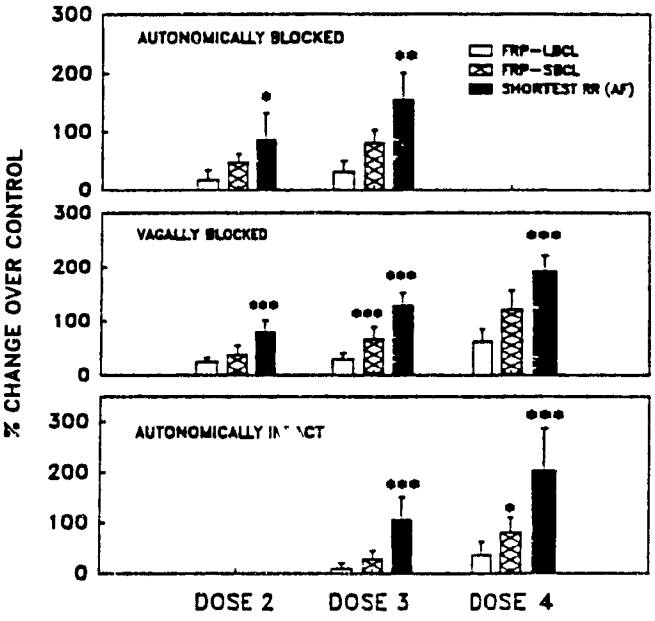

Fig. 3. Changes in the AVFRP period at the longest cycle length (FRP-LBCL) and at the shortest cycle length (FRP-SBCL) available during each drug dose in each dog Each value indicates the percentage of change compared to control AVFRP at the same absolute cycle length in each dog The increase in AVFRP at LBCL and SBCL were compared to changes in the shortest RR interval during atrial fibrillation an indirect index of AVFRP during the latter arrhythmia. *P < 05, **P < 01, ***P < 001 compared to drug-induced increase in AVFRP at long cycle lengths

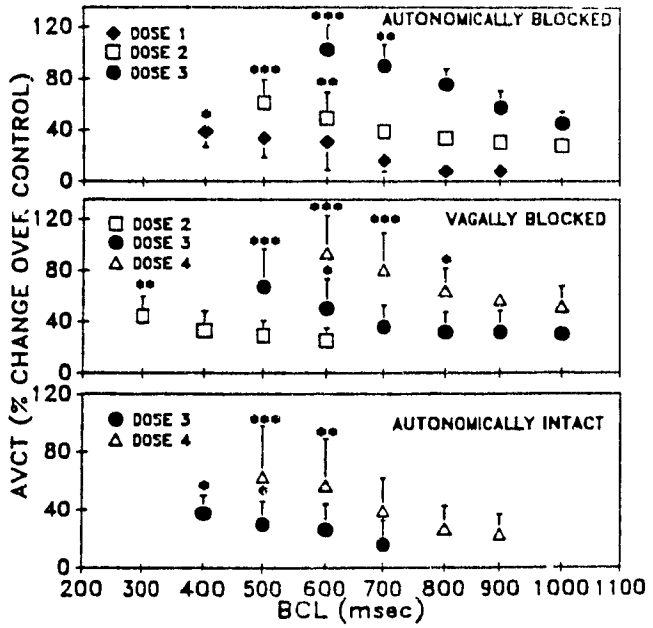

Fig. 4 Rate-dependent changes in AVCT resulting from diltiazem Values are shown as a percentage of change compared to the predrug control value at the same cycle length *P < 05, **P < 01, ***P < 001 compared to the effect of diltiazem at the longest cycle length available for a given drug dose in a given set of dogs

Rate-dependent effects of diltiazem in autonomically intact animals. We have shown previously that diltiazem has rate-dependent effects on AV nodal refractoriness (Talajic and Nattel, 1986), and that these rate-dependent effects result in selective antiarrhythmic actions during atrial fibrillation (Talajic *et al.*, 1989) and AV re-entrant tachycardias (Talajic *et al.*, 1990). Those studies were performed using dogs with *beta* adrenergic and vagal blockade, to minimize any complicating effect of autonomic reflex changes. Ellenbogen *et al* (1985) showed that verapamil produced rate-dependent changes in AH interval in patients not on *beta* blockers, but did not report changes in AV refractoriness. In the current study we found that, whereas autonomic reflexes decrease the magnitude of diltiazem's effects on the AV node for any given plasma concentration (fig. 1), diltiazem's actions continue to depend strongly on the frequency of AV nodal activation. The pattern of frequency-dependent drug action is similar for a given magnitude of drug effect whether dogs are autonomically intact, vagally blocked or exposed to combined *beta* adrenergic and muscarinic cholinergic receptor blockade (figs. 2 and 4, table 2). If the reflex response to calcium antagonists results from peripheral vasodilation and changes in the baroreflex mechanism, as suggested previously (Oesterle and Schroeder, 1982), changes in heart rate might not greatly alter the reflex response to diltiazem because peripheral vasodilating action is not directly dependent on heart rate

Preserved rate-dependent actions in the presence of intact autonomic tone allows for selective depression of supraventricular tachyarrhythmias For example, dose 3 of diltiazem increased AVERP by 1 ± 38% at a heart rate of 100/min and by 31 ± 40% at a heart rate of 150/min (P < 001) in intact dogs whereas WBCL was increased by an average of 83% Therefore, this dose of diltiazem, which produced plasma concentrations very similar to those resulting from chronic p o therapy in humans (Roth *et al*, 1986), had no measurable effect on AV nodal conduction at rates comparable to sinus rhythm but caused marked interference with AV conduction during tachycardia. The potential role of selective rate-dependent increases in AV node refractoriness by diltiazem has been shown in an animal model of AV re-entrant tachycardia (Talajic *et al* 1990)

The rapid atrial input during atrial fibrillation would be expected to maximize diltiazem's depressant effect on the AV node As shown in figure 3, dose 3 increased the shortest RR

TABLE 3

Changes in atrial fibrillation produced by diltiazem in dogs with varying background autonomic tone

The mean RR interval shortest RR interval and S D of RR intervals (S D RR) were obtained by constructing RR interval histograms during each experimental condition All data are presented as the mean ± S D

	Mean RR	%	Shortest RR	%	S D RR	%
			Autonomically intact (n = 7)			
Control	225 ± 27	(–)	138 ± 18	(–)	49 ± 6	(–)
Dose 3	534 ± 198**	(133 ± 61)†	297 ± 101**	(106 ± 46)	157 ± 93**	(216 ± 170)
Dose 4	751 ± 219***	(242 ± 102)	415 ± 108***	(204 ± 83)	213 ± 49***	(363 ± 104)
			Vagally blocked (n = 6)			
Control	230 ± 23	(–)	163 ± 14	(–)	33 ± 7	(–)
Dose 2	456 ± 44***	(97 ± 12)	302 ± 31**	(79 ± 22)	77 ± 17**	(155 ± 11)
Dose 3	622 ± 95***	(169 ± 26)	374 ± 58***	(128 ± 25)	100 ± 46**	(186 ± 70)
Dose 4	038 ± 291***	(351 ± 100)	476 ± 38***	(193 ± 29)	222 ± 104**	(580 ± 354)
			Autonomically blocked (n = 8)			
Control	293 ± 62	(–)	208 ± 45	(–)	51 ± 19	(–)
Dose 1	558 ± 232	(88 ± 67)	298 ± 81	(39 ± 34)	178 ± 143	(257 ± 145)
Dose 2	882 ± 447**	(200 ± 128)	387 ± 123**	(86 ± 46)	302 ± 212*	(525 ± 402)
Dose 3	1058 ± 207***	(300 ± 109)	461 ± 75***	(154 ± 47)	425 ± 56***	(923 ± 379)

*P < 05 **P < 01 ***P < 001 compared ton control † values shown in brackets are percentage increases relative to the corresponding drug-free control value

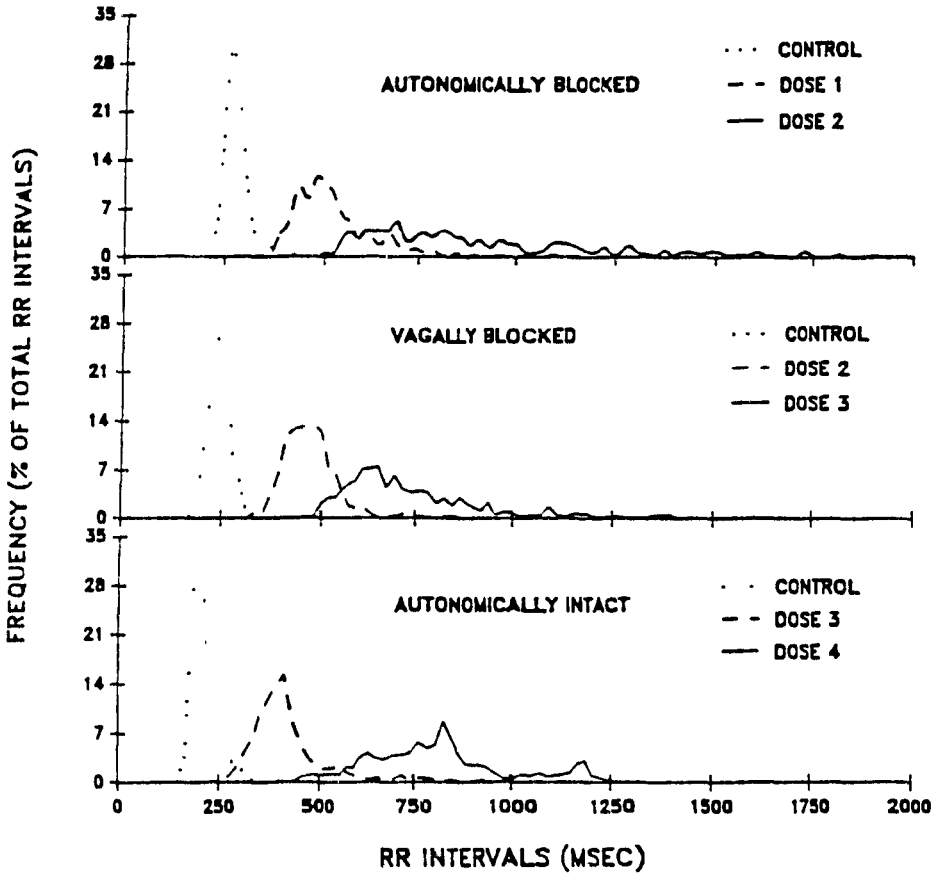

Fig. 5. RR interval histograms for the ventricular response to atrial fibrillation from one representative dog in each group (20 msec bins for RR, 500 RR intervals/histogram). Results are shown for predrug control and two drug doses. Progressively larger doses of diltiazem are needed to achieve a similar effect as autonomic reflex responses are less inhibited Note also the much greater splaying out of the histogram at the highest dose in autonomically blocked dogs compared to vagally blocked or intact dogs

interval (a measure of AVFRP) during atrial fibrillation by 106 ± 46% in autonomically intact dogs, an effect almost 12 times as large as its effect on AVFRP at cycle lengths comparable to sinus rhythm in humans (9 ± 11%, P < 001). Rate-dependent increases in refractoriness explain the observation that doses of diltiazem which do not importantly alter AV conduction during sinus rhythm can produce clinically significant reductions in the ventricular response rate during atrial fibrillation (Theisen *et al* 1985, Steinberg *et al*., 1987)

Role of changes in vagal tone in response to diltiazem. All available calcium antagonists are known to be peripheral vasodilators and to cause reflex sympathetic activation (Serruys *et al*., 1983; Dodek and Ruedy, 1983; Singh *et al*., 1983). Sympathetic activation blunts the direct cardiac actions of calcium antagonists In some instances, reflex responses can quantitatively exceed the direct actions of calcium antagonists, increasing heart rate and/or cardiac output (Serruys *et al*., 1983, Bass and Friedemann, 1971, Vincenzi *et al*., 1976; Stone *et al*., 1980). Whereas increases in sympathetic tone are an important part

of the baroreflex response to vasodilation, reductions in parasympathetic tone are also potentially significant.

The expected response to the vasodilating action of a calcium antagonist is an increase (from basal conditions) in sympathetic tone and a decrease in vagal tone. These alterations counteract the effects of diltiazem on AV node conduction. The most direct way of assessing the modification of diltiazem's actions by changes in autonomic tone would be to measure noradrenaline and acetylcholine release from cardiac nerve endings in the presence of diltiazem, and apply interventions that would return noradrenaline and acetylcholine release to base-line levels. Figure 6 illustrates the above points, and shows how we understand our results. In the clinical situation (or the intact dog), diltiazem increases WBCL (from C to D at the right of figure 6). If base-line vagal tone were maintained (*i.e.*, a reduction in vagal activity in response to diltiazem prevented), WBCL would increase to the level indicated by (A) in figure 6. If, in addition, sympathetic tone was maintained at basal levels (*i.e.*, not increased in response to diltiazem), WBCL would increase further to level (B) in figure 6.

This experiment is technically unfeasible. We therefore evaluated the role of background autonomic tone indirectly, by studying dogs with vagal or sympathetic effects blocked under both control and drug conditions, and comparing the results to autonomically intact dogs. This approach assumes that the effects of diltiazem in an atropinized dog (in whom changes in the rate of acetylcholine release do not alter cardiac electrophysiology) are similar to the effects that would be seen if vagal tone could be maintained constant at the basal level during diltiazem infusion. Such an assumption is reasonable, but its validity is unproven. The response to two dose levels of diltiazem in our dogs is illustrated at the left of figure 6. Autonomically intact dogs show a dose-related increase in WBCL. Inasmuch as vagal tone is reduced by diltiazem, the final WBCL is similar after the drug in both intact dogs (with little vagal effect because of low vagal discharge rates after drug) and vagally blocked dogs. However, the predrug WBCL is shorter in vagally blocked dogs. Consequently, the change from base line to drug values is larger in vagally blocked dogs. Among autonomically blocked dogs, base-line WBCL is slightly increased, and values after diltiazem are increased further because of the lack of positive dromotropic effects from noradrenaline released in response to calcium channel blockade. We studied the effects of diltiazem in separate groups of dogs with the autonomics intact, blocked or vagally blocked. The base-line (preatropine) value of WBCL was greater among vagally blocked dogs than the control value in the intact group. This accounts for the fact that control WBCL (postatropine) among vagally blocked dogs is not shorter than for intact animals. Because of the larger preatropine WBCL in vagally blocked dogs, the postdiltiazem values are larger in this group than among control animals.

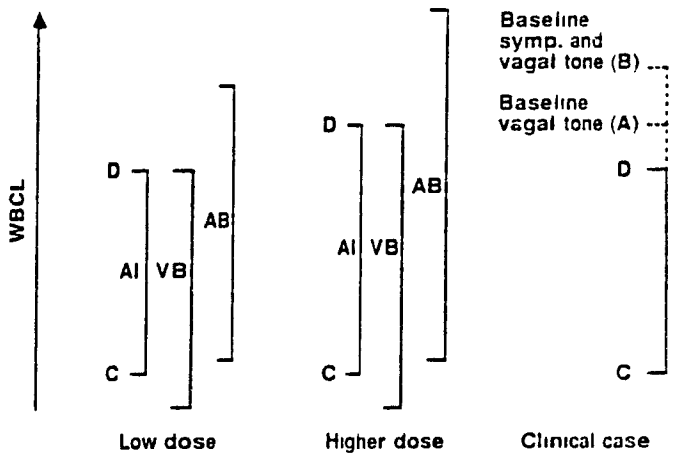

Fig. 6. Diagrammatic representation of diltiazem action on WBCL in dogs at two dose levels (low dose and higher dose). Each vertical bar represents the change in WBCL from predrug control (C) to postdrug (D) values in autonomically intact (AI), vagally blocked (VB) and autonomically blocked (AB) dogs. Shown at the right (clinical case) are the presumed changes in humans. Diltiazem increases WBCL from C to D, an effect resulting from the intrinsic action of the drug, as well as the action of reduced vagal and increased sympathetic (symp) tone in response to the drug. If vagal tone were increased to predrug values, WBCL would increase to the level shown by (A). If, in addition, sympathetic tone were reduced to predrug values, the level designated (B) would result.

Mechanisms of autonomic interactions with diltiazem. *Beta* adrenergic receptor stimulation results in increased calcium entry *via* cyclic AMP-dependent mechanisms (Brown and Yatani, 1986). This facilitates AV nodal conduction (Spear and Moore, 1973, Levy and Zieske, 1969), which is dependent on phase 0 calcium current in AV node cells (Zipes and Fischer 1974). Muscarinic cholinergic stimulation, in turn, suppresses AV node conduction (Spear and Moore, 1973, Levy and Zieske 1969). Increases in vagal tone can alter AV nodal conduction in two ways: 1) by inhibiting net phase 0 inward current *via* an enhanced acetylcholine-dependent outward current (Nishimura *et al.*, 1988) and/or 2) by accentuated antagonism of sympathetic effects (Takahashi and Zipes, 1983).

Interpretation of changes during atrial fibrillation is more complex than during 1:1 atrial pacing. Changes in atrial input rate can modify the ventricular response, complicating analysis. The evaluation of AV nodal refractory period and concealed conduction is limited by the use of indirect indices.

The sympathetic component of the reflex response appeared to be more important than vagal mechanisms during atrial fibrillation. The larger increases caused by diltiazem in mean RR interval during atrial fibrillation in autonomically blocked dogs appeared to be due to an increase in concealed conduction, as reflected in a splaying out in RR interval histograms (fig. 4) and changes in the S.D. of RR intervals (table 3). Qualitatively similar changes have been observed after sympathectomy in the absence of calcium antagonists (Moe and Abildskov, 1964). By increasing the difference between atrial and AV nodal effective refractory period, diltiazem causes a rate-dependent increase in the zone of concealment, thereby augmenting concealed conduction during atrial fibrillation (Talajic *et al.*, 1989). The present study shows that sympathetic influences are capable of decreasing this effect of diltiazem in the presence of atrial fibrillation. The lack of a difference between vagally blocked and intact dogs suggests that changes in vagal tone are less important than sympathetic activation during atrial fibrillation.

Limitations of the models used. The model of atrial fibrillation that we used is artificial, and its relationship to spontaneous atrial fibrillation has been questioned (Stracke *et al.*, 1971). We have shown previously that the ventricular response to electrically induced atrial fibrillation is similar to that for spontaneous atrial fibrillation in dogs (Talajic *et al.*, 1989). The relative amount of sympathetic activation and parasympathetic withdrawal associated with diltiazem administration in humans will depend on the specific clinical situation

and may not be the same as in our dog model. Because we showed that frequency-dependent actions occurred over a wide range of autonomic tone, such actions should occur during human arrhythmias as well.

A His bundle electrode was not used to document the site of conduction slowing and AV block in these experiments. In previous studies, we have shown that all of the AV conduction slowing and refractory period prolongation caused by calcium antagonists is due to changes in AV node function (Talajic and Nattel, 1986). Under control conditions, our measurements of AVERP sometimes reflect an upper limit to AV node refractoriness, because the atrial refractory period exceeded that of the AV node in several experiments.

Changes in the ventricular response to atrial fibrillation can result from changes in AV node function or in atrial input pattern. Diltiazem does not alter atrial refractoriness, as shown in this and previous work (Talajic *et al.*, 1989), or does it affect atrial conduction (Talajic and Nattel, 1986). On the other hand, both limbs of the autonomic nervous system can alter the properties of atrial tissue (DiPalma and Mascatello, 1951). Atrial input into the AV node cannot be measured directly *in vivo*, and we cannot exclude the possibility that changes in atrial input mediated some of the effects of altered autonomic tone during atrial fibrillation. These considerations do not apply to the rate-dependent changes in AVERP and AVFRP observed during 1:1 conduction, or to alterations in WBCL.

Regularization of ventricular response is sometimes observed after verapamil administration in humans (Schamroth, 1980), although in some series' it is relatively infrequent (Schwartz *et al.*, 1982). We did not observe this type of response to diltiazem, perhaps because of species differences (dog *vs.* humans) or differences between drugs (verapamil *vs.* diltiazem).

We did not attempt to quantify precisely the kinetics of drug effects on conduction upon sudden changes in heart rate, as in previous studies of autonomically blocked dogs (Talajic and Nattel, 1986), because of the complexities of kinetic analysis in the presence of dynamically changing autonomic tone produced by tachycardia. Although such studies would have been interesting, they are beyond the scope of the present manuscript.

Potential significance. This is the first study to evaluate quantitatively the interactions between diltiazem and the autonomic nervous system, and to consider rate-dependent properties of potential clinical relevance in the presence of varying autonomic tone. We have shown that intact autonomic reflexes shift the concentration-response curve of diltiazem so that higher concentrations are needed for the same effect on AV nodal conduction. This implies that *beta* blockade should increase the effect of diltiazem in humans for a given plasma concentration. In a recent multicenter trial (The Multicenter Diltiazem Postinfarction Trial Research Group, 1988), the occurrence of AV block among patients treated with diltiazem in the coronary care unit was concentration-related (Nattel *et al.*, 1989b). If *beta* blockade increases diltiazem's effect at any given plasma concentration, AV block should be more likely when a *beta* blocker and diltiazem are administered together than when the latter is given alone. In a series of 110 consecutive patients treated with diltiazem, Hossack (1982) noted AV block in 1 of 99 patients not taking *beta* blockers and in 3 of 11 patients on concomitant *beta* blocker therapy ($P < .01$, Fisher's exact test). A significant incidence of serious bradyarrhythmias has also been observed after concurrent i.v. of diltiazem and propranolol (Oesterle *et al.*, 1986).

The potentiation of the effects of diltiazem by *beta* blockade suggests that the combination of a *beta* blocker and diltiazem might prove to be useful in treating resistant cases of rapid atrial fibrillation or re-entrant tachyarrhythmias involving the AV node. Heart rate variation related to parasympathetic tone is reduced in humans by verapamil administration (Schwartz, 1989), a response consistent with a reduction in background vagal tone after calcium channel blockade. The role of vagal tone in the response to diltiazem may need to be considered when evaluating the effects of the drug in patients with altered vagal control, such as those taking digitalis, acetylcholinesterase inhibitors (*e.g.*, physostigmine in myasthenia gravis), and agents with anticholinergic properties.

Diltiazem, like other calcium antagonists, binds to calcium channels preferentially when they are in the activated or inactivated state, and unbinds during the diastolic period (Hondeghem and Katzung, 1984). Increases in AV nodal activation rate reduce the diastolic time available for drug unbinding, and should therefore magnify diltiazem's actions. This has been shown to occur in the absence of autonomic reflex responses (Talajic and Nattel, 1986), but the current manuscript is the first to document this phenomenon over a range of background autonomic tone. We have shown previously that the rate-dependent actions of diltiazem can contribute importantly to beneficial effects during experimental atrial fibrillation (Talajic *et al.*, 1989) and AV re-entrant tachycardia (Talajic *et al.*, 1990) in autonomically blocked dogs. The present experiments demonstrate similar phenomena in autonomically intact animals, indicating further their potential relevance for understanding the antiarrhythmic actions of diltiazem in patients with intact autonomic function.

Acknowledgments

The authors thank Randi Elituv-Feder, Nancy Turmel, Carol Matthews and Christine Villemaire for technical assistance; Lise de Repentigny for typing the manuscript; and Nordic Pharmaceuticals (Montreal, Quebec, Canada) for supplying the diltiazem and internal standard used in the study.

References

Bass, O. and Friedemann, M.: Ein beitrag zum anti-arrhythmischen wirkungsmechanismus von verapamil. Schweiz. Med. Wochenschr. **101**: 792–799, 1971.

Billette, J.: Atrioventricular nodal activation during periodic premature stimulation of the atrium. Am. J. Physiol. **252**: H163–H177, 1987.

Billette, J., Nadeau, R. A. and Roberge, F. Relation between the minimum RR interval during atrial fibrillation and the functional refractory period of the AV junction. Cardiovasc. Res. **8**: 347–351, 1974.

Billette, J., Roberge, F. A. and Nadeau, R. A.. Role of the atrioventricular junction in determining the ventricular response to atrial fibrillation. Can. J. Physiol. Pharmacol. **53**: 575–585, 1975.

Brown, A. M. and Yatani, A. Ca and Na channels in the heart. *In* The Heart and Cardiovascular System, ed. by H. A. Fozzard, E. Haber, R. A. Jennings, A. M. Katz and H. E. Morgan, pp. 627–636, Raven Press, New York, 1986.

DiPalma, J. R. and Mascatello, A. V. Analysis of the actions of acetylcholine, atropine, epinephrine and quinidine on heart muscle of the cat. J. Pharmacol. (Phila.) **101**: 243–48, 1951.

Dodek, A. and Ruedy, J. Calcium blockers for cardiac disease: Therapeutic implications. Can. Med. Assoc. J. **128**: 911–914, 1983.

Ehara, T. and Kaufmann, R.. The voltage- and time-dependent effects of (−)-verapamil on the slow inward current in isolated cat ventricular myocardium. J. Pharmacol. Exp. Ther. **207**: 49–55, 1978.

Ellenbogen, K. A., German, L. D., O'Callaghan, W. G., Colavita, P. G., Marchese, A. C., Gilbert, M. R. and Strauss, H. C. Frequency-dependent effects of verapamil on atrioventricular nodal conduction in man. Circulation **72**: 344–352, 1985.

Goldstein, A.. Biostatistics, MacMillan Co., New York, 1964.

Hondeghem, L. M. and Katzung, B. G. Antiarrhythmic agents: The modulated receptor mechanism of action of sodium and calcium channel blocking drugs. Annu. Rev. Pharmacol. Toxicol. **24**: 387–423, 1984.

Hossack, K. F. Conduction abnormalities due to diltiazem. N. Engl. J. Med. **307**: 953–954, 1982.

Kanaya, S. and Katzung, B. G. Effects of diltiazem on transmembrane potential and current of right ventricular papillary muscle of ferrets. J. Pharmacol. Exp. Ther. **228**: 245–251, 1984.

LEE, K. S AND TSIEN, R W Mechanism of calcium channel blockade by verapamil D600, diltiazem and nitrendipine in single dialysed heart cells Nature (Lond.) **302:** 790–794, 1983

LEVY, M N AND ZIESKE, H · Autonomic control of cardiac pacemaker activity and atrioventricular transmission. J Appl Physiol **27:** 465–470, 1969

MCDONALD, T. F , PELZER, D AND TRAUTWEIN, W On the mechanism of slow calcium channel block in heart Pflugers Arch **385:** 175–179, 1980

MOE, G. K. AND ABILDSKOW, J A . Observations on the ventricular dysrhythmia associated with atrial fibrillation in the dog heart. Circ Res **14:** 447–460, 1964

NATTEL, S , FEDER-ELITUV, R., MATTHEWS, C , NAYEBPOUR, M AND TALAJIC M : Concentration dependence of class III and beta-adrenergic blocking effects of sotalol in anesthetized dogs J. Am. Coll. Cardiol. **13.** 1190–1194, 1989a

NATTEL, S , TALAJIC, M , O'CONNOR K , GOLDSTEIN, R E. AND MCCANS, J Determinants and significance of diltiazem plasma concentration in a large multicenter post-infarction trial (Abstract) Circulation **80:** (Suppl II), II-51, 1989b.

NISHIMURA, M , HABUCHI, Y , HIROMASA, S AND WATANABE, Y Ionic basis of depressed automaticity and conduction by acetylcholine in rabbit AV node. Am. J. Physiol **255:** H7-H14, 1988.

OESTERLE, S N , ALDERMAN, E. L., BEIER-SCOTT, L., BAIM, D. S , ROTHMAN, M. T. AND SCHROEDER, J. S . Diltiazem and propranolol in combination: Hemodynamic effects following acute intravenous administration. Am Heart J **111:** 489–497, 1986

OESTERLE, S N AND SCHROEDER, J . Calcium-entry blockade, beta-adrenergic blockade, and the reflex control of circulation. Circulation **65:** 669–670, 1982.

ROTH, A , HARRISON, E., MITANI, G , COHEN, J., RAHIMTOOLA, S. H AND ELKAYAM, U . Efficacy and safety of medium- and high-dose diltiazem alone and in combination with digoxin for control of heart rate at rest and during exercise in patients with chronic atrial fibrillation. Circulation **73:** 316–324, 1986.

SACHS, L.. Applied Statistics, Springer-Verlag, New York, 1984

SCHAMROTH, L : The clinical use of intravenous verapamil Am. Heart J **100:** 1070–1075, 1980.

SCHWARTZ, J. B . *In vivo* evidence for parasympathetic inhibition by verapamil. Circulation **80:** (Suppl. II), II-599, 1989

SCH ·ARTZ, J. B , KEEFE, D , KATES, R E., KIRSTEN, E AND HARRISON, D C.. Acute and chronic pharmacodynamic interaction of verapamil and digoxin in atrial fibrillation. Circulation **65:** 1163-1170, 1982.

SERRUYS, P. W , VANHALEWEYK, G. L. J. AND HUGENHOLTZ, P G . The hemodynamic effects of the calcium channel blocking agents. *In* Calcium Channel Blocking Agents in the Treatment of Cardiovascular Disorders. ed. by P. H. Stone and E M Antman. pp. 203–239, Futura Publisning, Mount Kisco. New York, 1983

SHENASA. M , FROMER M , FAUGERE. G., NADEAU. R , LEBLANC, R A , LAMBERT. C AND SADR-AMELI. M A.. Efficacy and safety of intravenous and oral diltiazem for Wolff-Parkinson-White syndrome. Am. J Cardiol **59:** 301–306, 1987

SINGH, B N., NADEMANEE, K. AND BAKY, S H : Calcium antagonists. Clinical use in the treatment of arrhythmias. Drugs **25:** 125–153, 1983

SPEAR. J. F AND MOORE, E N Influence of brief vagal and stellate nerve stimulation on pacemaker activity and conduction within the atrioventricular conduction system of the dog Circ Res 32. 27–41, 1973

STEINBERG, J S , KATZ, R J , BREN, G B , BUFF L A AND VARGHESE P J Efficacy of oral diltiazem to control ventricular response in chronic atrial fibrillation at rest and during exercise J Am Coll Cardiol 9 405–411 1987

STONE P H , ANTMAN, E M , MULLER, J E AND BRAUNWALD E Calcium channel blocking agents in the treatment of cardiovascular disorders Part II Hemodynamic effects and clinical applications Ann Intern Med 93 886–904, 1980

STRACKEE J , HOELEN A J , ZIMMERMAN N E AND MEIJLER F L Artificial atrial fibrillation in the dog An artifact ? Circ Res **28:** 441–445 1971

TAKAHASHI, N AND ZIPES D P Vagal modulation of adrenergic effects on canine sinus and atrioventricular nodes Am J Physiol **244** H775–H781 1983

TALAJIC, M AND NATTEL, S Frequency dependent effects of calcium antagonists on atrioventricular conduction and retractoriness Demonstration and characterization in anesthetized dogs Circulation **74** 1156–1167, 1986

TALAJIC, M , NAYEBPOUR M , JING, W AND NATTEL, S Frequency dependent effects of diltiazem on the AV node during experimental atrial fibrillation Circulation **80:** 380–389, 1989

TALAJIC M., PAPADATOS D , VILLEMAIRE, C , NAYEBPOUR, M AND NATTEL S Antiarrhythmic actions of diltiazem during experimental atrioventricular reentrant tachycardias Circulation **81:** 334–342 1990

THE MULTICENTER DILTIAZEM POSTINFARCTION TRIAL RESEARCH GROUP The effect of diltiazem on mortality and reinfarction after myocardial infarction N Engl. J Med **319:** 385–392, 1988

THEISEN, K , HAUFE, M , PETERS, J , THEISEN F AND JAHRMARKER, H Effect of the calcium antagonist diltiazem on atrioventricular conduction in chronic atrial fibrillation. Am J Cardiol **55** 98–102 1985

TUNG, L. AND MORAD, M Voltage- and frequency-dependent block of diltiazem on the slow inward current and generation of tension in frog ventricular muscle Pflugers Arch **398:** 189–198, 1983

VILLEMAIRE, C , TALAJIC, M AND NATTEL, S Electrophysiologic effects of α-adrenergic receptor stimulation (Abstract) Circulation **80** (Suppl II), II 131 1989

VINCENZI, M., ALLEGRI, P , GABALDO, S , MAIOLINO, O AND OMETTO, R Hemodynamic effects caused by i.v administration of verapamil in healthy subjects Arzneim Forsch **26** 1221–1223, 1976

YEH, S J , KOU, H C., LIN, F C., HUNG, J S AND WU, D Effects of oral diltiazem in paroxysmal supraventricular tachycardia Am J Cardiol **52:** 271–278, 1983

ZIPES D P AND FISCHER J C Effects of agents which inhibit the slow channel on sinus node automaticity and atrioventricular conduction in the dog Circ Res **34:** 184–192, 1974

Send reprint requests to. Dr Stanley Nattel Montreal Heart Institute, 5000 E. Belanger Street, Montreal, Quebec, H1T 1C8, Canada

CHAPTER 8

General Conclusion and Directions for Future Research

The research conducted for this thesis is presented as a compilation of articles, and discussion of the results is well covered in the individual discussion sections of each paper. Therefore, in order to avoid redundancy, this general conclusion will focus mainly on the significance of the model developed in this study, and suggestions for future research and on the cellular mechanisms of the rate-dependent properties of the AV node.

Significance of the model and its potential application to studying AV node physiology

This study demonstrates that a mathematical model based on rate- and time-dependent AV nodal properties can accurately predict AV nodal behavior over a wide range of heart rates. Several mathematical models of AV nodal conduction have been described (Heethar et al, 1973; Van der Tweel, 1986, Honerkam, 1983; Shrier et al, 1987) However, none of the models can explain the variety of nodal responses to heart rate changes. Each model has been developed based on specific assumptions and conditions and cannot be used to explain other nodal behaviors. In addition, there are several theoretical models and computer simulations of AV nodal behavior that do not involve experimental confirmation.

To our knowledge, this is the first model of AV nodal conduction which is able to predict the changes in nodal conduction over a wide range of pacing rates. To develop this model we developed quantitative indices of the three rate sensitive properties of the AV node: AV nodal recovery, fatigue, and facilitation. Among these properties, AV node recovery has been most widely used to explain nodal behaviors. Mobitz

1924, Decherd and Ruskin, 1946). Recently, Shrier et al (1987) used AV nodal recovery characteristics to predict conduction patterns observed during second degree AV block in man. However, it is well known that the AV node recovery curve is dependent on heart rate (Lewis and Master , 1925, Ferrier and Dressel, 1974) and the model developed by Shrier et al (1987) varied depending on the heart rate at which the AV recovery curve was constructed In fact their model was able to predict experimental results only when the recovery curve was constructed at a very rapid rate In addition, the development of fatigue observed during prolonged rapid heart rate changes the degree of block, which suggests that this property should be taken into consideration to explain the nodal response during second degree AV block. This property was not considered in Shrier's model and their model was not able to explain the changes in the degree of AV block observed during prolong rapid pacing

Recently, in our laboratory, these three properties were used to develop a unified model of AV node conduction to predict dynamic changes in Wenckebach periodicity (Talajic et al, 1990). This model was able to predict different patterns of AV block observed following abrupt changes in atrial rate There is evidence from our model that facilitation plays an important role in the model and improves the accuracy of the model (Figure 2-10)

So far this model has been successfully used to predict the changes in AV conduction observed during constant atrial pacing and nodal behavior observed during second degree AV block. Billette and colleagues using isolated rabbit hearts in an <u>in vitro</u> system have shown that the interactions between these three properties explain the rate-induced

changes in functional refractory period (Billette and Metayer, 1989). Yet there are other type of nodal responses occurring in response to ramp changes in activation rate (Loeb et al, 1985), multiple step changes in atrial rate (Loeb et al, 1987), and ventricular responses to atrial fibrillation which have not been studied using the model developed in this study. It would be interesting to assess the ability of the model to explain these responses. It would also be of interest to apply this analysis approach and tools to clinical situations in man to understand nodal behavior under different situations, and to see whether these properties can be similarly quantified in man.

Underlying mechanisms

1- AV node Recovery

1.1- AA or HA

One of the major problems in the characterization of AV nodal function is its apparent dependence on the interval chosen as the measure of recovery time, which has an important impact on the interpretation of the nodal response. Two kinds of approaches can be used to construct the AV recovery curve, AA-AH or HA-AH relationship. Levy and Meytes (1974) first proposed the use of an index of the time between the exit of the impulse from the node and the subsequent nodal input, the PP interval, as an indicator of the nodal recovery time. Levy et al (1974) emphasized on the use of the RP-PR (VA-AV) relationship and showed that changing the VA interval during tachycardia prevents AV nodal block, whereas the same rate of tachycardia with constant AA resulted in Wenckebach block. Moreover, Billette and Matayer (1989) using the same relationship

(HA-AH) found the origins of rate-induced variations of functional refractory period in rabbit AV node. However other investigators (Ferrier and Dresel, 1974; Simson et al, 1978; Simson et al, 1981) have challenged the rationale of using the HA time as a recovery index, and argued for the AA interval as a better indicator of the recovery time This issue can only be addressed by direct microelectrode studies of the isolated AV node, and cannot be resolved by the type of approach presented in this thesis

1.2- The mechanism of AV nodal recovery

In order to discus underlying mechanisms of AV nodal recovery several factors should be taken into consideration 1- AV nodal cells remain partially refractory up to two hundred milliseconds after repolarization (Meredith et al, 1968), resulting in decremental conduction within the N region (Paes de Carvalho and de Almeida, 1960; Hoffman et al, 1959) 2- An electrically silent period occurs between activation of N and NH cells and increases in duration as N cells become activated more prematurely (Billette et al, 1976; Billette, 1987) This period, possibly due to slow activation across an electrotonically-coupled gap, accounts for most of the additional delay in the AV conduction during increased rates. Therefore, both the recovery of source current in the N region (calcium current), and the recovery of excitability in NH cells are determinants of the delay (Billette et al, 1976; Billette, 1987). So far, there are no data on the recovery of the slow inward current from inactivation in the AV node. One way to test this is voltage clamp experiments performed on the small specimens of the AV node (Kokubun et

al, 1982; Noma et al, 1980; Nishimura, 1988) or in single, enzymatically dissociated AV node cells (Nakayama et al, 1984). A two-pulse protocol where two depolarizing steps can be separated by a recovery voltage step of variable duration can be used to determine the time constant of recovery of slow inward current in the AV node. Since the voltage dependence of inactivation and activation of T-type calcium current is at more negative potential than the L-type calcium current, it is quite likely that the recovery of slow inward current in the AV node is due to recovery of L-type current. The time constant of recovery of I_{si} in ventricular muscle has been reported to be 20 msec in cow (Reuter and Scholz, 1977b), 50 msec in sheep (Reuter,1973), 55 in pig (Gettes and Reuter, 1974), and 125 in cat (Trautwein et al, 1975). In sheep Purkinje fibers it has been found to be 670 msec (Gibbons and Fozzard, 1975), and in guinea pig atrial muscle 571 msec (Schulz, 1978). Recently, Hirano et al (1989) found that recovery from inactivation of L-type current in canine cardiac Purkinje cells was voltage dependent and begins at voltage positive to those where recovery of T-type current occurs. The half time of recovery of L-type current was found to be in the range of 100 msec. This remains to be assessed in AV node cells at a voltage similar to the AV node cell resting potential. We have found that the time constant of the AV nodal recovery curve is in the range of 60-80 msec. Therefore, it is possible to compare the time constant of recovery of L-type current with the above recovery time constant.

Potassium current, with its slow kinetics, may contribute to pacemaker depolarization (Carmeliet and Vereecke, 1979). Recently, Belardinelli et al (1989) explained postrepolarization refractoriness and Wenckebach periodicity in single guinea pig ventricular myocytes in terms of the

voltage dependence and slow kinetics of potassium outward currents This makes I_K current a possible candidate for the mechanism of rate-dependent conduction slowing in the AV node and AV nodal recovery curve Since accumulation or depletion of potassium in the extracellular space makes it difficult to study the kinetics of I_K current in multicellular preparation, the contribution of I_K current to AV nodal recovery should be studied in single cells of the AV node

1 3- Slow recovery of excitability

Not only does the recovery of source current in the N region of the AV node determine AV node recovery, but the recovery of excitability in the NH region is also important in this regard. Previous studies using the Purkinje fiber-sucrose gap model (Jalife, 1983) showed that progressive prolongation and eventual failure of proximal to distal activation during the Wenckebach phenomenon can be explained in terms of delayed recovery of excitability of the distal element during diastole (NH cells in the case of AV node) One way to test this is current injection experiments performed on small specimens of the AV node or single cells of AV node. Using this technique, a stimulus response curve can be generated Delmar et al (1989) studied the above relationship in the single guinea pig ventricular myocytes and found that the recovery of cell excitability during diastole was a slow process that outlasted the action potential. They related this to postrepolarization refractoriness, as previously demonstrated in the AV node (Meredith et al, 1968).

1.4- Effects of autonomic manipulations on the AV node recovery

We found that autonomic nervous system significantly modulates the recovery of the AV node (chapter 3 and 4; Figure 3.3 & 4.2). Vagal stimulation delays recovery, whereas sympathetic stimulation accelerates it. Iijima et al (1985) found that the inactivation time course of I_{Ca} in isolated single atrial cells of the guinea-pig was not affected by 10^{-7} molar ACh. However they found that ACh increased K^+ currents which had a progressive deactivation (relaxation) with a time constant of 111 ± 16 msec. This later observation was also reported by Nishimura et al (1988) who found that ACh-dependent potassium current shows time dependent relaxation after repolarization. In addition Shimoni et al (1987) found that ACh slows calcium current repriming in single guinea pig ventricular myocyte. Either of the above effects, or a combination of them, could account for the retardation of the AV nodal recovery observed in our study (chapter 3). However, none of these possible mechanisms has been studied in AV nodal cells. One way to test these is voltage clamp experiments performed in isolated single nodal cells to study the selective effects of ACh on recovery of I_{Ca} current and I_K current.

Nishimura et al (1988) found that ACh significantly changes the passive electrical properties of the AV node. This has profound effects on the excitability of nodal cells. This should be taken into consideration to explain the changes in AV nodal recovery. Analysis of the ACh induced changes in cable properties of AV node and their effects on nodal excitability would be of interest in this regard.

The effects of sympathetic stimulation on nodal recovery is also poorly understood. It has been shown that the increase in amplitude of I_{Ca} by catecholamines occurs without any changes in activation or inactivation kinetics, the current reversal, or ion selectivity of the channel (Reuter and Scholz, 1977a) On the other hand, beta adrenergic stimulation has shown to accelerate the recovery of slow channel action potentials (Tsuji et al, 1985), and to promote reactivation of calcium current in single guinea pig ventricular myocytes (Shimoni et al 1987) Therefore, it is possible that an acceleration of the recovery of calcium current from inactivation contributes to the more rapid recovery of AV nodal conduction observed with beta adrenergic stimulation in our experiments (chapter 4) Voltage-clamp experiments can be conducted in a small specimen of the AV node or in isolated single AV nodal cells to determine the effects of isoproterenol on the recovery of slow inward current from inactivation

2-Fatigue

Meredith et al (1968) found that steady-state rate-induced changes in nodal conduction time (fatigue) were associated with an increased diastolic excitability threshold. They looked at the time course with which conduction velocity changes after a change in rate of stimulation. They observed an initial change of conduction velocity in the first beat, followed by a slower, more gradual change The initial change is probably due to incomplete recovery, but this cannot account for the slower changes (fatigue) developed over many beats They did not systematically study concomitant changes in action potential characteris-

tics. This would provide useful information in understanding the process of fatigue. Beat to beat recording of nodal activation time together with the transmembrane potential ($\dot{V}_{max}$, action potential amplitude, action potential duration (APD), and take-off potentials) from nodal cells during rate-induced fatigue would reveal the following information

1-The site(s) of fatigue development One of the key questions regarding fatigue is the site(s) of its development It is possible that fatigue occurs in the proximal portion (AN cells), central portion (N cells), distal portion (NH) of AV node, or between N and NH cells One way to determine this is the simultaneous recording of cell activation time and total nodal activation time (AH interval) in one preparation during rate-induced fatigue The fatigue-induced changes in total nodal activation time (AH interval) can be compared with the fatigue induced changes in activation time of the cell types (AN, N, and NH) In addition, Billette (1987) found that an electrically silent period (gap) occurs between activation of N and NH cells and its duration increases as rate increases It is possible that development of fatigue reflects the beat by beat increases in the duration of the gap In this case the magnitude of fatigue (delta AH) can be compared to the magnitude of rate induced prolongation of the gap

2-To relate the rate-induced fatigue to the changes in action potential characteristics, the magnitude and time course of fatigue can be compared with the magnitude and time course of rate induced changes in action potential duration, $\dot{V}_{max}$, action potential amplitude and take-off potential

Although the above electrophysiological studies characterize the process of fatigue in the AV node and can give us useful data to understand this phenomenon, the underlying physicochemical mechanism remains unknown. Possible mechanisms are:

2.1-Intracellular accumulation of Ca^{2+}

The rate of rise of action potential of AV node is very slow, suggesting that I_{Na} is small or lacking in the nodal cell. Calcium current is the major time-dependent inward current in AV node cells. The calcium channels are highly selective to calcium ions (Ruters and Scholz, 1977, Lee and Tsien, 1984). The relative permeability sequence of cardiac calcium channel for divalent ions is $Ca^{++}>Sr^{++}>Ba^{++}$. However, when the extracellular Ca^{++} concentration is very low (<0.1nM), monovalent ions can pass through the calcium channel. The permeability sequence for monovalent ions is $Li^{+}>Na^{+}>K^{+}>Cs^{+}$. At normal calcium concentration, these monovalent ions are less permeant through calcium channels than are divalent cations. Therefore, it is possible that during repetitive action potentials at the fast rate there is an accumulation of calcium in the intracellular space which causes fatigue to be developed. This can be measured by calcium sensitive microelectrodes, calcium sensitive dyes, or the bioluminescent protein aequorin method (Kihara et al, 1989). The time course and magnitude of calcium accumulation can be then compared with the time course and magnitude of fatigue reported in our experiments. The mechanism by which intracellular accumulation of calcium causes fatigue could be related to the increased intercellular

coupling resistance caused by an increase calcium This is discussed in more detail in the next section.

2.2-Increased intercellular coupling resistance caused by increased intracellular Ca^{2+}.

The sequence of excitation of the various regions of the heart involves the propagation of action potentials through electrical coupled cells. This provided by a specialized structure known as the gap junction. Conduction velocity is directly related to junctional conductance and both the upstroke velocity and amplitude of the action potential (Jack et al, 1983). A number of factors have shown to affect the junctional conductance and increase intercelluar resistance Acute myocardial ischemia results in a slowing of conduction that becomes more pronounced when the stimulation frequency is increased (El-Sherif et al, 1975) It is known that $\dot{V}_{max}$ (Gettes, 1986) and conduction velocity are decreased, and internal longitudinal resistance (r_i) is increased (Gettes et al, 1985, Kleber et al, 1987) in acute ischemia Hirzel et al (1989) found that these changes in acute ischemia are increased as the heart rate increases They also found that the beneficial effect of verapamil (a calcium channel blocker) during ischemia, are in part due to the prevention of rate-dependent cellular uncoupling possibly by blocking calcium entry into the cell and consequently reducing longitudinal resistance (i_L) It is possible that the same situation as in ischemia occurs during fatigue development in the AV node, and intracellular accumulation of Ca in AV nodal cells causes an increase in intercellular coupling resistance To test this one can measure internal

longitudinal resistance (r_i) by the voltage ratio method (Buchanan et al, 1986; Hiramatsu et al, 1989) in superfused rabbit AV node. This method allows one to measure the time course and magnitude of rate-induced increase in r_i during fatigue development in one preparation.

2.3-Accumulation of adenosine

The release of endogenous adenosine has been previously implicated in the origin of fatigue observed in isolated guinea pig hearts (Jenkins and Belardinelli, 1988). However, the selective effects of rate-induced fatigue were not considered in their study and the adenosine output was measured from the entire heart perfusate. Moreover, the rabbit heart which was shown to have less adenosine receptors and to respond less to adenosine administration (Froldi and Belardinelli, 1990), shows similar rate-induced selective fatigue (approximately 11 msec) to that in anesthetized dogs (chapter 2, Fig. 2.9). Therefore, adenosine may not be an essential factor in the development of fatigue. Studies can be designed to determine the role of adenosine on independently and selectively determined rate-induced fatigue effects primarily in the rabbit heart and, for comparison purposes, in the guinea pig which has more adenosine receptors than the rabbit. Pharmacological tools such as: exogenous adenosine and dipyridamole (an adenosine uptake blocker) can be used to determine the effects of elevated adenosine on fatigue, and BW-A1433 (an adenosine antagonist) can be used to block the effects of adenosine.

2.4-Changes in resting membrane potential due to extracellular accumulation of potassium

It is well documented that resting membrane potential (RMP) become depolarized at high rates of stimulation (Hoffman and Suckling, 1954, Kline and Morad, 1978). The changes in RMP upon stimulation depends on both rate and duration of pacing. During long periods of pacing at a fast rate (1-5 minute), after an initial depolarization there is a progressive membrane repolarization which exceeds the RMP before pacing, even though stimulation continues (Glitsch, 1973, Vassalle, 1970). This phenomenon is known as overdrive suppression. The mechanism by which this occurs has been related to changes in the extracellular potassium concentration. Extracellular concentration of K^+ in cardiac tissue is about 4 mM, and can be increased as much as 1 mmol/litre in a single action potential. This can be increased further during a train of action potentials (Kline and Morad, 1978). Kline and Morad (1978) measured rate-induced changes in the clefts of frog ventricular muscle by K^+ sensitive microelectrodes and found that the time course of the increase of the extracellular K^+ concentration during a short period of stimulation was similar to the time course of membrane depolarization. In a similar study of rabbit atrium, Kunze (1977) found that during longer periods of fast stimulation there was an initial potassium accumulation which followed by a decline of the K^+ concentration, which even undershot the baseline value. These observation indicated that the initial membrane depolarization is due to K^+ accumulation and the later repolarization is due to a decay of K^+ concentration. The mechanism by which repolarization occurs has been attributed to the K^+ accumulation-

stimulated Na^+-K^+ pump (Vassalle, 1970; Glitsch, 1973). When the rate of stimulation increases K^+ will be accumulated within the cleft, and Na^+ will be accumulated intracellularly. This will increase the activity of the Na^+-K^+ pump which exports three Na^+ ions and imports two K^+ ions at the expense of hydrolysis of adenosine triphosphate (ATP). The resulting extrusion of net positive charge generates outward current (the pump is electrogenic), which repolarizes the RMP (Thomas, 1972; Glitsch, 1982). It has been shown that rate-induced changes in RMP are abolished by procedures known to inhibit the Na^+-K^+ pump-e.g. metabolic inhibitors, low temperatures, cardiac glycosids, and Li^+ substitution for Na^+ in the bathing solution (Vassalle, 1970; Glitsch, 1973; Kodama et al, 1977).

In the case of rate-induced fatigue in the AV node, it is possible that activation of Na^+-K^+ pump hyperpolarizes the RMP. This may reduce excitability in the AV node, and cause fatigue. The first attempt should be to measure rate-induced changes in the extracellular concentration of K^+ in the AV node using K^+-sensitive microelectrodes to obtain the relationship between the changes in K^+ concentration, RMP, excitability, and conduction velocity. These can be compared to the rate-induced changes in AH interval (fatigue) in the same preparation. The second attempt should be to block the Na^+-K^+ pump to determine if fatigue is altered.

3-FACILITATION

The cellular processes governing AV nodal facilitation are largely unknown. As explained in the first chapter, this property describes the facilitatory effect of closely coupled atrial impulses an the conduction

of a subsequent beat. Billette (1987) showed that premature AV nodal action potentials can have a decreased duration, possibly providing a cellular basis for facilitation. This can be explained by the theoretical illustration in Fig. 8.1., in which a schematic drawing of an atrial electrogram, the action potential of an AVN cell, and a His electrogram is shown. The upper tracing represents the atrial electrogram A_1 is last basic beat and A_2 is a premature beat introduced at progressively shorter A_1A_2 intervals. In panel A, as the A_1A interval decreases, diastolic recovery time (RT) decreases and activation time (AT) of the AV node cell with reference to the atrial electrogram is increased. In panel C, curve 1 shows the relationship between activation time and recovery time. In panel B, a single atrial impulse with a short coupling interval, A_1A', is introduced before the test impulse A. As a result of the decreased action potential duration of A' (which provides a longer diastolic recovery time, RT), an A_2 at the same coupling interval as in panel A (A_1A_2=$A'A_2$) has a shorter activation time. This is shown by a leftward shift of the recovery curve (curve 2 in panel C).

This can be tested by recording transmembrane potentials from nodal cells during periodic premature stimulation to correlate direct nodal conduction with concomitant changes in activation of various nodal cells and changes in action potential duration. If a decreased PD of distal portion of the AV node provides a longer recovery time (RT), one can study the relationship between the prematurity-induced changes in RT and the degree of facilitation in the same preparation.

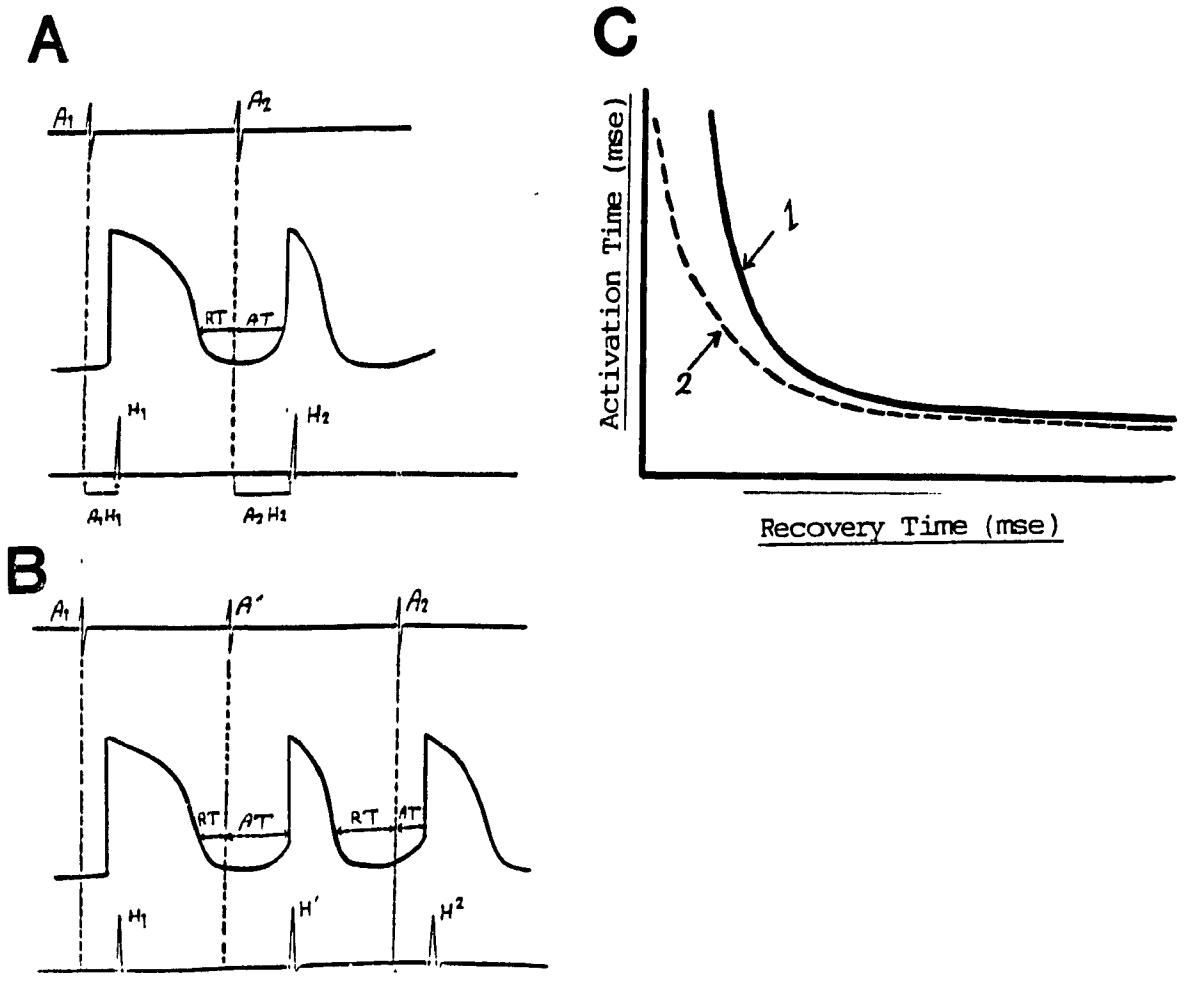

Figure 8 1-Theoretical illustration of facilitation (see text for explanation.)

We found that vagal stimulation decreased facilitation while sympathetic stimulation did not change the degree of facilitation (chapter 3 and 4). Vagal stimulation or ACh administration are known to shorten the APD (Hoffman and Cranefield, 1960; Mazgalev et al, 1986, West and Todo, 1967) The ACh-induced APD shortening attenuates the action potential shortening resulting from prematurity (Mubagwa and Carmeliet, 1985). This could possibly account for the decreased facilitation observed in our study (chapter 3) This can be tested using the experimen-

tal protocol explained above before and after vagal stimulation or ACh administration. The effects of catecholamines on the cardiac action potential are complex, and depend on species and concentration. Low concentrations (nanomolar) of norepinephrine prolong the action potential, whereas higher concentrations (micromolar) causes action potential shortening (Bennett and Begenisich, 1987). The unaltered facilitation by isoproterenol that we observed in our study might be due to a lack of effect on APD by isoproterenol. A detailed microelectrode study would need to be done to investigate the effects of isoproterenol on AV nodal action potential duration and facilitation.

Clinical relevance of frequency-dependent drug action

A desirable goal of antiarrhythmic drug therapy is to terminate or suppress tachycardia without affecting impulse initiation or propagation at physiologic heart rates (Hondeghem and Katzung, 1984, Grant et al, 1984). Association of a drug with the ionic channel occurs predominantly during the upstroke and plateau phase of the action potential while dissociation occurs predominantly during diastole (Hondeghem and Katzung, 1984, Grant et al, 1984). When the drug is bound to its receptor site in the channel, that channel can no longer conduct. Thus, as the driving rate of a preparation is increased, the diastolic interval becomes shortened, and there is less time for the drug to dissociate from the channels and to recover from block. The faster the heart rate, the greater the steady-state channel blockade, and thus the greater depression in $\dot{V}_{max}$ and conduction velocity.

The most common type of supraventricular arrhythmia involving the AV node is reentrant AV tachycardia. In order to initiate the arrhythmia,, an early extrasystole is necessary. If an early extrasystole is viewed as a very rapid single beat tachyarrhythmia, a drug that rapidly binds to the receptor during phase zero of action potential, and dissociates entirely during diastole would be a drug of choice. However, in the case of sustained tachycardia, a drug which has a longer time constant of recovery would be desirable A drug that increases the magnitude of fatigue, even though it fails to prevent sustained AV nodal reentrant tachycardia, would have a therapeutic effect by reducing the rate of a tachycardia. Since the importance of facilitation in induction and termination of tachycardia is not known, more studies are needed to evaluate the role of facilitation and effects of antiarrhythmic drugs on this property and arrhythmia.

Statement of Original Contributions.

The research presented in this thesis contributes to knowledge in three areas of study concerning the frequency-dependent properties of the AV node, modulation of the frequency-dependent properties by autonomic nervous system, and implications of frequency-dependence for arrhythmias and antiarrhythmic drugs.

1-The experiments reported here contribute to establishing a new model of the frequency-dependent properties of the AV node that might be used to study the response of the AV node to the changes in rate, and to evaluate the effects of interventions on AV nodal function. The original contribution to the characterization and quantification of the components of the model are listed below

1-1. The degree of facilitation-induced leftward shift of the AV recovery curve was found to be an exponential function of facilitation cycle length (FCL)

1-2 Facilitation has no effect on the time constant of AV node recovery and AH_{∞}

1-3. The facilitation-induced leftward shift of the AV recovery curve can be quantified in terms of changes in HA interval for any given AH interval

1-4 The development of AV nodal fatigue was found to be a monoexponential function of beat number

1-5. The time constant for the onset of fatigue was found to be independent of HA interval

1-6 The magnitude of AH changes caused by fatigue at any steady-state HA interval was found to be a monoexponential function of HA interval

1-7. A mathematical equation incorporating quantitative indices of nodal recovery, facilitation, and fatigue accurately predicts the changes in AH interval at any steady-state heart rate

2 A detailed study of the autonomic modulation of the frequency-dependent properties of the AV node was presented This study revealed that

2-1. Negative dromotropic action of vagal nerve stimulation on the AV node was found to be frequency-dependent.

2-2 Underlying mechanisms of this rate-dependent effect were found to be related to the effects of vagal stimulation on the three rate-sensitive properties of the AV node as follow:

2-2-1. Vagal stimulation slowed AV node recovery in a voltage dependent way

2-2-2. The magnitude of facilitation was reduced by vagal stimulation

2-2-3. The magnitude of rate-induced fatigue increased by vagal stimulation, without altering its time course

2-2-4 Mathematical prediction of vagal effects on AV conduction revealed that over 50% of overall vagal action at rapid rates is due to slowing of recovery.

2-3. The degree of beta-adrenergic stimulation and blockade significantly alters the rate-dependent properties of the AV node. These studies revealed that

2-3-1. Beta-blockade increased the recovery time constant while beta-adrenergic stimulation by isoproterenol decreased it

2-3-2. Beta-blockade significantly increased the amount of rate dependent AV nodal fatigue, while isoproterenol decreased it

2-3-3. Neither isoproterenol nor beta-blockade altered AV node facilitation.

2-3-4. A mathematical model based on the above information accurately predicted enhanced rate-dependent conduction slowing with beta-blockade, and reduced rate-dependent slowing with isoproterenol

3. Theoretical considerations and previous observations suggest that depressant effects of calcium channel blockers on the AV node functions should be amplified by tachyarrhythmias This thesis presents the relevance of these concepts to the antiarrhythmic efficacy of calcium channel blockers The original contribution to these concepts are as follow

3-1 Results from these studies revealed that the rate dependent action of diltiazem account for its therapeutic effects during atrial fibrillation and atrioventricular reentrant tachycardia Mechanisms of these effects are listed below

3-1-1 Both of the determinants of the ventricular response to atrial fibrillation (AV node functional refractory period, and concealed AV nodal conduction) increased as the rate accelerated in the presence of diltiazem

3-1-2. The effects of diltiazem were significantly amplified during atrial fibrillation

3-1-3. Diltiazem produced a tachycardia-related suppression of AV nodal conduction during atrioventricular reentrant tachycardia.

3-1-4 The selective depressant effects of diltiazem during AV reentrant tachycardia was found to be related to diltiazem's effect on the minimum pathway for reentry, or wavelength.

3-2 This thesis provides evidence that in spite of alteration in the magnitude of diltiazem's effect by the autonomic tone, frequency-dependent diltiazem effects remained unaltered and account for its beneficial effect during tachycardia. Modulation of diltiazem's effect by autonomic tone are listed below:

3-2-1. Autonomic reflexes reduced diltiazem's effect for any given plasma concentration.

3-2-2. The autonomic modulation pf the diltiazem's effect was found to be related to both sympathetic enhancement and parasympathetic withdrawal.

REFERENCES

Bennet PB, and Begenisich TB (1987): Catecholamines modulate the delayed rectifying potassium current (I_K) in guinea pig ventricular myocytes Pflugers Arch 410;217-219.

Billette J, Janse MJ, Van Caplle FJL, Anderson RH, Touboul P, Durrer D (1976): Cycle-length-dependent properties of AV nodal activation in rabbit hearts. Am J Physiol 231.1129-1139.

Billette J (1987): Atrioventricular activation during periodic premature stimulation of the atrium Am J Physiol 252.H163-H177

Billette J, Matayer R (1989): Origin, domain, and dynamics of rate induced variations of functional refractory period in rabbit atrioventricular node. Circ Res 65 164-175

Buchanan JW, Oshita S, Fujino T, Gettes LS (1986) A method for measurement of internal longitudinal resistance in papillary muscle Am J Physiol,251 H210-H217.

Carmeliet E, and Vereecke J (1979) Electrogenesis of the action potential and automaticity In: Berne RM, Sperelakis N, Geiger SP (eds) Handbook of physiology, section 2 The cardiovascular system, Volume I The heart, American Physiological Society, Bethesda, pp 269-334

Decherd GM, Ruskin A (1946) The mechanism of Wenckebach type of A-V block Br Heart J 8:6-16

Delmar M, Michaels DC, and Jalife J (1989a) Slow recovery of excitability and Wenckebach phenomenon in the single guinea pig ventricular myocyte. Circ Res 65,761-774

Delmar D, Glass L, Michaels DC, and Jalife J (1989b) Ionic basis and analytical solution of the Wenckebach phenomenon in guinea pig ventricular myocytes. Circ Res 65,775-788

El-Sherif N, Scherlag BJ, Lazzara R (1975) Electrode catheter recording during malignant ventricular arrhythmia following experimental acute myocardial ischemia Circulation 51 1067-1074

Ferrier GR, Dresel PF (1974) Relationship of the functional refractory period to conduction in the atrioventricular node Circ Res 35 204-214

Froldi G, and Belardinelli L (1990): Species-dependent effects of adenosine on heart rate and atrioventricular nodal conduction Mechanism and physiological implications Circ Res 67 960-972

Gettes LS, and Reuter H (1974) Slow recovery from inactivation of inward currents in mammalian myocardial fibres J Physiol 240,703-724.

Gettes LS, Buchanan JW Jr, Saito T, Kagiyama Y, Oshita S, Fujino T (1985): Studies concerned with slow conduction in Zipes DP Jalife J (eds) Cardiac Electrophysiology and Arrhythmias Orlando, Fla, Grune&Stratton Inc, pp 81-87

Cottes LS (1986). Effect of ischemia on cardiac electrophysiology. In Fozzard HA, Haber E, Jennings RB, Katz AM, Morgan HE (eds) The heart and cardiovescular system. New York Ravan Press, publishers pp. 1317-1341.

Gibbons WR, and Fozzard HA (1975): Slow inward current and contraction of sheep cardiac Purkinje fibers J Gen. Physiol 65,367-384

Glitsch HG (1973) An effect of the electrogenic sodium pump on the membrane potential in beating guinea pig atria Pflugers Arch. Ges Physiol 344,169-180.

Glitsch HG (1982): Electrogenic Na pumping in the heart Ann Rev Physiol 44:389-400.

Grant AO, Starmer CF, Strauss HC (1984). Antiarrhythmic drug action Blockade of the inward sodium current Circ Res 55 427

Heethaar RM, Van Der Gon JJD, and Meijler FL (1973) Mathematical model of A-V conduction in the rat heart Cardiovasc Res 7 103-114

Hiramatsu Y, Buchanan JW, Knisley SB, Koch GG, Kropp S, and Gettes LS (1989): Influence of Rate-Dependent Cellular Uncoupling on Conduction Change During Simulated Ischemia in Guinea Pig Papillary Muscles Effect of Verapamil Cir Res 65:95-107).

Hirano Y, Fozzard HA, January CT (1989): Characteristics of L- and T-type Ca^{2+} currents in canine cardiac Purkinje cells. Am J Physiol 256 H1478-H1492

Hoffman BF, and Suckling EE (1954): Effect of heart rate on cardiac membrane potentials and the unipolar electrogram Am J Physiol 179,123-130

Hoffman BI, Paes de Carvalho A, Mello WC, Cranefield PF (1959) Electrical activity of single fibers of the atrioventricular node Circ Res 7 11-18

Hoffman and Cranefield (1960): Electrophysiology of the heart McGraw Hill, N Y.

Hondeghem LM, and Katzung BG (1984) Antiarrhythmic agents the modulated receptor mechanism of action of sodium and calcium channel blocking drugs. Ann Rev Pharmacol Toxicol 24:387

Honerkamp J (1983) The heart as a system of coupled nonlinear oscillators J Math Biol 18:69-88.

Iijima T, Irisawa H, Kameyama M (1985) Membrane currents and their modification by acetylcholine in isolated single atrial cells of the guinea-pig. J. Physiol 359;485-501

Jalife J (1983): The sucrose gap preparation as a model of AV nodal transmission Are dual pathways necessary for reciprocation and AV nodal echoes? PACE 6 1106-1122

Jack JJB, Nobel D, Tsien RW (1983) Electrical flow in excitable cells. London, Oxford University Press, P 518.

Jenkins JR, and Belardinelli (1988)· Atrioventricular nodal accomodation in isolated guinea pig hearts physiological significance and role of adenosine Circ Res 63·97-116

Kihara Y, Grossman W, and Morgan JP (1989) Direct measurement of changes in intracellular calcium transients during hypoxia, ischemia, and reperfusion of the intact mammalian heart Circ Res 65·1029-1044

Kleber AG, Riegger CB, Janse MJ (1987). Electrical uncoupling and increase of extracellular resistance after induction of ischemia in isolated, arterially perfused rabbit papilary muscle Circ Res. 61,271-279.

Kline RP, and Morad M (1978): Potassium efflux in heart muscle during activity: Extracellular accumulation and its implications J Physiol. 280,537-558

Kodama I, Hirata Y, Ando S, Toyama J, and Yamada K (1977) The mechanism of overdrive suppression-activation of electrogenic sodium pump following overdrive. J Mole. Cell Cardiol 9,36

Kokubun S, Nishimura M, Noma A, and Irisawa H (1982) Membrane currents in the rabbit atrioventricular node cell Pfluger's Arch 394 15 22

Kunze DL (1977)· Rate-induced changes in extracellular potassium in the rabbit atrium Circ Res 41,122-127

Lee KS, Tsien RW (1984) High selectivity of calcium channels in single ventricular heart cells of the guinea pig J Physiol 354 253-272

Levy MN, Martin H, Zieske, and Adler (1974): Role of positive feedback in the atrioventricular nodal Wenekebach phenomenon Circ Res. 34·697-710

Lewis T, Master AM (1924) Observation upon conduction in the mammalian heart AV conduction Heart, 12.209-269.

Loeb JM, deTarnowsky JM, Warner MR, Whitson CC (1987) Dynamic interactions between heart rate and atrioventricular conduction Am J Physiol; 249·H505-H511

Loeb JM, de Tarnowsky JM, Whitson CC, Warner MR (1987) Atriozentricular nodal accomodation. rate- and time-dependent effects Am J Physiol, 252:H578-H584.

Mazgalev T, Dreifus LS, Michelson EL, Pelleg A (1986) Vagal, induced hyperpolarization in atrioventricular node Am J Physiol 251;H631-H643.

Meredith BJ, Mendez C, Mueller WJ, Moe GK (1967) Electrical excitability of atrioventricular nodal cells. Circ Res 21,167-179.

Mobitz W (1924): Uber die unvollstandige Storung der Erregungs-uberleitung zwischen Vorhof und Kammer des menschlichen Herzens. Zeit Gesamte Exp Med;41:180-237.

Mubagwa K, Carmeliet E (1983): Effects of acetylcholine on electrophysiological properties of rabbit cardiac Purkinje fibers. Circ Res 53;740-751.

Nakayama T, Kurachi Y, Noma A, and Irisawa H (1984): Action potential and membrane currents of single pacemaker cells of the rabbit heart. Pflugers Arch. 402:248-257.

Nishimura M, Habuchi Y, Hiromasa S, and Watanabe Y (1988): Ionic basis of depressed automaticity and conduction by acetylcholine in rabbit AV node. Am. J. Physiol. 255(Heart Circ. Physiol. 24):H7-H14.

Noma A, Irisawa H, Kokubun S, Kotake H, Nishimura M, Watanabe Y (1980): Slow current sysyem in the A-V node of the rabbit. Nature 285:228-229.

Paes de Carvalho A, de Almeida DF (1960): Spread of activity through the AV node. Circ Res 8:801-809.

Reuter H (1973): Time- and voltage-dependent contractil responses in mammalian cardiac muscle. Eur. J. Cardiol. 1;177-181

Reuter H and Scholz H (1977a): The regulation of the Ca conductance of cardiac muscle by adrenaline. J. Physiol. (Lond.) 264;49-62.

Reuter H and Scholz H (1977b): A study of the ion selectivity and kinetic properties of calcium dependent slow inward current in mammalian cardiac muscle. J Physiol 264:17-47.

Schulz JJ (1978): Staircase response in guinea-pig atrial muscle. J. Physiol. 284,51p.

Simson MB, Spear JF, and Moore EN (1978): Electrophysiological studies in AV nodal Wenckebach cycles. Am. J. Cardiol. 41:244-258.

Simson MB, Spear JF, Moore EN (1981): Stability of an experimental atrioventricular reentrant tachycardia in dogs. Am J Physiol;240:H947-H953.

Shimoni Y, Spindler AJ, Nobel D (1987): The control of calcium current reactivation by catecholamines and acetylcholine in single ginea-pig ventricular myocytes. Proc R Soc Lon 239;267-278.

Shrier A, Dubarsky H, Rosengarten M, Guevara MR, Nattel S, Glass L (1987): Prediction of complex atrioventricular conduction rhythms in humans with use of the atrioventricular nodal recovery curve. Circulation; 76:1196-1205.

Talajic M, Papadatos D, Glass L, Villemaire C, Nattel S (1990): Mechanism of dynamic changes in Wenckebach-type AV block. J Am Coll Cardio; 15:201A.

Thomas RC (1972): Electrogenic sodium pump in nerve and muscle cells. Physiol Rev 52,563-594.

Tsuji Y, Inoue D, Pappano AJ (1985): Beta-adrenoceptor agonist accelerates recovery from inactivation of calcium-dependent action potentials. J Mol Cell Cardiol 17,517-521.

Trautwein W, McDonald TF, and Tripathi O (1975): Calcium conductance and tension in mammalian ventricular muscle. Pflugers Arch Gen Physiol 354,55-74.

Van Der Tweel I, Herbschleb JN, Borst C, and Meijler FL (1986): Deterministic model of the canine atrio-ventricular node as a periodically perturbed, biological oscillator. J Appl Cardiol 1:157-173.

Vassalle M (1970): Electrogenic suppression of automaticity in sheep and dog Purkinje fibers. Circ Res 27,361-377.

West TC, Toda N (1967): Response of the A-V node of the rabbit to stimulation of itracardiac cholinergic nerves. Circ Res 20,13-21.

APPENDIX

LIST OF ABBREVIATIONS

AA interval	Preceding atrial activation
ACh	Acetylcholine
AERP	Atrial Effective Refractory Period
AF	Atrial Fibrillation
APD	Action potential duration
AVCT	Atrioventricular conduction time
AVERP	Atrioventricular effective refractory period
AVFRP	Atrioventricular functional refractory period
AVN	Atrioventricular Node
AVRT	Atrioventricular Reentrant Tachycardia
BCL	Basic Cycle Length
cAMP	Cyclic adenosine 3',5'-monophosphate
cGMP	Cyclic guanosine 5'-monophosphate
CMT	Circus movement tachycardia
c_m	Capacity of the fiber per unit length
ECG	Electrocardiogram
EDTA	Ethylenediaminetetraacetic
FAC	Facilitation
FAT	Fatigue
FCL	Facilitation Cycle Length
GTP	Guanosine 5'-triphosphate
HA interval	Preceding His bundle interval
HBE	His bundle electrogram
I_f	The hyperpolarization activated current
$I_{K.ACh}$	Acetylcholine stimulated potassium outward current
I_K	Delayed rectifier potassium current
I_{Na}	Sodium inward current
I_{si}	Slow inward calcium current
I_{to}	Transient outward current
Rec	Recovery
r_i	The internal resistance of the cardiac fiber
r_m	The membrane resistance
RMP	Resting membrane potential
RRP	Relative refractory period
SVT	Supraventricular tachycardia
TTX	Tetrodotoxin
V_{max}	The maximum rate of rise of membrane potential during phase zero of action potential
WBCL	Wenckebach Cycle Length
WPW	Wolff-Parkinson-White